5-1-2019

Assessing Simulated Transmissivity in Numerical Flow Models of Complex Hydrogeology

Afan Tarar
afan.tarar@gmail.com

ASSESSING SIMULATED TRANSMISSIVITY IN NUMERICAL FLOW MODELS OF COMPLEX HYDROGEOLOGY

By

Afan Mahmood Tarar

Bachelor of Science- Molecular and Cellular Biology
University of Nevada, Las Vegas
2012

A thesis submitted in partial fulfillment
of the requirements for the

Master of Science- Geoscience

Department of Geoscience
College of Sciences
The Graduate College

University of Nevada, Las Vegas
May 2019

UNLV | GRADUATE COLLEGE

Thesis Approval

The Graduate College
The University of Nevada, Las Vegas

February 5, 2019

This thesis prepared by

Afan Mahmood Tarar

entitled

Assessing Simulated Transmissivity in Numerical Flow Models of Complex Hydrogeology

is approved in partial fulfillment of the requirements for the degree of

Master of Science- Geoscience
Department of Geoscience

David Kreamer, Ph.D.
Examination Committee Chair

Kathryn Hausbeck Korgan, Ph.D.
Graduate College Dean

Wayne Belcher, Ph.D.
Examination Committee Member

Michael Nicholl, Ph.D.
Examination Committee Member

Sajjad Ahmed, Ph.D.
Graduate College Faculty Representative

Abstract

Accurately extracting a meaningful transmissivity, a target value within one order of magnitude of field estimates, in numerical models poses a significant challenge when modeling complex groundwater systems. Aquifer transmissivity is directly proportional to the aquifer thickness and the estimated aquifer hydraulic conductivity. In complex geologic conditions (especially in fractured systems) with multiple heterogeneous and anisotropic hydrogeologic units, transmissivity can vary over several orders of magnitude.

To extract a meaningful value of transmissivity from a numerical model, a simple five-layer MODFLOW model was constructed. Each layer in the model was assigned a fixed hydraulic conductivity and thickness. The model simulates multiple pumping scenarios with varying combinations of hydraulic conductivity, aquifer thicknesses, and locations of the well screen to simulate aquifer tests.

Two extraction methods, the Screen Interval and Layer Summation, were used to extract transmissivity values from the five-layer model, and first compared to model-assigned transmissivity values and then to transmissivity estimated from simulated pumping tests using the Cooper-Jacob Approximation. A similar process was repeated with a more complex groundwater model, the Death Valley regional groundwater-flow system v. 2.0 numerical model. However, in the Death Valley regional groundwater-flow system v. 2.0 numerical model analysis, the Screen Interval and Layer Summation values were compared to field estimated values, not model-assigned transmissivity values.

The results of these comparisons show that transmissivity values extracted from a numerical model can vary many orders of magnitude from model assigned transmissivity values, and in the case of the Death Valley regional groundwater-flow system v. 2.0 numerical model, field estimated transmissivity. However, out of the 30 pumping scenarios run, the Screen Interval method transmissivity values were all within half an order of magnitude with the model input transmissivity and was found to be the most sensitive to the variation in transmissivity in both the simple five-layer model and Death Valley regional groundwater-flow system v. 2.0 numerical model. The Screen Interval extraction method may provide the most meaningful comparison of transmissivity between model results and field estimates.

Table of Contents

List of Tables

List of Figures

Introduction

Numerical models that incorporate the physical properties of aquifers, such as hydraulic conductivity (K), storativity (S), and transmissivity (T), are used to predict groundwater movement. Flow in the natural system is assumed to follow a governing equation that relates these properties to hydraulic head (h). Numerical modeling is used to attain an approximate solution for the governing equation, and hence groundwater flow through one of several numerical techniques, including finite-difference, finite-volume, or finite-element (e.g., Driscoll, 1987; Anderson and Woessener, 1992). The resulting numerical solution is an approximation containing uncertainties that result from: the choice of governing equation, numerical errors in the solution, and incomplete conceptualization of the groundwater flow system. In spite of these limitations, numerical models are widely used to predict water resource availability in policy and land management decisions. Thus, it is critical to explore and understand the accuracy of numerical models used for such purposes.

Hydrogeologic systems typically consist of multiple geologic layers of varying thicknesses that are composed of aquifers and confining layers. An aquifer can be defined as "a saturated permeable geologic unit that can transmit significant quantities of water under ordinary hydraulic gradients" (Freeze and Cherry, 1979, p. 47). A hydraulic gradient is the slope of the water potential and drives its flow (e.g., Fetter, 1994). The confining layers are "less-permeable beds in a stratigraphic sequence" that are not sufficiently permeable to allow production wells within them (Freeze and Cherry, 1979, p. 47). Because of the geological complexity in both material and structure, aquifers transmit water at different volumetric flow rates. The hydraulic conductivity of a geologic unit is a value describing the ability to transmit water under a hydraulic gradient (e.g., Lohman, 1979). Transmissivity (T) is defined as "the rate at which

water of the prevailing kinematic viscosity is transmitted through a unit width of the aquifer under a unit hydraulic gradient" (Lohman, 1979, p. 6). The T values are calculated by multiplying the horizontal saturated hydraulic conductivity (K) (hereafter-called hydraulic conductivity) by the thickness of an aquifer (e.g., Driscoll, 1987). Typically, T values are estimated from a field aquifer test and field experiments that monitor the water level response in a well, which is screened within a productive unit of an aquifer when water is pumped. In many cases, however, it is not clear which geological units and their associated thicknesses are influencing the T value being estimated (e.g., the thickness of the whole aquifer unit, the thickness of the well screen, or the physical property of certain geological layers).

In order to construct accurate groundwater models (simulations that mimic natural groundwater flow processes), it is essential to provide values of hydraulic conductivity that reflect the influences of the geologic materials on groundwater flow. Typically, K values are used as input for numerical models. Due to the lack of sufficient knowledge on the groundwater systems, uncertainties exist in hydrogeologic conceptualization of the target systems. One of the uncertainties is the choice of thickness (b) of an aquifer and/or confining unit that best represents the physical system. During model calibration, modelers can calculate simulated T values and compare them to the T values estimated from aquifer tests. In this study, b is the variable that will be adjusted and calibrated. The selected b values must reflect the field-estimated T and consider the complexity of multi-layered stratigraphy. To extract a T from the numerical model and make an appropriate comparison with the field estimated T values, modelers need to assess what representative b value better fits the field estimates.

The goal of this research is to assess the effectiveness of two different methodologies for extracting a value for T from a multi-layer aquifer simulation that best fits a field estimated T

value. The two methods are (1) the summation of all Ts of each model layer that the well penetrates, the Layer Summation (or LS method), and (2) the summation of all Ts in model layers where there is well screen, the Screened Interval method (or SI method). This study is expected to improve the selection of parameters in groundwater modeling by providing a comparison between model-derived and aquifer test-derived T values.

Purpose and Scope

The purpose of this work is to test different methods to extract T from a numerical groundwater-flow model and to evaluate which extraction method is more representative of real-world groundwater flow system. Two extraction methods, the Screen-Interval (SI), and Layer Summation (LS) methods are used with a simplified five-layer model and compared to model-assigned (input) T values. To mimic real-world aquifer tests the model was pumped and the simulated time and drawdown values were analyzed using the Cooper-Jacob Approximation (CJA) to obtain a T value. Simulated T values estimated using the CJA were compared to the values from the model extracted using the SI and LS methods. A similar analysis was used to extract T from a more complex multi-layer groundwater flow model Death Valley regional groundwater-flow system v. 2.0 (DVRFS v. 2.0) and compared to field estimated T values.

Background

Aquifer transmissivity and hydraulic conductivity estimate the ease with which water can move through permeable and fractured rock or unconsolidated materials such as gravel, sand, or silt. In field conditions, aquifer (pumping or slug) tests provide an estimate of T. MODFLOW-2005 uses K values, not T, as model input. When extracting a meaningful T from a numerical model and comparing this value to field estimated values, choosing a representative aquifer thickness for model input (particularly whether to use the entire model layer thickness or just the screen interval thickness) becomes a crucial factor. Field values of T and storativity (S) can be estimated using the Cooper-Jacob Approximation (CJA). In 1946, Cooper and Jacob developed a method to estimate T by using the semi-log relationship between drawdown and the $\log_{10}$ value of time. The CJA draws a "best fit" straight line down the log time versus drawdown curve (see Methods section for complete explanation).

Halford (2016) published FORTRAN programs called TCOMP to extract T values from MODFLOW models. TCOMP attempts to compare simulated T to aquifer-test estimated T values during model calibration. TCOMP sums the T of the entire thickness of the model cell to extract T values and shows that it is successful when calculating large T values, specifically values that exceed 3,000 ft^2/day (Halford, 2016). However, TCOMP is limited since it heavily relies on "professional judgment" for simulating the affected volumes and identifying affected model cells (Halford, 2016).

Since numerical models are just approximations of nature and no model perfectly matches field conditions, there is bound to be error with the T values extracted using the LS and SI methods. In a study published in 2016, Halford and others ran model simulations with known T

values and concluded that an error range of two times the known T as acceptable when interpreting T values from aquifer test results. For this study, T values ranging up to an order of magnitude are assumed to include the actual value.

Death Valley Regional Groundwater-Flow System Model v. 2.0 (DVRFS v. 2.0)

DVRFS v. 2.0 (Belcher and others, 2017) is an extensive, geologically complex numerical groundwater flow model of the Death Valley region. Groundwater in this regional system originates as recharge in nearby mountains, flowing in the subsurface through carbonate-rock aquifers, and discharging at lowland springs (Belcher and others, 2017). Arid conditions in the region limit groundwater recharge from precipitation, which mostly occurs at higher altitudes, and there is effectively no recharge at lower altitude areas (Belcher and others, 2017). Interbasin flow, groundwater flow through multiple valleys that are separated by bordering mountains, is a crucial component to our conceptual understanding of groundwater movement in the Great Basin. While interbasin flow does vary between the various basins, it is common and mostly driven by the hydraulic conductivity of the hydrogeologic units (HGUs) and recharge (Belcher and others, 2009). For the simple five-layer model each of the five layers is considered a different hydrogeologic unit (HGU).

Within DVRFS, D'Agnese (1997) described regional groundwater flow as occurring within three sub-regions: northern, central, and southern Death Valley. The location of recharge and discharge areas, regional hydraulic gradients, the occurrence of hydrogeologic units and structures, and water chemistry were used to define these sub-regions. The direction of groundwater flow across the boundaries of these sub-regions are based on estimates provided in Harill and Bedinger (2010). Figure 1 shows the extent of the model and the geologically complex area it encompasses (Belcher and others, 2017).

The DVRFS 2.0 model was constructed using MODFLOW-2005 and has 194 rows, 160 columns, and 16 layers (Belcher and others, 2017). In DVRFS 2.0 model cells are 1,500 meters (m) on a side and the thickness ranges from 50 m to greater than 300 m (Belcher and others, 2017). Apart from model layer one, which is thicker locally, the model layer thickness increases at greater depths in the model (Belcher and others, 2017). The Recharge Package (RCH) simulates precipitation-based recharge, the Drain Package (DRN) simulates springs and evapotranspiration areas (Belcher and others, 2017). The Hydrogeologic Unit Flow (HUF) package simulates horizontal conductivity, vertical anisotropy, and storage and the geometry of HGUs (Belcher and others, 2017).

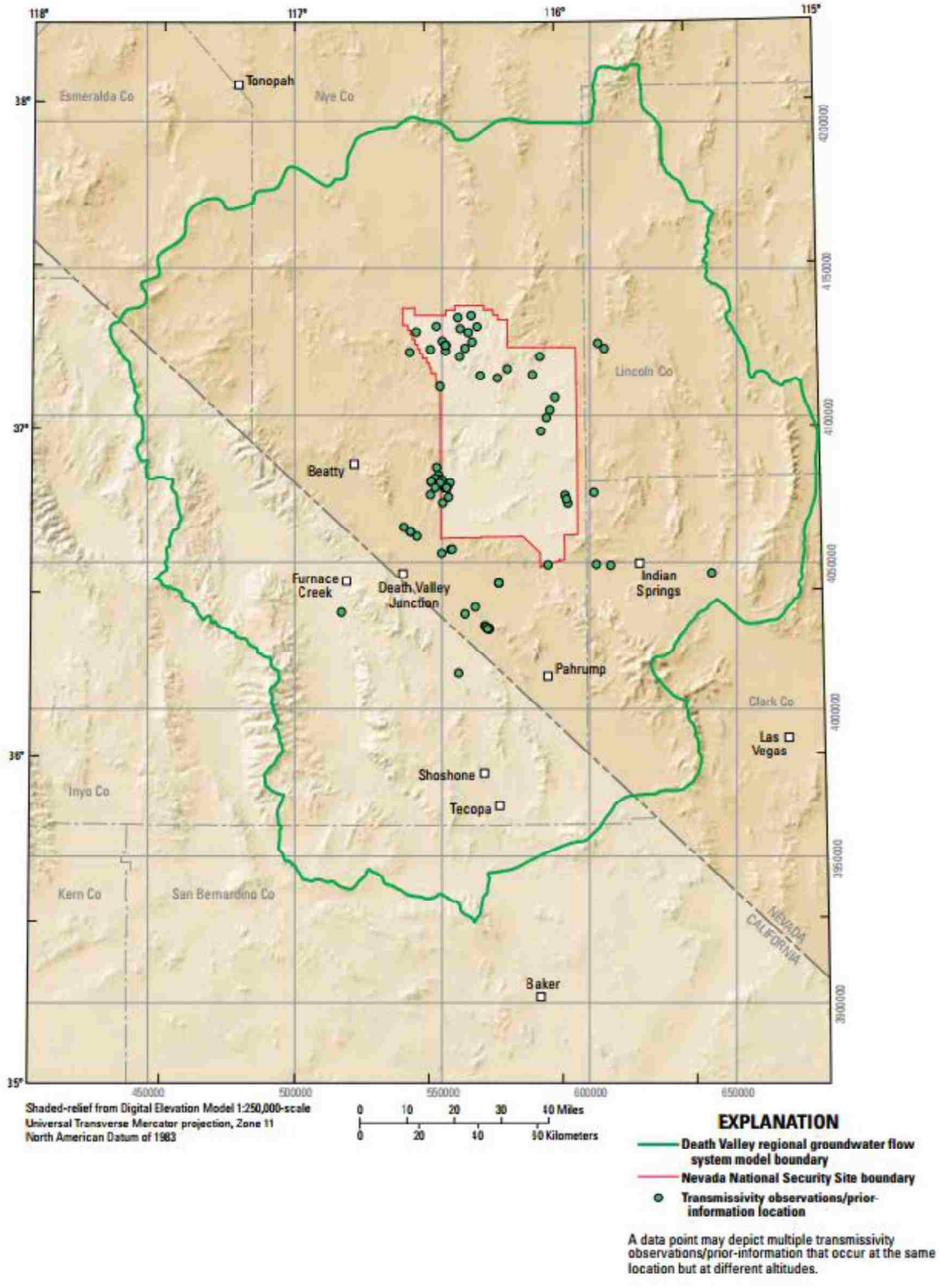

Figure 1 - Death Valley Regional Groundwater System model area from Belcher and others, 2017.

Methods

A simple five-layer model was constructed using MODFLOW-2005 (Harbaugh, 2005) and used to determine which extraction method, LS or SI is most appropriate to extract T from a groundwater model. The K values of this hypothetical model simulate a regressive stratigraphical sequence (layers with greater values of K on top of layers with lesser values). Initially, the T values extracted using these methods were compared to model-assigned T values. Then, the five-layer numerical model was stressed by pumping nodes to simulate pumping aquifer tests that produce changing hydraulic head values over time. The results of the simulated pumping tests are graphically analyzed using the CJA to assess the effect of multiple layers with varying hydraulic conductivities on the resulting transmissivity and then compared to the extracted T values. The resulting T estimates are used to assess the most appropriate method to extract T values in complex groundwater flow models.

A similar analysis was then applied to the DVRFS v. 2.0 (Belcher and others, 2017) to use a more complex, published model and test the robustness of the SI and LS methods. Developing a defined methodology to extract T from numerical models may not be exact in all cases, especially considering the uncertainty and complexity of some groundwater models.

ModelMuse (Winston, 2009), "a graphical user interface (GUI) for MODFLOW", was used to construct the simple five-layer model. Model Viewer (Hsieh and Winston, 2002) provided the three-dimensional results of each model run and whether the cone of depression (radius of influence) touched the model boundaries. GW Chart extracted and displayed the head values of each model cell after pumping. Finally, Microsoft Excel © was used for data organization and to construct drawdown graphs.

Aquifer Test Analysis

Theis (1935) defined hydraulic conductivity multiplied by the thickness of an aquifer (b) as a single term to represent the transmission capability (T) of the entire thickness of an aquifer. Theis (1935) showed that deriving T and S in an aquifer can be accomplished by analyzing drawdown and recovery data collected during pumping tests. Values of T and S are estimated by comparing the Theis type log-log curve to drawdown data. Cooper and Jacob (1946) developed a method to estimate T using the semi-log relationship between drawdown and the $\log_{10}$ value of time. The Cooper-Jacob Approximation (CJA) draws a "best fit" straight line through the log time versus drawdown curve for late- time values (Figure 2). The CJA is defined as:

$$s = \frac{2.3Q}{4\pi T}\log\frac{2.25Tt}{r^2S} \quad (1)$$

where:

1. r = radial distance from pumping well to observation well (L)
2. s = drawdown (L) over one log cycle
3. S = storativity (dimensionless)
4. Q = pumping rate (L^3/T)
5. t = time elapsed over one log cycle (T)
6. T = transmissivity (L^2/T)

The line through the late the late time data were fit manually (Figure 2).
The CJA (Cooper and Jacob, 1946) assumes:

1. the pumping well fully penetrates the aquifer;
2. the aquifer is homogeneous, isotropic in the aquifer;

3. the aquifer is of infinite extent;
4. the well diameter is infinitesimal;
5. instantaneous discharge with a drop-in head value;
6. the aquifer is fully confined;
7. the discharge is constant;
8. the aquifer has a constant thickness

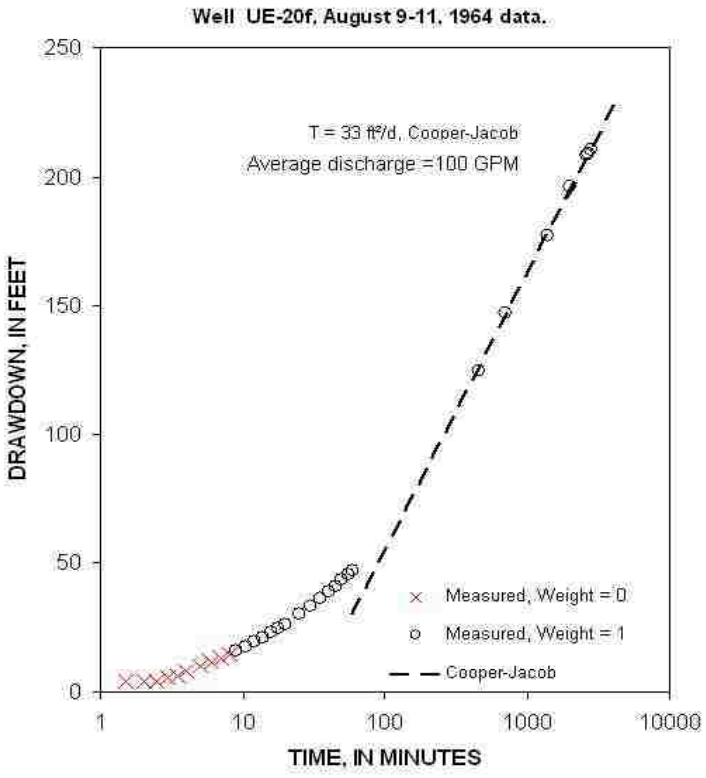

Figure 2 - Cooper- Jacob Approximation (source http://nevada.usgs.gov/water/AquiferTests/nts_singlewell_UE-20f.cfm?studyname=nts_singlewell_UE-20f)

The solution of the CJA is valid when the amount of time since the aquifer was pumped is large enough that the value for u, a dimensionless time parameter, is less than 0.01 or the radius

of the well that is being pumped to the observation well is small enough that u stays below 0.01 (Kruseman and de Ritter, 2000). It also should be noted that error can be relatively small when values above 0.01 are used (Kruseman and de Ritter, 2000).

MODFLOW-2005

MODFLOW-2005 (Harbaugh, 2005) is a 3D block centered finite-difference numerical modeling code that approximates the solution of the groundwater-flow equations. The finite-difference technique produces matrices of algebraic equations from the complex partial differential questions that the computer can then solve (Anderson and Woessener, 1992). In the finite-difference method, head values are calculated at the node and this is the average head value for the entire cell surrounding that node (Anderson and Woessener, 1992). Similar to other numerical methods, the algebraic equations are solved iteratively until convergence to an approximate solution. Convergence is defined as when a predefined threshold of the difference between iterative values (residuals) at the nodes is reached. These progressively smaller residuals reach a point where further iteration is believed not to change the model's final estimated values appreciably. MODFLOW-2005 solves for the water level, net discharge, and flow rate – the rate at which the water is either added or subtracted from the system (Harbaugh, 2005). Multi Node Well Package 2 (MNW2) allows the user to set the pumping rate and the model dynamically determines the flow rates layer by layer (Konikow and others, 2009). It also allows the user to input the various different screen intervals, rather than parsing out the intervals by assigning different pumping rates to different layers (Konikow and others, 2009). Numerical techniques are much more practical and robust than analytical solutions for groundwater flow in heterogeneous and anisotropic media.

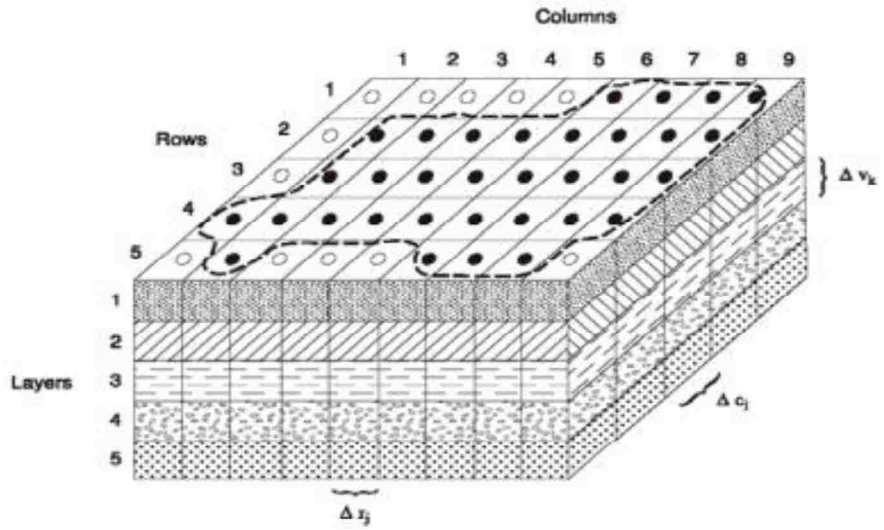

Figure 3 - Schematic of MODFLOW finite-difference grid (from Harbaugh, 2005). The filled in black nodes are the active cells, while the unfilled white nodes are inactive cells.

In a finite-difference grid, the head is calculated at the node in the center of the cell (Figure 3). Δr_j is the width of a cell in the row direction for any column, Δc_j is the width of the cell in the column direction for any given row, and Δv_k is the thickness of the cell in any layer (Harbaugh, 2005). The MNW2 Package (Konikow and others, 2009) is used to set up the various pumping scenarios. MNW2 allows the user to designate a screen length for a well that can penetrate multiple model layers (including partial penetration). MNW2 calculates the flow rates layer by layer, distributing the pumping over the designated screen lengths.

Other Modeling Tools

ModelMuse (Winston, 2009), Model Viewer (Hsieh and Winston, 2002), GW Chart (Winston, 2000) and Microsoft Excel were used to build and analyze the simple five-layer numerical model. ModelMuse is a GUI for MODFLOW-2005, making it possible to set up the model without having to code it in MODFLOW-2005. Model Viewer visualizes the simulation

results and was used to ensure that the model was functional and, as mentioned on page 7 above, that the cone of depression did not intersect the model boundaries. GW Chart extracts and displays head values from any cell in a MODFLOW-2005 file during the simulation. These head values were exported to Microsoft Excel which was used to produce the CJA graphs and to estimate values for T.

Numerical Model Setup

A simple five-layer model was constructed to simulate changes in K at depth. This model contains 299 rows and 299 columns with homogenous and isotropic properties in each model cell. The top and bottom of the model domain are no-flow boundaries with constant head boundaries on sides of the model. These boundary conditions were used to make the simple five-layer model into a confined aquifer and make it similar to DVRFS v. 2.0. Each of the five layers is 10 meters thick giving a total model thickness of 50 meters. Model cells are 100 m by 100 m in the x and y directions. The total model area is 8.94×10^8 m^2. A large model area was constructed to ensure that any simulated cone of depression would not intersect the model boundaries.

Simulating a confined aquifer, water-levels were set with a piezometric surface of 60 meters, resulting in a water surface 10 meters above the top of the model. Table 1 presents the hydraulic properties of each layer in the simple five-layer numerical model. The horizontal K arithmetic mean is 0.2222 m/day and the vertical K geometric mean is 0.000045 m/d, which makes vertical flow negligible when considering the entire 5-layer profile.

Table 1 - Numerical model hydraulic properties

	Model Layer	Horizontal Hydraulic Conductivity (m/day)	Vertical Hydraulic Conductivity (m/day)	Specific Storage (1/m)
Top layer	1	1	0.1	0.001
⋮	2	0.1	0.01	0.001
⋮	3	0.01	0.001	0.001
⋮	4	0.001	0.0001	0.001
Bottom layer	5	0.0001	0.00001	0.001

Several pumping scenarios were run with well screens at various intervals (Figure 4). The simulated pumping well has a radius of 0.15 meters and pumps 100 m^3/day. A total of 31 stress periods were simulated with each day-long stress period divided into two half-day time steps. A total of 30 scenarios simulate various combinations of partially- and fully-penetrating pumping wells. Figure 4 depicts all 30 tests run using the simple five-layer model simulation. Each layer is 10 meters in thickness, grey layers are screened; black layers, that is intervals with casing but not well screen, still penetrated by the well. The number within the layer shows the length of the well screen interval in the calculation (for example in Test 16, layer 1, the well screen is 5 meters in length).

Before the pumping simulations were run a hypothetical case was modeled to test the functionality of the MODFLOW-2005 model. The test model was a homogeneous version of the model described above, with each model layer assigned a K of 1 meter/day, resulting in a T of 50 m^2/day. Pumping was simulated in a single fully penetrating well located in the center of the grid. Analysis of the drawdown using the CJA gave a T value of 23 m^2/day, and analysis using the Theis (1935) method gave a value of 25 m^2/day, both of which are within a factor of two

from the model assigned T of 50 m^2/day. This comparison between the values estimated using the Theis and CJA methods demonstrates that the CJA can be used reliably to estimate values of T in this study.

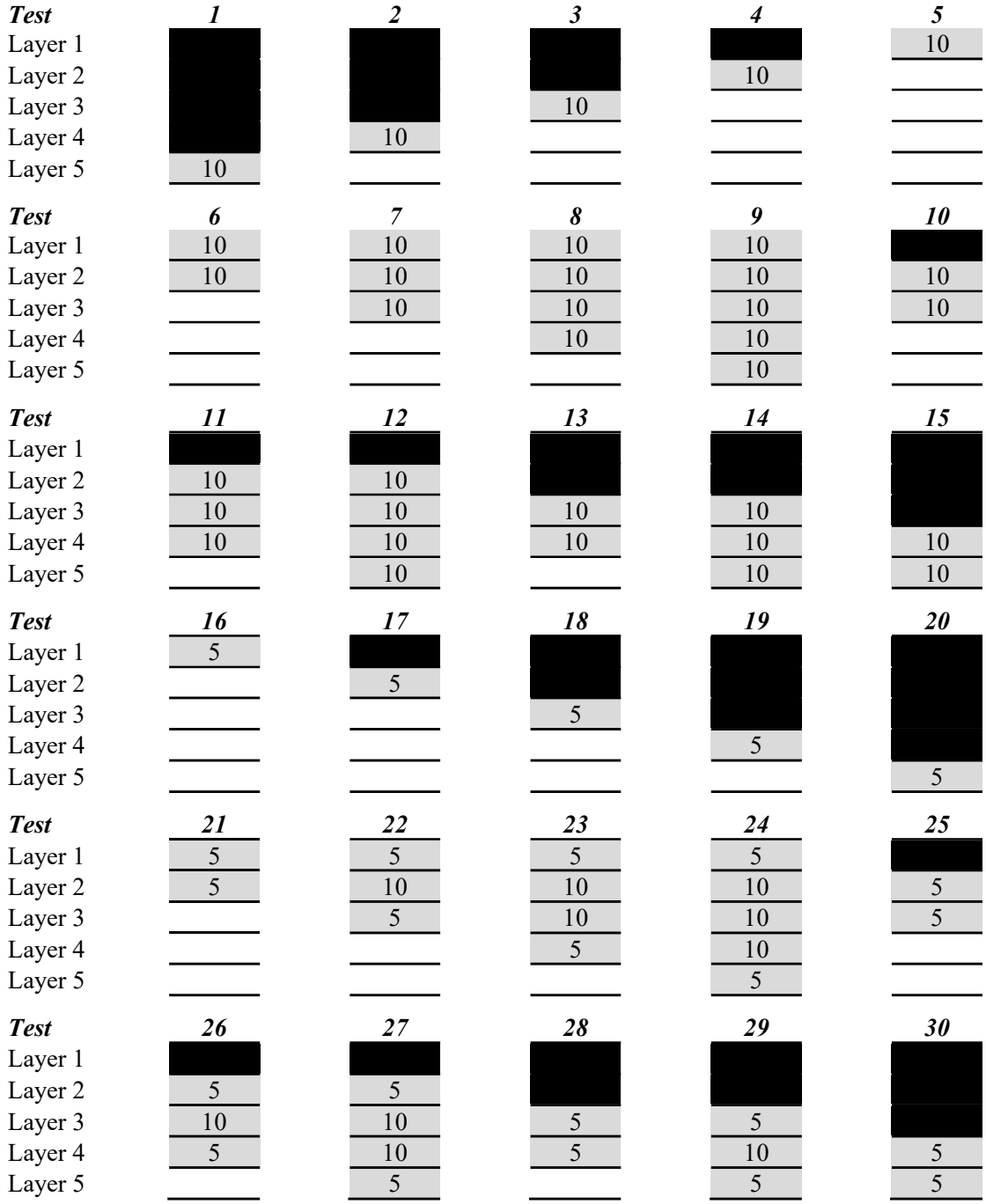

Figure 4 - Pumping Scenarios Test (T) run 1-6, in each model layer. Unscreened intervals, that is intervals with casing but not well screen, still penetrated by the well (black); Screened intervals (grey) (S); blank, that is, undrilled intervals not penetrated by either unscreened casing or well screen (white); Meters of screen in each interval (number in grey).

Extracting Simulated Transmissivities

For the five-layer model, both K and b are assumed input values, therefore, the model-assigned T (called TI in this study) is designated for each test run and represents a reference value for that test run's transmissivity. In numerical test simulations where there is only one layer that was screened (Tests 1-5 and 16-20, Figure 4), the assigned transmissivity TI is just the product of the individual K for that layer times that individual model layer's thickness. For the other tests where there are multiple layers that are screened (Test 6-15 and 21-30, Figure 4), the assigned TI value is the sum of the calculated T values for each of the layers in the screened interval, that is, the arithmetic sum of the product K(b) for all the layers that are screened. TI is calculated for each model test run.

Then, different T values are extracted from the five-layer numerical model scenarios represented in Figure 4. These extracted values are alternative transmissivity values for comparison (similarity or contrast) with the TI values, and with the CJA estimated transmissivity for both the numerical model test scenarios and the field DVRFS v. 2.0 model.

Specifically, there are two extraction methods investigated in this study: layer summation (LS), Equation 3, and screened interval (SI) Equation 4. As stated above, the values of T extracted from these LS and SI methods are compared to the model-assigned TI values and the CJA-estimated T values in the five-layer model. In the case of the DVRFS v 2.0 model, the LS and SI derived T values are compared to field-estimated T values.

$$T = K_{HGU} b_{HGU} \tag{2}$$

where:

1. T = Transmissivity
2. K = Hydraulic Conductivity (horizontal)
3. b = Thickness
4. HGU = Hydrogeologic unit, in this case the model layer.

The two methods used to extract T values from both numerical models are:

1. **Layer Summation (LS)** - Summation of transmissivities in all layers that the well penetrates, that is, taking the product of each layer's hydraulic conductivity (K_i) times its corresponding thickness (bi) for each (n) hydrogeologic unit (HGU)) and summing them, including both the screened and non-screened intervals that the well penetrates, but not layers without well penetration (called blanks or blank intervals).

$$T_x = \sum_{1}^{n} K_i \, b_i \tag{3}$$

2. **Screen Interval (SI)** - Multiplying hydraulic conductivity of each HGU (K_{HGU}) times its corresponding HGU layer thickness (considering only the HGUs in the well-screened interval), and then summing just those well screen interval (b_{SI}) T values. During scenarios where the well only partially penetrates the HGU, the SI method only takes the well screen length, not the entire thickness of the HGU.

$$\sum_{1}^{n} T = K_{HGU}\, b_{SI} \tag{4}$$

Model runs in which the well penetrates multiple layers, the LS method sums the T for each layer that is penetrated. Both the TI and SI methods only sum the T for the layers in which the well screen is located, with the difference being the SI method multiplies by the thickness of the well screen interval and the TI method multiplies by the thickness of the entire model layer. The two methods used to extract T from the five-layer model, LS and SI, are then applied to DVRFS v. 2.0 for a similar analysis.

Assessing Transmissivity Extraction Methods

Transmissivity values are extracted from numerical models using the LS and SI methods. To assess the accuracy of these methods, the values of TI are divided by both extraction methods. A $\log_{10}$ of the results are plotted against a 1:1 plot of extraction methods (LS versus TI, and SI versus TI). Points plotted against the 1:1 line indicate the degrees of magnitude from the TI. The point value closest to the 1:1 line, is considered "best-fit". T values estimated using CJA were subject to the same process, where CJA T was divided by the T value obtained from an extraction method (SI or LS) and a $\log_{10}$ of the results were plotted against a 1:1 line. Additionally, DVRFS v. 2.0 field T values are divided by each of the T extraction methods (SI and LS) and similarly, $\log_{10}$ of the result is plotted against the 1:1 line, resulting in "best-fit" values. Results from these assessments are presented in sections 5 and 6, respectively.

Pumping Test Simulation Results

Pumping test simulations were run for 30 different scenarios in the five-layer model. Drawdown over time initially shows layers affected by pumping. Results are plotted on a semi-log graph and analyzed using the CJA. CJA-estimated T values were then compared to the extracted T from equations 2-3 and TI (see tables 3-6).

Model values (table 2) were grouped based upon the order of magnitude difference between either TI or CJA values ("known" T values) and T extracted using either the LS or SI methods in the five-layer model. TI and CJA values were also compared using the same methodology. Similarly, for DVRFS v. 2.0, the groupings were based on the order of magnitude difference between the field estimated T values and T extracted using the LS or SI method.

To compare the extraction methods to the "known" T values, five groupings (Bin Value) were developed based upon orders of magnitude difference between, CJA or TI referred to as KV in the table and the different extraction methods (EM) which are either the LS or SI methods (Table 2). These Bin Values were calculated between the results of "known" KV methods and "extracted" EM methods, and this was done to determine logarithmic differences in the five-layer numerical model scenarios, and between field estimated T and the different extraction methods for DVRFS v. 2.0. Various pumping scenarios (Figure 4) were evaluated and results are presented and compared in the Tables 4 thru 6 (Appendix 1) that include values of TI, T values extracted using LS or SI method, associated normalization and degree of magnitude, and Bin value. Tables 7 and 8 (Appendix 2) contain values of T estimated using CJA, T values extracted using LS or SI method, associated normalization and degree of magnitude, and Bin value.

Table 2 - Bin Value grouping based on the magnitude difference between known or estimated T values.

Range of Values (Log_{10} of KV/EM)	Bin Value
$\lvert x \rvert \leq 0.5$	1
$0.5 < \lvert x \rvert \leq 1$	2
$1 < \lvert x \rvert \leq 2$	3
$2 < \lvert x \rvert \leq 3$	4
$\lvert x \rvert > 3$	5

Known value (KV, which is either TI or CJA) and transmissivity extraction method (TEM, which is either the LS and SI methods) and whose results are shown in Tables 4 thru 10 and appear in the Appendices (1-3). Bin Value is the grouping based on the magnitude orders difference between methods. Table 3 summarizes all model run results and includes transmissivity values for the CJA, SI, TI, and LS.

Table 3 -Transmissivity calculated using various methods. Cooper-Jacob Approximation (CJA) - Value estimated using CJA associated with drawdown; Screened Interval (SI) method - equation 4; T-Input (TI) method – model assigned transmissivity- equation 2; Layer Summation (LS) – equation 3

Test	Transmissivity-Input (m^2/day)	Cooper-Jacob Approximation (m^2/day)	Screened Interval (m^2/day)	Layer Summation (m^2/day)
1	0.001	19.291	0.001	11.111
2	0.010	73.307	0.010	11.110
3	0.100	610.890	0.100	11.100
4	1.000	6108.897	1.000	11.000
5	10.000	20362.991	10.000	10.000
6	11.000	1832.669	11.000	11.000
7	11.100	254.283	11.100	11.100
8	11.110	6.545	11.110	11.110
9	11.111	4.073	11.111	11.111
10	1.100	229.084	1.100	11.100
11	1.110	20.343	1.110	11.110
12	1.111	4.582	1.111	11.111
13	0.110	43.635	0.110	11.110
14	0.111	5.086	1.111	11.111
15	0.011	7.636	0.011	11.111
16	10.000	45816.729	5.000	10.000
17	1.000	9163.346	0.500	11.000
18	0.100	1309.049	0.050	11.100
19	0.010	166.606	0.005	11.110
20	0.001	17.454	0.001	11.111
21	11.000	833.031	5.500	11.000
22	11.100	335.318	6.050	11.100
23	11.110	30.544	6.105	11.110
24	11.111	2.932	6.111	11.111
25	1.100	591.184	0.550	11.100
26	1.110	40.685	0.605	11.110
27	1.111	2.932	0.611	11.111
28	0.110	75.109	0.055	11.110
29	0.111	5.086	0.061	11.111
30	0.011	7.331	0.0055	11.111

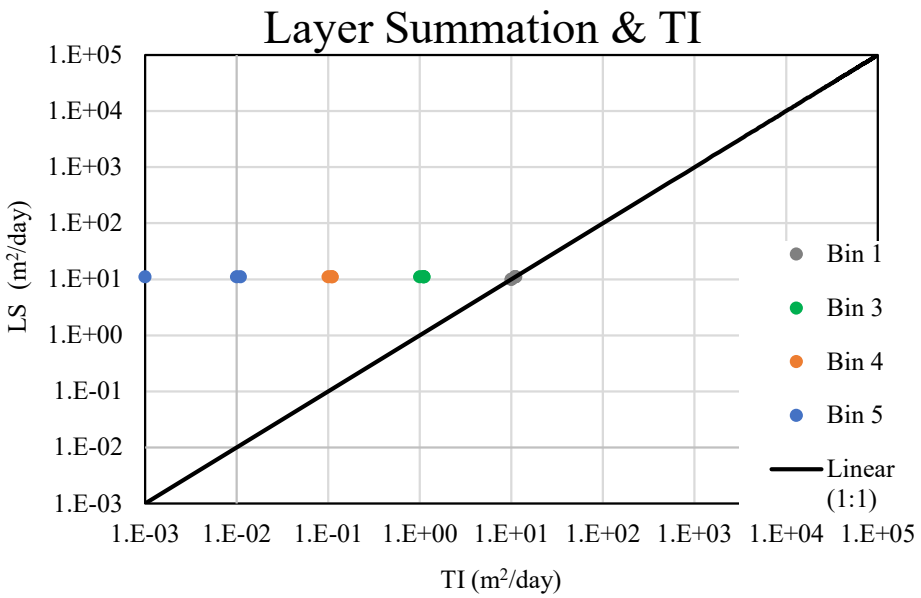

Figure 5 - Comparison of Layer Summation (LS) method with model assigned transmissivity values (TI). Bins = Grouping based on orders of magnitude difference between TI and LS. Bin 1: $|x| \leq 0.5$; Bin 2: $0.5 < |x| \leq 1$; Bin 3: $1 < |x| \leq 2$, Bin 4: $2 < |x| \leq 3$; Bin 5: $|x| > 3$. Some values are not visible because they overlay with each other.

Figure 5 shows the relationship of TI versus the LS method (equation 2) and shows the orders of magnitude difference between TI values and LS values. Raw data for these model runs is listed in Table 4 (Appendix 1). Of the 30 model runs, 33 % of values are in Bin 1, 0 % in Bin 2, 27 % in Bin 3, 20 % in Bin 4, and 20 % in Bin 5. In Figure 5, T values from the TI and LS methods range from maximums of 11.111 m^2/day and 11.111 m^2/day (respectively) and minimums of 0.001 m^2/day and 10 m^2/day (respectively). Average values for TI and LS were calculated to be 3.932 m^2/day and 11.020 m^2/day with standard deviations of 4.925 and 0.275, respectively.

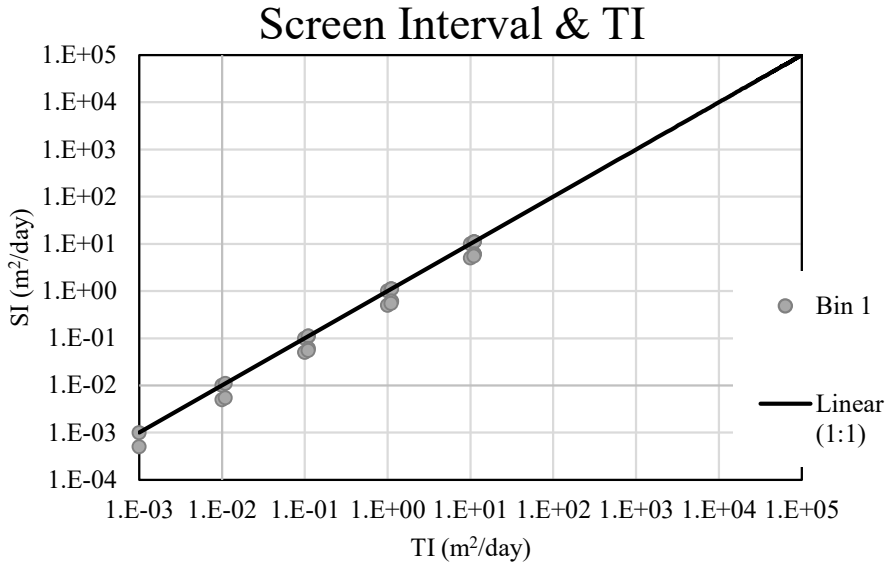

Figure 6 - Comparison of Screen Interval (SI) method with model assigned T values (TI). Bins = Grouping based on orders of magnitude difference between TI and LS. Bin 1: $|x| \leq 0.5$; Bin 2: $0.5 < |x| \leq 1$; Bin 3: $1 < |x| \leq 2$, Bin 4: $2 < |x| \leq 3$; Bin 5: $|x| > 3$. Some values are not visible because they overlay with each other.

Figure 6 shows the relationship the TI versus the SI (equation 4) and the order of magnitude difference between TI values and SI values. Table 5 (Appendix 1) lists the various T values extracted using this technique. All extracted T values using this method fell into Bin 1. In Figure 6, T values from the TI method and SI methods range from maximums of 11.111 m^2/day and 11.111 m^2/day (respectively) and minimums of 3.932 m^2/day and 3.006 m^2/day (respectively). Average values for TI and SI are 3.932 m^2/day and 3.006 m^2/day with standard deviations of 4.925 and 4.051, respectively.

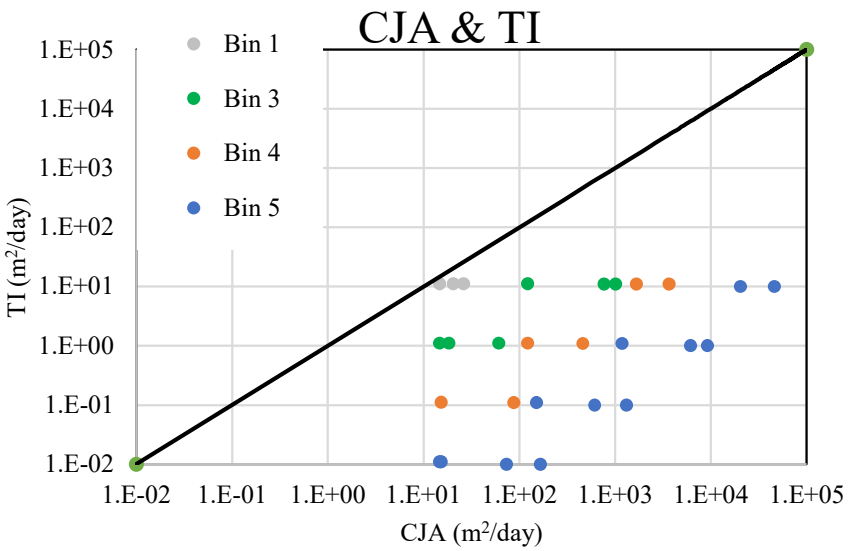

Figure 7 - Comparison of model assigned transmissivity values (TI) with Cooper-Jacob Approximation estimates (CJA). Bins = Grouping based on orders of magnitude difference between TI and LS. Bin 1: $|x| \leq 0.5$; Bin 2: $0.5 < |x| \leq 1$; Bin 3: $1 < |x| \leq 2$, Bin 4: $2 < |x| \leq 3$; Bin 5: $|x| > 3$. Some values are not visible because they overlay with each other.

Figure 7 shows the relationship between CJA values versus the TI (equation 2) and shows the order of magnitude difference between TI values and CJA estimated values. Table 6 (Appendix 1) lists the TI values and compares them to those estimated using the CJA. Of the 30 total tests run, 13 % were in Bin 1, 6 % were in Bin 2, 23 % were in Bin 3, 23 % in Bin 4, and 33 % in Bin 5. In Figure 7, T values from the CJA and TI methods range from maximums of 45,817 m^2/day and 11 m^2/day (respectively) and minimums of 15 m^2/day and 0.001 m^2/day (respectively). Average values for CJA and TI are 3,103 m^2/day and 4 m^2/day with standard deviations of 8,884 and 4.925, respectively.

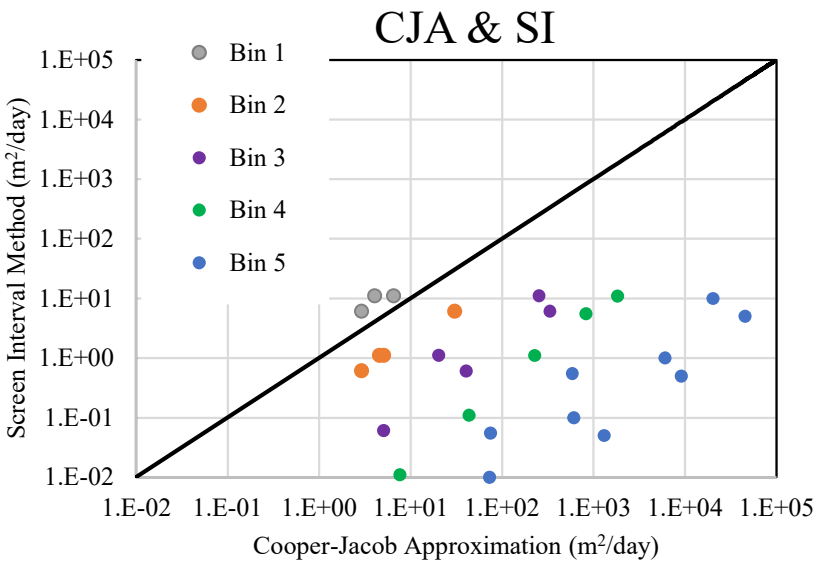

Figure 8 - Comparison of transmissivity (T) values extracted using the Screen Interval (SI) method with T values estimated using the Cooper-Jacob Approximation (CJA). Bins = Grouping based on orders of magnitude difference between TI and LS. Bin 1: $|x| \leq 0.5$; Bin 2: $0.5 < |x| \leq 1$; Bin 3: $1 < |x| \leq 2$, Bin 4: $2 < |x| \leq 3$; Bin 5: $|x| > 3$. Some values are not visible because they overlay with each other.

Figure 8 shows the relationship between the CJA values versus the SI method (equation 4) and shows the order of magnitude difference between CJA estimated values and SI values. Table 7 (Appendix 2) gives the full account of the various T values extracted using this technique. Of the 30 total tests run, 10 % fell into Bin 1, 0 in Bin 2, 17 % in Bin 3, 27 % in Bin 4, and 47% in Bin 5. In Figure 8, T values from the CJA versus SI methods range from maximums of 45,817 m^2/day and 11 m^2/day (respectively), and minimums of 3 m^2/day and 0.001 m^2/day (respectively). Average values for CJA and SI were calculated to be 2,932 m^2/day and 3 m^2/day, with standard deviations of 8,914 and 4.03, respectively.

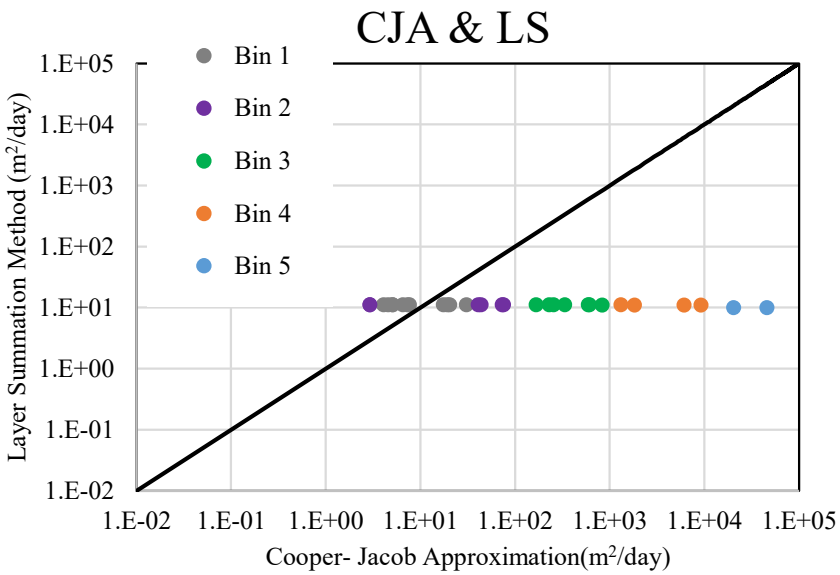

Figure 9 - Comparison of transmissivity (T) values extracted using the Layer Summation (LS) method with T values estimated using the Cooper-Jacob Approximation (CJA). Bins = Grouping based on orders of magnitude difference between TI and LS. Bin 1: $|x| \leq 0.5$; Bin 2: $0.5 < |x| \leq 1$; Bin 3: $1 < |x| \leq 2$, Bin 4: $2 < |x| \leq 3$; Bin 5: $|x| > 3$. Some values are not visible because they overlay with each other.

Figure 9 shows the relationship between the CJA versus the LS (equation 4) and shows the order of magnitude difference between CJA estimated values and LS values. Table 8 (Appendix 2) gives the full account of the various T values extracted using this technique. Of the 30 model runs, 37 % fell into Bin 1, 20% in Bin 2, 23 % in Bin 3, 13% in Bin 4, and 7% in Bin 5. In Figure 9, T values from the CJA and LS methods range from a maximum of 45, 816 m^2/day and 11.11 m^2/day (respectively), and a minimum of 2.93 m^2/day and 10.00 m^2/day respectively. Average values for CJA and LS were calculated to be 2932 m^2/day and 11.11 m^2/day, with standard deviations of 8,914 and 4.05, respectively.

Application to DVRFS v. 2.0

An analysis like that applied to the five-layer model runs was used on DVRFS v. 2.0. However, instead of comparing the Ts extracted using LS and SI methods to the TI or CJA T values, they were compared to field-estimated Ts. Figures 10 and 11 present the results for the SI and the LS methods being applied to DVRSF v. 2.0 respectively and compared to field estimates of T.

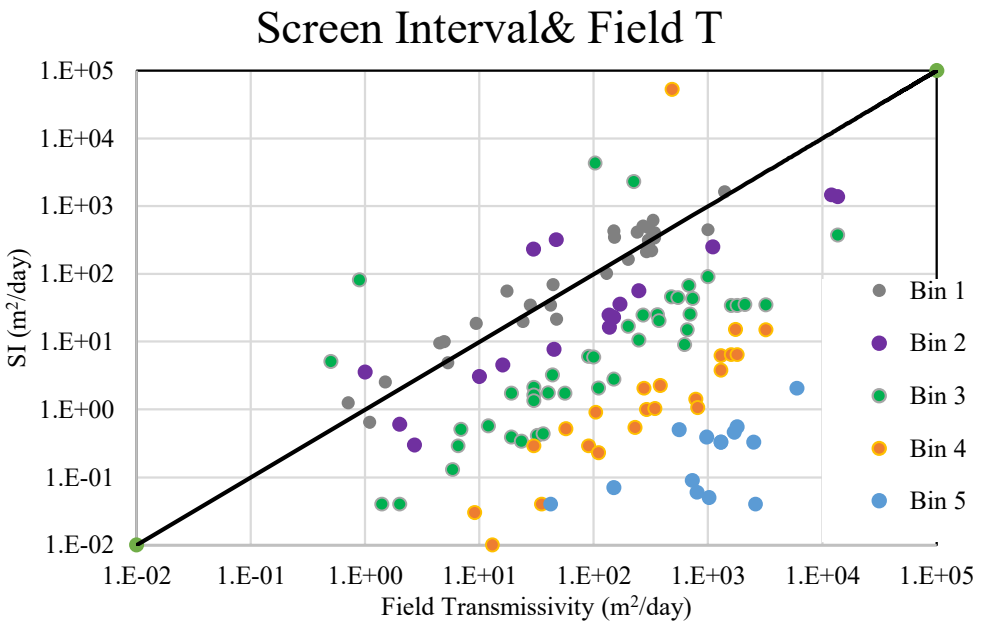

Figure 10 - Comparison of transmissivity (T) values extracted using Screen Interval (SI) method with Field Transmissivity. Bins = Grouping based on orders of magnitude difference between TI and LS. Bin 1: $|x| \leq 0.5$; Bin 2: $0.5 < |x| \leq 1$; Bin 3: $1 < |x| \leq 2$, Bin 4: $2 < |x| \leq 3$; Bin 5: $|x| > 3$. Some values are not visible because they overlay with each other.

Figure 10 shows the results of the field T values versus the SI values in DVRFS v. 2.0. Table 10 (Appendix 3 presents the various T values extracted using this technique. Out of 116 wells, 26 were in Bin 1, 15 were in Bin 2, 42 were in Bin 3, 21 in Bin 4, and 14 were in Bin 5. 51 % of the values are within one order of magnitude of the field values and 74 % are within two orders of magnitude (Belcher and others, 2017).

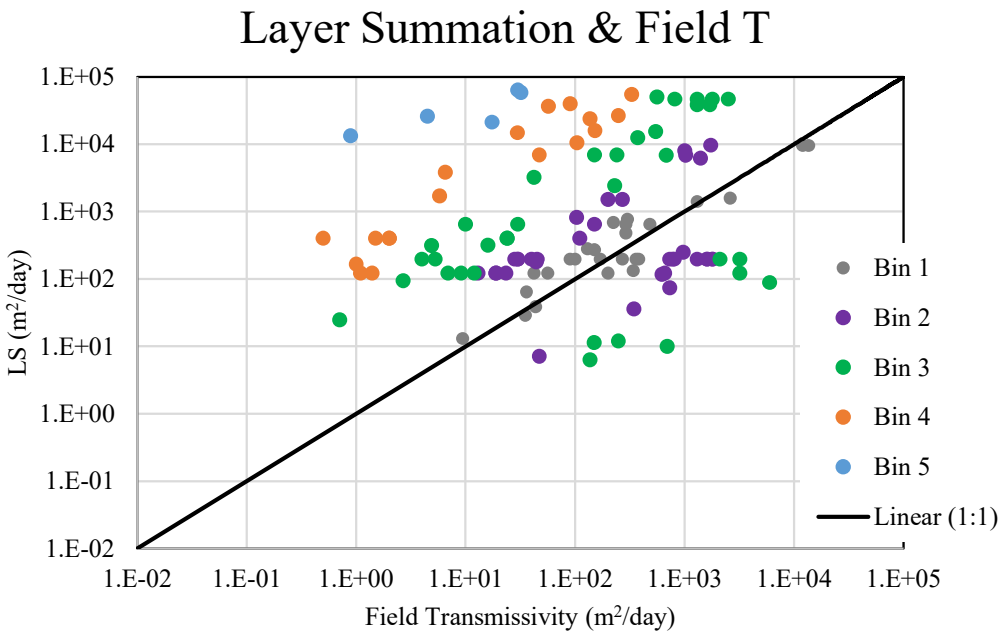

Figure 11 - Comparison of transmissivity (T) values extracted using the Layer Summation (LS) method with Field Transmissivity. Bins = Grouping based on orders of magnitude difference between TI and LS. Bin 1: $|x| \leq 0.5$; Bin 2: $0.5 < |x| \leq 1$; Bin 3: $1 < |x| \leq 2$, Bin 4: $2 < |x| \leq 3$; Bin 5: $|x| > 3$. Some values are not visible because they overlay with each other.

Figure 11 shows the results of the field T values versus LS values in DVRFS v. 2.0. Table 11 (Appendix 3) gives the full account of the various T values extracted using this technique. Of the 116 wells, LS method has 26 values in Bin 1, 33 in Bin 2, 35 in Bin 3, 19 in Bin 4, and 5 in Bin 5. 22 % of the values within one order of magnitude and 50 % are within two orders of magnitude.

Discussion

The results of the T comparisons are mixed. While comparing TI values to Ts extracted using the LS and SI methods was relatively straightforward, comparing the CJA estimated Ts to LS and SI T values gives mixed results. CJA comparisons do get complicated due to: model error, model conditions not exactly follow the assumptions of the CJA (such as full penetration i.e. complete screening), and the limitations of the CJA method. Using the SI and LS methods to extract T from DVRFS v 2.0 provides much clearer results.

Limitations

The simulations used in this study violated the assumptions listed for the CJA (Aquifer Test Analysis). The CJA assumptions that this experiment does not adhere to are:

1. The control well is fully penetrating
2. Water is released instantaneously from storage
3. The diameter of pumping well is infinitely small
4. The aquifer is of an infinite extent
5. There is no vertical hydraulic conductivity

By violating the assumptions listed above, the model incompletely mimics a real-world aquifer test. Similar to real-world aquifer tests, various model runs were conducted where the well is partially penetrating the aquifer and in many runs the well is only partially penetrating any given layer. However, since the well had been pumping for 31 days, there is adequate time for the well to stabilize and provide an accurate drawdown curve (Halford and others, 2006). The aquifer is not of infinite extent, but the cone of depression never reaches the model boundaries, thus effectively being infinite in extent. The well has a radius of 0.15 meters, indicating that an

instant response to the change in hydraulic head is not possible. Since the well radius is smaller than the model cell, this violation does hold and could lead to possible well-bore storage effects. Additionally, the set-up of the experiment could bias the results, with there being confined aquifer layers on both the top and bottom of the model and only horizontal K was considered when calculating T. It should be noted that the lines through the CJA late time data were drawn manually and the late time data were assumed to be linear.

The low number of negative-log values when comparing the CJA T estimates to the two different extraction methods and TI (Figures 7-9) indicate that in comparison the CJA T was overestimated. The values estimated using the CJA are consistently greater than the TI values.

During the pumping simulation on the top layers of the model, the transmissivity tended to be greater due to three reasons: (1) the value of K is greater in the higher units, (2) the simulated pumping discharge caused only small drops in head thus causing over-estimation of T, and (3) flow from lower layers could be pulled upward and influence the head values. Examining the CJA estimated T values, the T values in the lower layers (e.g. Tests are less than the higher conductivity ones, from layer 3 and above.)

Limitations of the CJA could play a role when addressing the abnormally large T value estimates where the pumping is primarily occurring in top layers, which have greater K values. While the CJA estimated T values follow the trend of lesser values in the less conductive layers and greater T values in the more conductive layers (for example, note differences in Tests 1-5 in Figure 4 and Appendices 4 and 5), the values estimated when primarily pumping in top two layers are greater than pumping in any other layer. Because there was little to no drawdown from these layers, it affects the scale of the semi-log graph and the steepness of the CJA line. These values are a clear overestimation (for example Tests 5, 6, ,16, and 21 in Appendix 5). The CJA

method is also dependent on the expertise of the hydrologist when drawing a straight-line through the curve. Different hydrologists could produce different CJA lines and have different T estimates (Halford and others, 2006).

Results

Noting that the well in the model is not infinitely small in diameter which violates an assumption of the CJA, and limitations of the CJA, the conceptual model of fluid flow through the model layers is consistent with the model results. For example, in Test #1 the noted drawdown in the screened interval (layer 5) is shallow and steepens upward through the column to the surface and drawdown in occurring in the top 4 layers (Figure 12). This result is expected and conforms to expected drawdown in a confined aquifer. All drawdown graphs for each test can be found in Appendix 4.

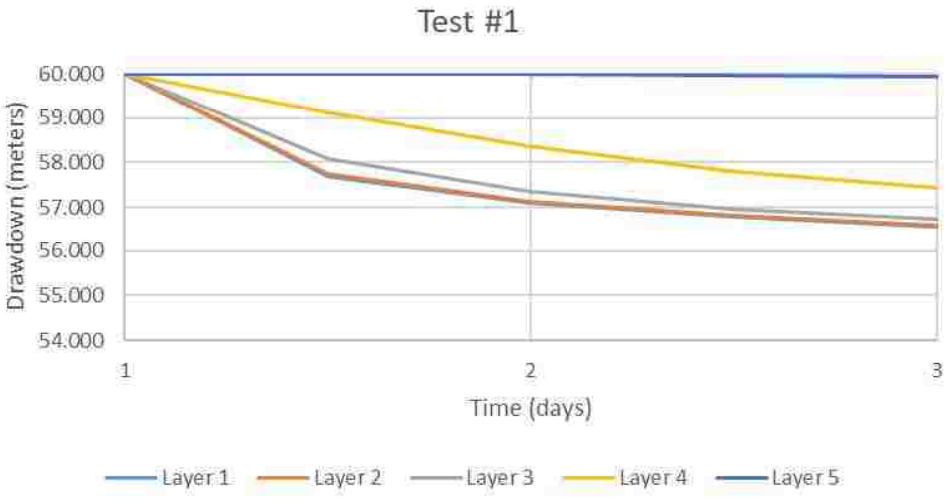

Figure 12 - Early drawdown of Test #1

Drawdown trends found in Test #1 were consistent through all the drawdown graphs (see Appendix 4). There was virtually no drawdown when the well screen was exclusively placed in the greater hydraulic conductivity layers. This trend remains consistent in model runs in which the well is partially screened.

This drawdown trend explains the greater values of T estimated using the CJA in Tests 5, 6, 16, and 17 (see Tables 4-6, Appendix 1). With little to no drawdown, the CJA gave greater T values. Examining the CJA estimated T values, the T values in the lower layers are less than the ones from layer 3 and above.

Another result which follows the drawdown trend is the observed greater T values for Tests 4, 5, 6, 16, and 17. The greater CJA estimated T values for these model runs are expected since they are all in the top two layers where there is virtually no drawdown (Appendix 4). Due to the small amount of drawdown, numerical error in the model can affect these results. Appendix 5 contains the semi-log graphs for all the layers in the various model runs. In all test runs, layer 5 had a delay in its drawdown.

In the first part of the experiment, where TI is compared to LS and SI, the SI method returned values that matched TI relatively closely (Tables 5, Appendix 1). All the T values extracted using the SI method in this comparison were in Bin 1. The only differences between SI and TI values occurred when the well partially penetrated a layer and even then, the difference was within one order of magnitude. T values extracted using the LS method needed to be summed, causing them to be over-estimated (Figure 5 and Table 4, Appendix 1). Since the LS method sums all the layers that the well penetrates, the T value becomes influenced by the greater K values in the higher model layers.

When pumping the five-layer model, the results are complicated. Making a relative comparison between the TI and the CJA reveals a positive correspondence between high T values and low T values; for example, when the TI T is a high value there is a corresponding CJA value, and when there is a low TI value, the CJA value is lower. This variability indicates that the configuration of different layers and the varying screen intervals can affect CJA T estimates. Figure 8 shows how the SI values in each Bin show a positive correspondence when compared to CJA values. In Figure 9, the LS values stay relatively constant. Table 6 shows that most of the values calculated by the LS method are around 11.1. However, the LS method does not show any trend but rather provides the same value for T (Figures 5 and 9). This method is not sensitive to the lower end T values (Figures 5 and 9). The SI method shows more variance since the values extracted using this method are more sensitive to the HGUs with lesser K values (Figure 6).

For DVRFS v. 2.0, the SI method resulted in an extracted T values that were closer to the field estimated values. Of 116 T values extracted using the SI method, 51% lie within one order of magnitude of the field estimated T values, 74% are within two orders of magnitude, and 26% are more than two orders of magnitude from their field estimated T. (Belcher and others, 2017).

Conclusions

It is apparent that accurately extracting a T from a numerical groundwater model can be complex. Transmissivity varies over several orders of magnitude in relatively short distances, especially in complex and heterogeneous geology (especially fractured systems). The procedure of this analysis was, to build a simple five-layer model to simulate a real-world pumping test. T values in an aquifer test are affected by the configuration of HGUs and differing depths and thickness of the well screen interval. Comparing the T values extracted using the SI and LS methods to the CJA values, the results were mixed. The LS method had 43 % of its values within two orders of magnitude of the CJA estimated T, superior to the 10 % of the SI method. Using the simple five-layer model, the SI and LS methods were tested to assess which extraction method provides more values that match TI values. Finally, these two extraction methods were applied to DVRFS v. 2.0.

When analyzing the results of the LS method (Table 4) its limitations become apparent, with similar maximum and minimum values of 11.111 m^2/day and 11.020 m^2/day, respectively. Graphing the results of the LS to TI comparison shows values running straight along the middle of the graph and do not show any sensitivity to the T values on the lower end. In contrast, the SI to TI comparison fluctuates more and captures a broader range of values. The LS method skews to greater T values, as reported by Belcher and others (2017) since it is heavily influenced by the layers with the greater K values. The SI method shows a broader range of results and is more sensitive to T values on the lower end of the graph.

The different simulations used in this study did not fully conform to assumptions listed in the CJA. Additionally, the CJA method itself has limitations, being dependent on the expertise of

the hydrologist to draw the “best” fit line. Model approximation can also contribute to adding more error in the calculations. There were several model runs where the simulated drawdown was small and more susceptible to numerical error in the model. While the five-layer model did behave like a confined aquifer when it was pumped it should be noted that some of the results estimated using CJA were abnormally large.

When the SI and LS methods were applied to a complex model, DVRFS v. 2.0, the results are much clearer, with more T values being within two orders of magnitude of the field estimated T using the SI method than the LS method (Belcher and others 2017). As in the previous five-layer model, the T values extracted using the LS method were dominated by the layers with greater Ks, which is expected and consistent with the findings of Belcher and others (2017).

The data suggest that the SI method provides the most accurate comparison of model T values with field estimates. This is clear when applying this method to model assigned T values and the field estimated T values in DVRFS v. 2.0. These results are consistent with Belcher (2001) where the SI was used to calculate K values from aquifer test derived T in wells from the Death Valley region. Furthermore, this suggests that the screen interval thickness plays a crucial role in field estimated T values.

Appendix 1

This appendix contains Tables 4-6 which compare the TI T value to LS, SI, and CJA.

Table 4 -Transmissivity value from T-Input (TI) and Layer Summation (LS) Method with associated normalized difference and degrees of magnitude from model run. Log Value = Log_{10} of the dividend of T-Input and LS.; Bin Value = Grouping based on the magnitude difference between TI and LS. Test = Scenario run, see Figure 4.

Test	T-Input(m^2/day)	Layer Summation (m^2/day)	TI/LS	Log Value	Bin Value
Test 1	0.0010	11.1110	0.0001	-4.0458	5
Test 10	1.1000	11.1000	0.0991	-1.0039	3
Test 11	1.1100	11.1100	0.0999	-1.0004	3
Test 12	1.1110	11.1110	0.1000	-1.0000	3
Test 13	0.1100	11.1100	0.0099	-2.0043	4
Test 14	0.1110	11.1110	0.0100	-2.0004	4
Test 15	0.0110	11.1110	0.0010	-3.0044	5
Test 16	10.0000	10.0000	1.0000	0.0000	1
Test 17	1.0000	11.0000	0.0909	-1.0414	3
Test 18	0.1000	11.1000	0.0090	-2.0453	4
Test 19	0.0100	11.1100	0.0009	-3.0457	5
Test 2	0.0100	11.1100	0.0009	-3.0457	5
Test 20	0.0010	11.1110	0.0001	-4.0458	5
Test 21	11.0000	11.0000	1.0000	0.0000	1
Test 22	11.1000	11.1000	1.0000	0.0000	1
Test 23	11.1100	11.1100	1.0000	0.0000	1
Test 24	11.1110	11.1110	1.0000	0.0000	1
Test 25	1.1000	11.1000	0.0991	-1.0039	3
Test 26	1.1100	11.1100	0.0999	-1.0004	3
Test 27	1.1110	11.1110	0.1000	-1.0000	3
Test 28	0.1100	11.1100	0.0099	-2.0043	4
Test 29	0.1110	11.1110	0.0100	-2.0004	4
Test 3	0.1000	11.1000	0.0090	-2.0453	4
Test 30	0.0110	11.1110	0.0010	-3.0044	5
Test 4	1.0000	11.0000	0.0909	-1.0414	3
Test 5	10.0000	10.0000	1.0000	0.0000	1
Test 6	11.0000	11.0000	1.0000	0.0000	1
Test 7	11.1000	11.1000	1.0000	0.0000	1
Test 8	11.1100	11.1100	1.0000	0.0000	1
Test 9	11.1110	11.1110	1.0000	0.0000	1

Table 5 - Transmissivity value from T-Input (TI) and Screen Interval (SI) Method with associated normalized difference and degrees of magnitude from model run. Log Value = Log_{10} of the dividend of T-Input and SI.; Bin Value = Grouping based on the magnitude difference between TI and LS. Test = Scenario run, See Figure 4.

Test	TI Input (m^2/day)	SI (m^2/day)	TI/SI	Log Value	Bin Value
Test 14	0.1110	0.1110	1.0000	0.0000	1
Test 1	0.0010	0.0010	1.0000	0.0000	1
Test 2	0.0100	0.0100	1.0000	0.0000	1
Test 3	0.1000	0.1000	1.0000	0.0000	1
Test 4	1.0000	1.0000	1.0000	0.0000	1
Test 5	10.0000	10.0000	1.0000	0.0000	1
Test 6	11.0000	11.0000	1.0000	0.0000	1
Test 7	11.1000	11.1000	1.0000	0.0000	1
Test 8	11.1100	11.1100	1.0000	0.0000	1
Test 9	11.1110	11.1110	1.0000	0.0000	1
Test 10	1.1000	1.1000	1.0000	0.0000	1
Test 11	1.1100	1.1100	1.0000	0.0000	1
Test 12	1.1110	1.1110	1.0000	0.0000	1
Test 13	0.1100	0.1100	1.0000	0.0000	1
Test 15	0.0110	0.0110	1.0000	0.0000	1
Test 24	11.1110	6.1105	1.8183	0.2597	1
Test 23	11.1100	6.1050	1.8198	0.2600	1
Test 27	1.1110	0.6105	1.8198	0.2600	1
Test 22	11.1000	6.0500	1.8347	0.2636	1
Test 29	0.1110	0.0605	1.8347	0.2636	1
Test 26	1.1100	0.6050	1.8347	0.2636	1
Test 16	10.0000	5.0000	2.0000	0.3010	1
Test 17	1.0000	0.5000	2.0000	0.3010	1
Test 18	0.1000	0.0500	2.0000	0.3010	1
Test 19	0.0100	0.0050	2.0000	0.3010	1
Test 20	0.0010	0.0005	2.0000	0.3010	1
Test 21	11.0000	5.5000	2.0000	0.3010	1
Test 25	1.1000	0.5500	2.0000	0.3010	1
Test 28	0.1100	0.0550	2.0000	0.3010	1
Test 30	0.0110	0.0055	2.0000	0.3010	1

Table 6 - Transmissivity value from Cooper-Jacob Approximation (CJA) and T-Input (TI) with associated normalized difference and degrees of magnitude from model runs. Log Value = Log_{10} of the dividend of CJA and TI; Bin Value = Grouping based on the magnitude difference between CJA and TI. Test = Scenario run, see Figure 4.

Test	Cooper- Jacob Approximation (m^2/day)	T-Input (m^2/day)	CJA/TI	Log Value	Bin Value
Test 24	2.9323	11.1110	0.2639	-0.5785	2
Test 9	4.0726	11.1110	0.3665	-0.4359	1
Test 8	6.5452	11.1100	0.5891	-0.2298	1
Test 27	2.9323	1.1110	2.6393	0.4215	1
Test 23	30.5445	11.1100	2.7493	0.4392	1
Test 12	4.5817	1.1110	4.1239	0.6153	2
Test 11	20.3426	1.1100	18.3267	1.2631	3
Test 7	254.2828	11.1000	22.9084	1.3600	3
Test 22	335.3180	11.1000	30.2088	1.4801	3
Test 26	40.6853	1.1100	36.6534	1.5641	3
Test 14	5.0857	0.1110	45.8167	1.6610	3
Test 29	5.0857	0.1110	45.8167	1.6610	3
Test 21	833.0314	11.0000	75.7301	1.8793	3
Test 6	1832.6692	11.0000	166.6063	2.2217	4
Test 10	229.0836	1.1000	208.2579	2.3186	4
Test 13	43.6350	0.1100	396.6816	2.5984	4
Test 25	591.1836	1.1000	537.4396	2.7303	4
Test 30	7.3307	0.0110	666.4252	2.8238	4
Test 28	75.1094	0.1100	682.8127	2.8343	4
Test 15	7.6361	0.0110	694.1929	2.8415	4
Test 5	20362.9908	10.0000	2036.2991	3.3088	5
Test 16	45816.7292	10.0000	4581.6729	3.6610	5
Test 3	610.8897	0.1000	6108.8972	3.7860	5
Test 4	6108.8972	1.0000	6108.8972	3.7860	5
Test 2	73.3068	0.0100	7330.6767	3.8651	5
Test 17	9163.3458	1.0000	9163.3458	3.9621	5
Test 18	1309.0494	0.1000	13090.4941	4.1170	5
Test 19	166.6063	0.0100	16660.6288	4.2217	5
Test 20	17.4540	0.0010	17453.9921	4.2419	5
Test 1	19.2913	0.0010	19291.2544	4.2854	5

Appendix 2

This appendix contains Tables 7 and 8 which compare the CJA T value to LS and SI.

Table 7 - Transmissivity value from Cooper-Jacob Approximation (CJA) and Screen Interval (SI) with associated normalized difference and degrees of magnitude from model runs. Log Value = Log_{10} of the dividend of CJA and SI; Bin Value = Grouping based on the magnitude difference between CJA and SI. Test = Scenario run, See Figure 4

Test	CJA (m^2/day)	SI Method (m^2/day)	CJA/SI	Log Value	Bin Value
Test 9	4.0726	11.1110	0.3665	-0.4359	1
Test 24	2.9323	6.1105	0.4799	-0.3189	1
Test 8	6.5452	11.1100	0.5891	-0.2298	1
Test 12	4.5817	1.1110	4.1239	0.6153	2
Test 14	5.0857	1.1110	4.5775	0.6606	2
Test 27	2.9323	0.6105	4.8031	0.6815	2
Test 23	30.5445	6.1050	5.0032	0.6992	2
Test 11	20.3426	1.1100	18.3267	1.2631	3
Test 7	254.2828	11.1000	22.9084	1.3600	3
Test 22	335.3180	6.0500	55.4245	1.7437	3
Test 26	40.6853	0.6050	67.2484	1.8277	3
Test 29	5.0857	0.0605	84.0604	1.9246	3
Test 21	833.0314	5.5000	151.4603	2.1803	4
Test 6	1832.6692	11.0000	166.6063	2.2217	4
Test 10	229.0836	1.1000	208.2579	2.3186	4
Test 13	43.6350	0.1100	396.6816	2.5984	4
Test 15	7.6361	0.0110	694.1929	2.8415	4
Test 25	591.1836	0.5500	1074.8793	3.0314	5
Test 30	7.3307	0.0055	1332.8503	3.1248	5
Test 28	75.1094	0.0550	1365.6253	3.1353	5
Test 5	20362.9908	10.0000	2036.2991	3.3088	5
Test 3	610.8897	0.1000	6108.8972	3.7860	5
Test 4	6108.8972	1.0000	6108.8972	3.7860	5
Test 2	73.3068	0.0100	7330.6767	3.8651	5
Test 16	45816.7292	5.0000	9163.3458	3.9621	5
Test 17	9163.3458	0.5000	18326.6917	4.2631	5
Test 1	19.2913	0.0010	19291.2544	4.2854	5
Test 18	1309.0494	0.0500	26180.9881	4.4180	5
Test 19	166.6063	0.0050	33321.2576	4.5227	5
Test 20	17.4540	0.0005	34907.9842	4.5429	5

Table 8 - Transmissivity value from Cooper-Jacob Approximation (CJA) and Layer Summation (LS) with associated normalized difference and degrees of magnitude from model runs. Log Value = Log_{10} of the dividend of CJA and LS; Bin Value = Grouping based on the magnitude difference between CJA and LS. Test = Scenario run, See Figure 4

Test	CJA (m^2/day)	LS (m^2/day)	CJA/LS	Log Value	Bin Value
Test 24	2.9323	11.1110	0.2639	-0.5785	2
Test 27	2.9323	11.1110	0.2639	-0.5785	2
Test 9	4.0726	11.1110	0.3665	-0.4359	1
Test 12	4.5817	11.1110	0.4124	-0.3847	1
Test 14	5.0857	11.1110	0.4577	-0.3394	1
Test 29	5.0857	11.1110	0.4577	-0.3394	1
Test 8	6.5452	11.1100	0.5891	-0.2298	1
Test 30	7.3307	11.1110	0.6598	-0.1806	1
Test 15	7.6361	11.1110	0.6873	-0.1629	1
Test 20	17.4540	11.1110	1.5709	0.1961	1
Test 1	19.2913	11.1110	1.7362	0.2396	1
Test 11	20.3426	11.1100	1.8310	0.2627	1
Test 23	30.5445	11.1100	2.7493	0.4392	1
Test 26	40.6853	11.1100	3.6620	0.5637	2
Test 13	43.6350	11.1100	3.9275	0.5941	2
Test 2	73.3068	11.1100	6.5983	0.8194	2
Test 28	75.1094	11.1100	6.7605	0.8300	2
Test 19	166.6063	11.1100	14.9961	1.1760	3
Test 10	229.0836	11.1000	20.6382	1.3147	3
Test 7	254.2828	11.1000	22.9084	1.3600	3
Test 22	335.3180	11.1000	30.2088	1.4801	3
Test 25	591.1836	11.1000	53.2598	1.7264	3
Test 3	610.8897	11.1000	55.0351	1.7406	3
Test 21	833.0314	11.0000	75.7301	1.8793	3
Test 18	1309.0494	11.1000	117.9324	2.0716	4
Test 6	1832.6692	11.0000	166.6063	2.2217	4
Test 4	6108.8972	11.0000	555.3543	2.7446	4
Test 17	9163.3458	11.0000	833.0314	2.9207	4
Test 5	20362.9908	10.0000	2036.2991	3.3088	5
Test 16	45816.7292	10.0000	4581.6729	3.6610	5

Appendix 3

This appendix contains Tables 9-10 which compare the DVRFS 2.0 "field estimated" T values into LS and SI.

Table 9 - DVRFS 2.0 Transmissivity values from Cooper-Jacob Approximation and Screen Interval (SI) with associated normalized difference and degrees of magnitude from model runs. Log Value = Log_{10} of the dividend of CJA and SI; Bin Value = Grouping based on the magnitude difference between CJA and SI.

Well	Cooper-Jacob Approximation(m^2/day)	Screened Interval (m^2/day)	CJA/SI	Log Value	Bin Value
TOBS_ARMY1	484	52995	9.1.E-03	-2.0393895	4
TOBS_UE7NS	0.89	81.4	1.1.E-02	-1.9612131	3
TOBS_UE20E1	103	4321.39	2.4.E-02	-1.6227862	3
TOBS_U20A2WW	223.6	2,299.89	9.7.E-02	-1.0122353	3
TOBS_UE25P14	0.5	5.12	9.8.E-02	-1.0103424	3
TOBS_U3CN5	29.8	233.36	1.3.E-01	-0.893812	2
TOBSER2063	47	318.37	1.5.E-01	-0.8308343	2
TOBS_USWH3	1	3.57	2.8.E-01	-0.553033	2
TOBS_UE19I	17.4	56.02	3.1.E-01	-0.507788	1
TOBS_ER2062	150	430.9	3.5.E-01	-0.4582852	1
TOBS_TWA	151.5	346.63	4.4.E-01	-0.359456	1
TOBS_TW8	4.5	9.49	4.7.E-01	-0.3240354	1
TOBS_TW2	4.9	9.99	4.9.E-01	-0.3093346	1
TOBS_USWG2	9.4	18.49	5.1.E-01	-0.2938701	1
TOBS_AW	270	510.08	5.3.E-01	-0.2762754	1
TOBS_FSSW	330	617.88	5.3.E-01	-0.2723902	1
TOBS_U1535	0.71	1.25	5.7.E-01	-0.2466476	1
TOBS_ER2061	240	411.06	5.8.E-01	-0.233694	1
TOBS_UE25P13	1.5	2.53	5.9.E-01	-0.226514	1
TOBS_GNIT2	300	483.91	6.2.E-01	-0.2076451	1
TOBS_FL14	44	69.93	6.3.E-01	-0.2011922	1
TOBS_UE25C31	28	34.51	8.1.E-01	-0.0908468	1
TOBS_CLVFO1	340	405.41	8.4.E-01	-0.0764102	1
TOBS_USWWT10	1,400.00	1,637.07	8.6.E-01	-0.0679392	1
TOBS_4922DCC	300	317.46	9.5.E-01	-0.0245678	1
TOBS_W3WW	340	338.91	1.0E+00	0.00139453	1
TOBS_UE25C12	5.3	4.88	1.1E+00	0.03615695	1
TOBS_CLVFT1A	300	266.84	1.1E+00	0.05087358	1
TOBS_NCAPDR1	42	34.77	1.2E+00	0.0820446	1

Table 9 (cont'd) - DVRFS 2.0 Transmissivity values from Cooper-Jacob Approximation and Screen Interval (SI) with associated normalized difference and degrees of magnitude from model runs.

Well	Cooper- Jacob Approximation (m^2/day)	Screened Interval (m^2/day)	CJA/SI	Log Value	Bin Value
TOBS_UE25P12	24	19.81	1.2E+00	0.083322	1
TOBS_UE25P15	24	19.81	1.2E+00	0.083322	1
TOBS_DW	200	163.45	1.2E+00	0.087648	1
TOBS_UE20H	130	102.26	1.3E+00	0.104229	1
TOBS_UE18R	290	210.88	1.4E+00	0.138364	1
TOBS_AIP1	320	220.08	1.5E+00	0.162575	1
TOBS_USWH44	1.1	0.65	1.7E+00	0.228012	1
TOBS_TW3	47.2	21.56	2.2E+00	0.340283	1
TOBS_REVFT1	1,000.00	446.59	2.2E+00	0.350092	1
TOBS_UE25C13	4	1.64	2.4E+00	0.388526	1
TOBS_USWH61	10	3.06	3.3E+00	0.514421	2
TOBS_UE25P11	2	0.6	3.3E+00	0.520713	2
TOBS_WW3	16	4.52	3.5E+00	0.549222	2
TOBS_GNIO2]	1100	250.11	4.4E+00	0.643267	2
TOBS_UE19D	248	56.3	4.4E+00	0.643937	2
TOBS_UE25C21	170	35.56	4.8E+00	0.679521	2
TOBS_TW4	136.62	24.61	5.6E+00	0.744403	2
TOBS_UE25C32	45	7.74	5.8E+00	0.764438	2
TOBS_UE19C	149	23.04	6.5E+00	0.810745	2
TOBS_ATSTH1	12000	1470.6	8.2E+00	0.911687	2
TOBS_UE19FS	137	16.27	8.4E+00	0.9254	2
TOBS_W1WW	2.7	0.3	9.0E+00	0.955983	2
TOBS_ATSTH3	13,600.00	1,370.28	9.9E+00	0.99673	2
TOBS_NC9SX	680	67.35	1.0E+01	1.004152	3
TOBS_USWH65	480	46.15	1.0E+01	1.01706	3
TOBS_UE25C11	270	24.79	1.1E+01	1.037086	3
TOBS_USWH46	19	1.73	1.1E+01	1.040959	3
TOB_NCEWDP1S	1000	90.57	1.1E+01	1.042996	3
TOB_USWH411	200	16.87	1.2E+01	1.073915	3
TOBS_UE20D	546.5	44.53	1.2E+01	1.088916	3
TOBS_TW1	43.5	3.24	1.3E+01	1.128186	3
TOBS_USWH43	6.9	0.51	1.4E+01	1.134613	3
TOBS_USWH62	30	2.13	1.4E+01	1.14915	3
TOBS_UE25C14	360	24.88	1.4E+01	1.160526	3

Table 9 (cont'd) - DVRFS 2.0 Transmissivity values from Cooper-Jacob Approximation and Screen Interval (SI) with associated normalized difference and degrees of magnitude from model runs.

Well	Cooper-Jacob Approximation (m^2/day)	Screened Interval (m^2/day)	CJA/SI	Log Value	Bin Value
TOB_UE25C12	90	6.06	1.5E+01	1.171902	3
TOBS_UE25C25	100	5.92	1.7E+01	1.227788	3
TOBS_UE20J	733	43.35	1.7E+01	1.228078	3
TOBS_UE19GS	373	20.39	1.8E+01	1.26233	3
TOBS_UE25C34	30	1.63	1.8E+01	1.264516	3
TOBS_USWH41	12	0.57	2.1E+01	1.326096	3
TOBS_PM3	6.5	0.29	2.2E+01	1.345675	3
TOB_UE25C14	30	1.35	2.2E+01	1.346141	3
TOBS_UE25C24	40	1.75	2.3E+01	1.359705	3
TOBS_TW10	248.4	10.63	2.3E+01	1.368819	3
TOBS_UE19B1	696	25.35	2.7E+01	1.438568	3
TOBS_USWH45	56	1.73	3.2E+01	1.510393	3
TOB_USWH410	1.4	0.04	3.6E+01	1.553951	3
TOBS_ATSSH1	13600	376.2	3.6E+01	1.55812	3
TOB_UE25WT12	5.8	0.13	4.4E+01	1.638761	3
TOB_USWH413	660	14.96	4.4E+01	1.644715	3
TOBS_UE25P16	2	0.04	4.5E+01	1.655608	3
TOBS_UE25C17	1600	34.25	4.7E+01	1.669452	3
TOBS_USWH42	19	0.39	4.9E+01	1.692617	3
TOBS_UE25C18	1800	34.25	5.3E+01	1.720605	3
TOBS_KLON2	110	2.08	5.3E+01	1.722599	3
TOBS_USWH1	150	2.8	5.4E+01	1.729616	3
TOBS_UE25C23	2,100.00	35.28	6.0E+01	1.774706	3
TOBS_USWH4	23.3	0.34	6.8E+01	1.83333	3
TOB_USWG4	622	9	6.9E+01	1.839366	3
TOBS_WW5C	32	0.41	7.7E+01	1.887186	3
TOBS_USWH5	36	0.44	8.2E+01	1.91592	3
TOBS_UE25C33	3200	34.99	9.1E+01	1.961167	3
TOBS_WW5A	30	0.29	1.0E+02	2.010031	4
TOBS_SM10	57	0.52	1.1E+02	2.03799	4
TOBS_UE19E	104	0.91	1.1E+02	2.055713	4
TOBS_UE19H	1740	15.18	1.1E+02	2.059305	4

Table 9 (cont'd) - DVRFS 2.0 Transmissivity values from Cooper-Jacob Approximation and Screen Interval (SI) with associated normalized difference and degrees of magnitude from model runs.

Well	Cooper-Jacob Approximation (m^2/day)	Screened Interval (m^2/day)	CJA/SI	Log Value	Bin Value
TOBS_KLON1	275	2.06	1.3E+02	2.126204	4
TOBS_UE25C22	381	2.25	1.7E+02	2.227904	4
TOBS_UE25C26	1,300.00	6.22	2.1E+02	2.319846	4
TOB_USWH412	3200	14.96	2.1E+02	2.330321	4
TOBS_UE25C19	1,600.00	6.45	2.5E+02	2.394527	4
TOB_UE25C13	1800	6.45	2.8E+02	2.445679	4
TOBS_USWH63	290	1	2.9E+02	2.463485	4
TOBS_WW5B	90	0.29	3.1E+02	2.487821	4
TOBS_UE25A1	344	1.03	3.3E+02	2.523405	4
TOBS_USWH47	9.1	0.03	3.3E+02	2.524472	4
TOB_UE25WT14	1,300.00	3.78	3.4E+02	2.536543	4
TOB_NCEWDP3D	230	0.54	4.2E+02	2.625451	4
TOBS_UE25P17	110	0.23	4.8E+02	2.682316	4
TOBS_UE25C15	780	1.42	5.5E+02	2.738859	4
TOBS_SM3	810	1.06	7.7E+02	2.883795	4
TOBS_ER121	35	0.04	9.0E+02	2.953003	4
TOBS_USWH49	13	0.01	9.0E+02	2.954076	4
TOBS_SM5	560	0.5	1.1E+03	3.052619	5
TOBS_USWH48	42	0.04	1.2E+03	3.070581	5
TOBS_USWH64	150	0.07	2.2E+03	3.338187	5
TOBS_UE25ONC	970	0.39	2.5E+03	3.39524	5
TOBS_FCTW	6000	2.06	2.9E+03	3.465023	5
TOBS_SM4	1,800.00	0.55	3.3E+03	3.515092	5
TOBS_SM13	1700	0.46	3.7E+03	3.565972	5
TOBS_SM1	1,300.00	0.33	3.9E+03	3.595256	5
TOBS_SM2	1300	0.33	3.9E+03	3.595849	5
TOBS_18S5107	2,500.00	0.33	7.5E+03	3.875707	5
TOBS_UE25C16	730	0.09	7.9E+03	3.894887	5
TOB_UE25C11	800	0.06	1.3E+04	4.122413	5
TO_NCEWDP9SX	1020	0.05	1.9E+04	4.281914	5
TOBS_UE25WT3	2,600.00	0.04	6.4E+04	4.807674	5

Table 10 - DVRFS 2.0 Transmissivity values from Cooper-Jacob Approximation and Layer Summation (LS) with associated normalized difference and degrees of magnitude from model runs. Log Value = Log_{10} of the dividend of CJA and LS; Bin Value = Grouping based on the magnitude difference between CJA and LS.

Well	Cooper-Jacob Approximation (m^2/day)	Layer Summation (m^2/day)	CJA/LS	Log Value	Bin Value
TOBS_UE7NS	0.89	13307.85719	6.69E-05	-4.174718125	5
TOBS_TW8	4.5	26087.15348	1.72E-04	-3.76321418	5
TOBS_WW5A	30	63781.82429	4.70E-04	-3.327575682	5
TOBS_WW5C	32	58418.2325	5.48E-04	-3.261398435	5
TOBS_UE19I	17.4	21311.94708	8.16E-04	-3.088073881	5
TOBS_UE25P14	0.5	401.0891406	1.25E-03	-2.904270899	4
TOBS_SM10	57	36536.09093	1.56E-03	-2.806847224	4
TOBS_PM3	6.5	3849.527828	1.69E-03	-2.772494107	4
TOBS_U3CN5	29.8	14866.94245	2.00E-03	-2.698005396	4
TOBS_WW5B	90	40092.97702	2.24E-03	-2.648825796	4
TOBS_ARMY1	484	188422.5522	2.57E-03	-2.59028752	4
TOB_UE25WT12	5.8	1706.253872	3.40E-03	-2.468615656	4
TOBS_UE25P13	1.5	401.0891406	3.74E-03	-2.427149645	4
TOBS_UE25P16	2	401.0891406	4.99E-03	-2.302210908	4
TOBS_UE25P11	2	401.0891406	4.99E-03	-2.302210908	4
TOBS_UE19FS	137	23947.33038	5.72E-03	-2.242536539	4
TOBS_USWH3	1	167.0772279	5.99E-03	-2.222917261	4
TOBS_FSSW	330	54877.55047	6.01E-03	-2.220880778	4
TOBSER2063	47	6956.027338	6.76E-03	-2.170263422	4
TOBS_USWH44	1	121.8351398	8.21E-03	-2.085772566	4
TOB_USWH410	1	121.8351398	8.21E-03	-2.085772566	4
TOBS_UE19D	248	26586.73209	9.33E-03	-2.030213279	4
TOBS_TWA	151.5	15952.06956	9.50E-03	-2.022404402	4
TOBS_UE19E	104	10598.3708	9.81E-03	-2.008205771	4
TOBS_SM5	560	50719.32632	1.10E-02	-1.956985449	3
TOBS_NCAPDR1	42	3254.691066	1.29E-02	-1.889260481	3
TOBS_USWH61	10	648.4036067	1.54E-02	-1.811845422	3
TOBS_TW2	4.9	314.5179872	1.56E-02	-1.807449408	3
TOBS_SM3	810	46810.251	1.73E-02	-1.761855951	3
TOBS_UE25C13	4	196.5249248	2.04E-02	-1.691357647	3
TOBS_ER2062	150	6956.027338	2.16E-02	-1.666270021	3
TOBS_UE25C12	5.3	196.5249248	2.70E-02	-1.569141769	3
TOBS_SM2	1300	46810.251	2.78E-02	-1.556397618	3
TOBS_W1WW	2.7	94.84554055	2.85E-02	-1.545653152	3
TOBS_U1535	0.71	24.66056943	2.88E-02	-1.540744752	3
TOBS_UE19GS	373	12468.61414	2.99E-02	-1.524109353	3
TOBS_SM1	1300	38541.8609	3.37E-02	-1.471989327	3
TOBS_ER2061	240	6956.027338	3.45E-02	-1.462150038	3

Table 10 (cont'd) - DVRFS 2.0 Transmissivity values from Cooper-Jacob Approximation and Layer Summation (LS).

Well	Cooper-Jacob Approximation (m^2/day)	Layer Summation (m^2/day)	CJA/LS	Log Value	Bin Value
TOBS_UE20D	546.5	15418.25418	3.54E-02	-1.450445035	3
TOBS_SM4	1800	46810.251	3.85E-02	-1.415068465	3
TOBS_SM13	1700	38541.8609	4.41E-02	-1.355483758	3
TOBS_USWH62	30	648.4036067	4.63E-02	-1.334724167	3
TOBS_WW3	16	317.8466794	5.03E-02	-1.298097696	3
TOBS_18S5107	2500	46810.251	5.34E-02	-1.272400961	3
TOBS_USWH43	7	121.8351398	5.75E-02	-1.240674526	3
TOBS_UE25P12	24	401.0891406	5.98E-02	-1.223029662	3
TOBS_UE25P15	24	401.0891406	5.98E-02	-1.223029662	3
TOBS_USWH47	9	121.8351398	7.39E-02	-1.131530057	3
TOB_NCEWDP3D	230	2434.05057	9.45E-02	-1.024601761	3
TOBS_NC9SX	680	6918.814039	9.83E-02	-1.007522745	3
TOBS_USWH41	12	121.8351398	9.85E-02	-1.00659132	3
TOBS_USWH49	13	121.8351398	1.07E-01	-0.971829214	2
TOB_NCEWDP1S	1000	8021.615163	1.25E-01	-0.904261823	2
TOBS_UE20E1	103	817.1464257	1.26E-01	-0.899462661	2
TOBS_DW	200	1525.714681	1.31E-01	-0.882443329	2
TOBS_UE25C31	28	196.5249248	1.42E-01	-0.846259607	2
TO_NCEWDP9SX	1020	6918.814039	1.47E-01	-0.831431486	2
TOB_UE25C14	30	196.5249248	1.53E-01	-0.816296384	2
TOBS_UE25C34	30	196.5249248	1.53E-01	-0.816296384	2
TOBS_USWH42	19	121.8351398	1.56E-01	-0.807018965	2
TOBS_USWH46	19	121.8351398	1.56E-01	-0.807018965	2
TOBS_AW	270	1525.714681	1.77E-01	-0.752109561	2
TOBS_UE19H	1740	9649.334829	1.80E-01	-0.743948128	2
TOBS_USWH4	23	121.8351398	1.89E-01	-0.72404473	2
TOBS_UE25C24	40	196.5249248	2.04E-01	-0.691357647	2
TOBS_USWWT10	1400	6213.563368	2.25E-01	-0.647212696	2
TOBS_UE25C32	45	196.5249248	2.29E-01	-0.640205125	2
TOBS_USWH64	150	648.4036067	2.31E-01	-0.635754163	2
TOBS_FL14	44	180.1644084	2.44E-01	-0.612216324	2
TOBS_UE25P17	110	401.0891406	2.74E-01	-0.561848219	2
TOBS_U20A2WW	223.6	690.0853957	3.24E-01	-0.489431037	1
TOBS_USWH48	42	121.8351398	3.45E-01	-0.462523276	1
TOBS_4922DCC	300	768.5397106	3.90E-01	-0.408545058	1
TOBS_USWH63	290	648.4036067	4.47E-01	-0.349447424	1
TOB_UE25C12	90	196.5249248	4.58E-01	-0.339175129	1
TOBS_USWH45	56	121.8351398	4.60E-01	-0.337584539	1
TOBS_UE20H	130	280.0095709	4.64E-01	-0.333229524	1
TOBS_UE25C25	100	196.5249248	5.09E-01	-0.293417639	1
TOBS_USWH1	150	270.0066485	5.56E-01	-0.255283199	1

Table 10 (cont'd) - DVRFS 2.0 Transmissivity values from Cooper-Jacob Approximation and Layer Summation (LS).

Well	Cooper-Jacob Approximation (m^2/day)	Layer Summation (m^2/day)	CJA/LS	Log Value	Bin Value
TOBS_USWH5	36	64.23891052	5.60E-01	-0.251495666	1
TOBS_UE18R	290	481.0871392	6.03E-01	-0.219825749	1
TOBS_USWG2	9.4	13.0232919	7.22E-01	-0.141592921	1
TOBS_USWH65	480	648.4036067	7.40E-01	-0.130604185	1
TOBS_UE25C21	170	196.5249248	8.65E-01	-0.062968717	1
TOB_UE25WT14	1300	1416.701918	9.18E-01	-0.03733513	1
TOBS_TW1	43.5	38.72559112	1.12E+00	0.050491201	1
TOBS_ER121	35	29.14886693	1.20E+00	0.079446367	1
TOBS_ATSTH1	12000	9634.603276	1.25E+00	0.09534741	1
TOBS_UE25C11	270	196.5249248	1.37E+00	0.137946125	1
TOBS_ATSTH3	13600	9634.603276	1.41E+00	0.149705072	1
TOBS_ATSSH1	13600	9634.603276	1.41E+00	0.149705072	1
TOBS_UE25WT3	2600	1594.923852	1.63E+00	0.212233395	1
TOB_USWH411	200	121.8351398	1.64E+00	0.21525743	1
TOBS_UE25C14	360	196.5249248	1.83E+00	0.262884862	1
TOBS_UE25C22	381	196.5249248	1.94E+00	0.287507337	1
TOBS_W3WW	340	133.4569982	2.55E+00	0.406137565	1
TOBS_UE25C16	730	196.5249248	3.71E+00	0.569905221	2
TOBS_UE25ONC	970	249.7475076	3.88E+00	0.589270571	2
TOBS_UE25C15	780	196.5249248	3.97E+00	0.598676964	2
TOB_UE25C11	800	196.5249248	4.07E+00	0.609672348	2
TOB_USWG4	622	117.2279647	5.31E+00	0.72475916	2
TOB_USWH413	660	121.8351398	5.42E+00	0.73377137	2
TOBS_UE25C26	1300	196.5249248	6.61E+00	0.820525714	2
TOBS_TW3	47.2	7.111452243	6.64E+00	0.821983701	2
TOBS_UE25C17	1600	196.5249248	8.14E+00	0.910702344	2
TOBS_UE25C19	1600	196.5249248	8.14E+00	0.910702344	2
TOBS_UE25C18	1800	196.5249248	9.16E+00	0.961854866	2
TOB_UE25C13	1800	196.5249248	9.16E+00	0.961854866	2
TOBS_UE25A1	344	35.87121672	9.59E+00	0.981812335	2
TOBS_UE20J	733	74.16640345	9.88E+00	0.994896755	2
TOBS_UE25C23	2100	196.5249248	1.07E+01	1.028801656	3
TOBS_UE19C	149	11.39317325	1.31E+01	1.116541567	3
TOBS_UE25C33	3200	196.5249248	1.63E+01	1.21173234	3
TOBS_TW10	248.4	12.0048395	2.07E+01	1.315795234	3
TOBS_TW4	136.62	6.316147743	2.16E+01	1.335062001	3
TOB_USWH412	3200	121.8351398	2.63E+01	1.419377412	3
TOBS_FCTW	6000	88.78124906	6.76E+01	1.82983	3
TOBS_UE19B1	696	9.979005359	6.97E+01	1.843521984	3

Appendix 4

These are the drawdown graphs of the various tests run in the simple five-layer model. The y-axis represents the drawdown in meters, and the x-axis is the time in days. The model was run for a total of 31 days (broken down into 62 "steps") with a discharge (Q) of 100 m^3/day. The test numbers on top of each graph is a pumping scenario illustrated in Figure 4.

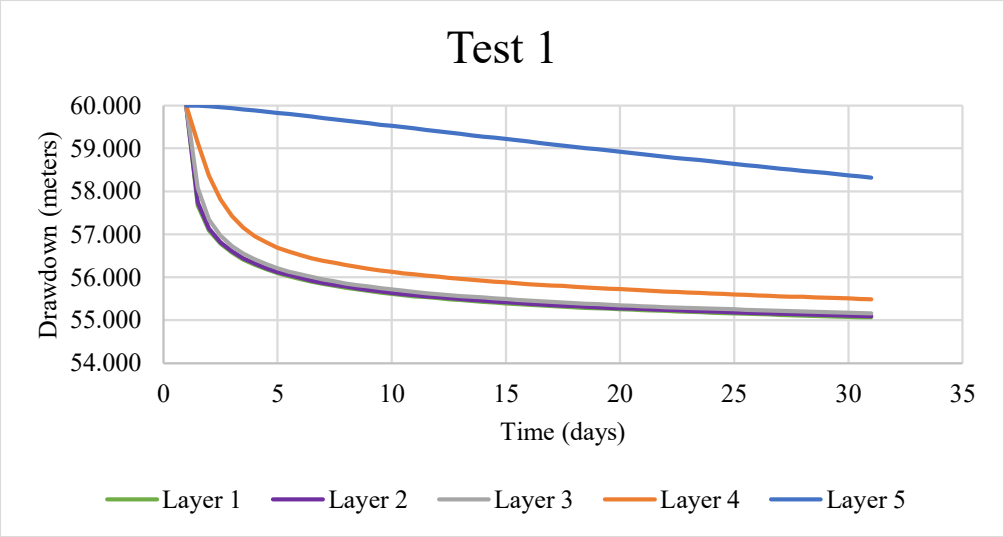

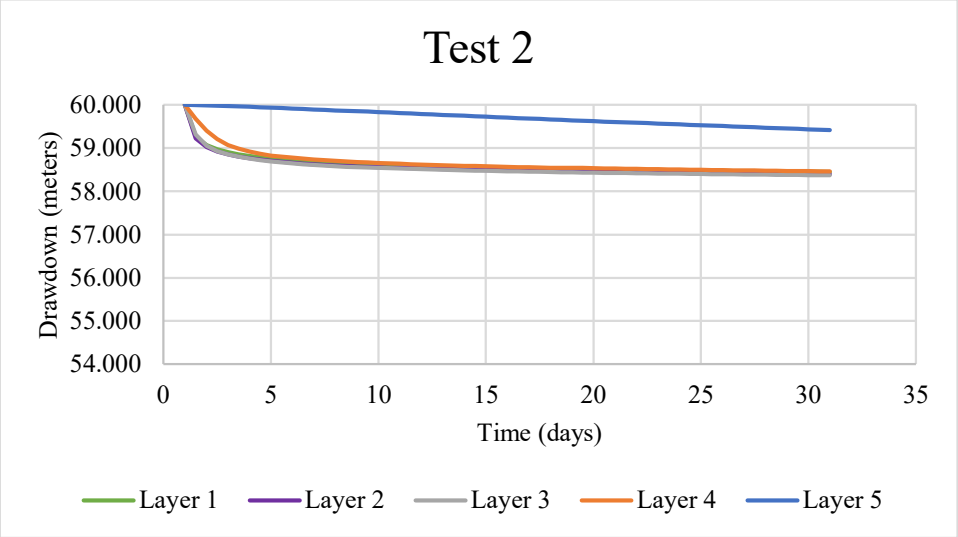
Test 2
60.000
59.000
58.000
57.000
56.000
55.000
54.000
Drawdown (meters)
0
5
10
15
20
25
30
35
Time (days)
Layer 1
Layer 2
Layer 3
Layer 4
Layer 5

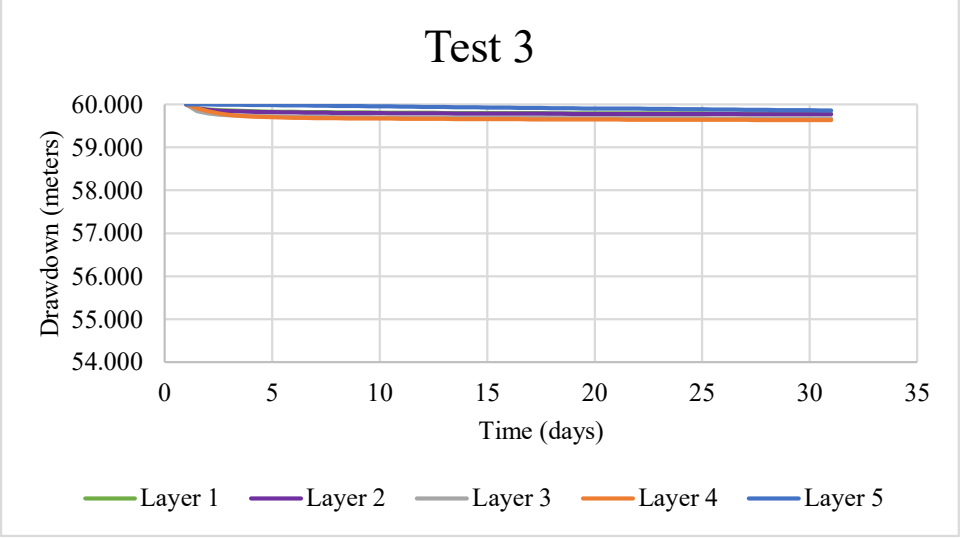
Test 3
60.000
59.000
58.000
57.000
56.000
55.000
54.000
Drawdown (meters)
0
5
10
15
20
25
30
35
Time (days)
Layer 1
Layer 2
Layer 3
Layer 4
Layer 5

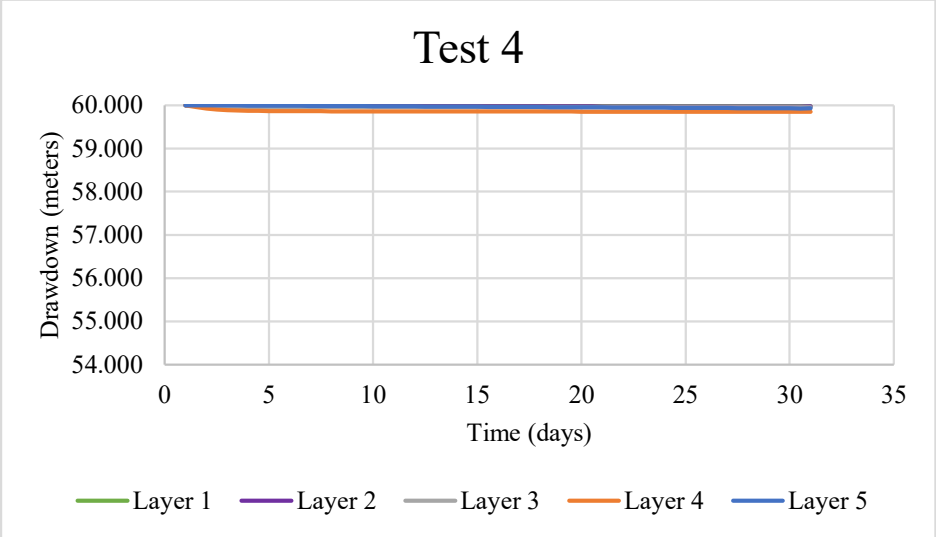
Test 4
60.000
59.000
58.000
57.000
56.000
55.000
54.000
Drawdown (meters)
0
5
10
15
20
25
30
35
Time (days)
Layer 1
Layer 2
Layer 3
Layer 4
Layer 5

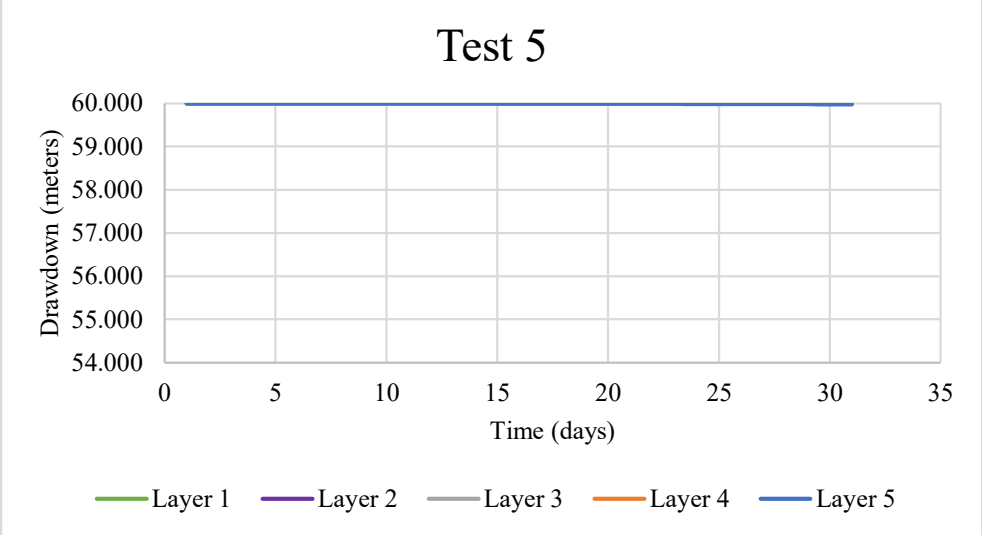
Test 5
60.000
59.000
58.000
57.000
56.000
55.000
54.000
Drawdown (meters)
0
5
10
15
20
25
30
35
Time (days)
Layer 1
Layer 2
Layer 3
Layer 4
Layer 5

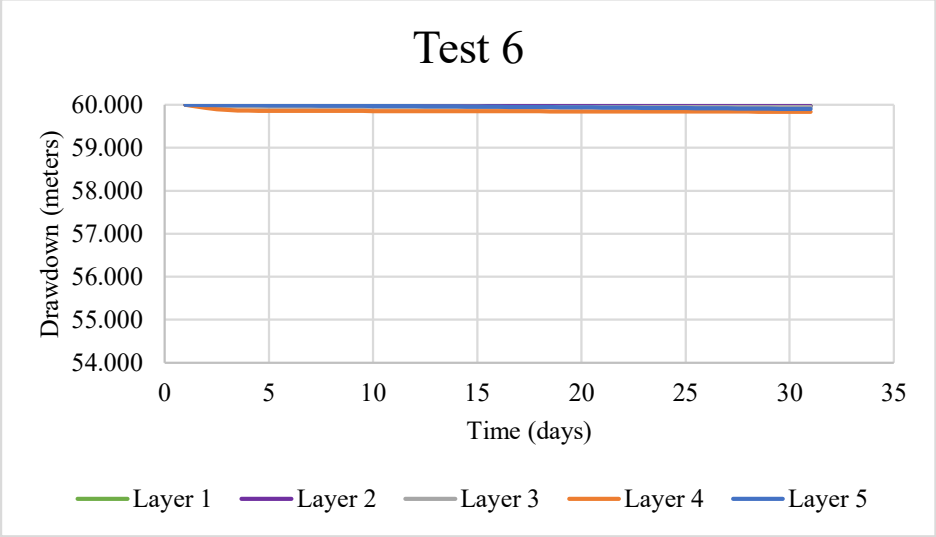
Test 6
60.000
59.000
58.000
57.000
56.000
55.000
54.000
Drawdown (meters)
0
5
10
15
20
25
30
35
Time (days)
Layer 1
Layer 2
Layer 3
Layer 4
Layer 5

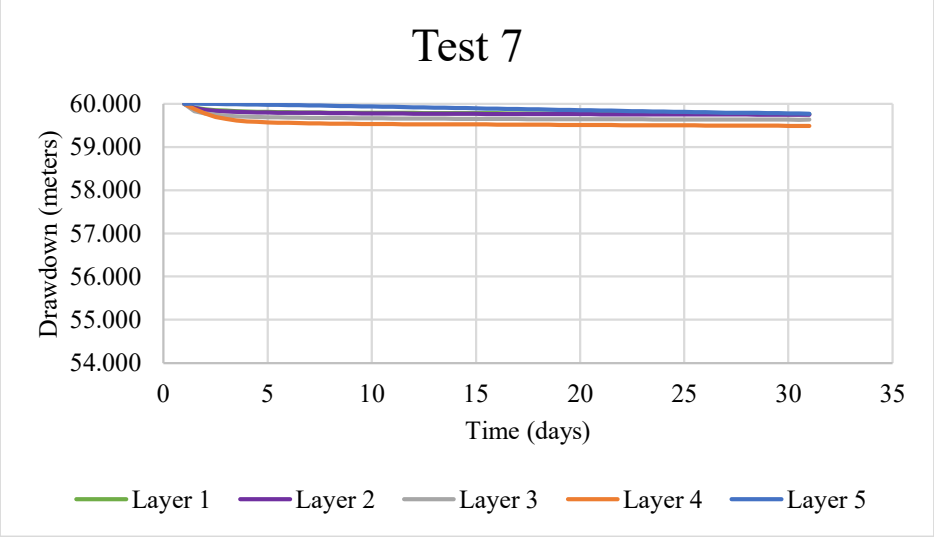
Test 7
60.000
59.000
58.000
57.000
56.000
55.000
54.000
Drawdown (meters)
0
5
10
15
20
25
30
35
Time (days)
Layer 1
Layer 2
Layer 3
Layer 4
Layer 5

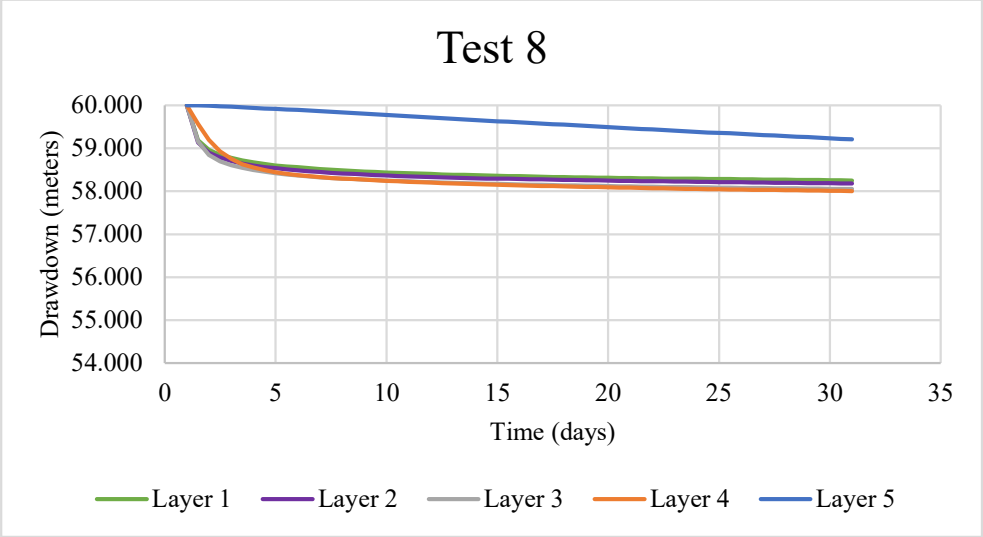
Test 8
60.000
59.000
58.000
57.000
56.000
55.000
54.000
Drawdown (meters)
0
5
10
15
20
25
30
35
Time (days)
Layer 1
Layer 2
Layer 3
Layer 4
Layer 5

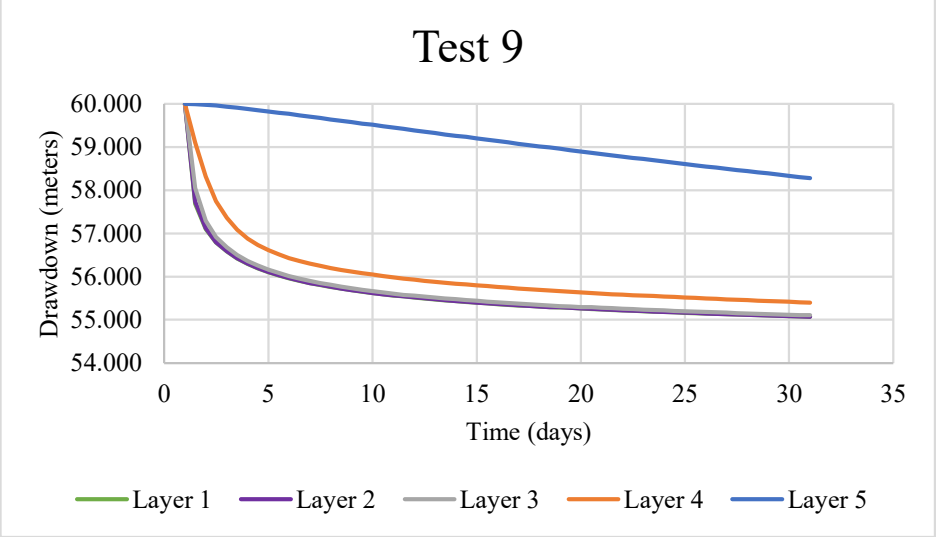
Test 9
60.000
59.000
58.000
57.000
56.000
55.000
54.000
Drawdown (meters)
0
5
10
15
20
25
30
35
Time (days)
Layer 1
Layer 2
Layer 3
Layer 4
Layer 5

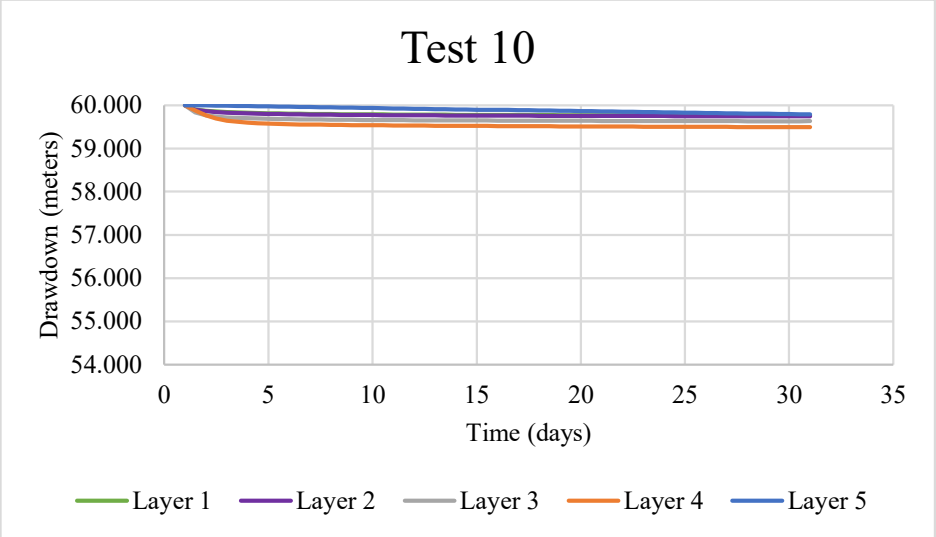
Test 10
60.000
59.000
58.000
57.000
56.000
55.000
54.000
Drawdown (meters)
0
5
10
15
20
25
30
35
Time (days)
Layer 1
Layer 2
Layer 3
Layer 4
Layer 5

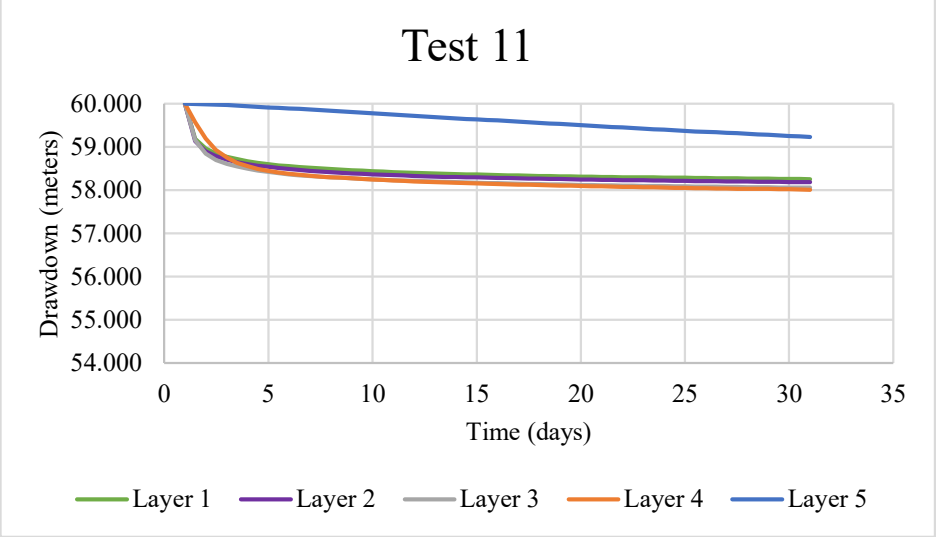
Test 11
60.000
59.000
58.000
57.000
56.000
55.000
54.000
Drawdown (meters)
0
5
10
15
20
25
30
35
Time (days)
Layer 1
Layer 2
Layer 3
Layer 4
Layer 5

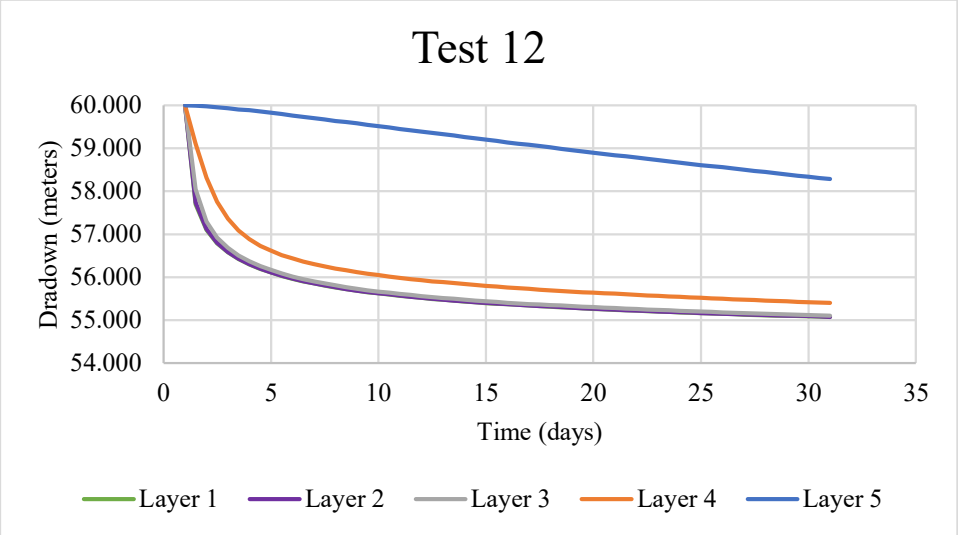
Test 12
60.000
59.000
58.000
57.000
56.000
55.000
54.000
Dradown (meters)
0
5
10
15
20
25
30
35
Time (days)
Layer 1
Layer 2
Layer 3
Layer 4
Layer 5

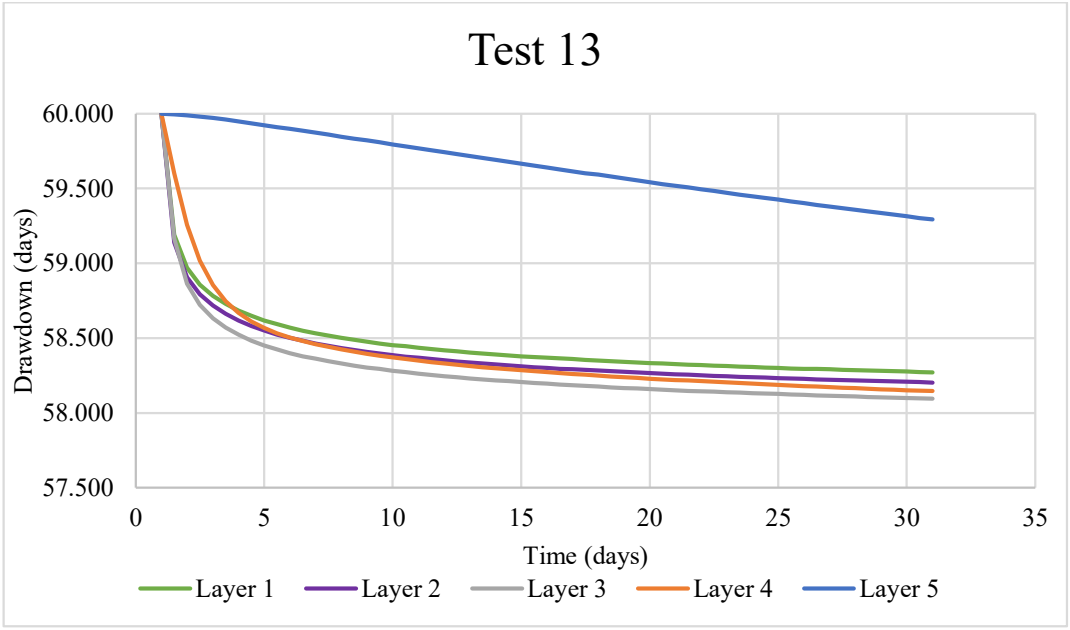
Test 13
60.000
59.500
59.000
58.500
58.000
57.500
Drawdown (days)
0
5
10
15
20
25
30
35
Time (days)
Layer 1
Layer 2
Layer 3
Layer 4
Layer 5

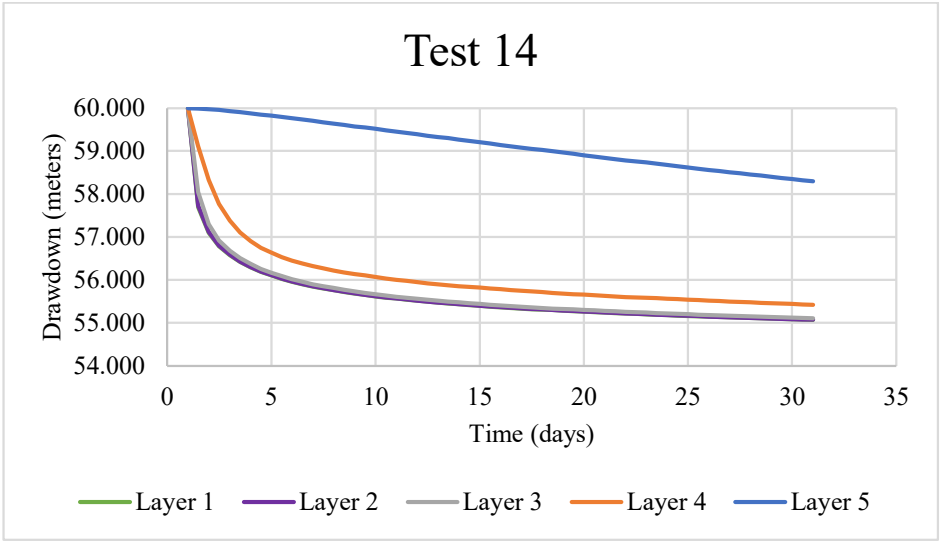
Test 14
60.000
59.000
58.000
57.000
56.000
55.000
54.000
Drawdown (meters)
0
5
10
15
20
25
30
35
Time (days)
Layer 1
Layer 2
Layer 3
Layer 4
Layer 5

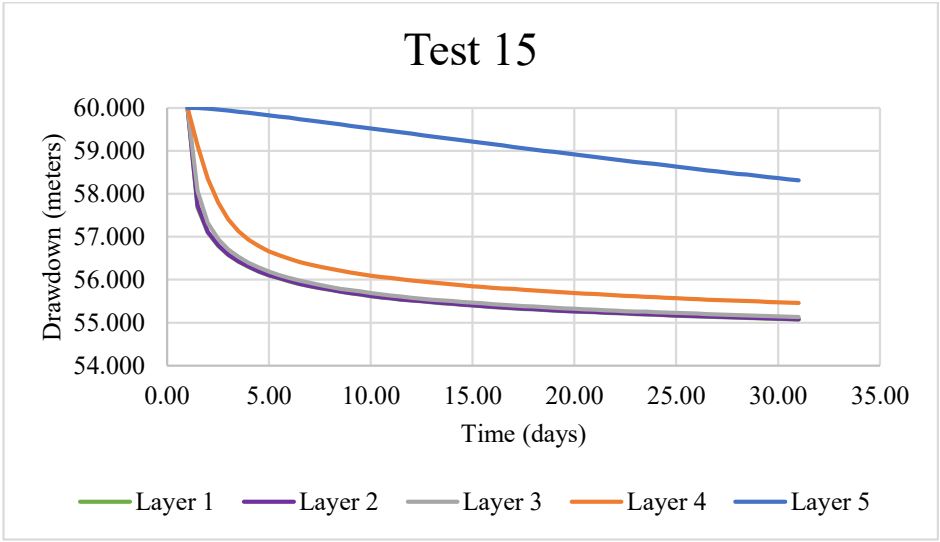
Test 15
60.000
59.000
58.000
57.000
56.000
55.000
54.000
Drawdown (meters)
0.00
5.00
10.00
15.00
20.00
25.00
30.00
35.00
Time (days)
Layer 1
Layer 2
Layer 3
Layer 4
Layer 5

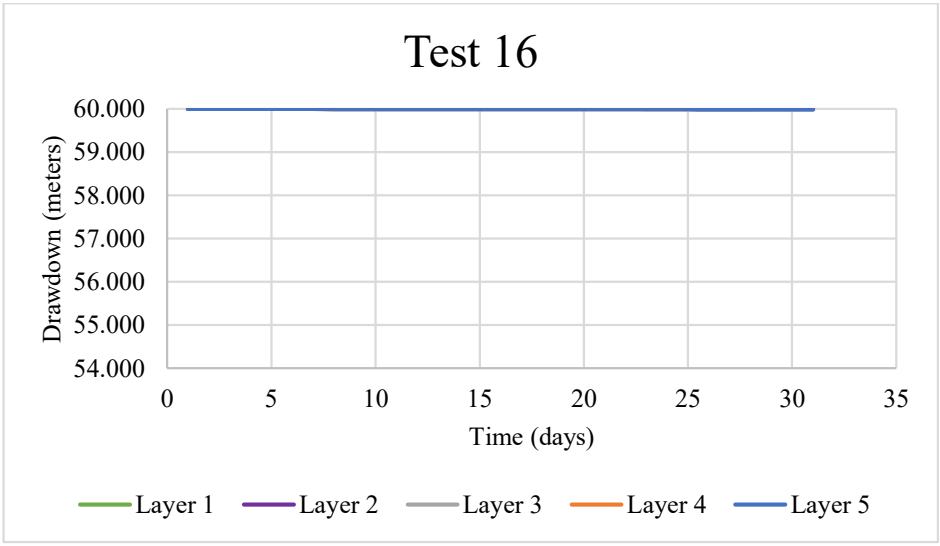
Test 16
60.000
59.000
58.000
57.000
56.000
55.000
54.000
Drawdown (meters)
0
5
10
15
20
25
30
35
Time (days)
Layer 1
Layer 2
Layer 3
Layer 4
Layer 5

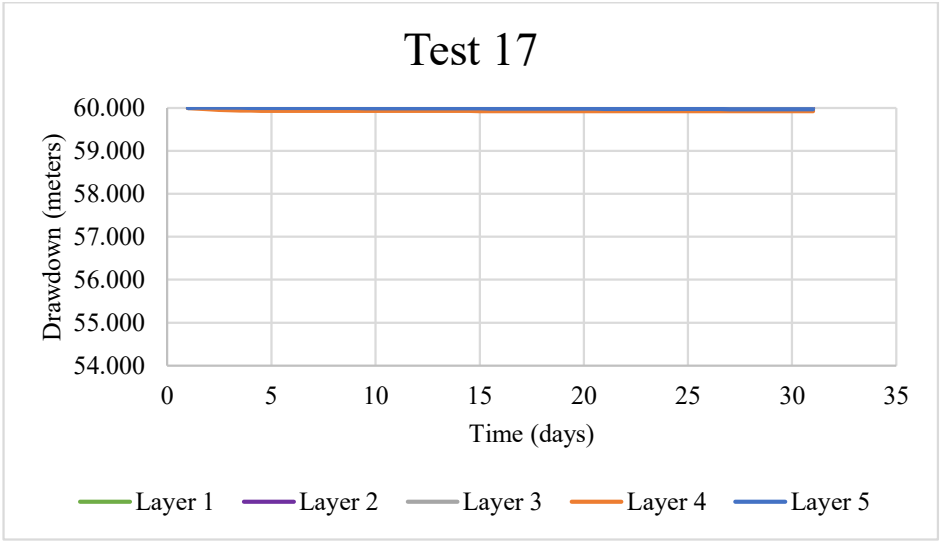
Test 17
60.000
59.000
58.000
57.000
56.000
55.000
54.000
Drawdown (meters)
0
5
10
15
20
25
30
35
Time (days)
Layer 1
Layer 2
Layer 3
Layer 4
Layer 5

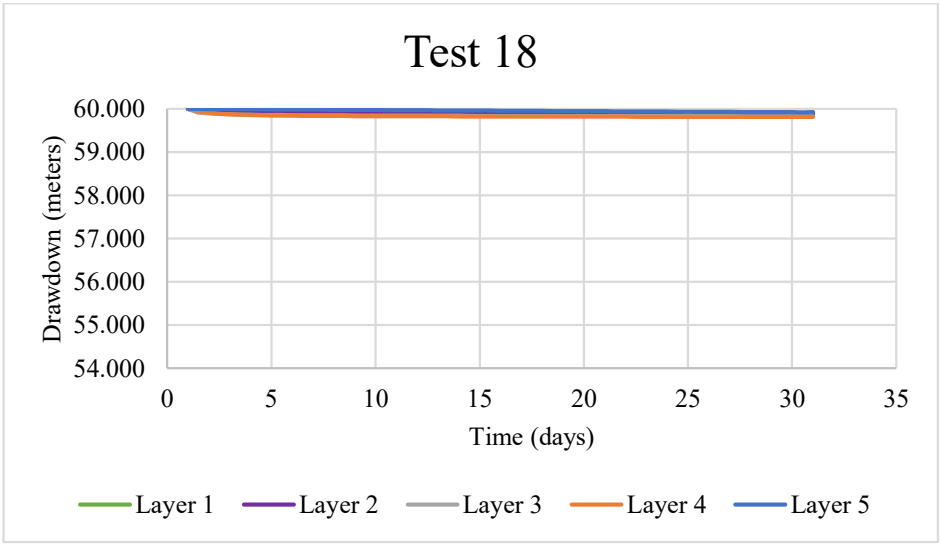
Test 18
60.000
59.000
58.000
57.000
56.000
55.000
54.000
Drawdown (meters)
0
5
10
15
20
25
30
35
Time (days)
Layer 1
Layer 2
Layer 3
Layer 4
Layer 5

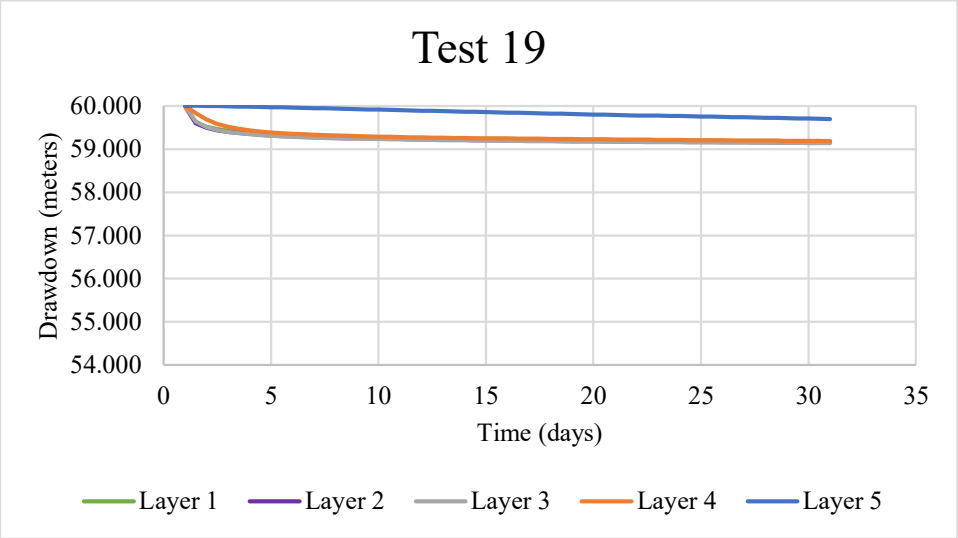
Test 19
60.000
59.000
58.000
57.000
56.000
55.000
54.000
Drawdown (meters)
0
5
10
15
20
25
30
35
Time (days)
Layer 1
Layer 2
Layer 3
Layer 4
Layer 5

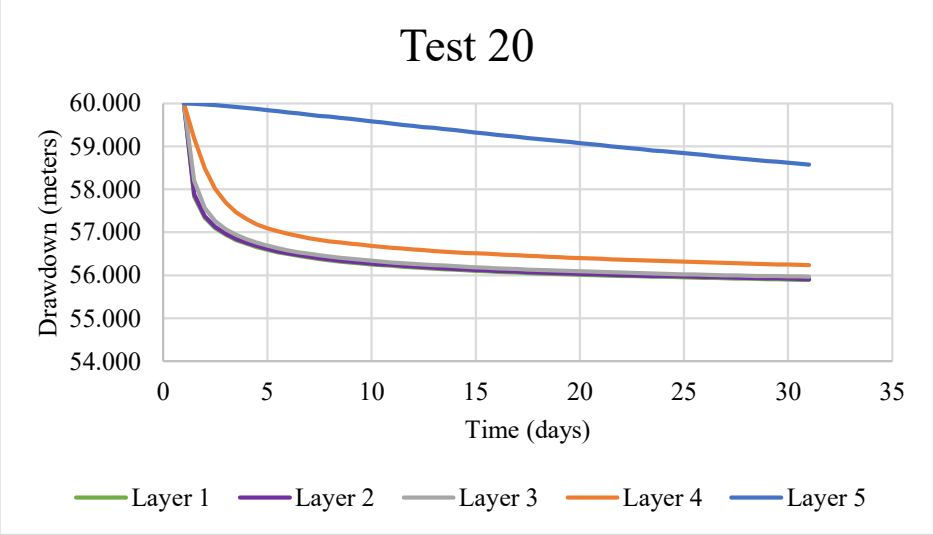
Test 20
60.000
59.000
58.000
57.000
56.000
55.000
54.000
Drawdown (meters)
0
5
10
15
20
25
30
35
Time (days)
Layer 1
Layer 2
Layer 3
Layer 4
Layer 5

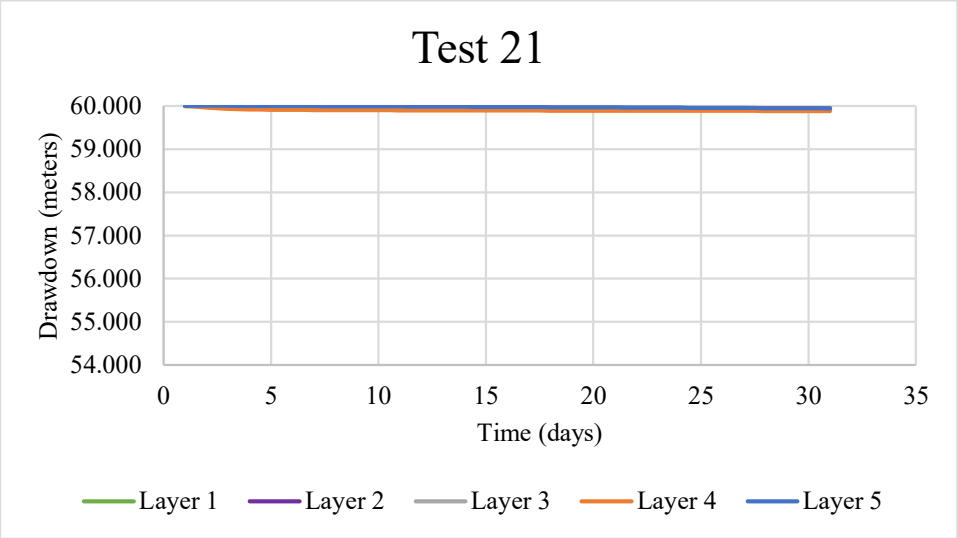
Test 21
60.000
59.000
58.000
57.000
56.000
55.000
54.000
Drawdown (meters)
0
5
10
15
20
25
30
35
Time (days)
Layer 1
Layer 2
Layer 3
Layer 4
Layer 5

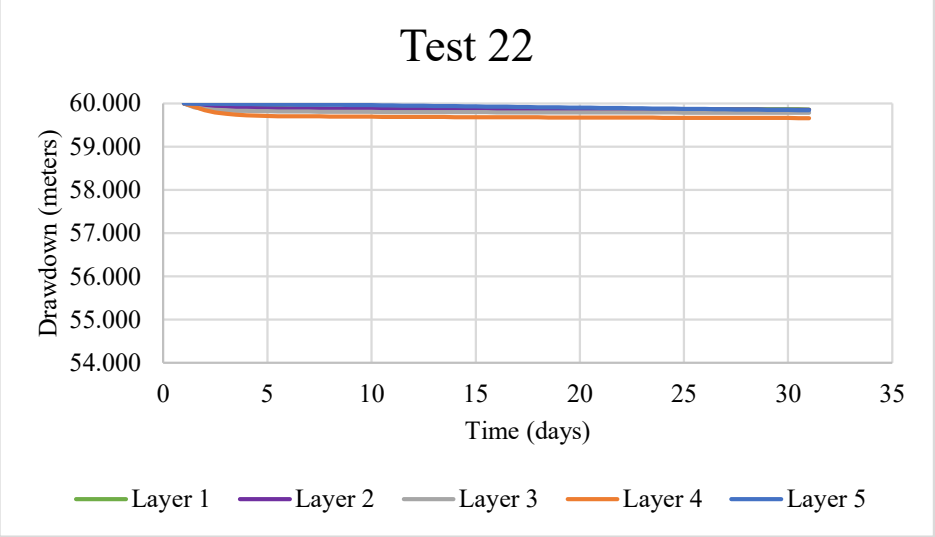
Test 22
60.000
59.000
58.000
57.000
56.000
55.000
54.000
Drawdown (meters)
0
5
10
15
20
25
30
35
Time (days)
Layer 1
Layer 2
Layer 3
Layer 4
Layer 5

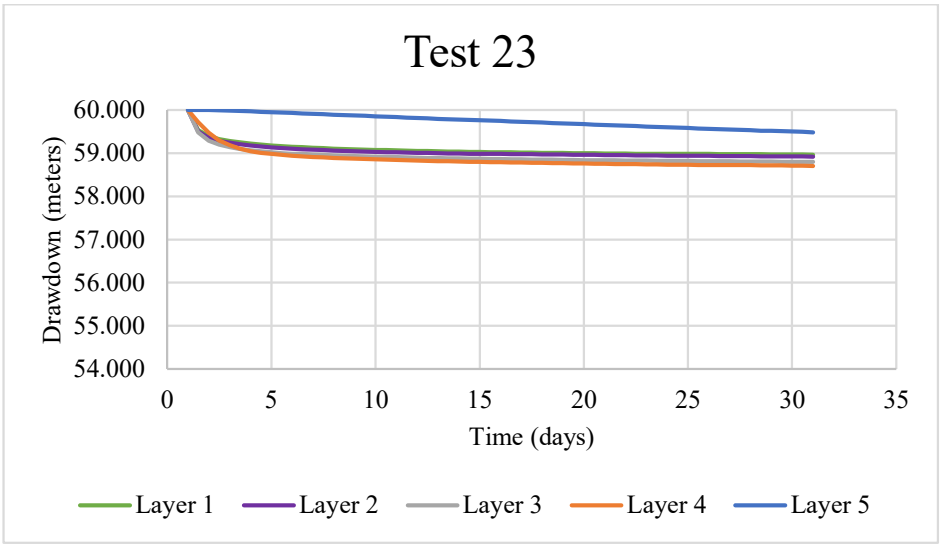
Test 23
60.000
59.000
58.000
57.000
56.000
55.000
54.000
Drawdown (meters)
0
5
10
15
20
25
30
35
Time (days)
Layer 1
Layer 2
Layer 3
Layer 4
Layer 5

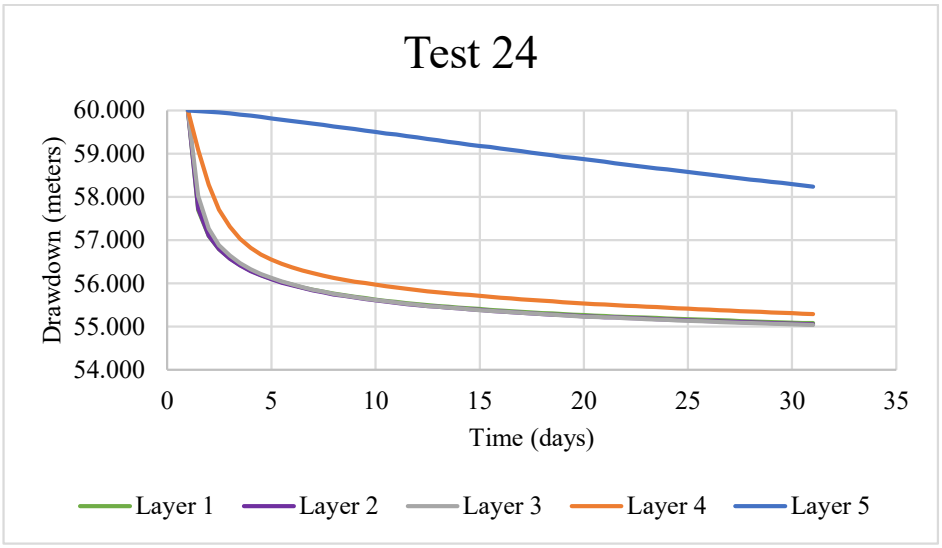
Test 24
60.000
59.000
58.000
57.000
56.000
55.000
54.000
Drawdown (meters)
0
5
10
15
20
25
30
35
Time (days)
Layer 1
Layer 2
Layer 3
Layer 4
Layer 5

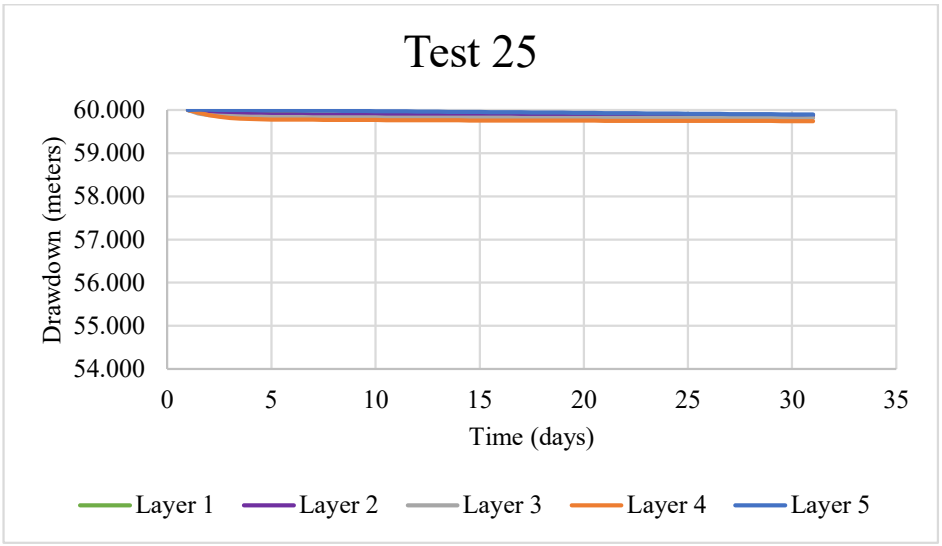
Test 25
60.000
59.000
58.000
57.000
56.000
55.000
54.000
Drawdown (meters)
0
5
10
15
20
25
30
35
Time (days)
Layer 1
Layer 2
Layer 3
Layer 4
Layer 5

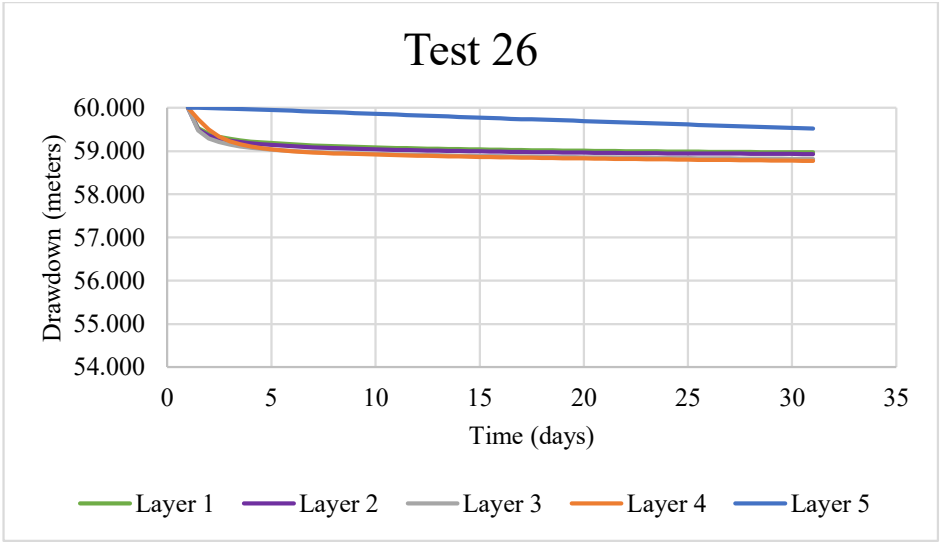
Test 26
60.000
59.000
58.000
57.000
56.000
55.000
54.000
Drawdown (meters)
0
5
10
15
20
25
30
35
Time (days)
Layer 1
Layer 2
Layer 3
Layer 4
Layer 5

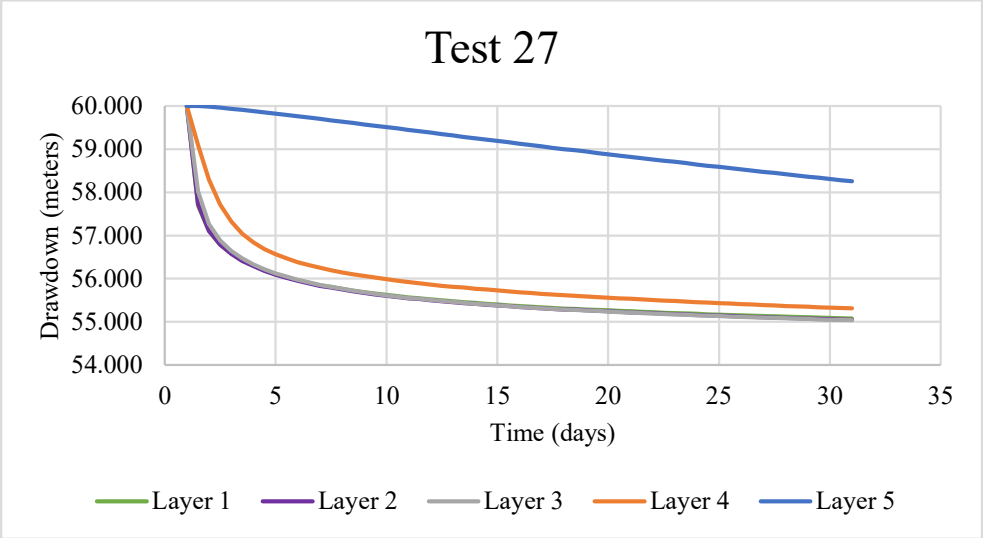
Test 27
60.000
59.000
58.000
57.000
56.000
55.000
54.000
Drawdown (meters)
0
5
10
15
20
25
30
35
Time (days)
Layer 1
Layer 2
Layer 3
Layer 4
Layer 5

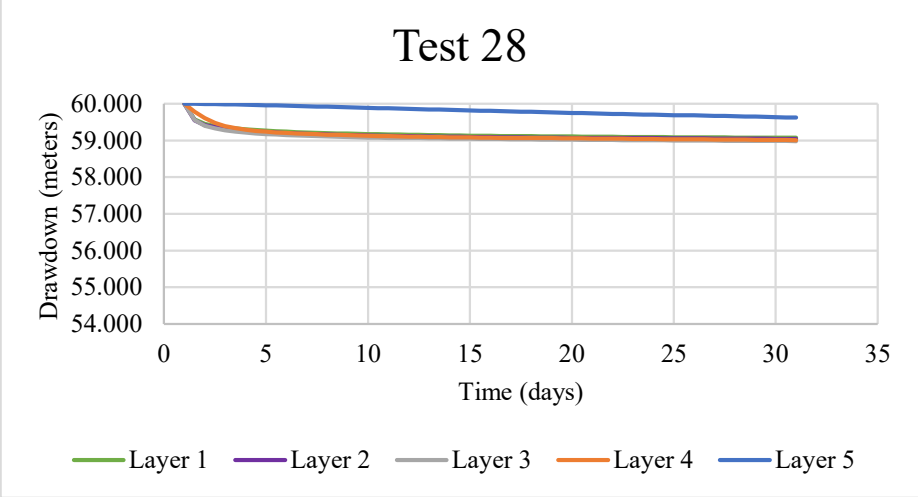
Test 28
60.000
59.000
58.000
57.000
56.000
55.000
54.000
Drawdown (meters)
0
5
10
15
20
25
30
35
Time (days)
Layer 1
Layer 2
Layer 3
Layer 4
Layer 5

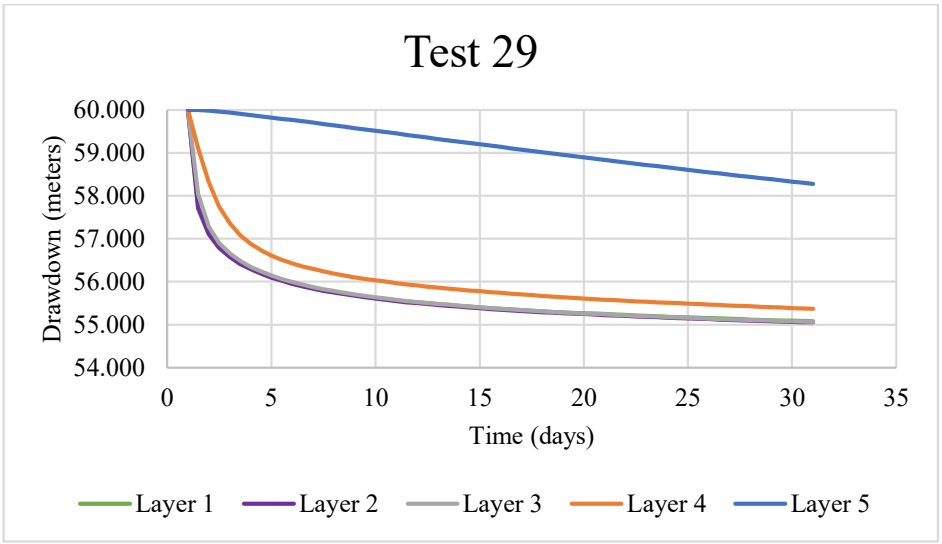
Test 29
60.000
59.000
58.000
57.000
56.000
55.000
54.000
Drawdown (meters)
0
5
10
15
20
25
30
35
Time (days)
Layer 1
Layer 2
Layer 3
Layer 4
Layer 5

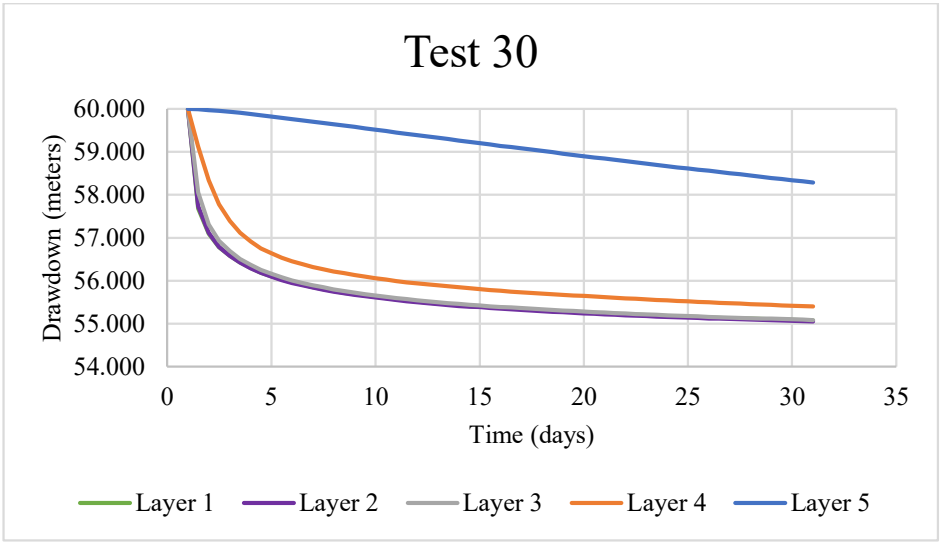
Test 30
60.000
59.000
58.000
57.000
56.000
55.000
54.000
Drawdown (meters)
0
5
10
15
20
25
30
35
Time (days)
Layer 1
Layer 2
Layer 3
Layer 4
Layer 5

Appendix 5

Semi-log drawdown graphs from the scenarios run in the experiment (see Figure 4). These graphs were drawn over the entire simulation period rather than a fixed amount of late time head drop, so the y axis scale will vary with each draw down graph.

Test 1

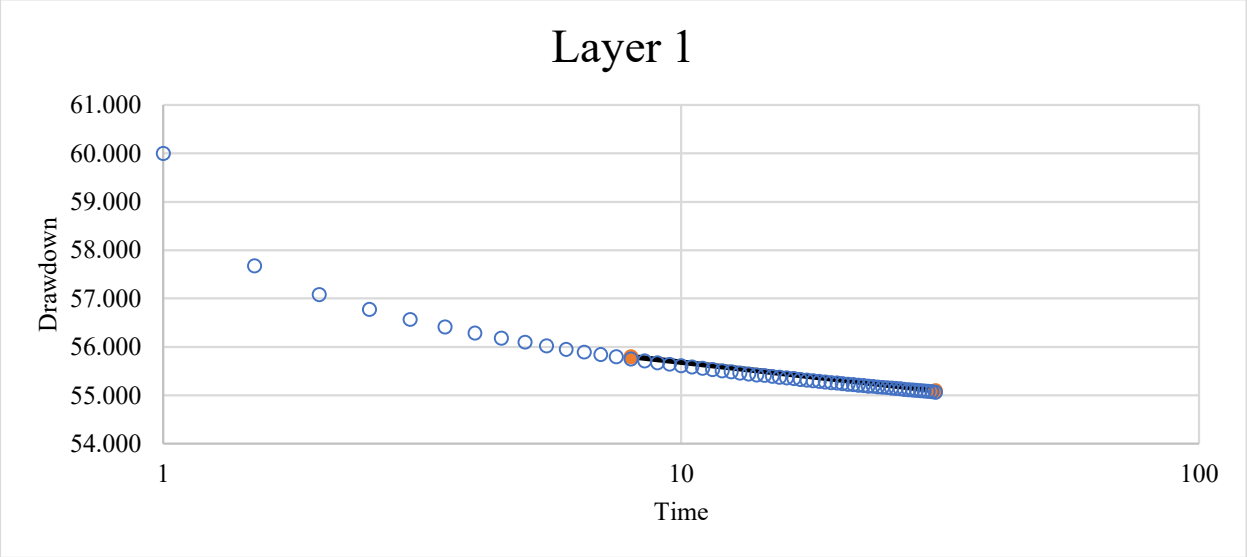

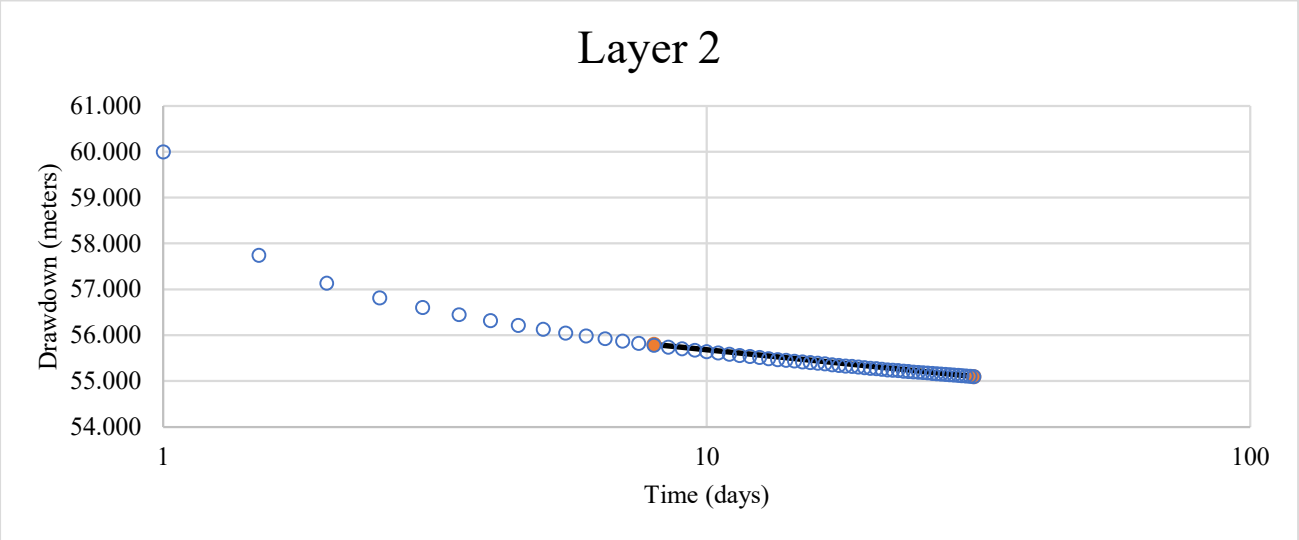
Layer 2
61.000
60.000
59.000
58.000
57.000
56.000
55.000
54.000
Drawdown (meters)
1
10
100
Time (days)

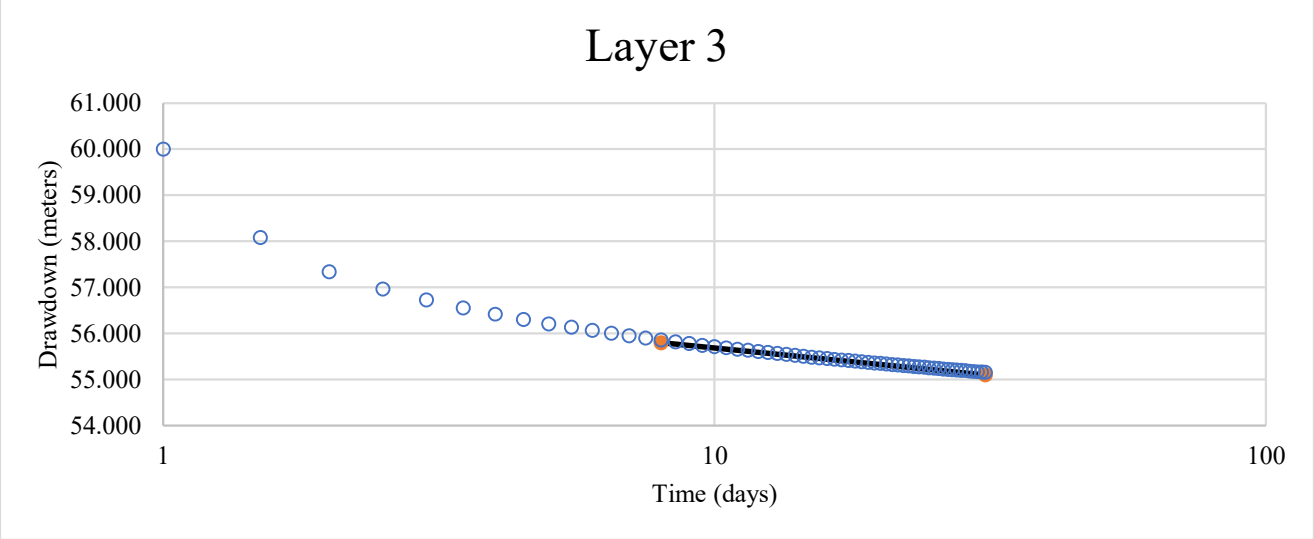
Layer 3
61.000
60.000
59.000
58.000
57.000
56.000
55.000
54.000
Drawdown (meters)
1
10
100
Time (days)

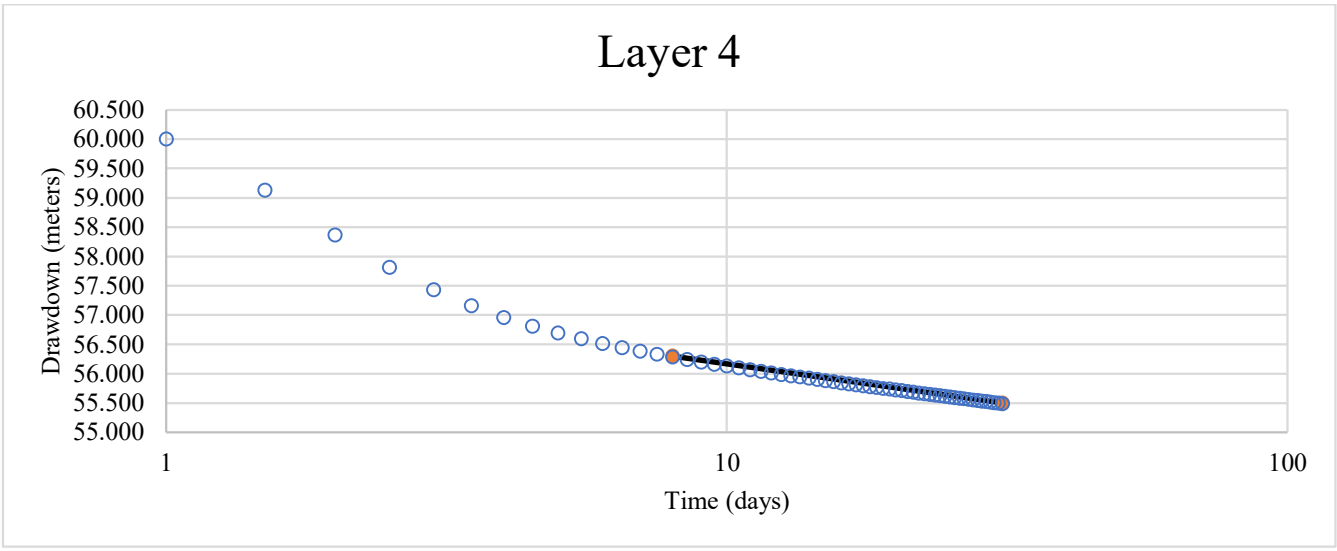
Layer 4
60.500
60.000
59.500
59.000
58.500
58.000
57.500
57.000
56.500
56.000
55.500
55.000
Drawdown (meters)
1
10
100
Time (days)

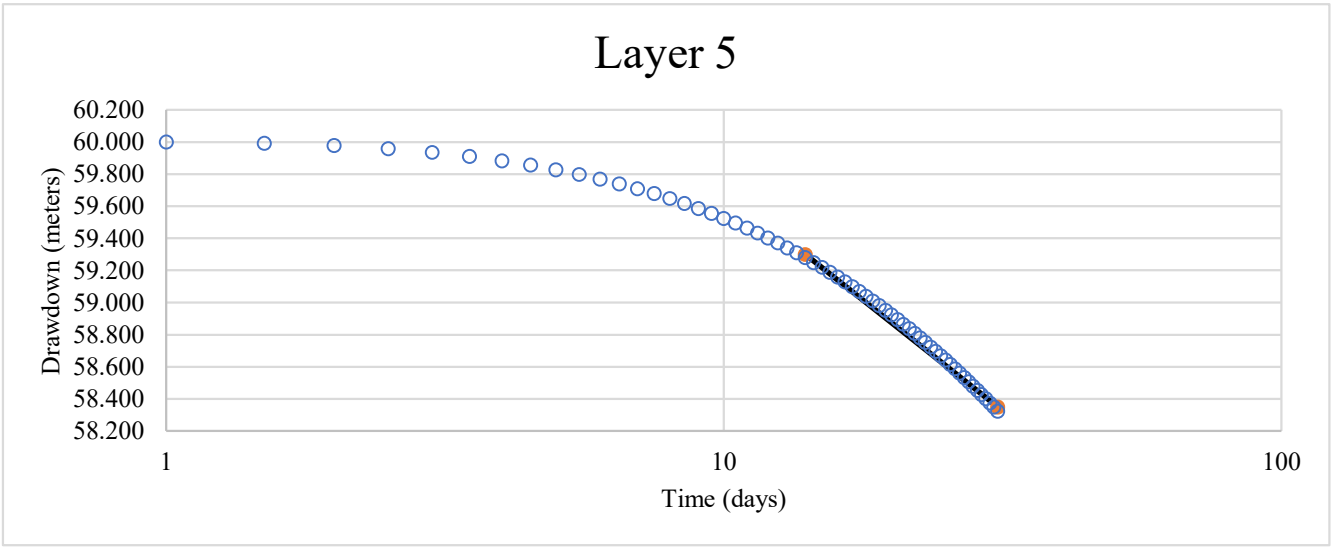
Layer 5
60.200
60.000
59.800
59.600
59.400
59.200
59.000
58.800
58.600
58.400
58.200
Drawdown (meters)
1
10
100
Time (days)

Test 2

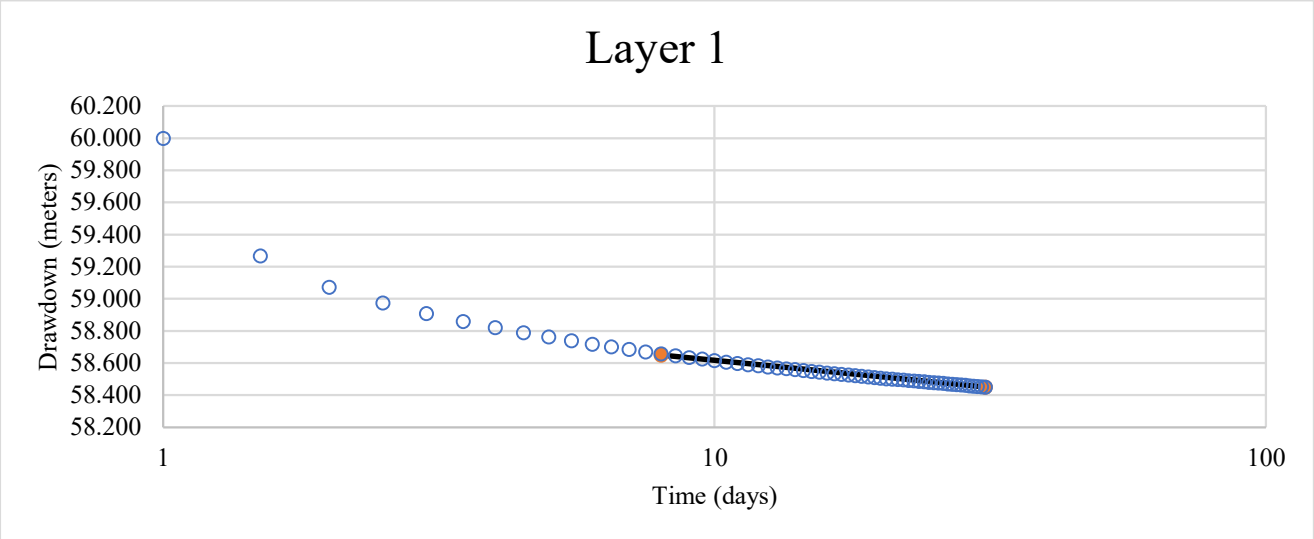
Layer 1
60.200
60.000
59.800
59.600
59.400
59.200
59.000
58.800
58.600
58.400
58.200
Drawdown (meters)
1
10
100
Time (days)

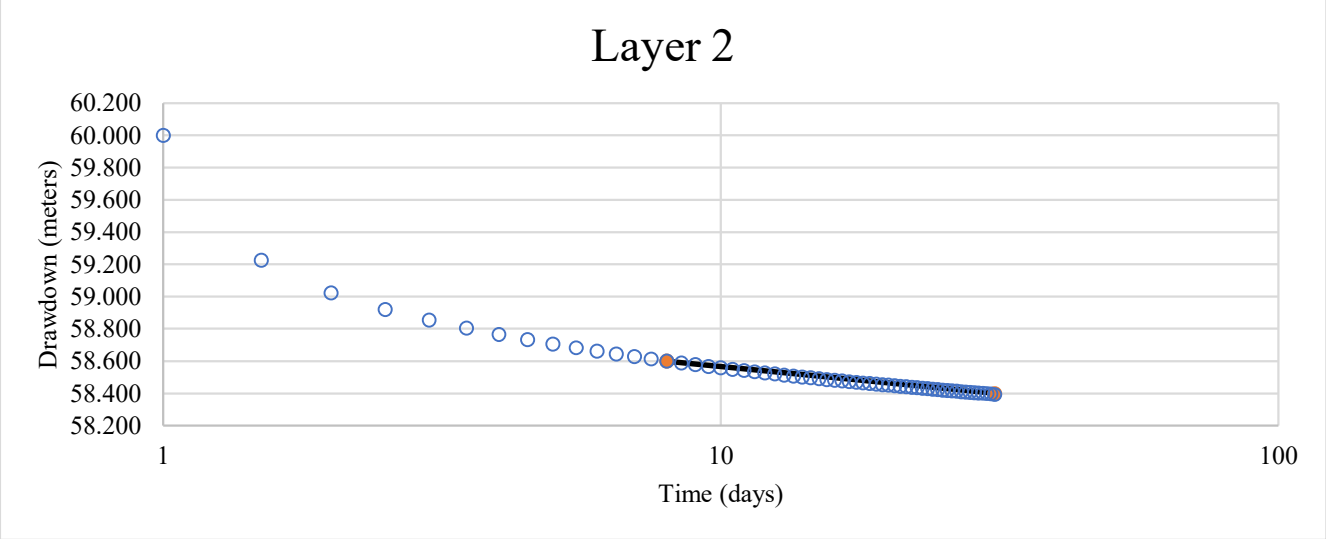
Layer 2
60.200
60.000
59.800
59.600
59.400
59.200
59.000
58.800
58.600
58.400
58.200
Drawdown (meters)
1
10
100
Time (days)

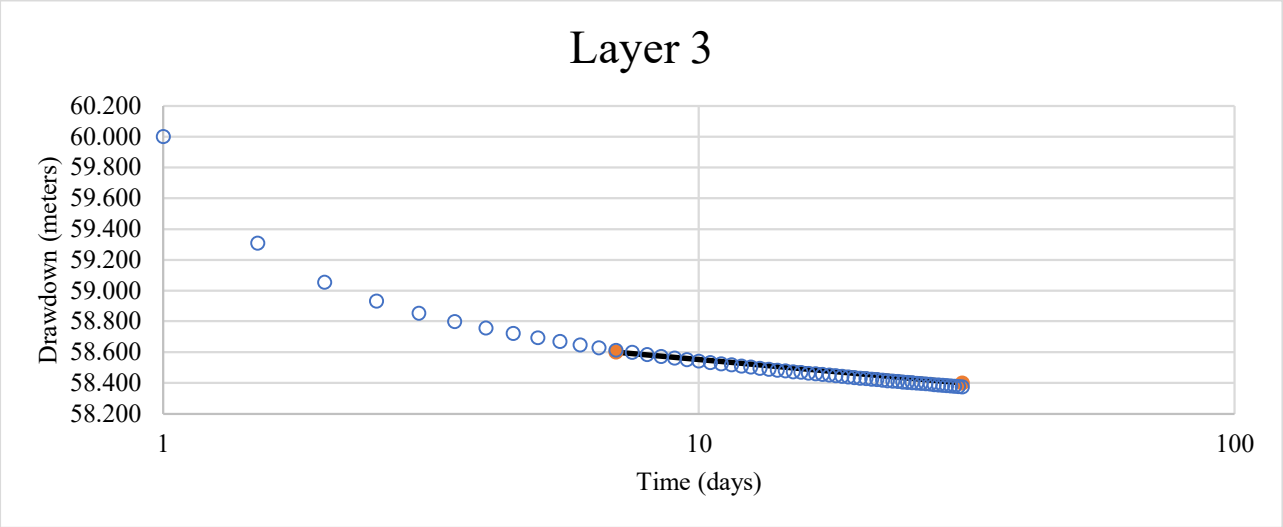
Layer 3
60.200
60.000
59.800
59.600
59.400
59.200
59.000
58.800
58.600
58.400
58.200
Drawdown (meters)
1
10
100
Time (days)

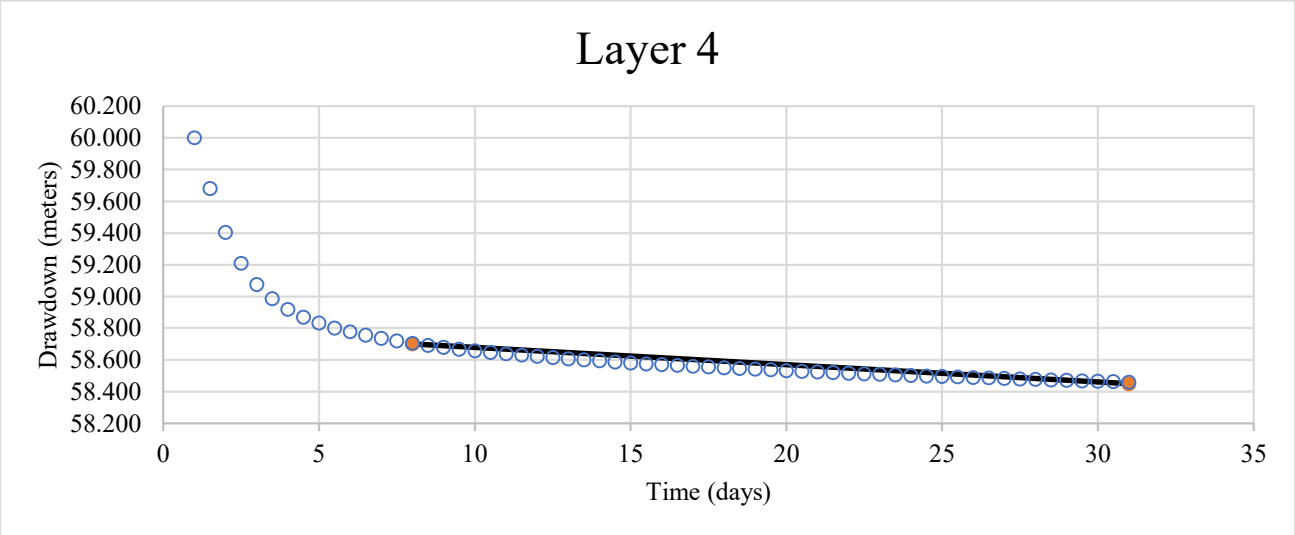
Layer 4
60.200
60.000
59.800
59.600
59.400
59.200
59.000
58.800
58.600
58.400
58.200
Drawdown (meters)
0
5
10
15
20
25
30
35
Time (days)

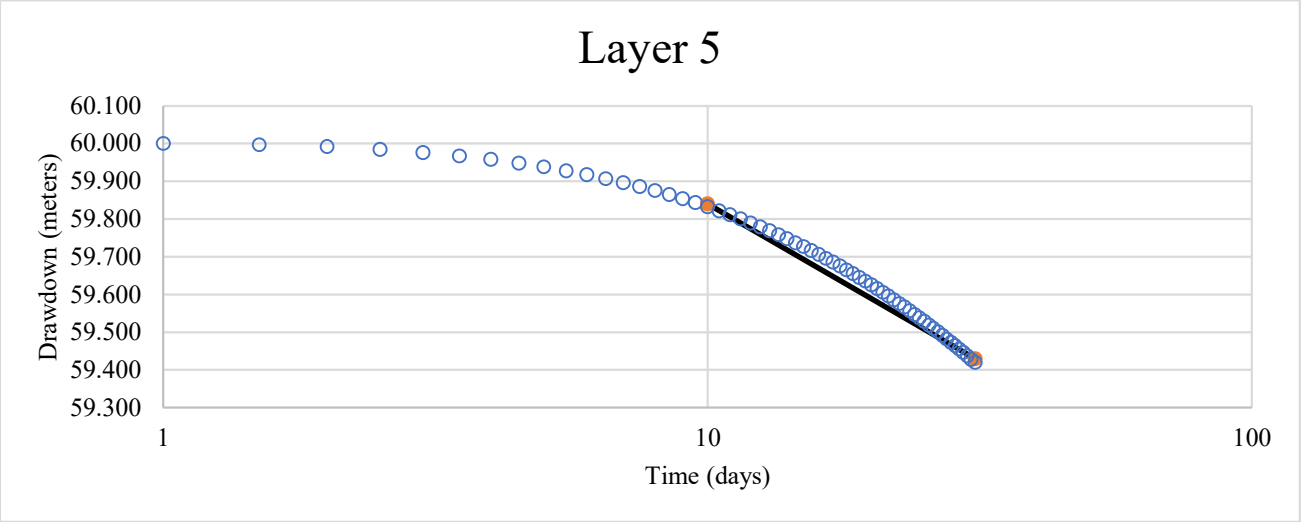
Layer 5
60.100
60.000
59.900
59.800
59.700
59.600
59.500
59.400
59.300
Drawdown (meters)
1
10
100
Time (days)

Test 3

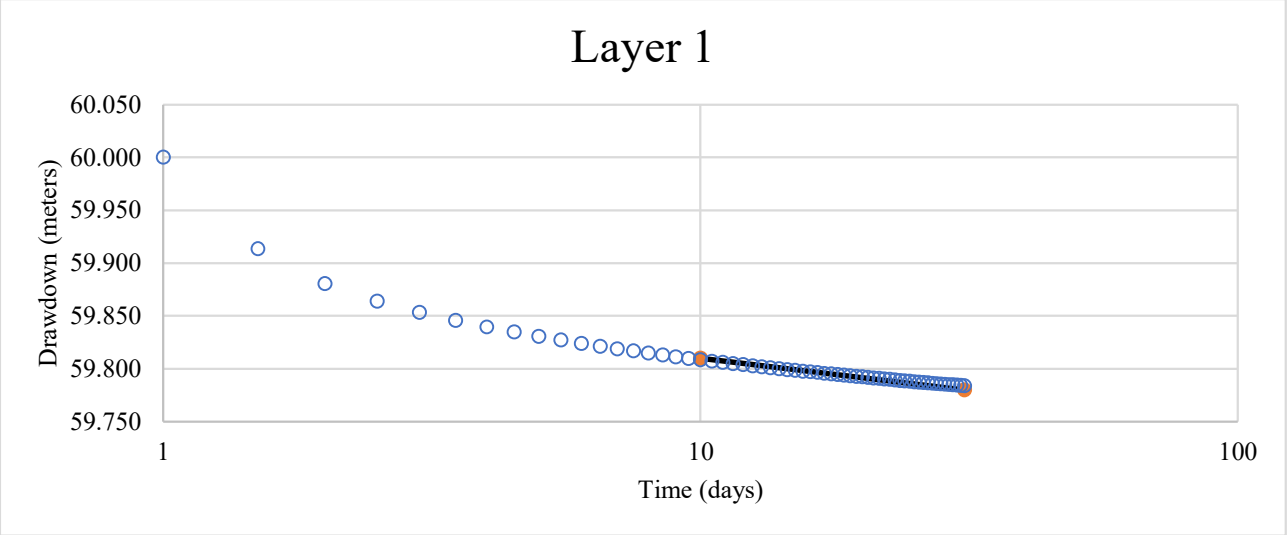
Layer 1
60.050
60.000
59.950
59.900
59.850
59.800
59.750
Drawdown (meters)
1
10
100
Time (days)

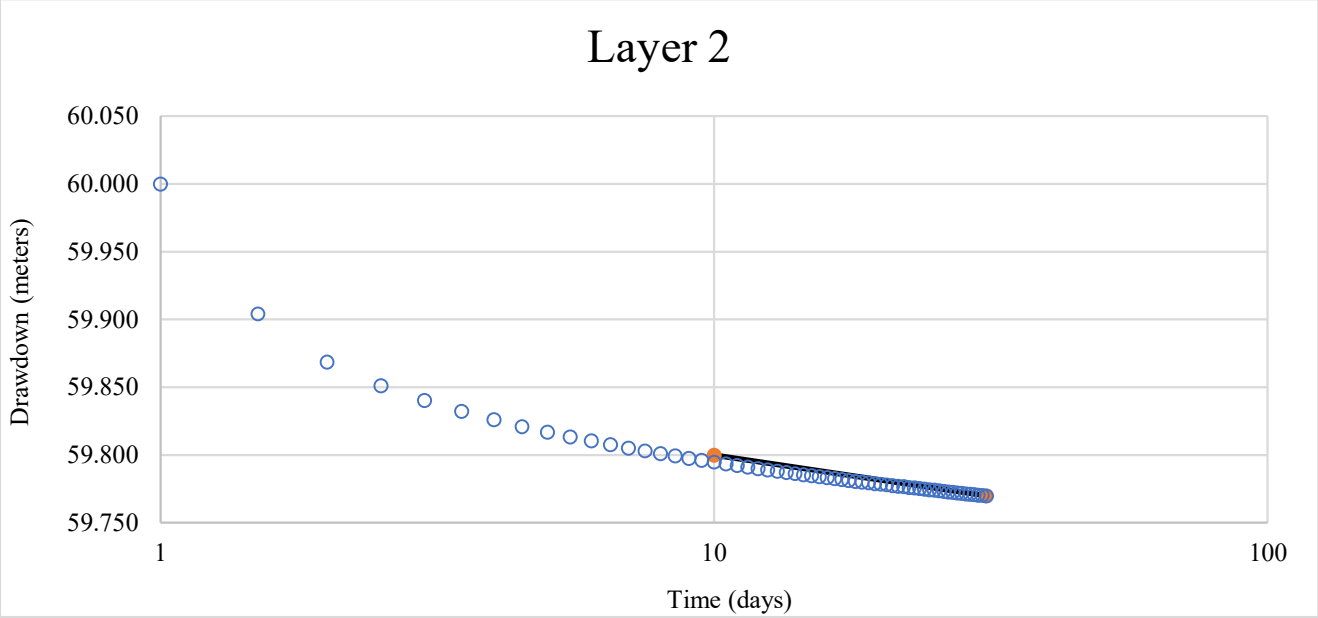
Layer 2
60.050
60.000
59.950
59.900
59.850
59.800
59.750
Drawdown (meters)
1
10
100
Time (days)

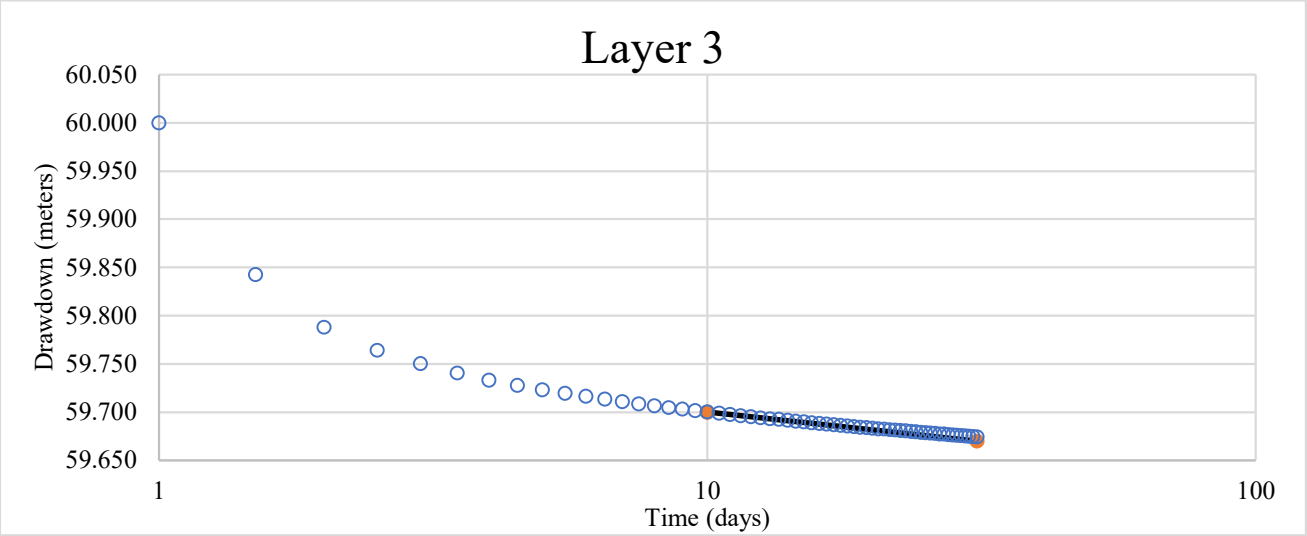
Layer 3
60.050
60.000
59.950
59.900
59.850
59.800
59.750
59.700
59.650
Drawdown (meters)
1
10
100
Time (days)

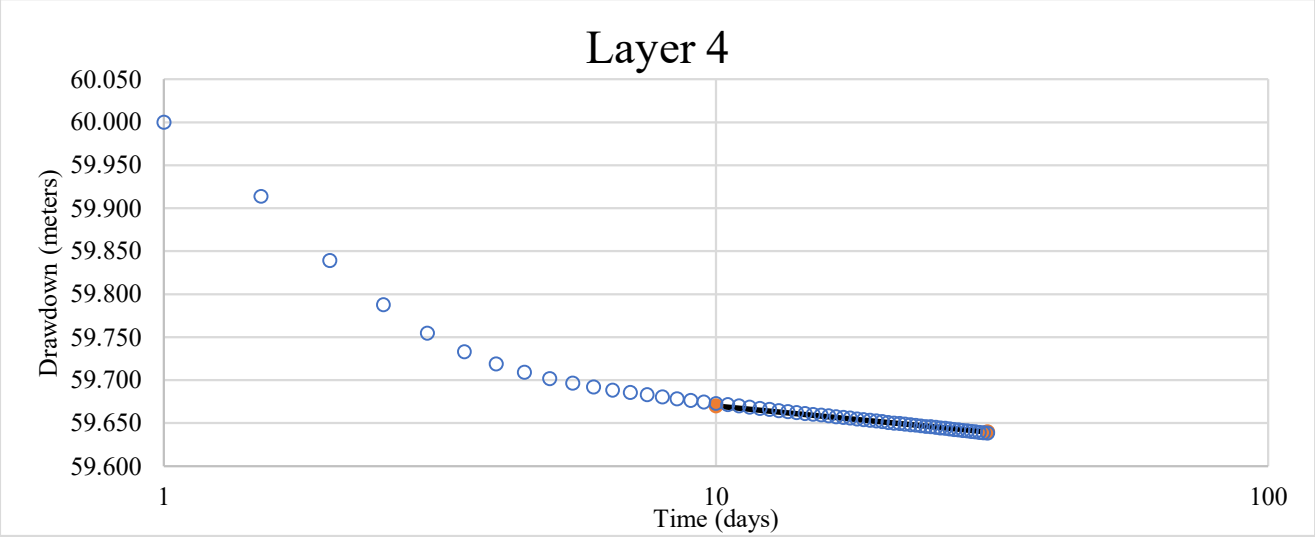
Layer 4
60.050
60.000
59.950
59.900
59.850
59.800
59.750
59.700
59.650
59.600
Drawdown (meters)
1
10
100
Time (days)

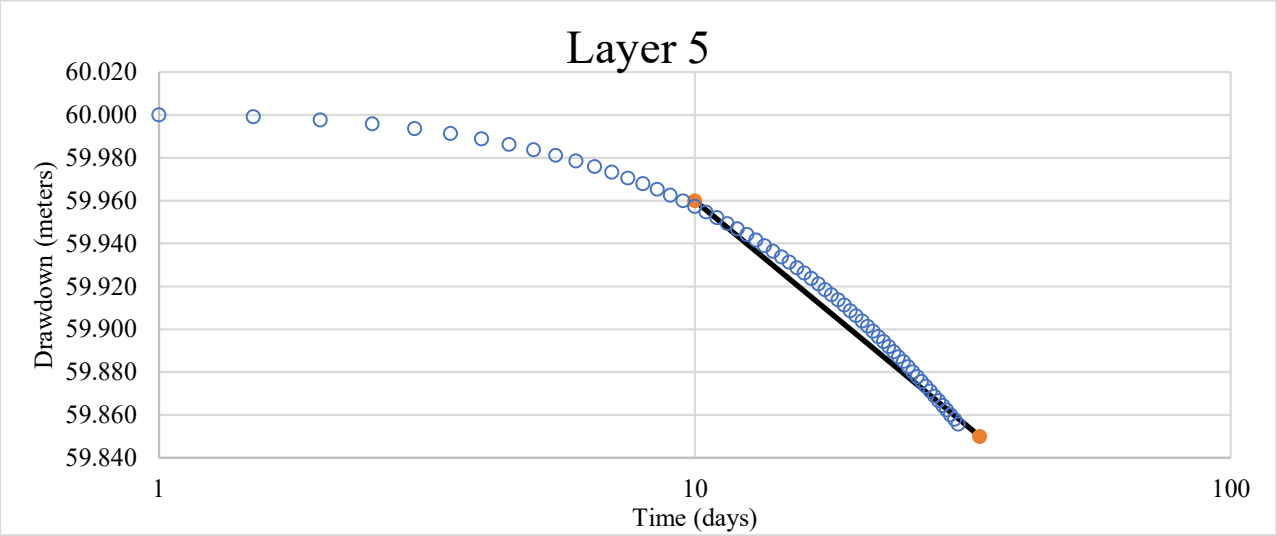
Layer 5
60.020
60.000
59.980
59.960
59.940
59.920
59.900
59.880
59.860
59.840
Drawdown (meters)
1
10
100
Time (days)

Test 4

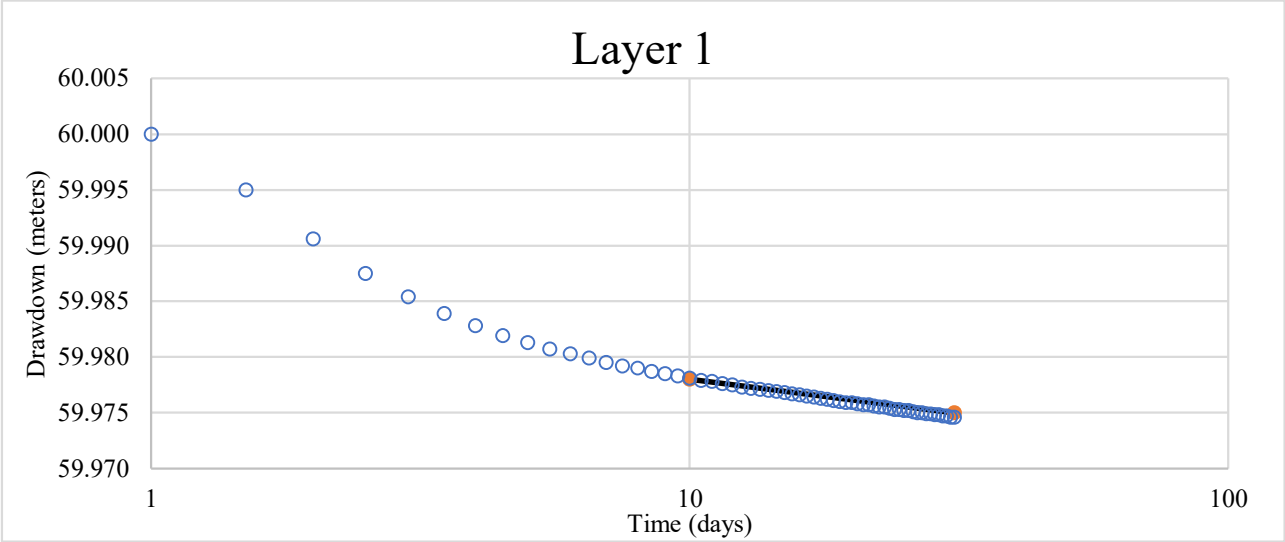
Layer 1
60.005
60.000
59.995
59.990
59.985
59.980
59.975
59.970
Drawdown (meters)
1
10
100
Time (days)

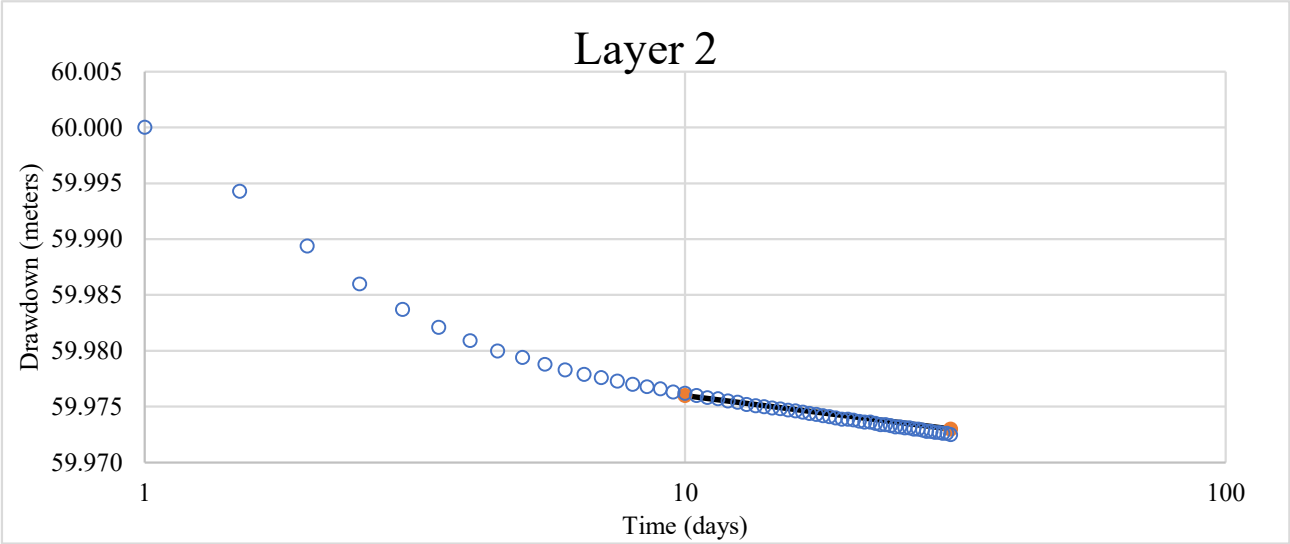
Layer 2
60.005
60.000
59.995
59.990
59.985
59.980
59.975
59.970
Drawdown (meters)
1
10
100
Time (days)

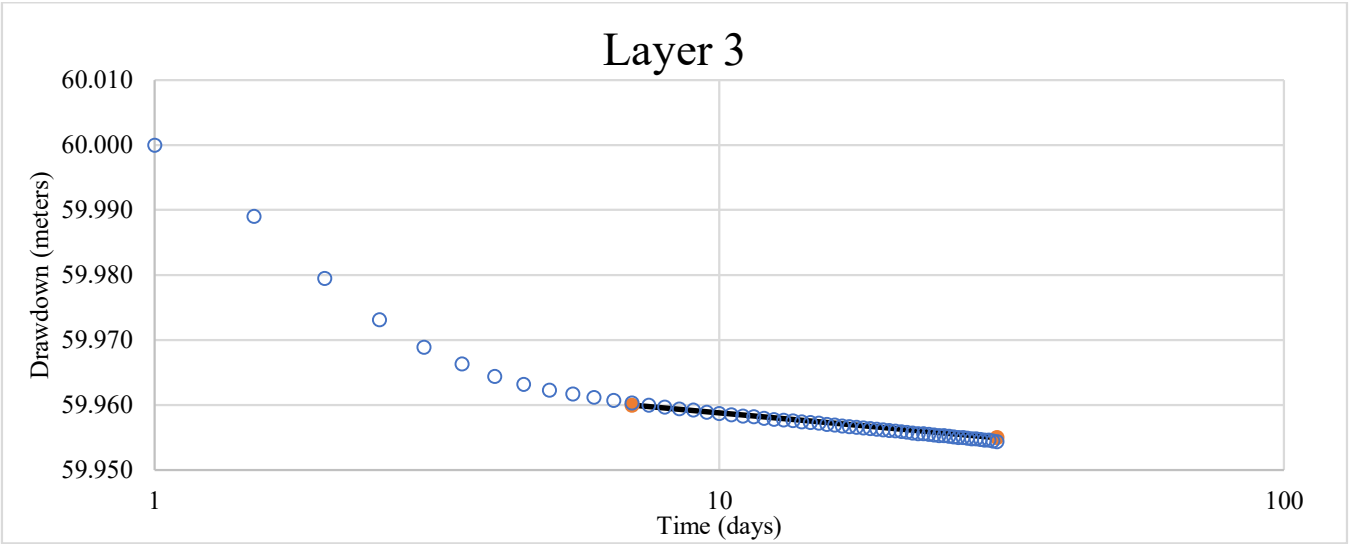
Layer 3
60.010
60.000
59.990
59.980
59.970
59.960
59.950
Drawdown (meters)
1
10
100
Time (days)

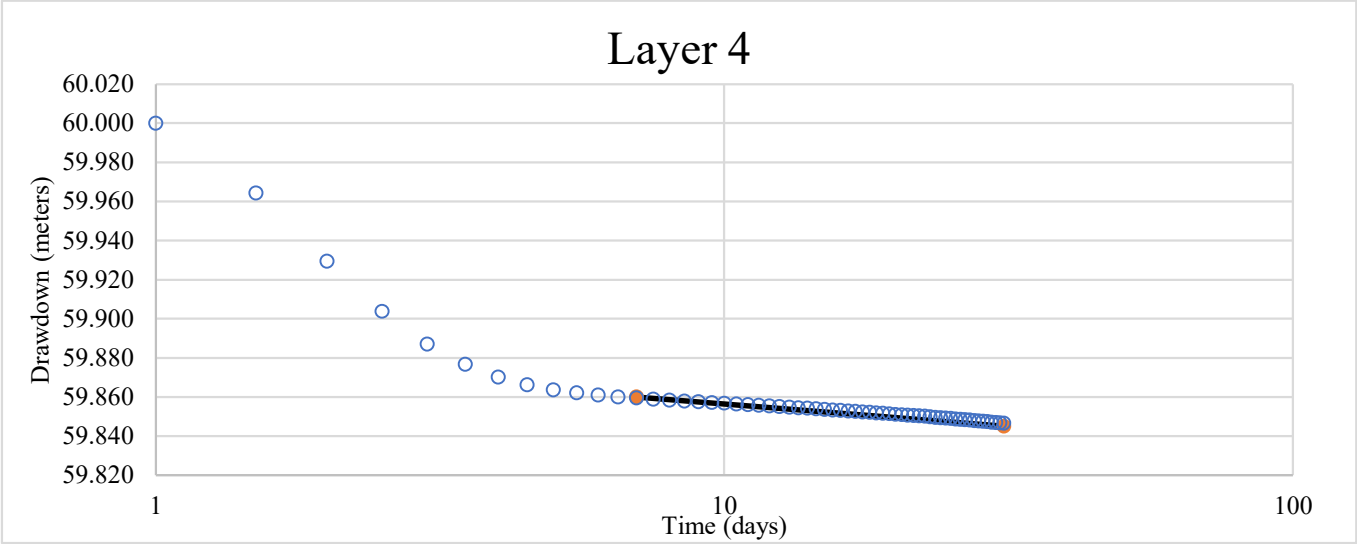
Layer 4
60.020
60.000
59.980
59.960
59.940
59.920
59.900
59.880
59.860
59.840
59.820
Drawdown (meters)
1
10
100
Time (days)

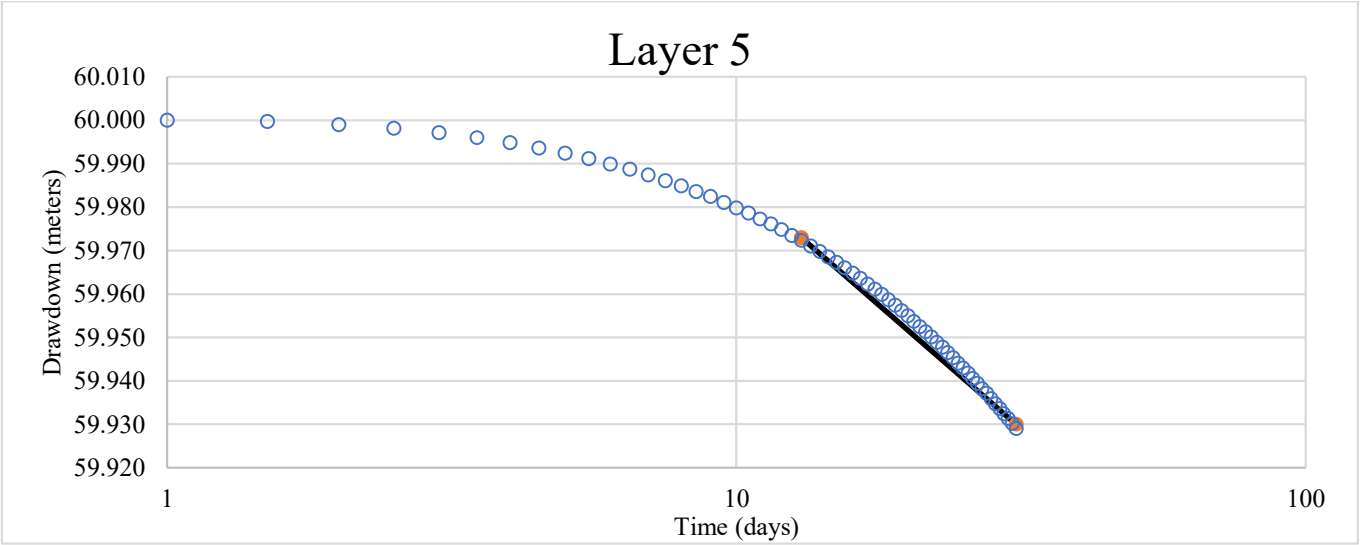
Layer 5
60.010
60.000
59.990
59.980
59.970
59.960
59.950
59.940
59.930
59.920
Drawdown (meters)
1
10
100
Time (days)

Test 5

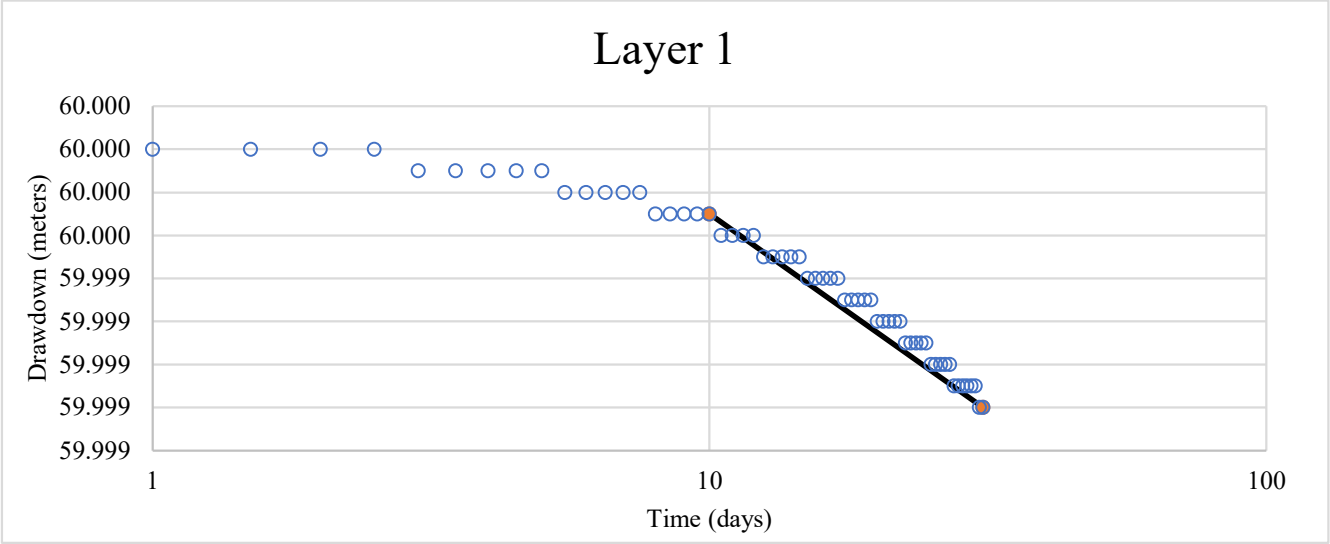
Layer 1
60.000
60.000
60.000
60.000
59.999
59.999
59.999
59.999
59.999
Drawdown (meters)
1
10
100
Time (days)

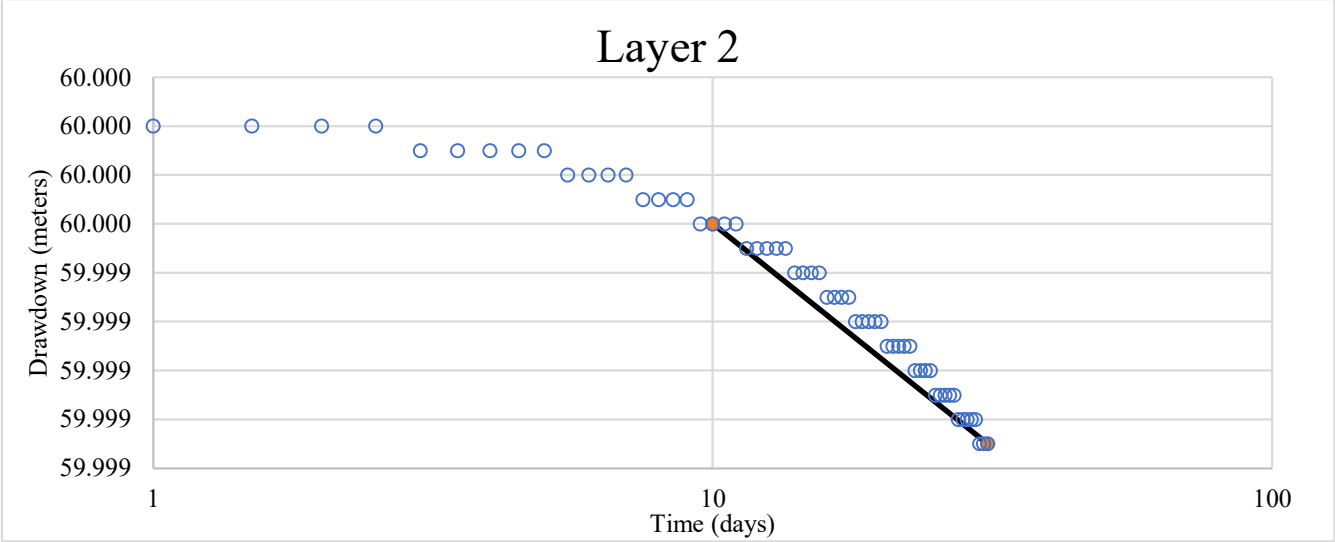
Layer 2
60.000
60.000
60.000
60.000
59.999
59.999
59.999
59.999
59.999
Drawdown (meters)
1
10
100
Time (days)

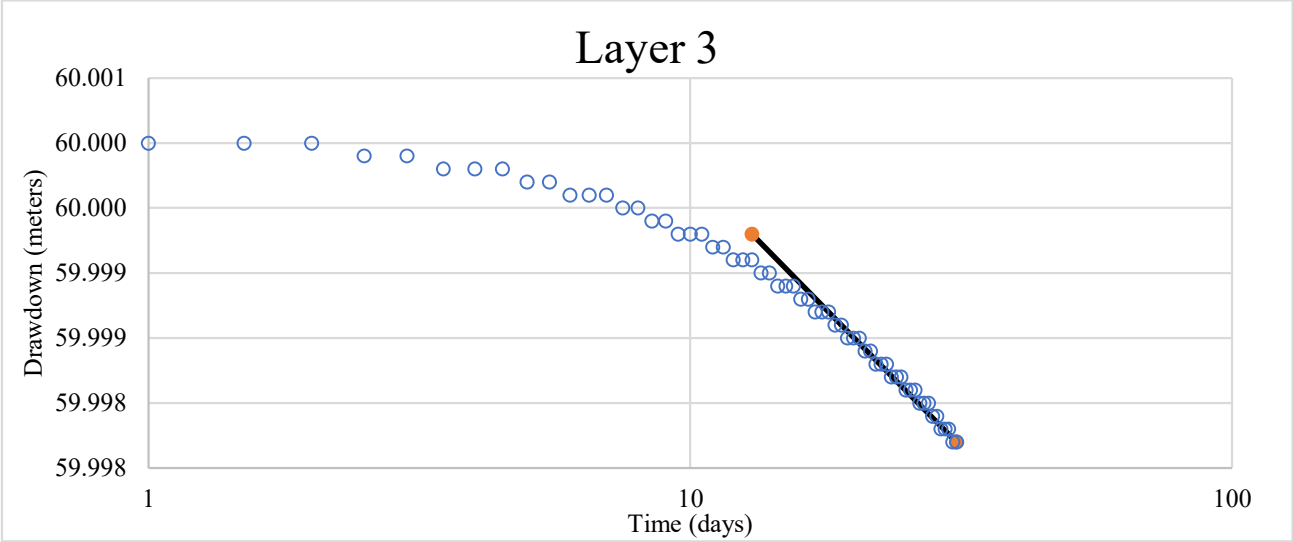
Layer 3
60.001
60.000
60.000
59.999
59.999
59.998
59.998
Drawdown (meters)
1
10
100
Time (days)

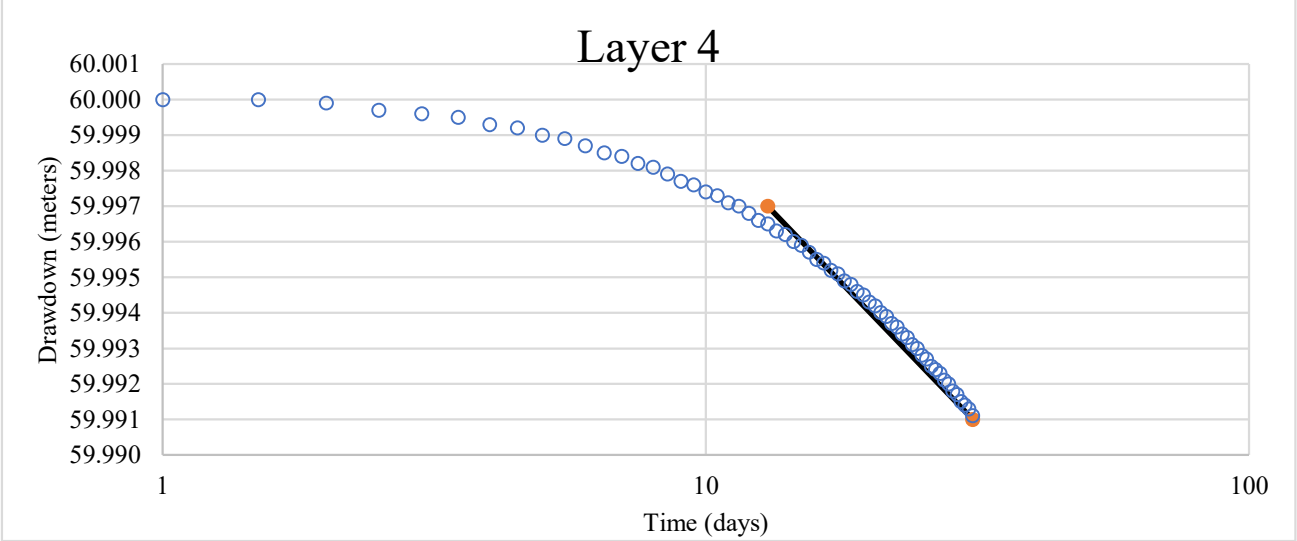
Layer 4
60.001
60.000
59.999
59.998
59.997
59.996
59.995
59.994
59.993
59.992
59.991
59.990
Drawdown (meters)
1
10
100
Time (days)

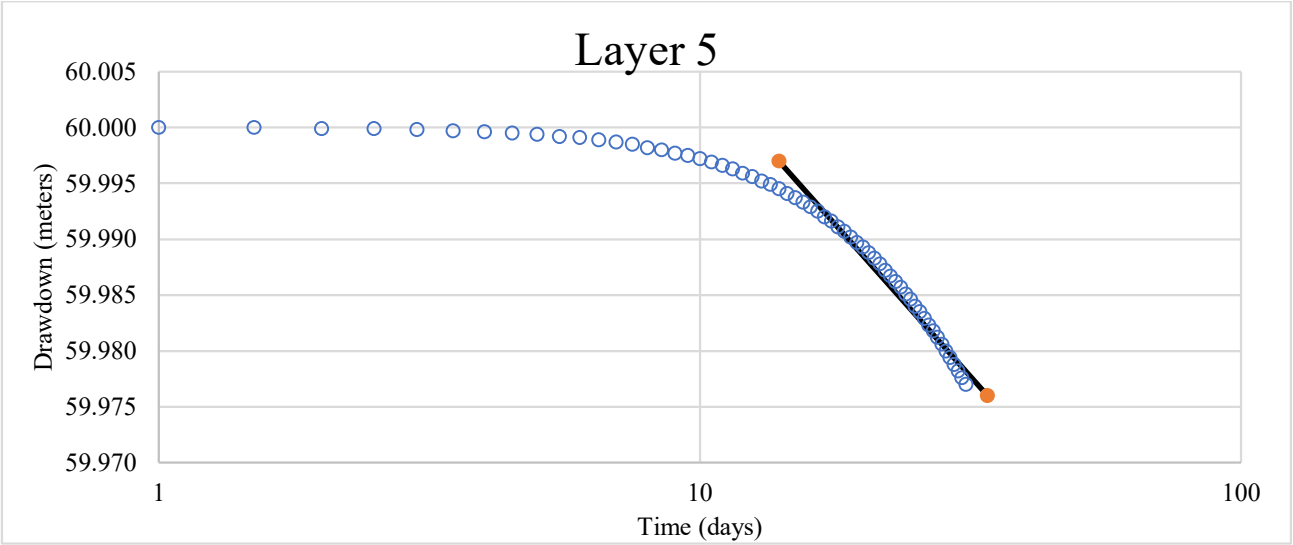
Layer 5
60.005
60.000
59.995
59.990
59.985
59.980
59.975
59.970
Drawdown (meters)
1
10
100
Time (days)

Test 6

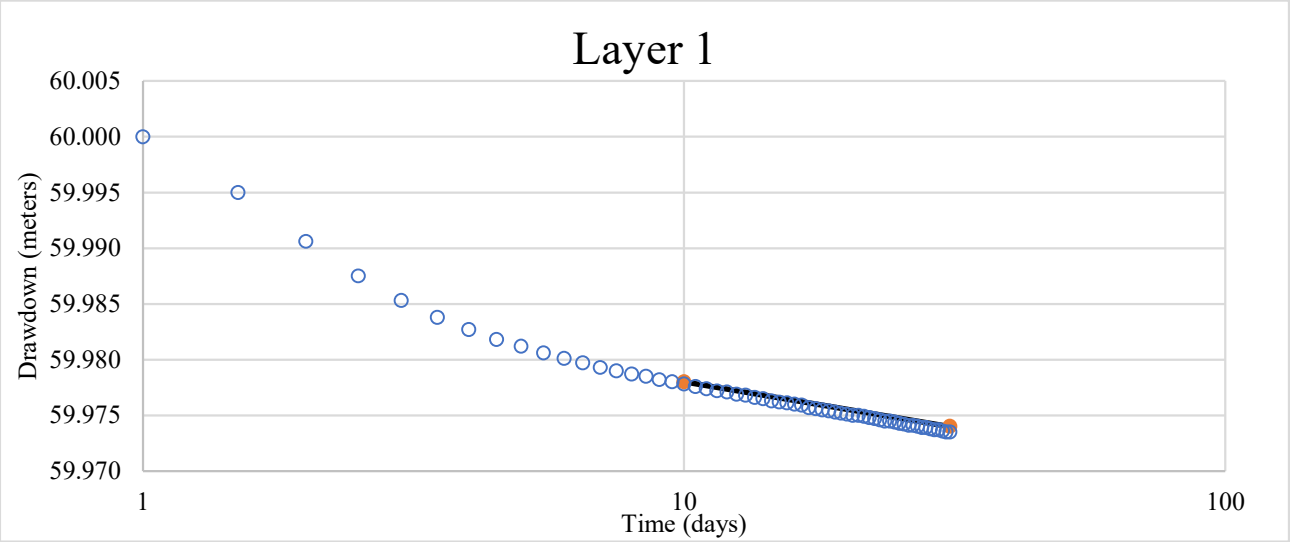
Layer 1
60.005
60.000
59.995
59.990
59.985
59.980
59.975
59.970
Drawdown (meters)
1
10
100
Time (days)

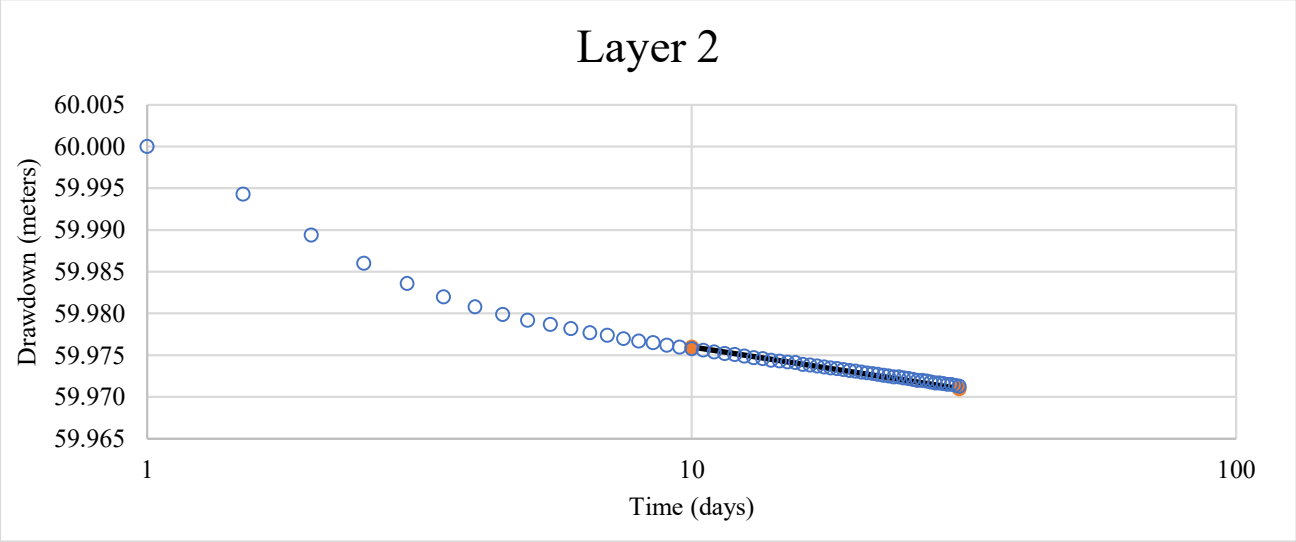
Layer 2
60.005
60.000
59.995
59.990
59.985
59.980
59.975
59.970
59.965
Drawdown (meters)
1
10
100
Time (days)

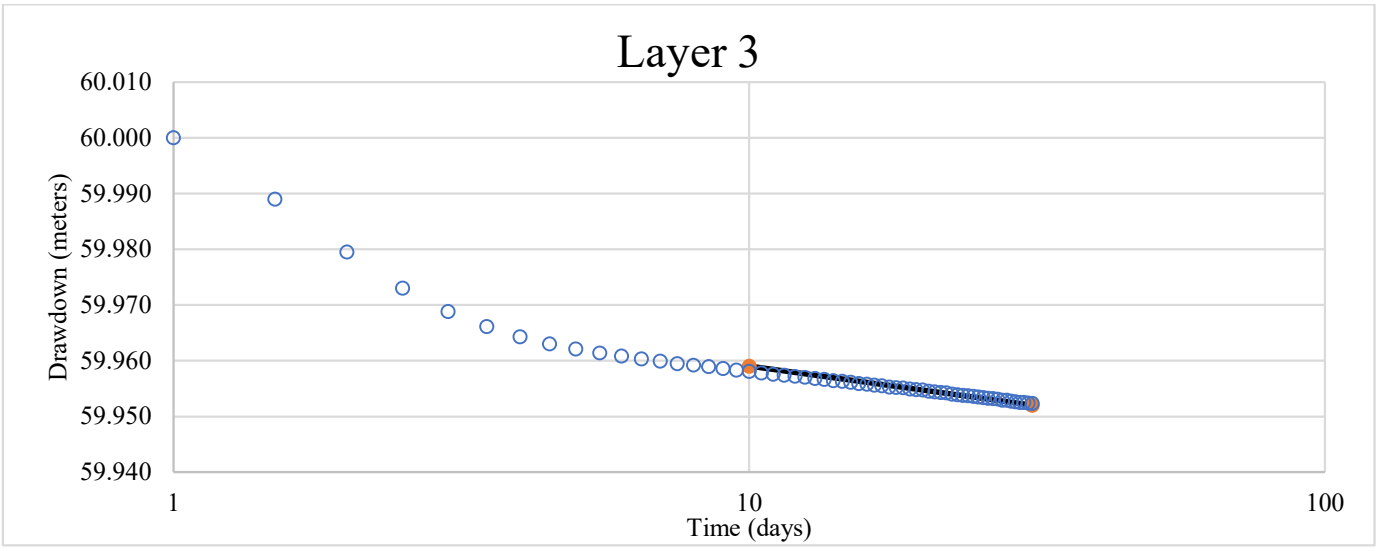
Layer 3
60.010
60.000
59.990
59.980
59.970
59.960
59.950
59.940
Drawdown (meters)
1
10
100
Time (days)

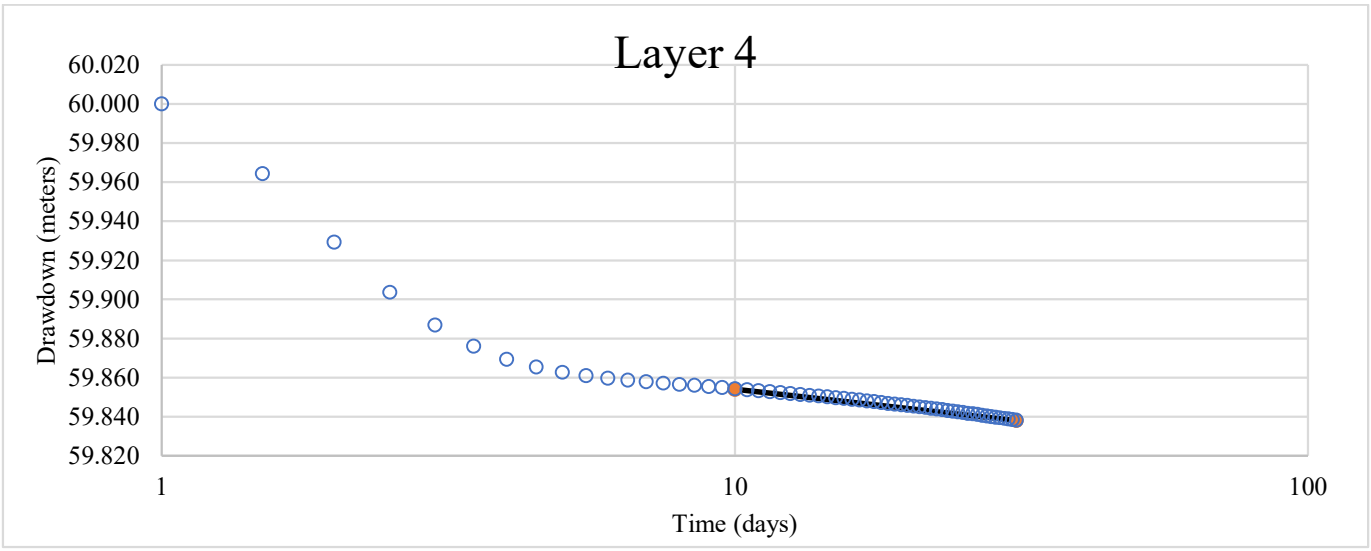
Layer 4
60.020
60.000
59.980
59.960
59.940
59.920
59.900
59.880
59.860
59.840
59.820
Drawdown (meters)
1
10
100
Time (days)

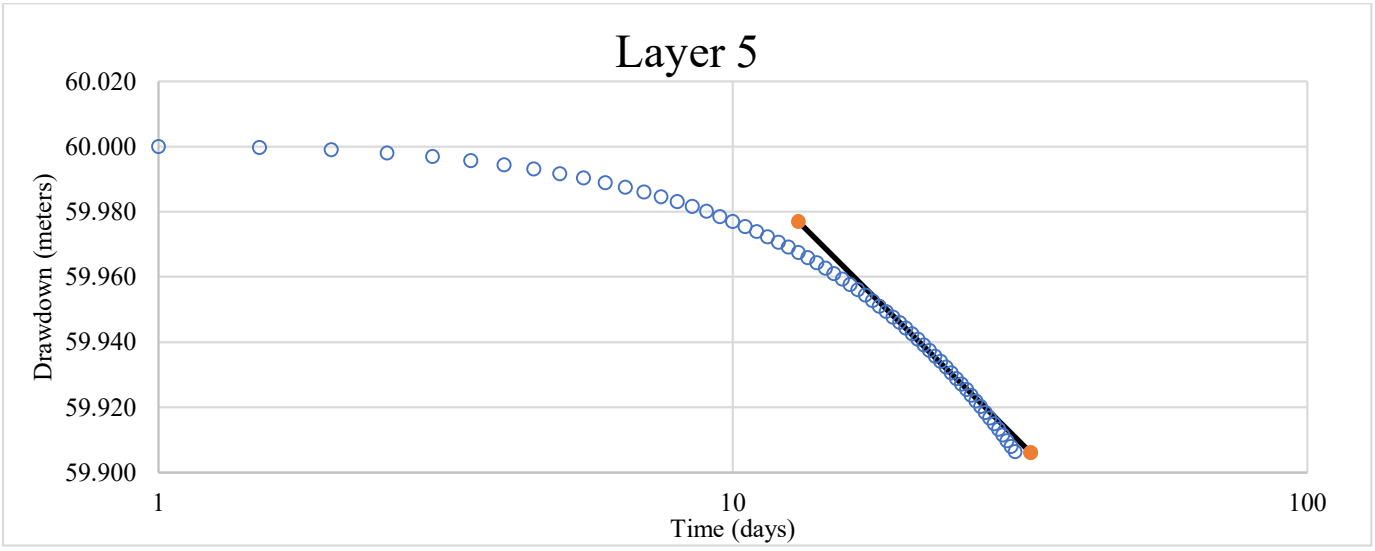
Layer 5
60.020
60.000
59.980
59.960
59.940
59.920
59.900
Drawdown (meters)
1
10
100
Time (days)

Test 7

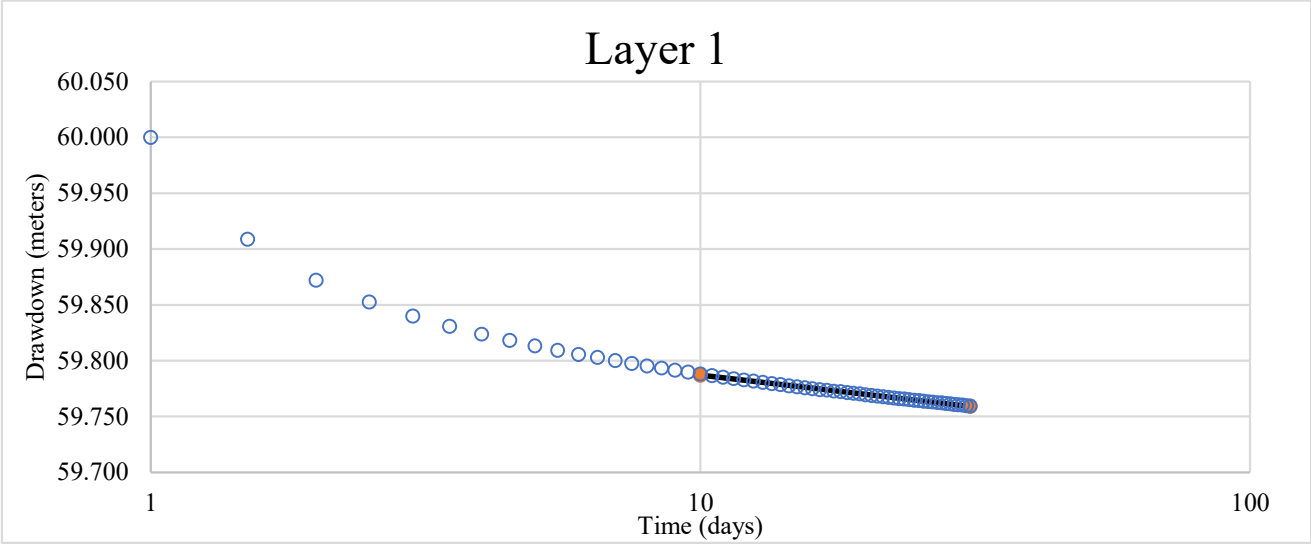
Layer 1
60.050
60.000
59.950
59.900
59.850
59.800
59.750
59.700
Drawdown (meters)
1
10
100
Time (days)

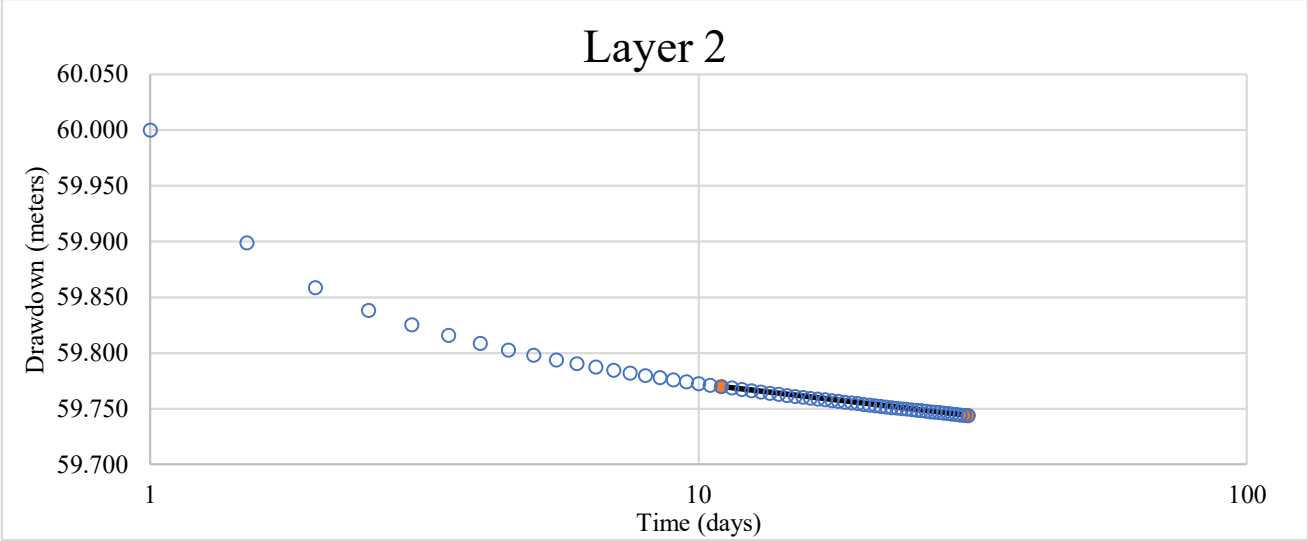
Layer 2
60.050
60.000
59.950
59.900
59.850
59.800
59.750
59.700
Drawdown (meters)
1
10
100
Time (days)

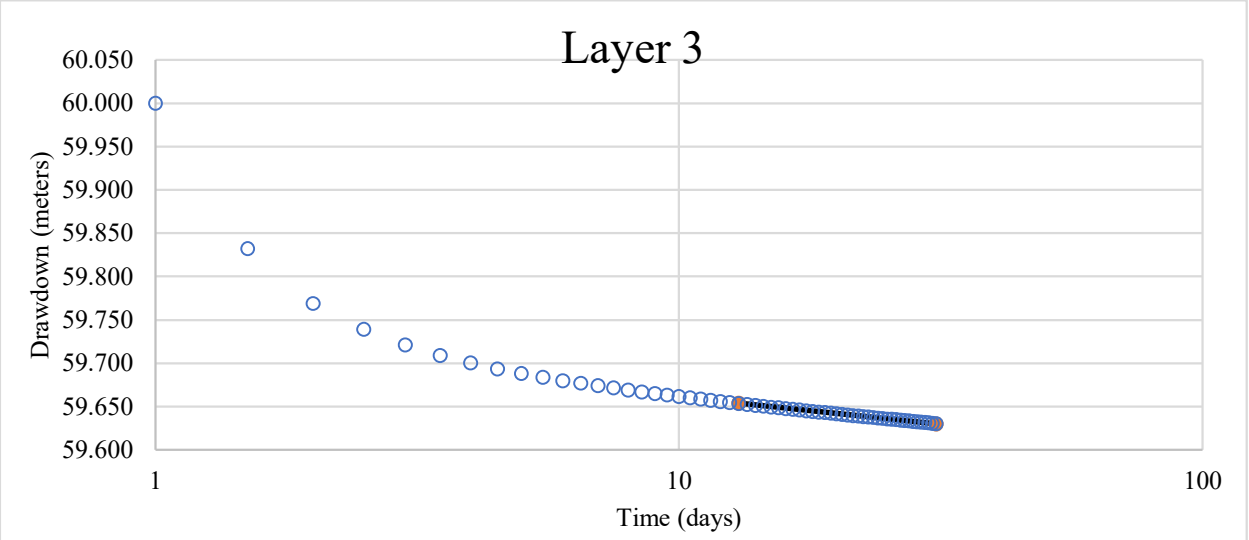
Layer 3
60.050
60.000
59.950
59.900
59.850
59.800
59.750
59.700
59.650
59.600
Drawdown (meters)
1
10
100
Time (days)

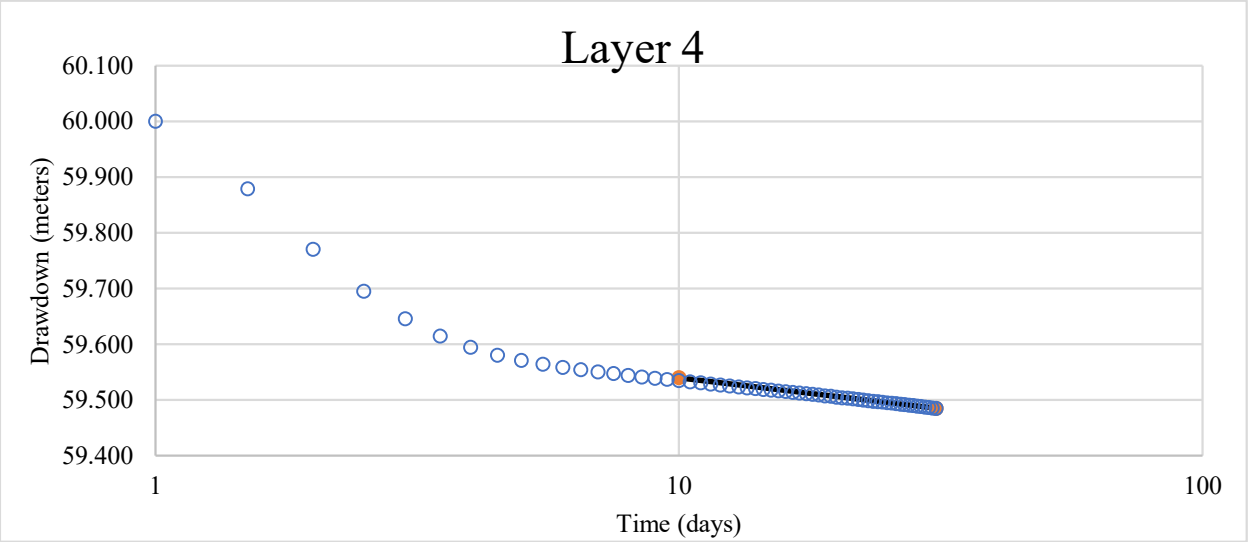
Layer 4
60.100
60.000
59.900
59.800
59.700
59.600
59.500
59.400
Drawdown (meters)
1
10
100
Time (days)

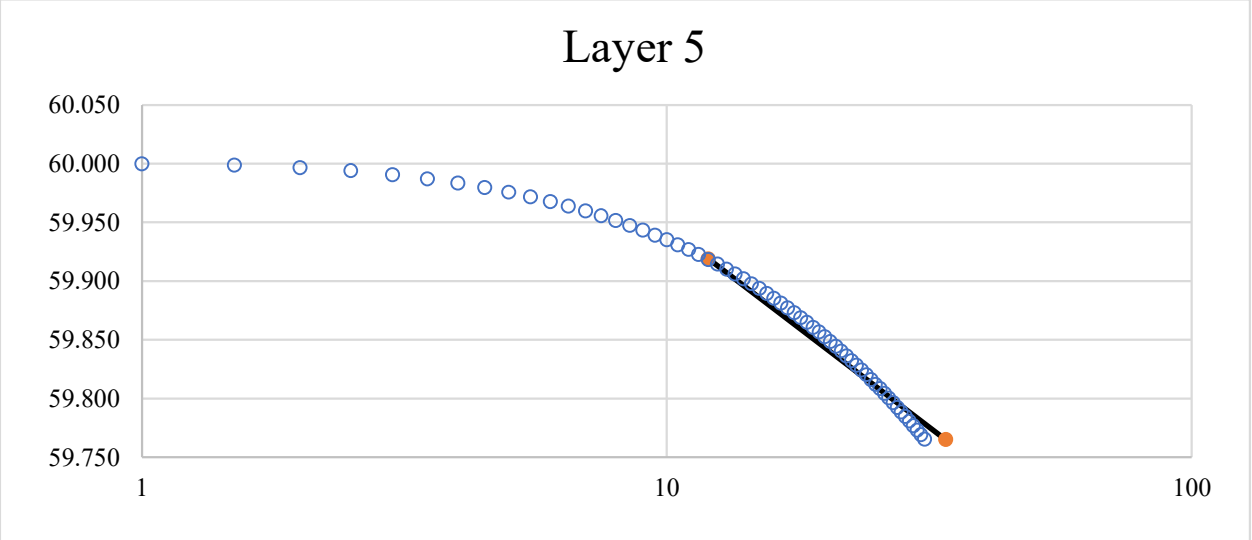
Layer 5
60.050
60.000
59.950
59.900
59.850
59.800
59.750
1
10
100

Test 8

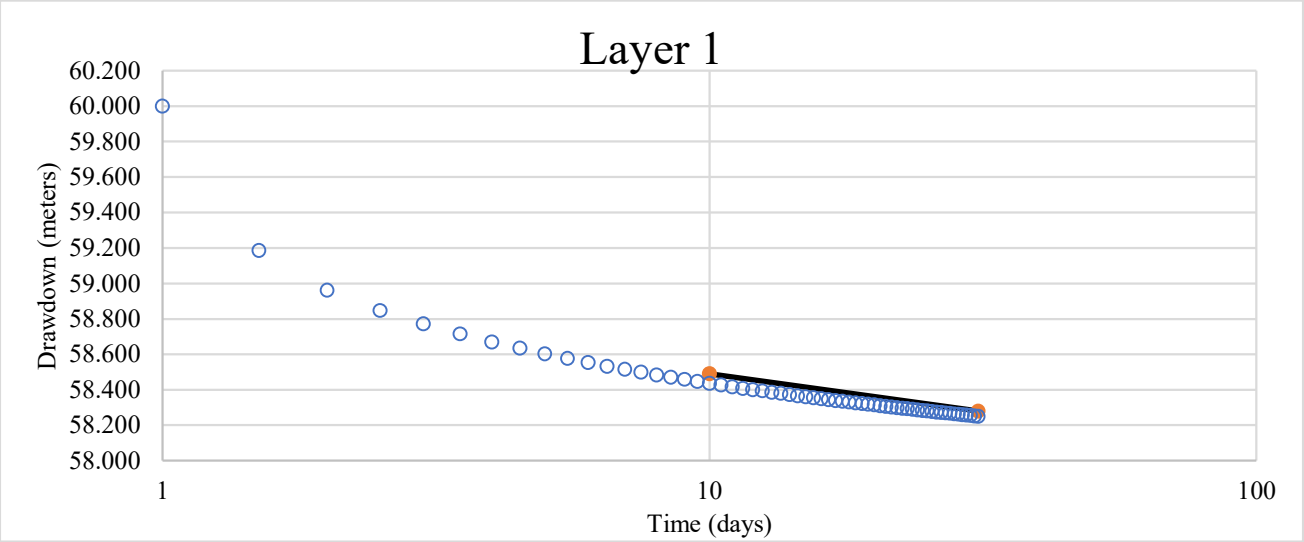
Layer 1
60.200
60.000
59.800
59.600
59.400
59.200
59.000
58.800
58.600
58.400
58.200
58.000
Drawdown (meters)
1
10
100
Time (days)

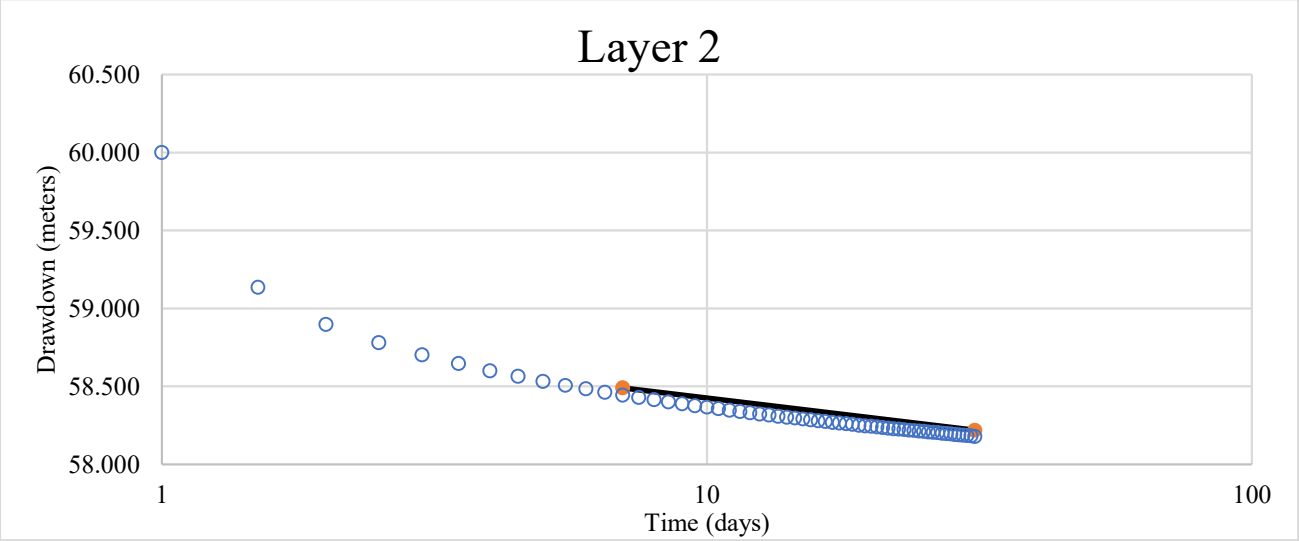
Layer 2
60.500
60.000
59.500
59.000
58.500
58.000
Drawdown (meters)
1
10
100
Time (days)

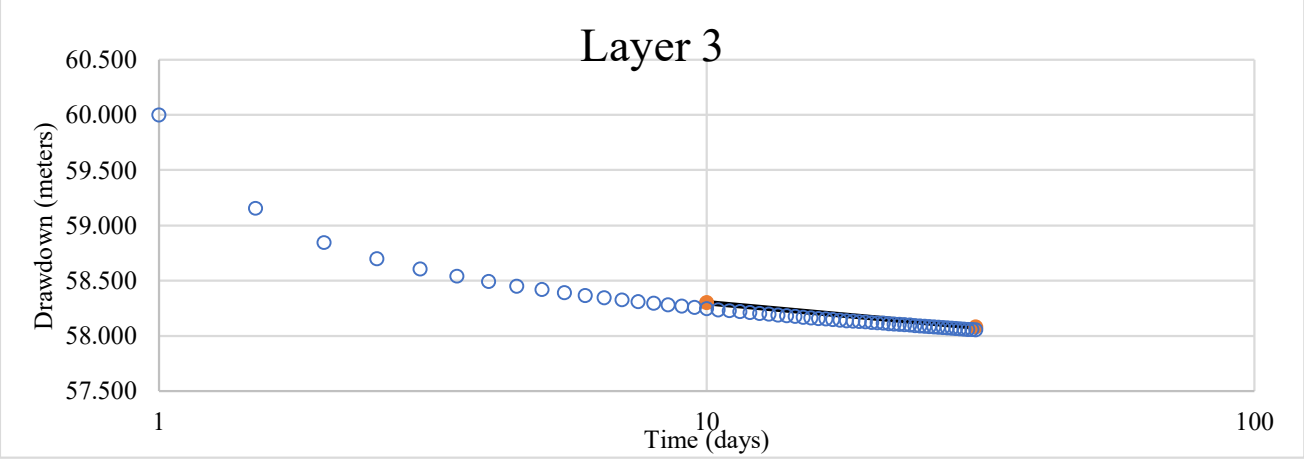
Layer 3
60.500
60.000
59.500
59.000
58.500
58.000
57.500
Drawdown (meters)
1
10
100
Time (days)

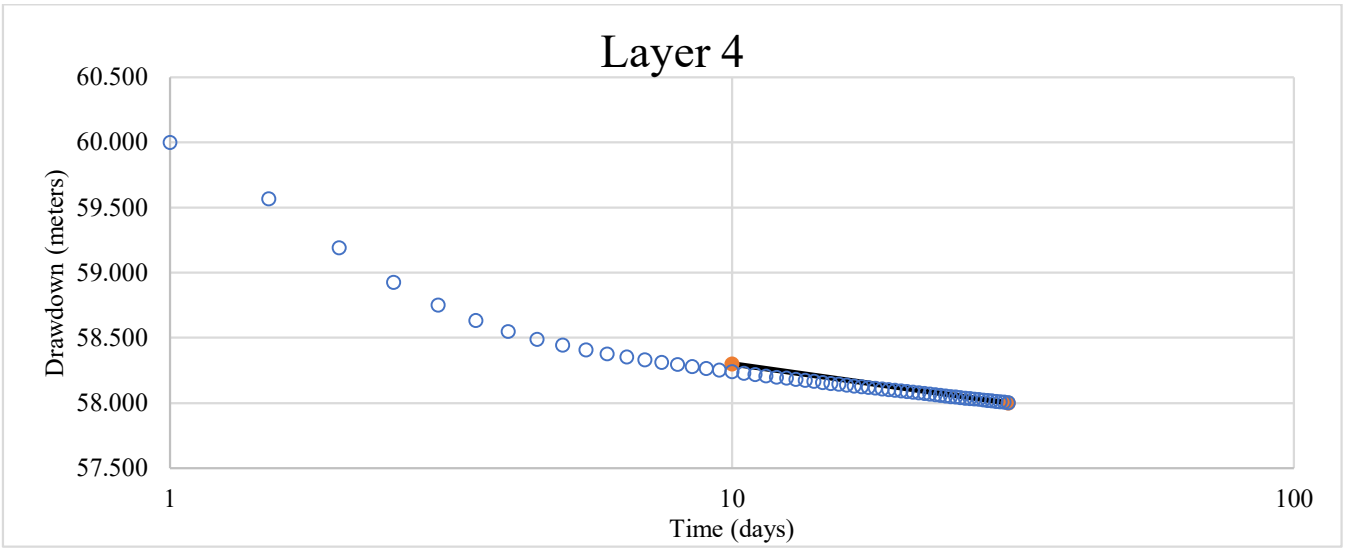
Layer 4
60.500
60.000
59.500
59.000
58.500
58.000
57.500
Drawdown (meters)
1
10
100
Time (days)

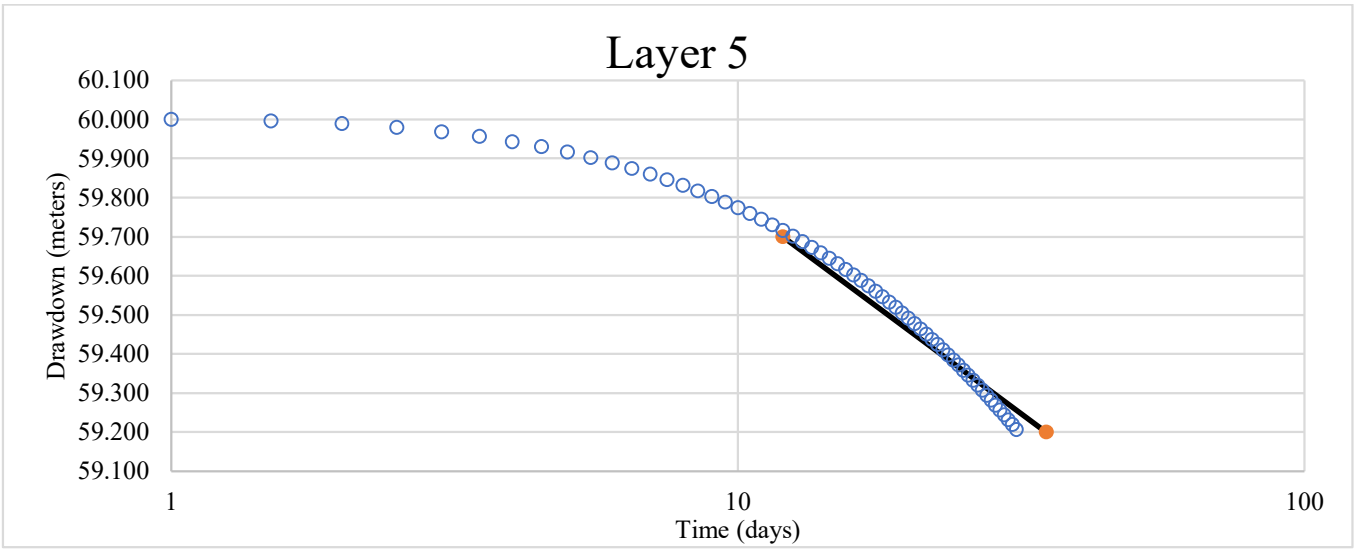
Layer 5
60.100
60.000
59.900
59.800
59.700
59.600
59.500
59.400
59.300
59.200
59.100
Drawdown (meters)
1
10
100
Time (days)

Test 9

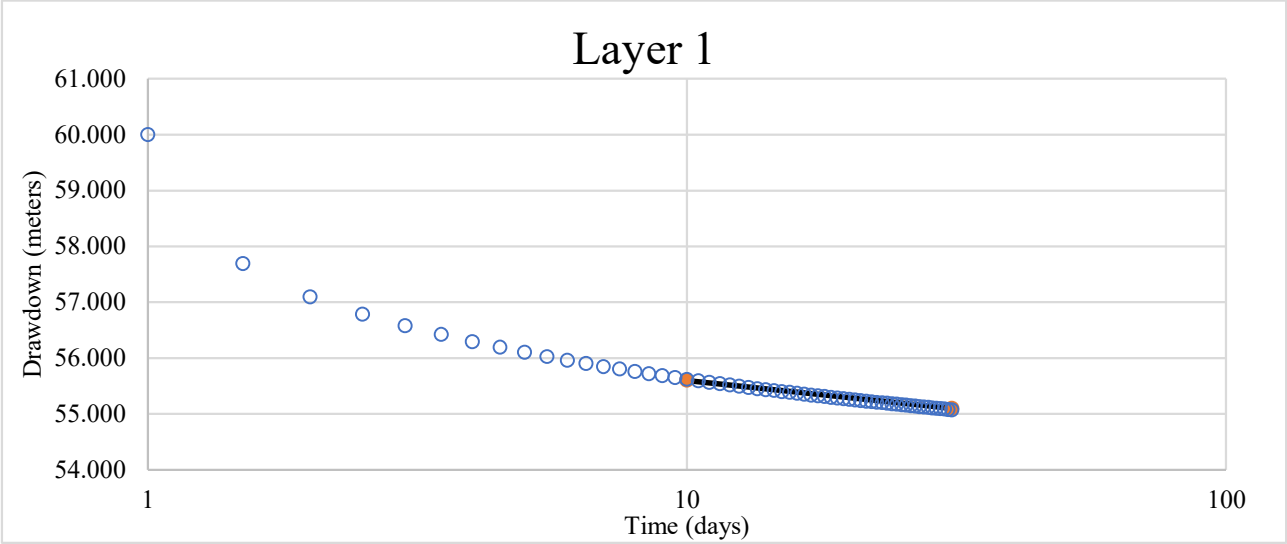
Layer 1
61.000
60.000
59.000
58.000
57.000
56.000
55.000
54.000
Drawdown (meters)
1
10
100
Time (days)

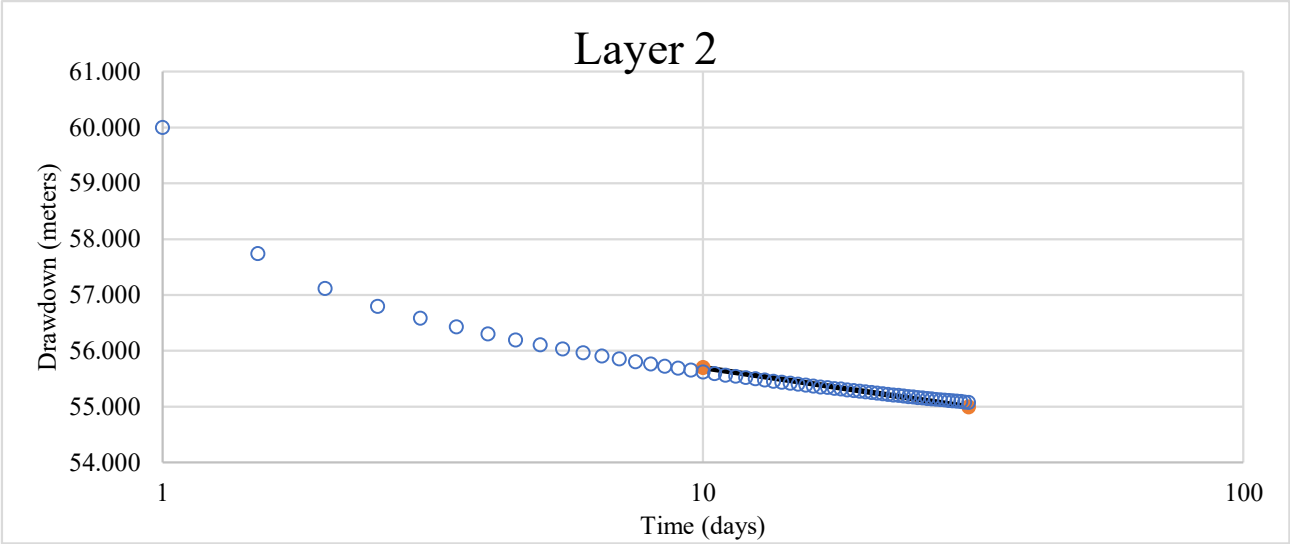
Layer 2
61.000
60.000
59.000
58.000
57.000
56.000
55.000
54.000
Drawdown (meters)
1
10
100
Time (days)

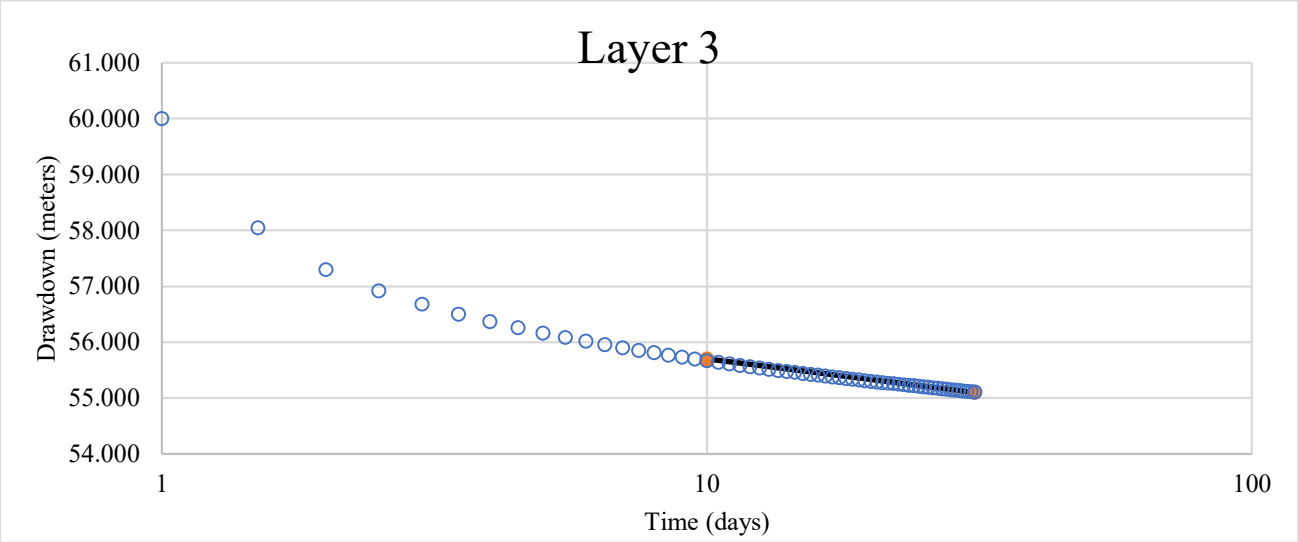
Layer 3
61.000
60.000
59.000
58.000
57.000
56.000
55.000
54.000
Drawdown (meters)
1
10
100
Time (days)

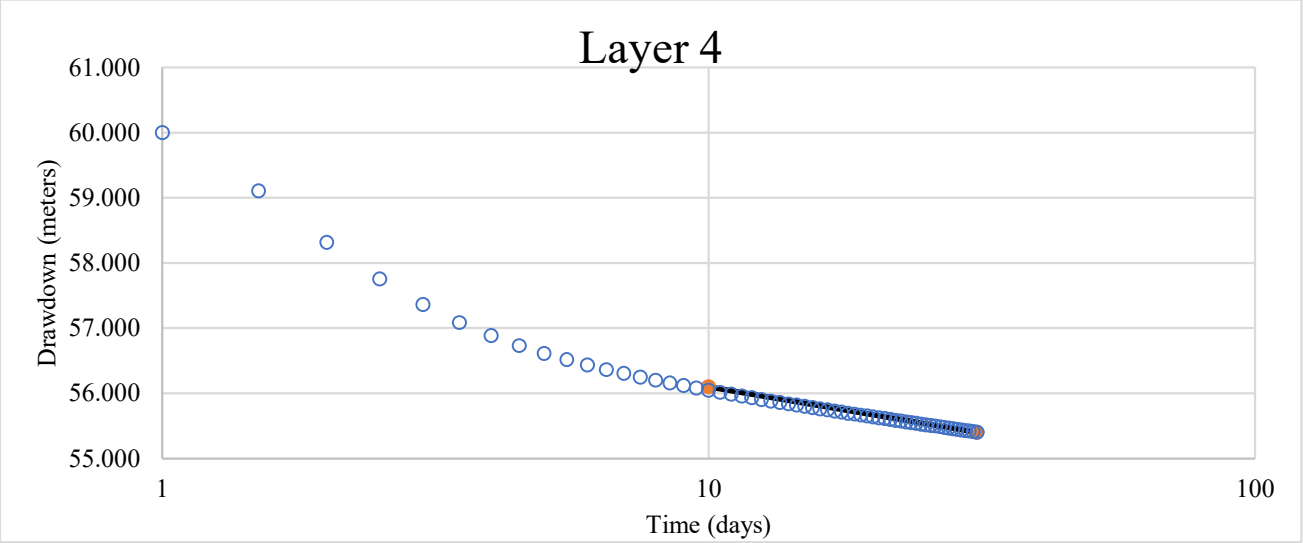
Layer 4
61.000
60.000
59.000
58.000
57.000
56.000
55.000
Drawdown (meters)
1
10
100
Time (days)

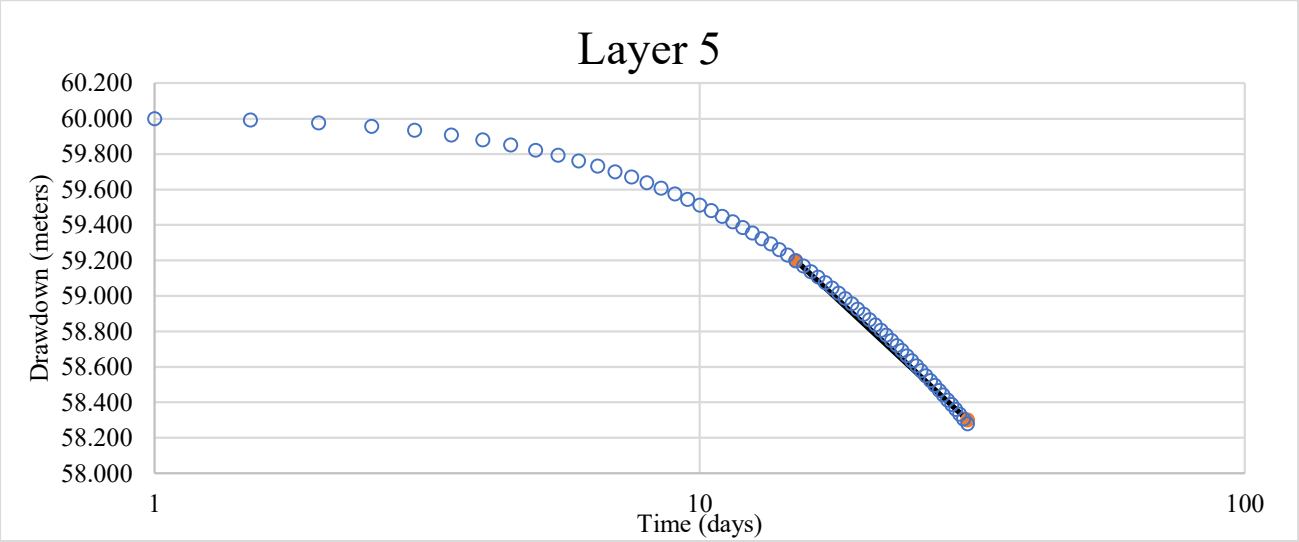
Layer 5
60.200
60.000
59.800
59.600
59.400
59.200
59.000
58.800
58.600
58.400
58.200
58.000
Drawdown (meters)
1
10
100
Time (days)

Test 10

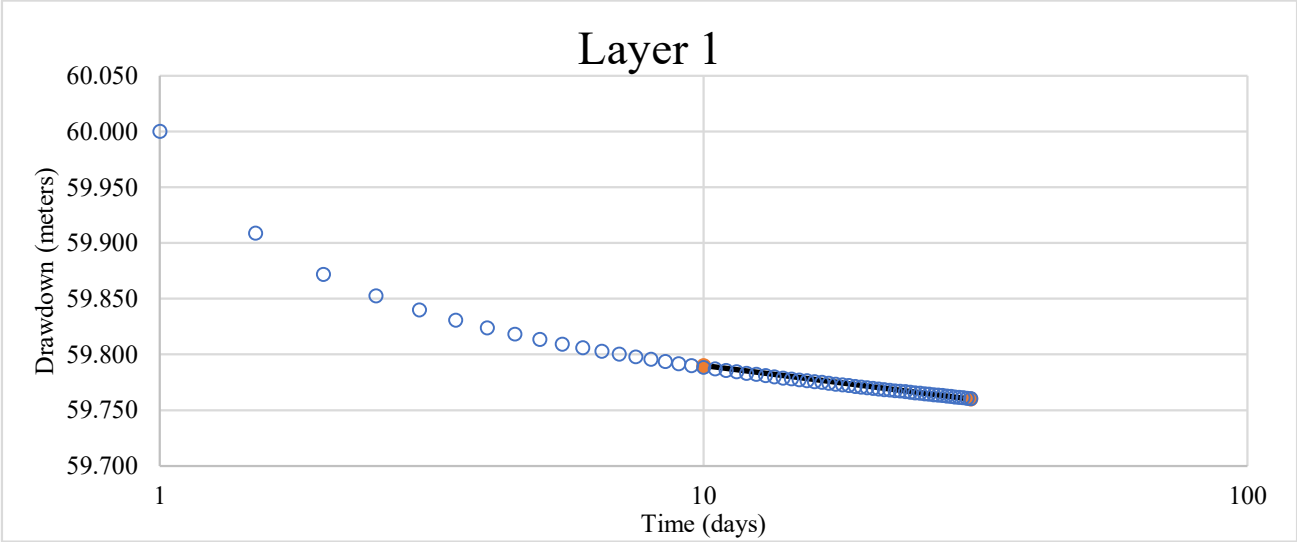
Layer 1
60.050
60.000
59.950
59.900
59.850
59.800
59.750
59.700
Drawdown (meters)
1
10
100
Time (days)

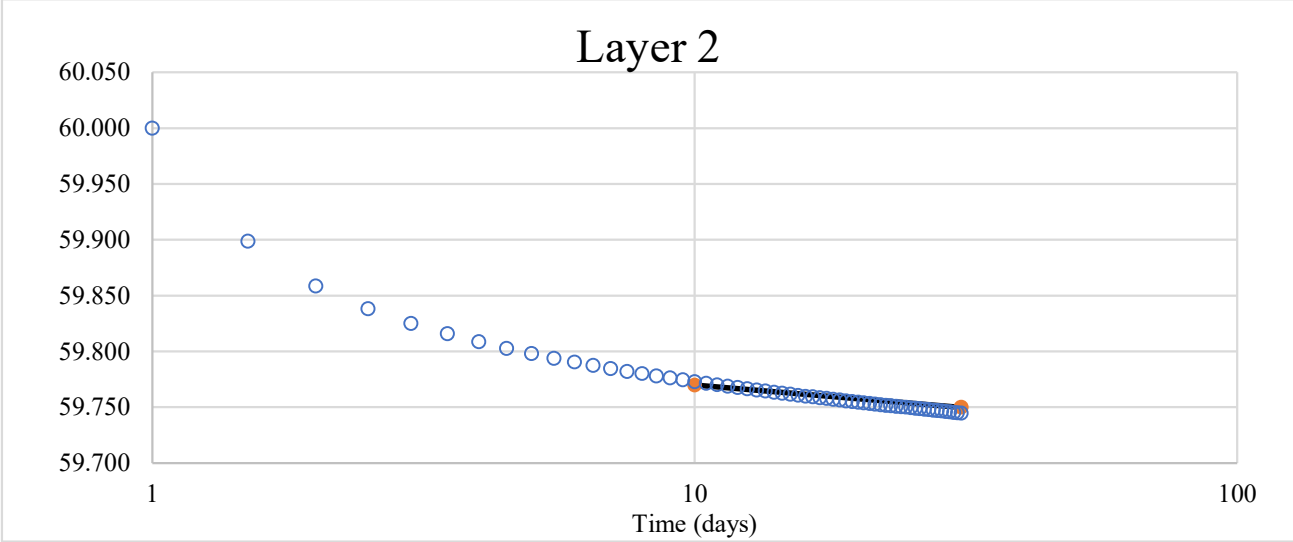
Layer 2
60.050
60.000
59.950
59.900
59.850
59.800
59.750
59.700
1
10
100
Time (days)

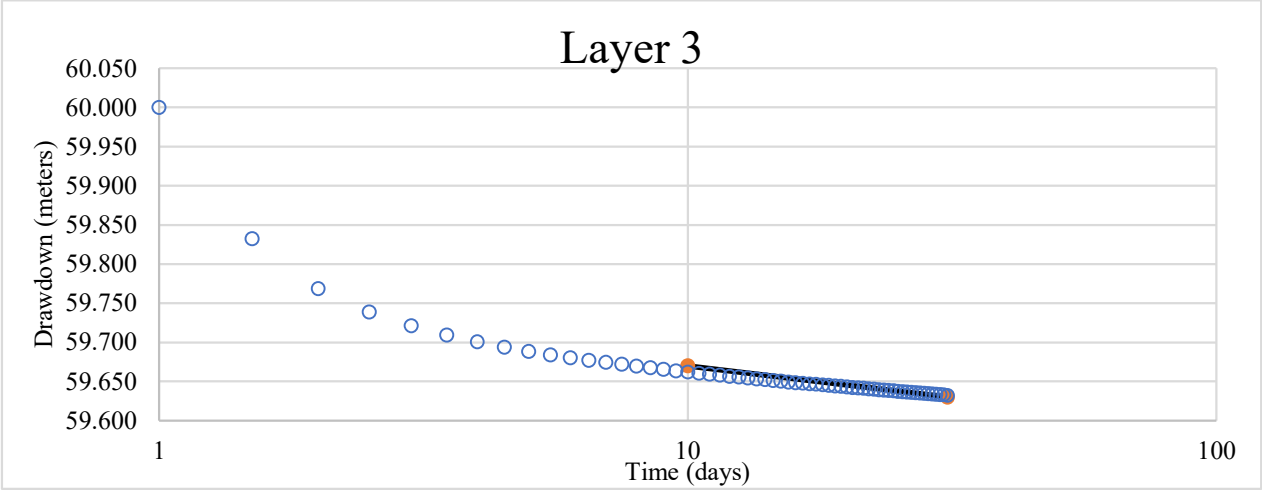
Layer 3
60.050
60.000
59.950
59.900
59.850
59.800
59.750
59.700
59.650
59.600
Drawdown (meters)
1
10
100
Time (days)

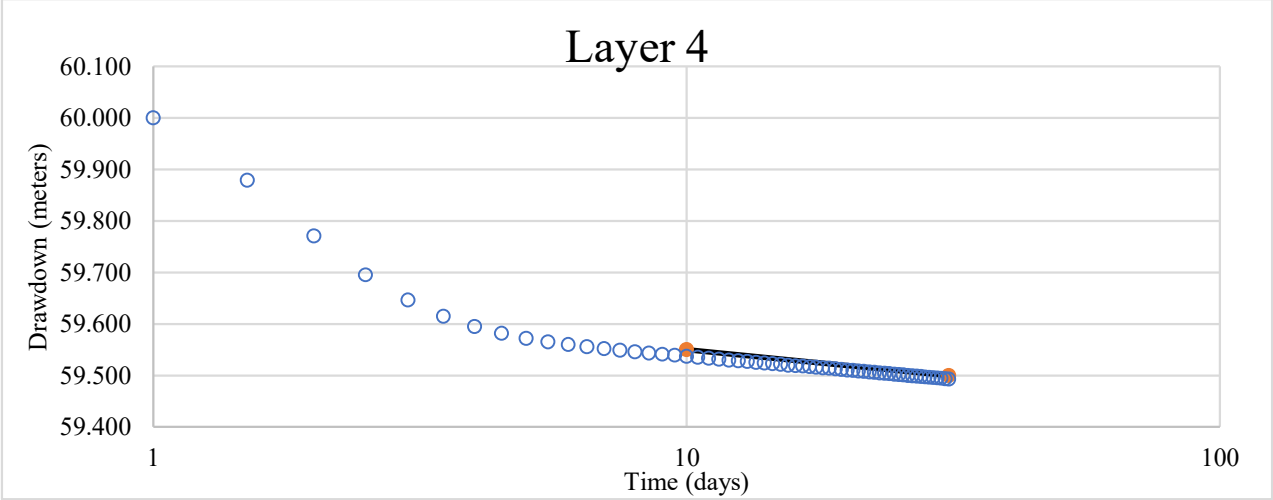
Layer 4
60.100
60.000
59.900
59.800
59.700
59.600
59.500
59.400
Drawdown (meters)
1
10
100
Time (days)

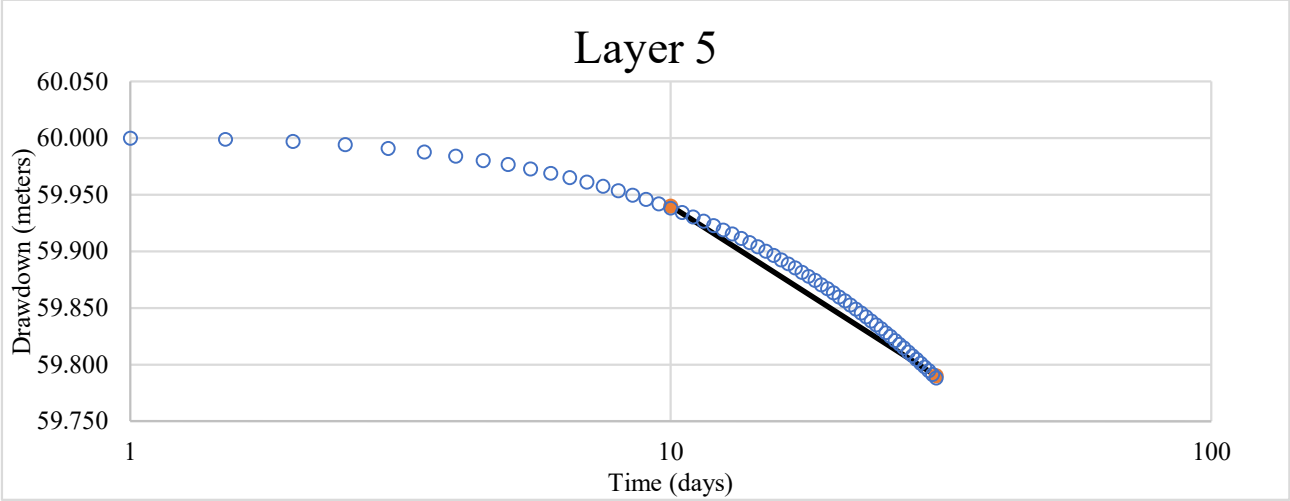
Layer 5
60.050
60.000
59.950
59.900
59.850
59.800
59.750
Drawdown (meters)
1
10
100
Time (days)

Test 11

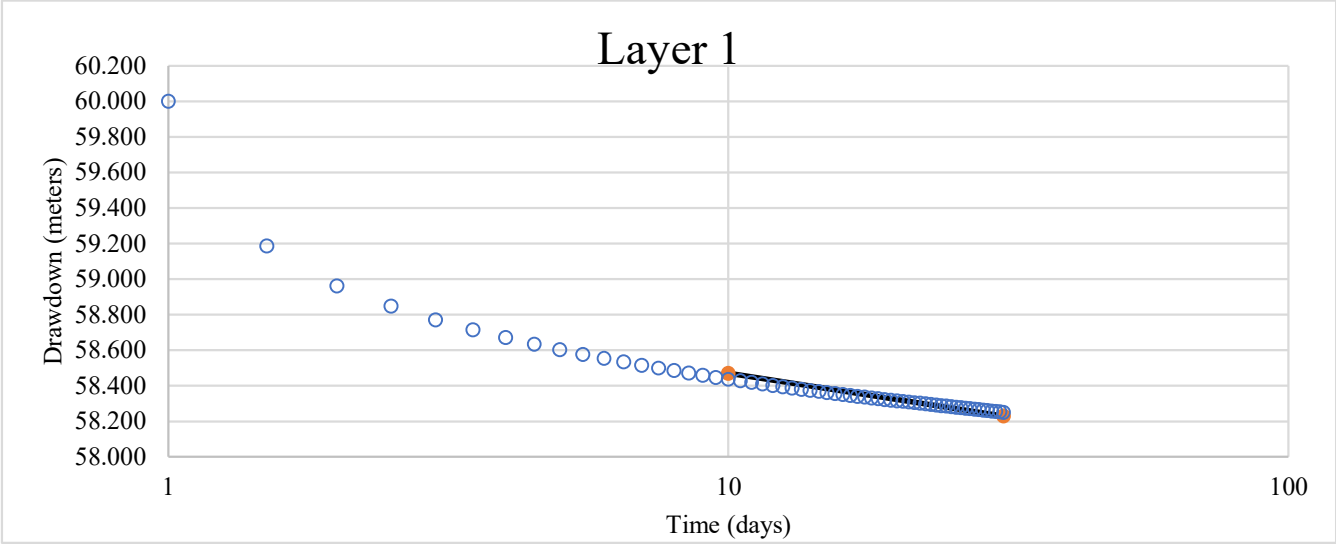
Layer 1
60.200
60.000
59.800
59.600
59.400
59.200
59.000
58.800
58.600
58.400
58.200
58.000
Drawdown (meters)
1
10
100
Time (days)

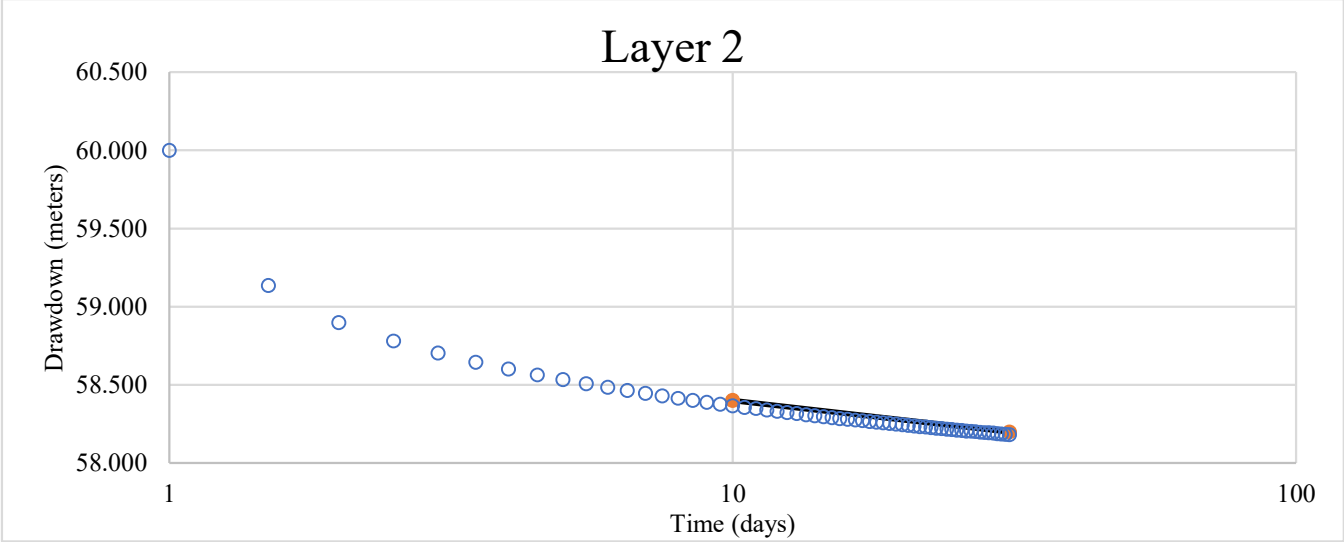
Layer 2
60.500
60.000
59.500
59.000
58.500
58.000
Drawdown (meters)
1
10
100
Time (days)

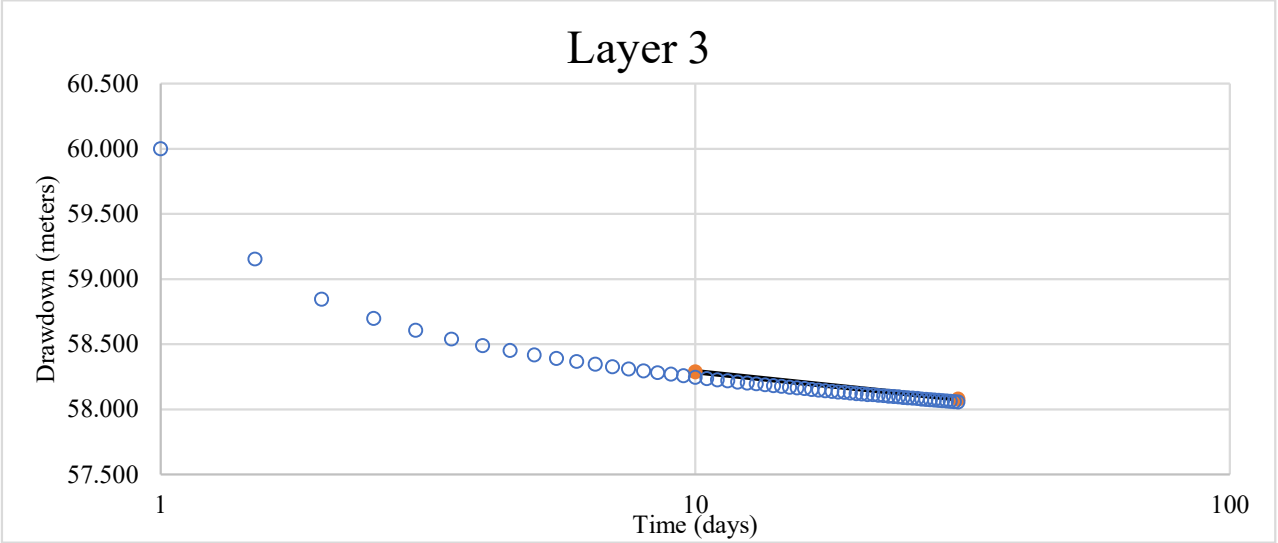
Layer 3
60.500
60.000
59.500
59.000
58.500
58.000
57.500
Drawdown (meters)
1
10
100
Time (days)

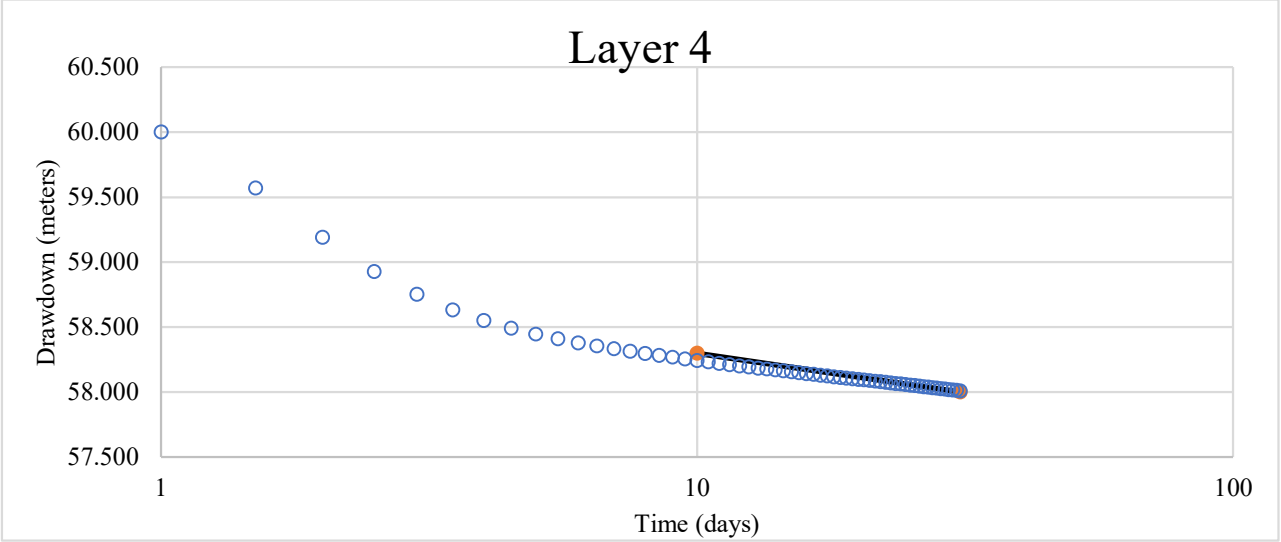
Layer 4
60.500
60.000
59.500
59.000
58.500
58.000
57.500
Drawdown (meters)
1
10
100
Time (days)

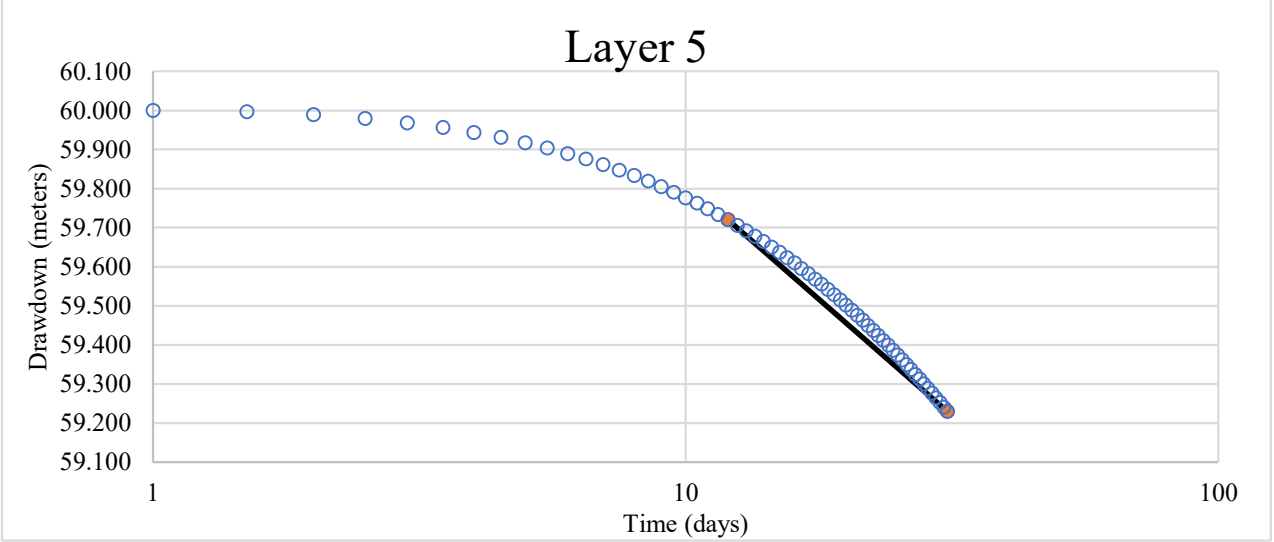
Layer 5
60.100
60.000
59.900
59.800
59.700
59.600
59.500
59.400
59.300
59.200
59.100
Drawdown (meters)
1
10
100
Time (days)

Test 12

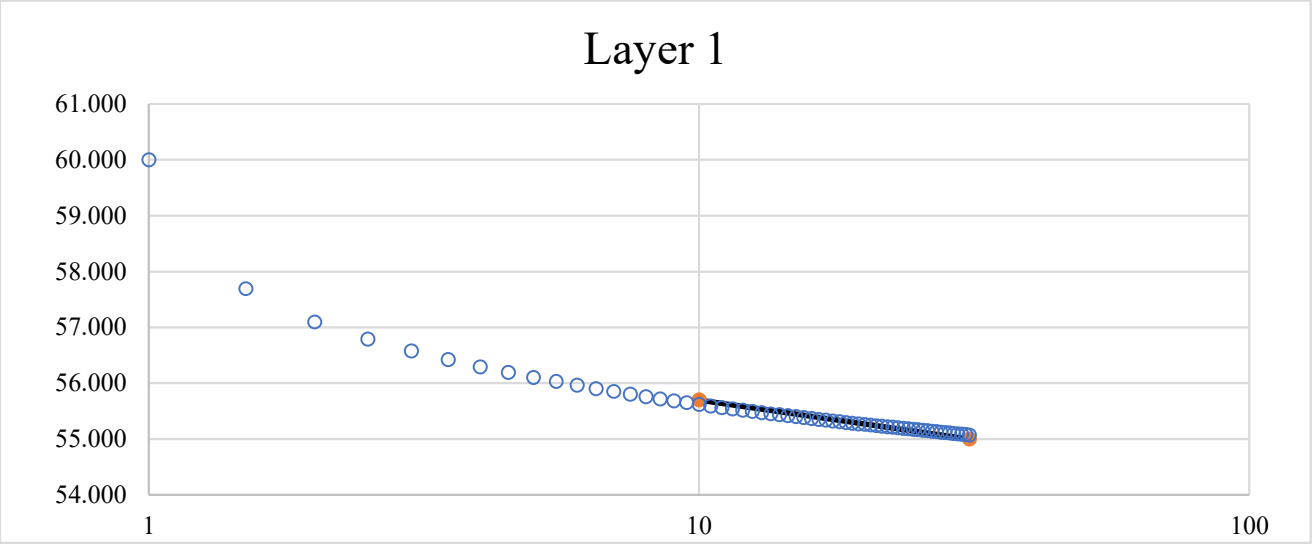
Layer 1
61.000
60.000
59.000
58.000
57.000
56.000
55.000
54.000
1
10
100

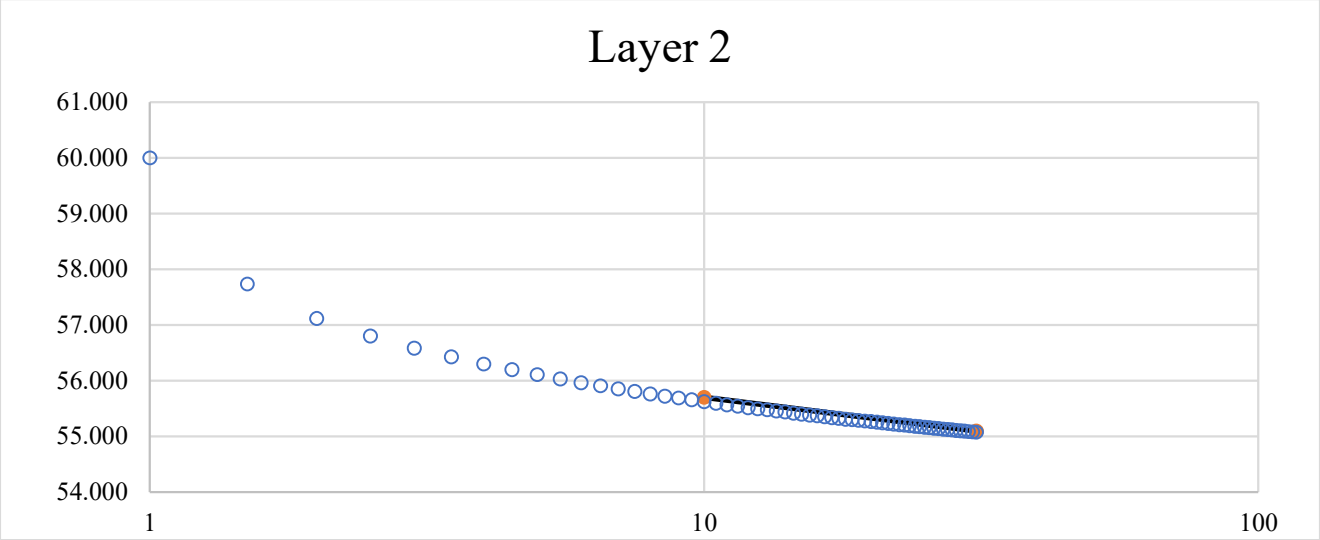
Layer 2
61.000
60.000
59.000
58.000
57.000
56.000
55.000
54.000
1
10
100

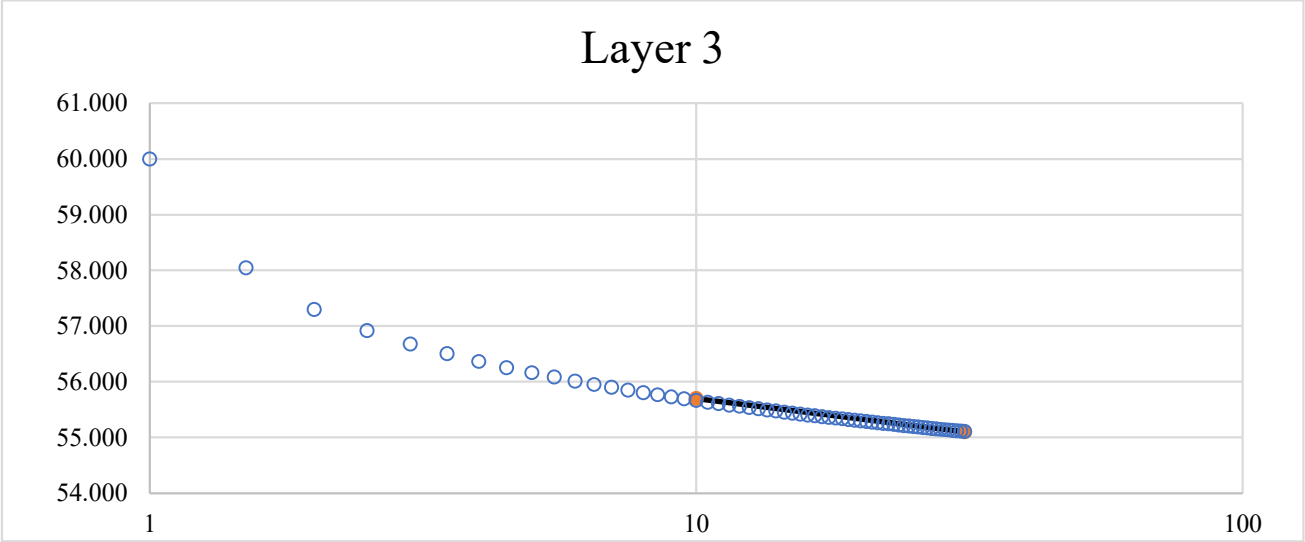
Layer 3
61.000
60.000
59.000
58.000
57.000
56.000
55.000
54.000
1
10
100

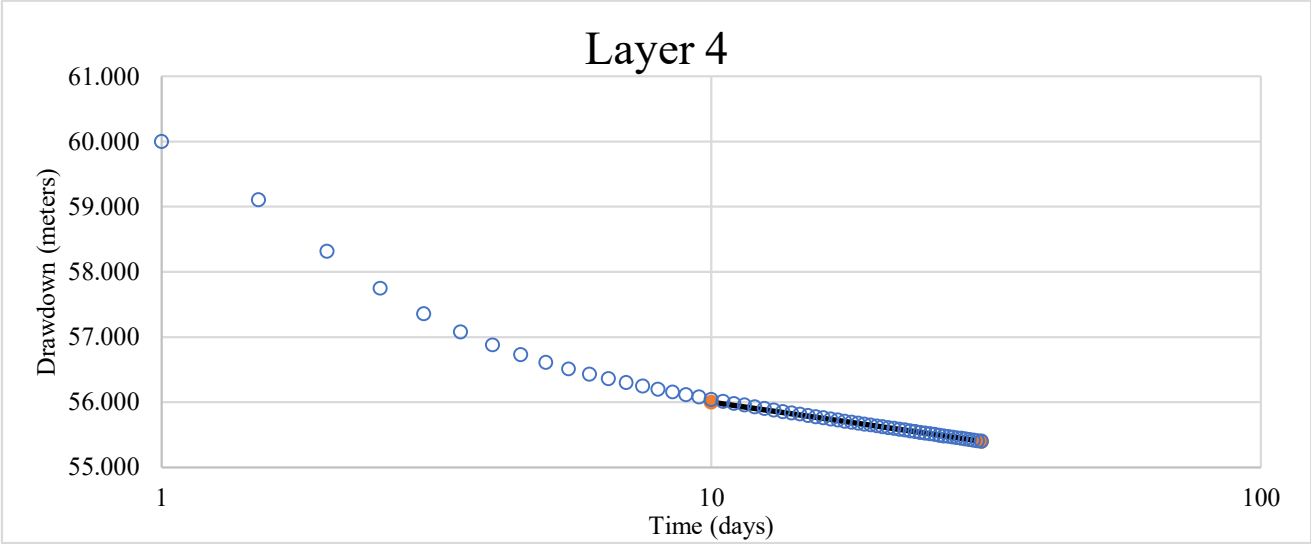
Layer 4
Drawdown (meters)
61.000
60.000
59.000
58.000
57.000
56.000
55.000
1
10
100
Time (days)

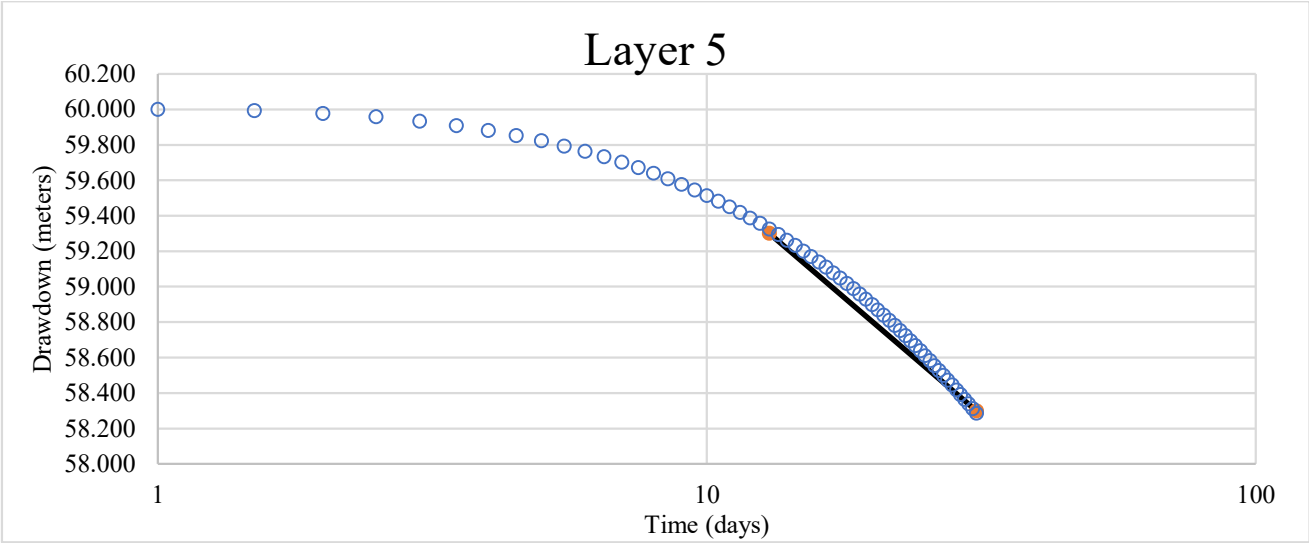
Layer 5
Drawdown (meters)
60.200
60.000
59.800
59.600
59.400
59.200
59.000
58.800
58.600
58.400
58.200
58.000
1
10
100
Time (days)

Test 13

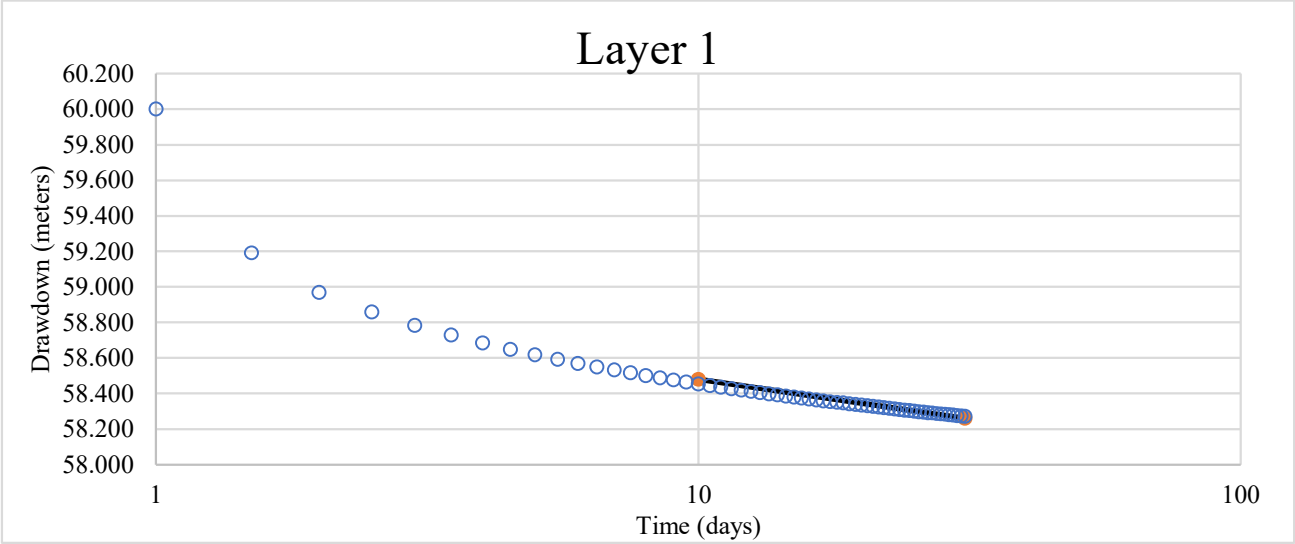
Layer 1
60.200
60.000
59.800
59.600
59.400
59.200
59.000
58.800
58.600
58.400
58.200
58.000
Drawdown (meters)
1
10
100
Time (days)

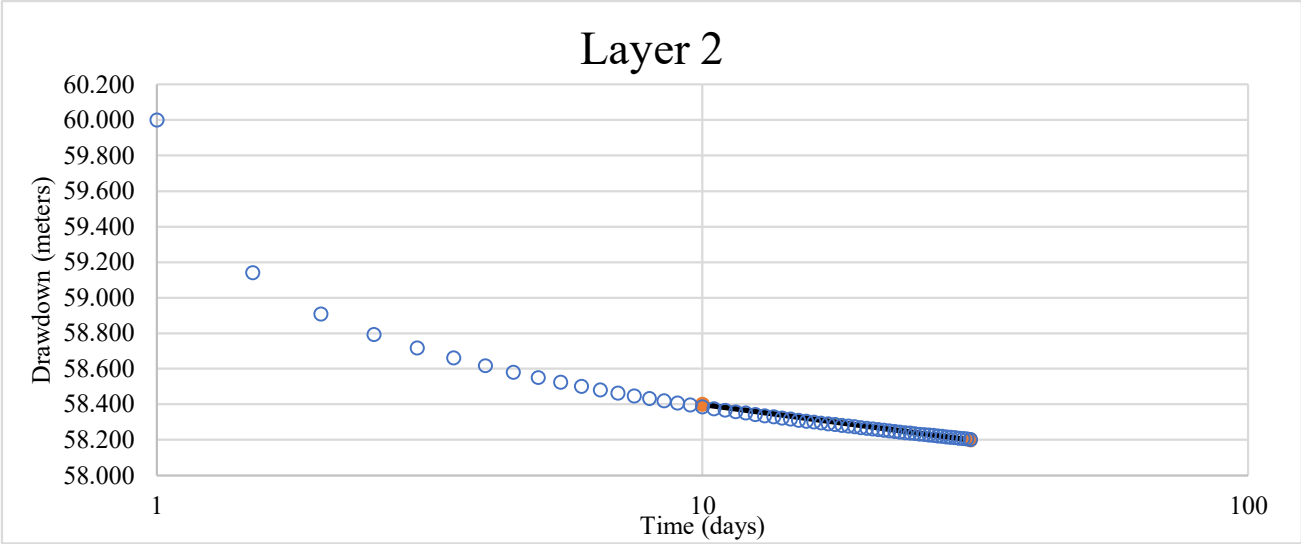
Layer 2
60.200
60.000
59.800
59.600
59.400
59.200
59.000
58.800
58.600
58.400
58.200
58.000
Drawdown (meters)
1
10
100
Time (days)

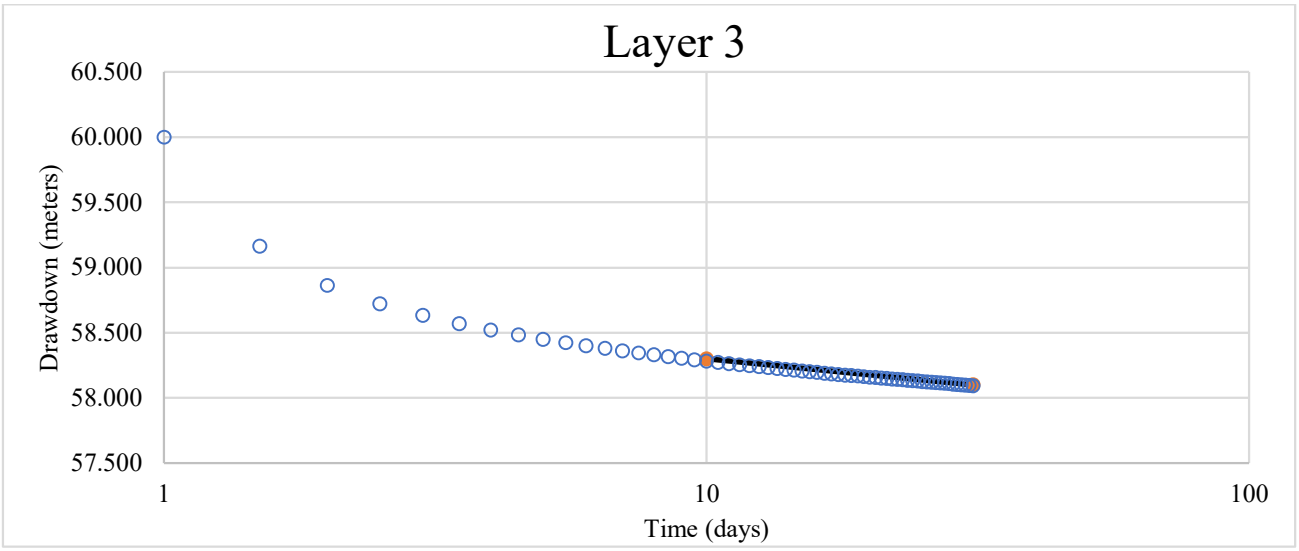
Layer 3
60.500
60.000
59.500
59.000
58.500
58.000
57.500
Drawdown (meters)
1
10
100
Time (days)

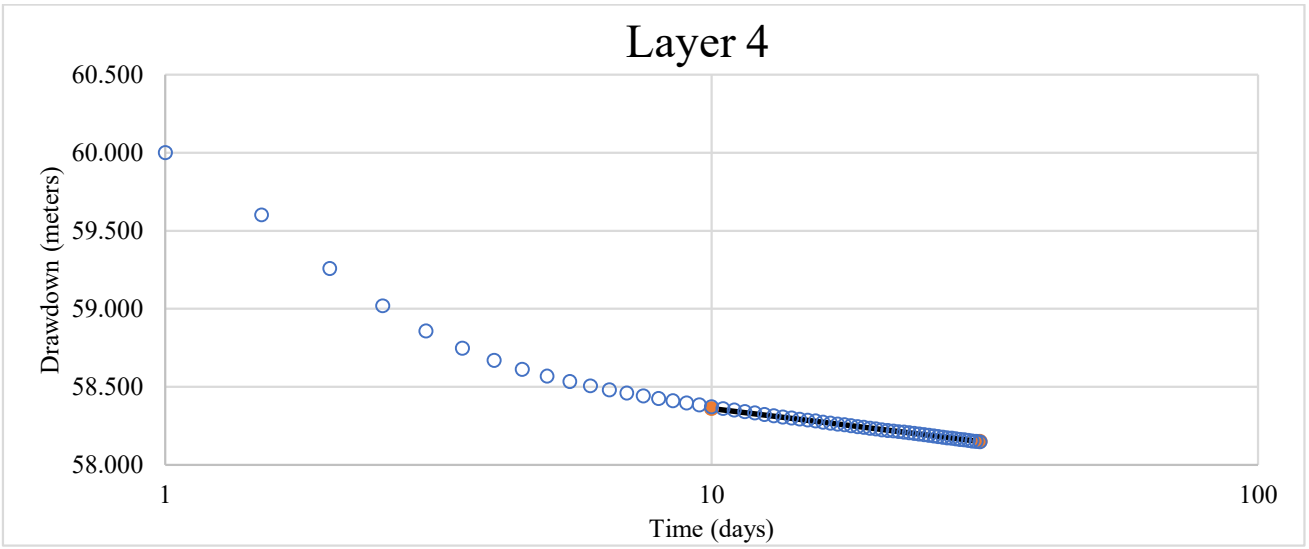
Layer 4
60.500
60.000
59.500
59.000
58.500
58.000
Drawdown (meters)
1
10
100
Time (days)

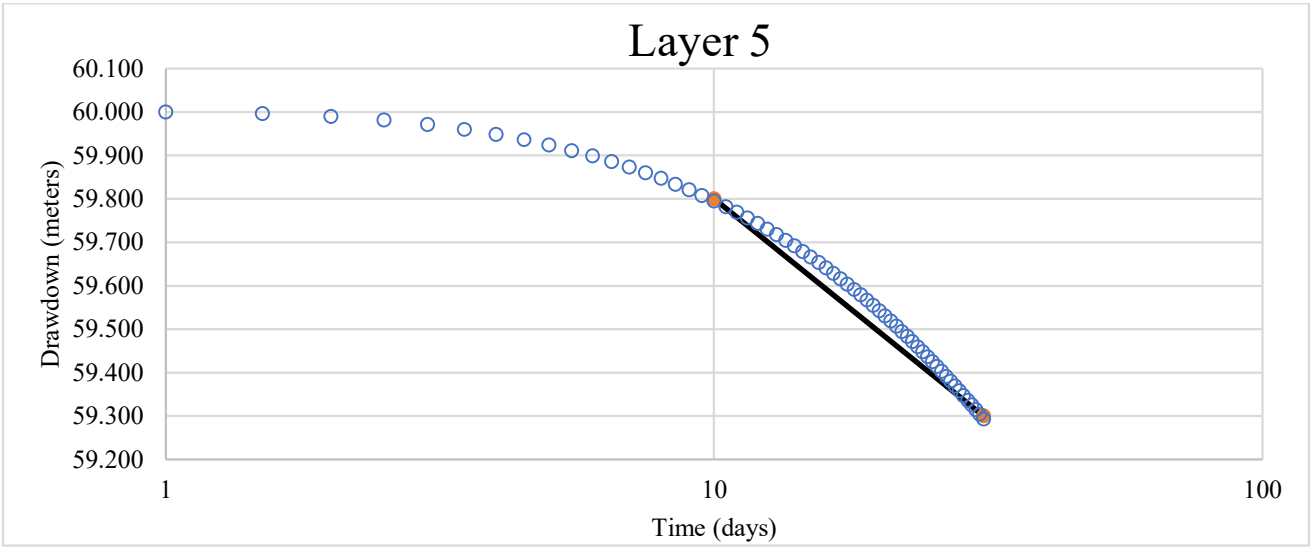
Layer 5
60.100
60.000
59.900
59.800
59.700
59.600
59.500
59.400
59.300
59.200
Drawdown (meters)
1
10
100
Time (days)

Test 14

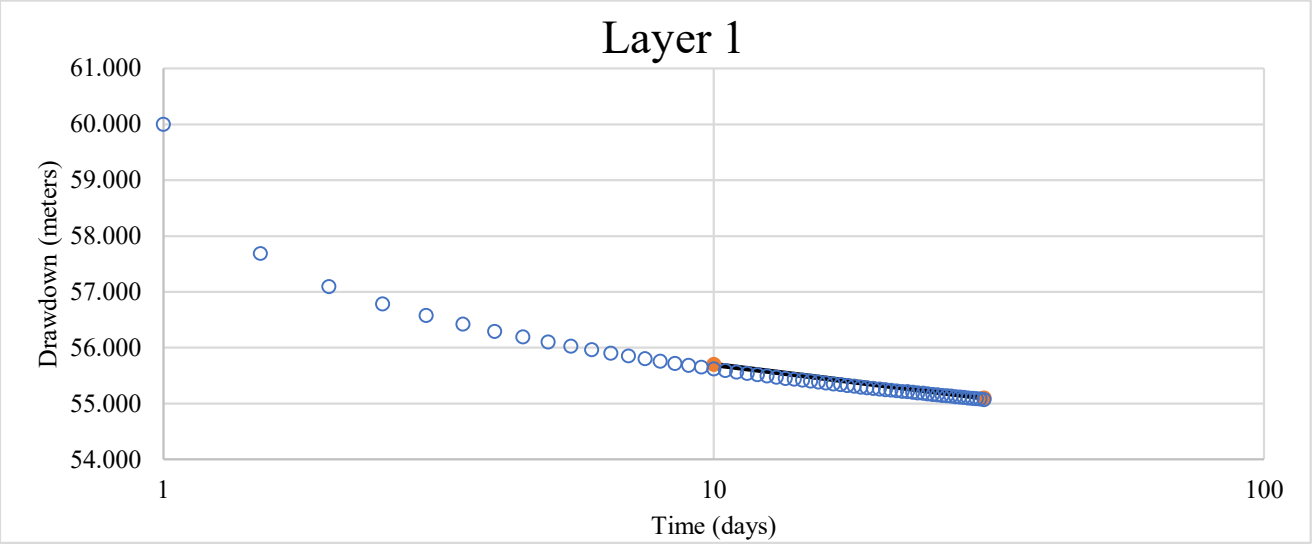
Layer 1
61.000
60.000
59.000
58.000
57.000
56.000
55.000
54.000
Drawdown (meters)
1
10
100
Time (days)

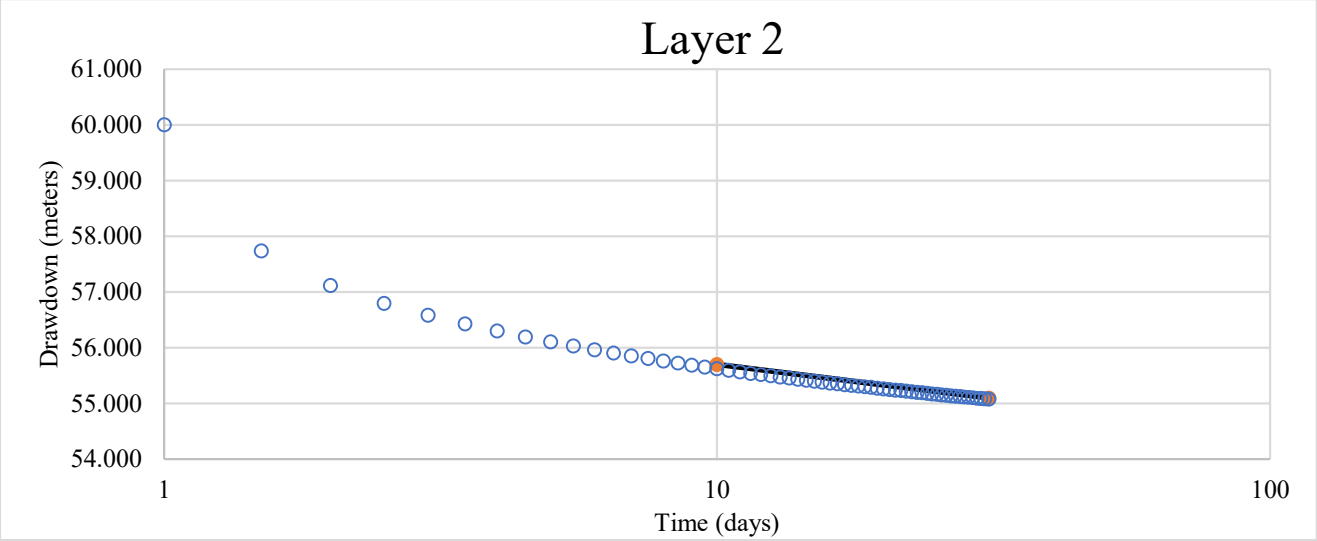
Layer 2
61.000
60.000
59.000
58.000
57.000
56.000
55.000
54.000
Drawdown (meters)
1
10
100
Time (days)

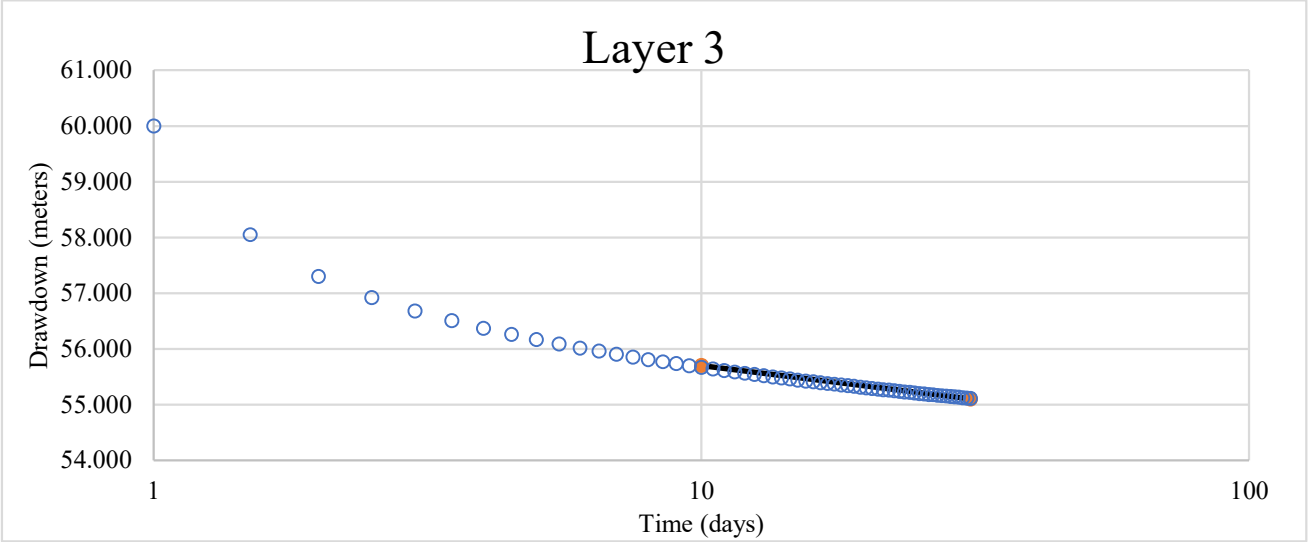
Layer 3
61.000
60.000
59.000
58.000
57.000
56.000
55.000
54.000
Drawdown (meters)
1
10
100
Time (days)

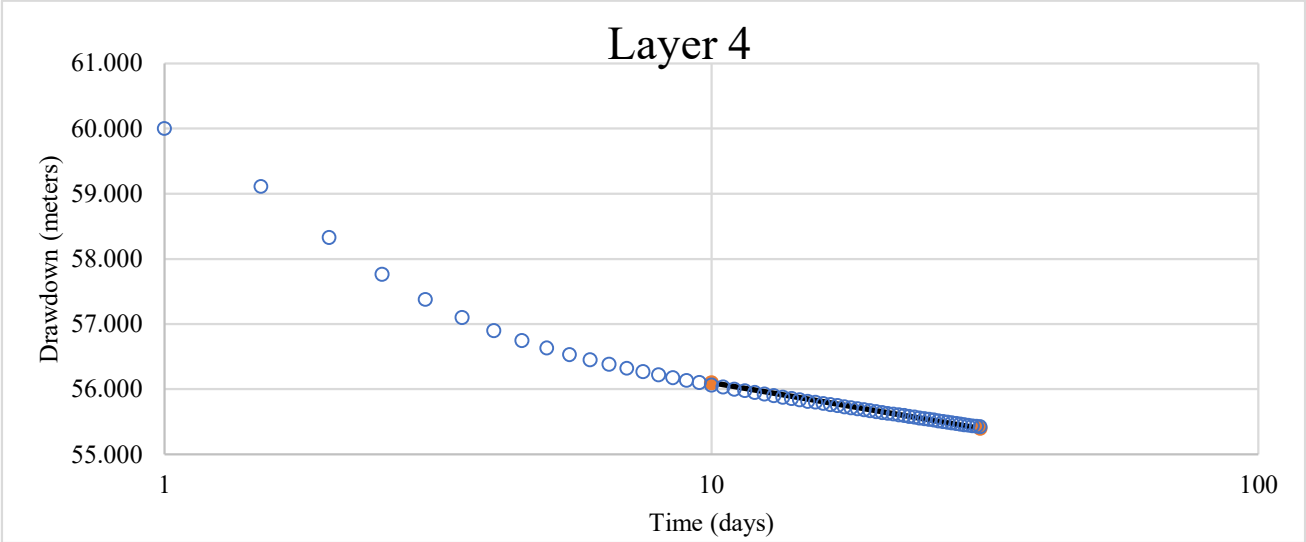
Layer 4
61.000
60.000
59.000
58.000
57.000
56.000
55.000
Drawdown (meters)
1
10
100
Time (days)

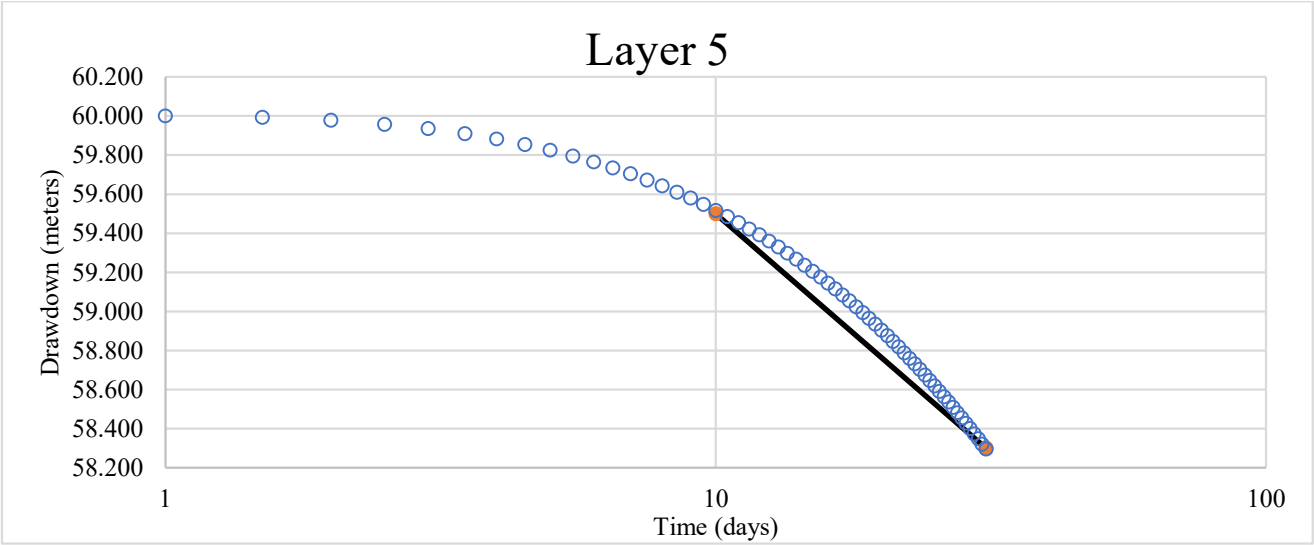
Layer 5
60.200
60.000
59.800
59.600
59.400
59.200
59.000
58.800
58.600
58.400
58.200
Drawdown (meters)
1
10
100
Time (days)

Test 15

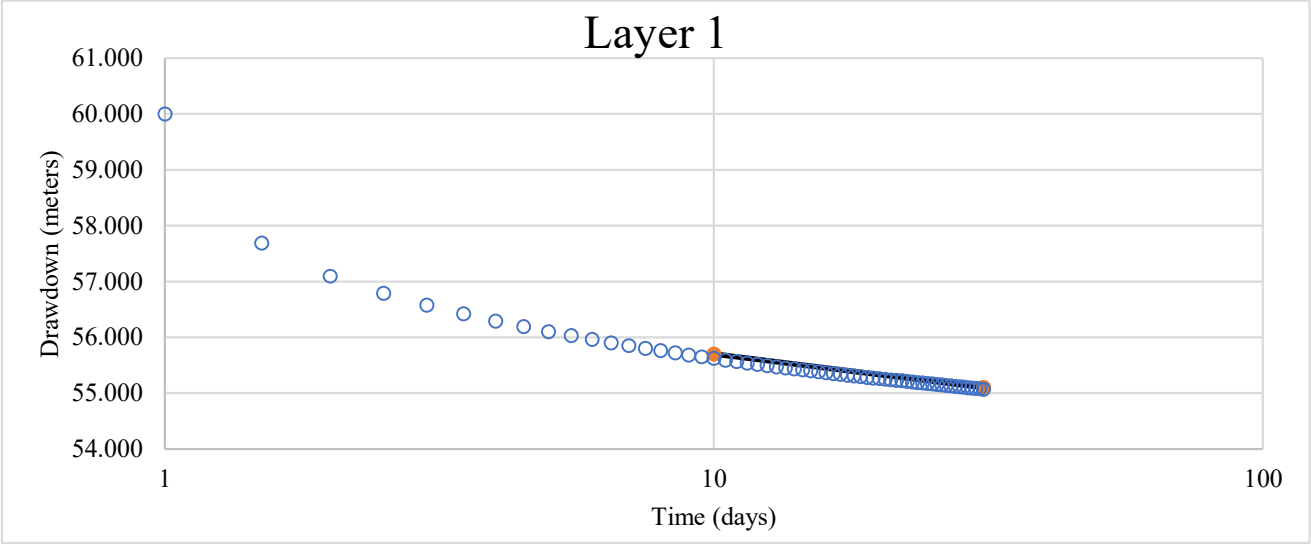
Layer 1
61.000
60.000
59.000
58.000
57.000
56.000
55.000
54.000
Drawdown (meters)
1
10
100
Time (days)

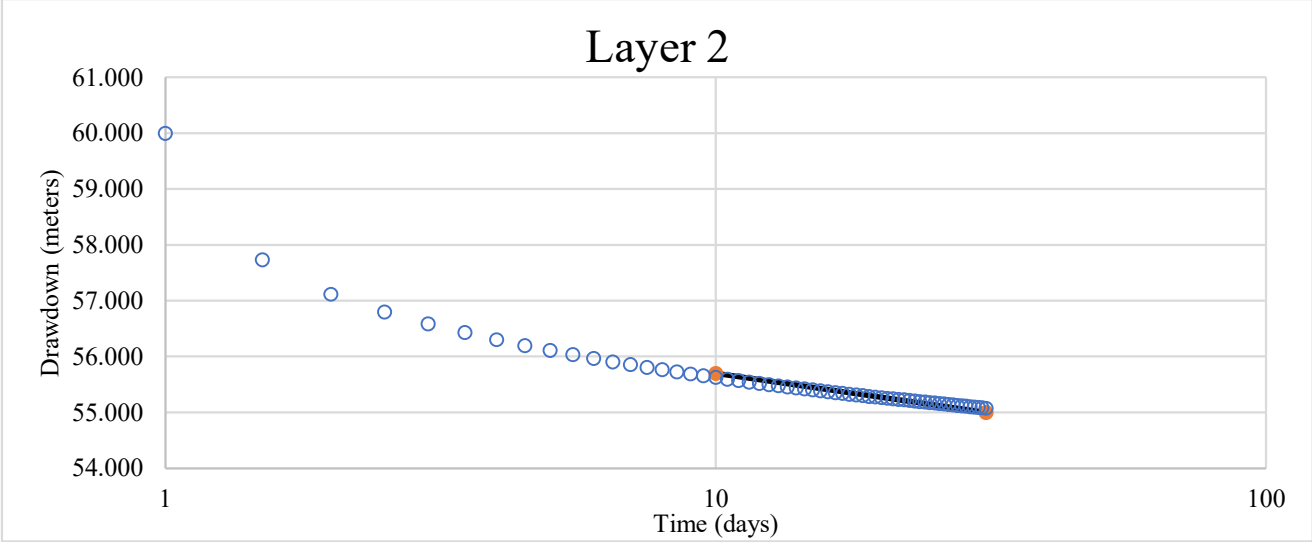
Layer 2
61.000
60.000
59.000
58.000
57.000
56.000
55.000
54.000
Drawdown (meters)
1
10
100
Time (days)

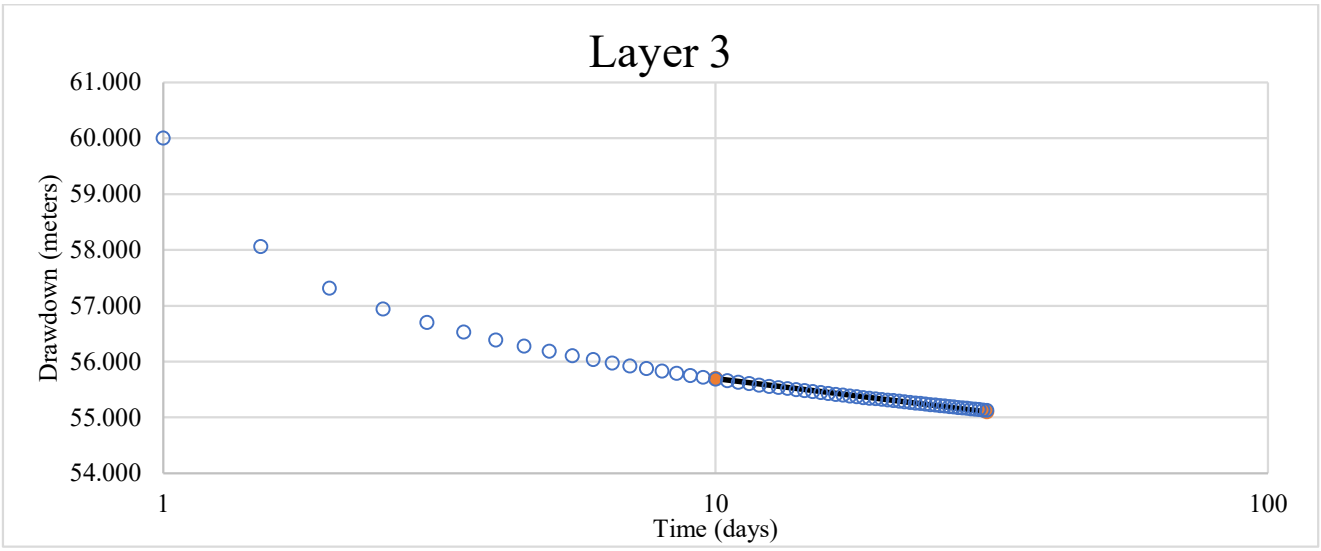
Layer 3
61.000
60.000
59.000
58.000
57.000
56.000
55.000
54.000
Drawdown (meters)
1
10
100
Time (days)

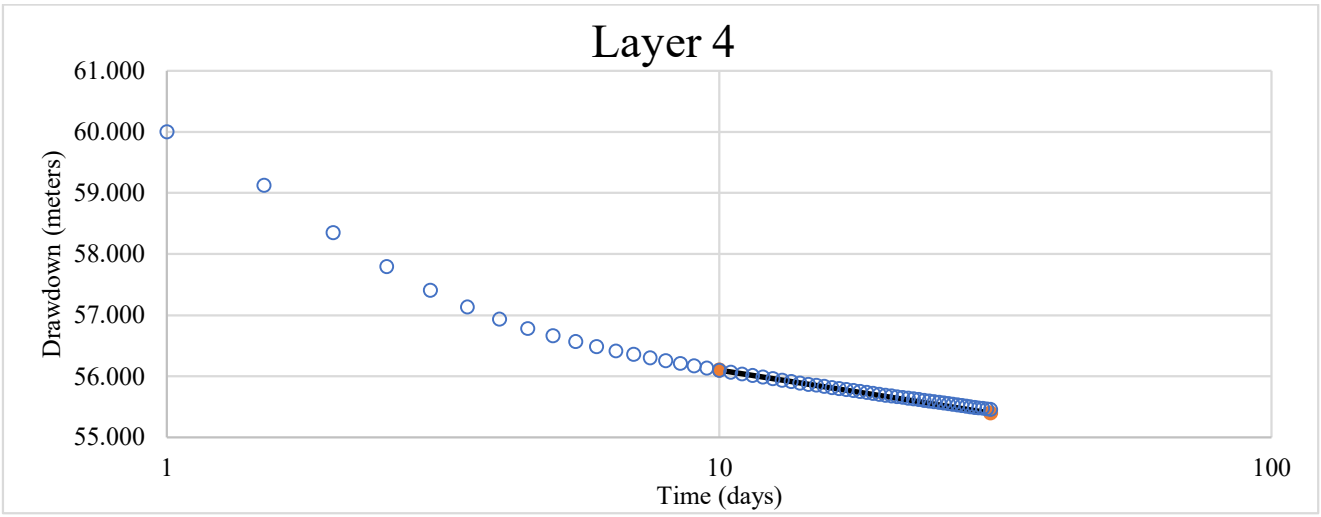
Layer 4
61.000
60.000
59.000
58.000
57.000
56.000
55.000
Drawdown (meters)
1
10
100
Time (days)

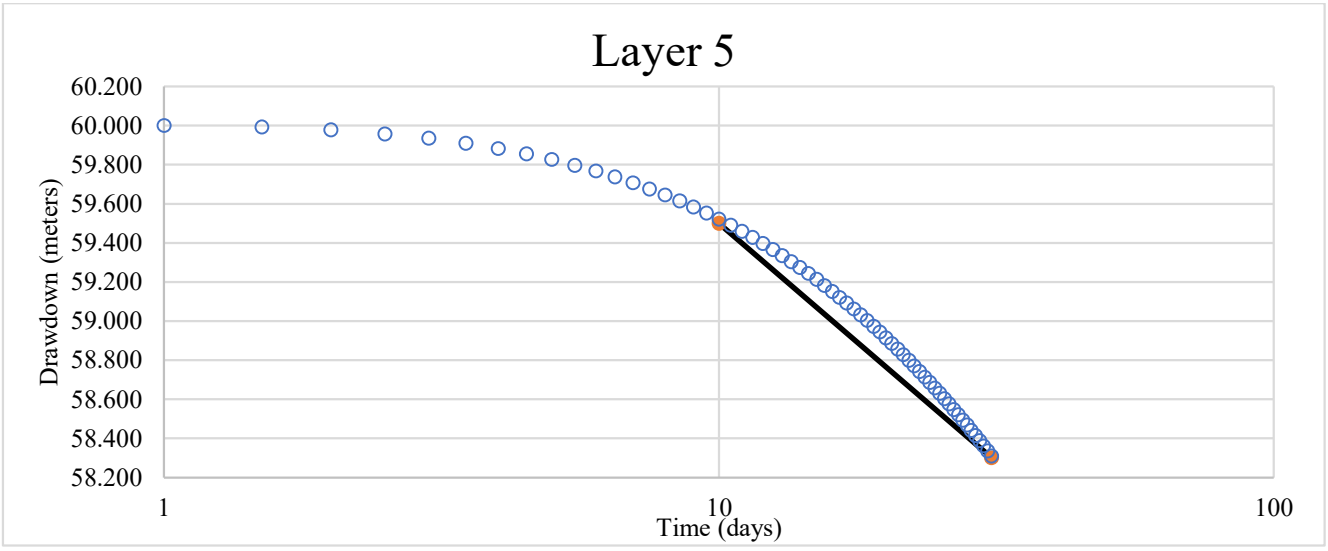
Layer 5
60.200
60.000
59.800
59.600
59.400
59.200
59.000
58.800
58.600
58.400
58.200
Drawdown (meters)
1
10
100
Time (days)

Test 16

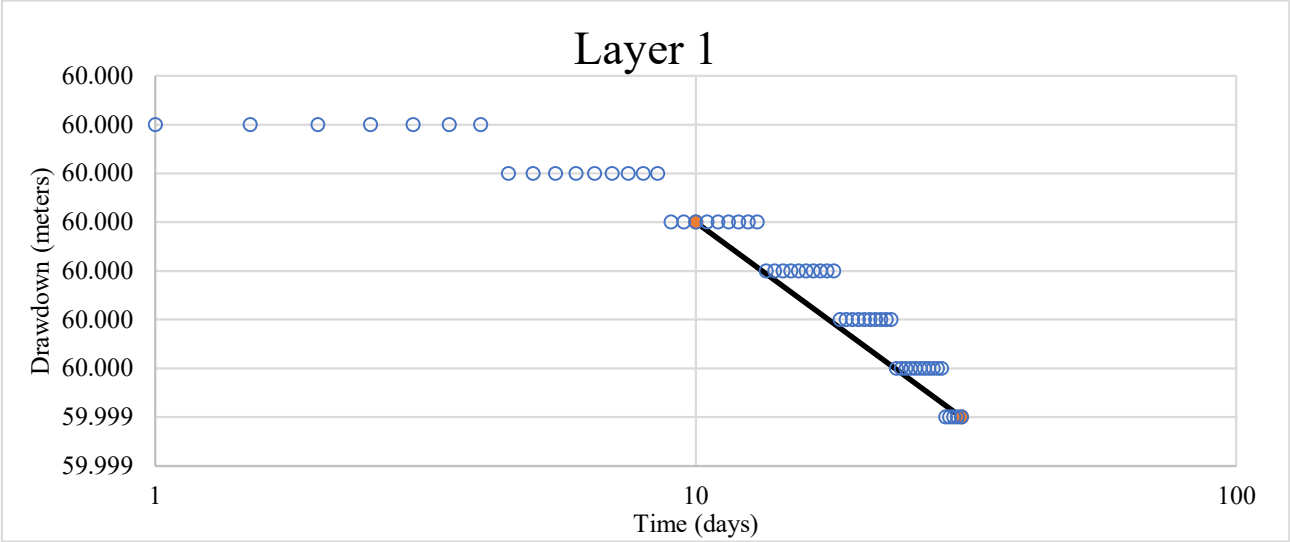
Layer 1
60.000
60.000
60.000
60.000
60.000
60.000
59.999
59.999
Drawdown (meters)
1
10
100
Time (days)

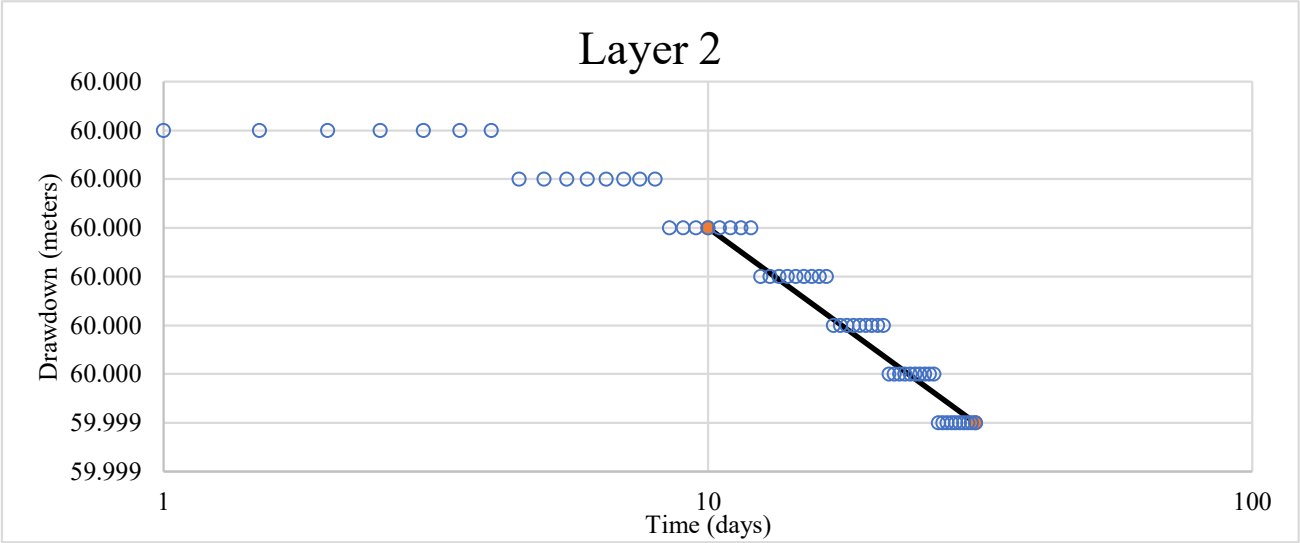
Layer 2
60.000
60.000
60.000
60.000
60.000
60.000
59.999
59.999
Drawdown (meters)
1
10
100
Time (days)

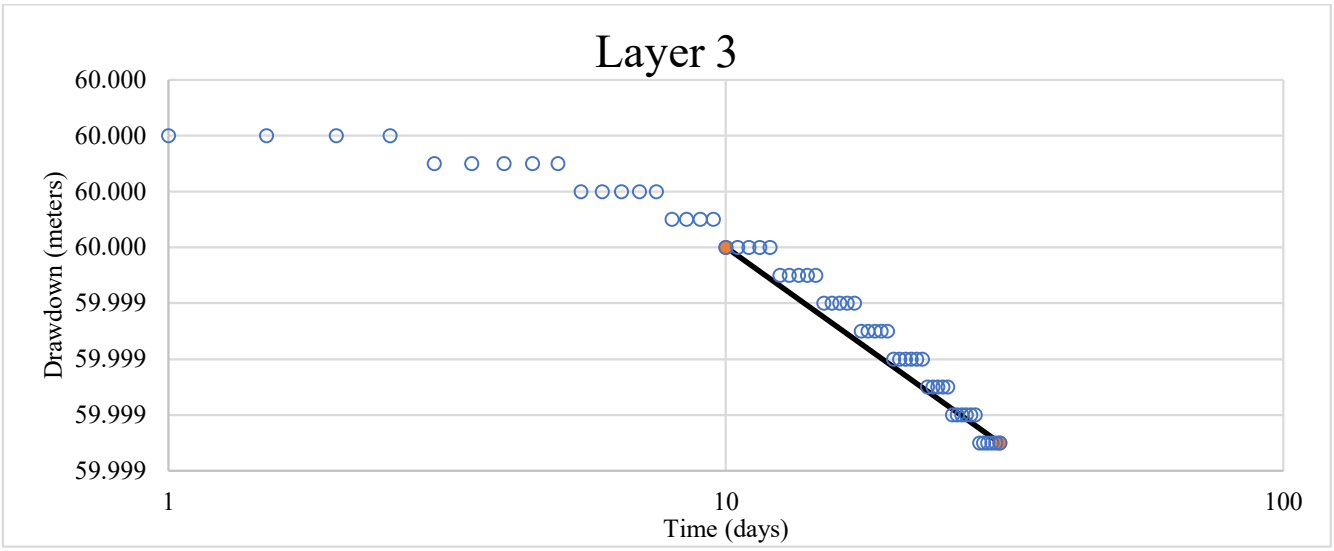
Layer 3
60.000
60.000
60.000
60.000
59.999
59.999
59.999
59.999
Drawdown (meters)
1
10
100
Time (days)

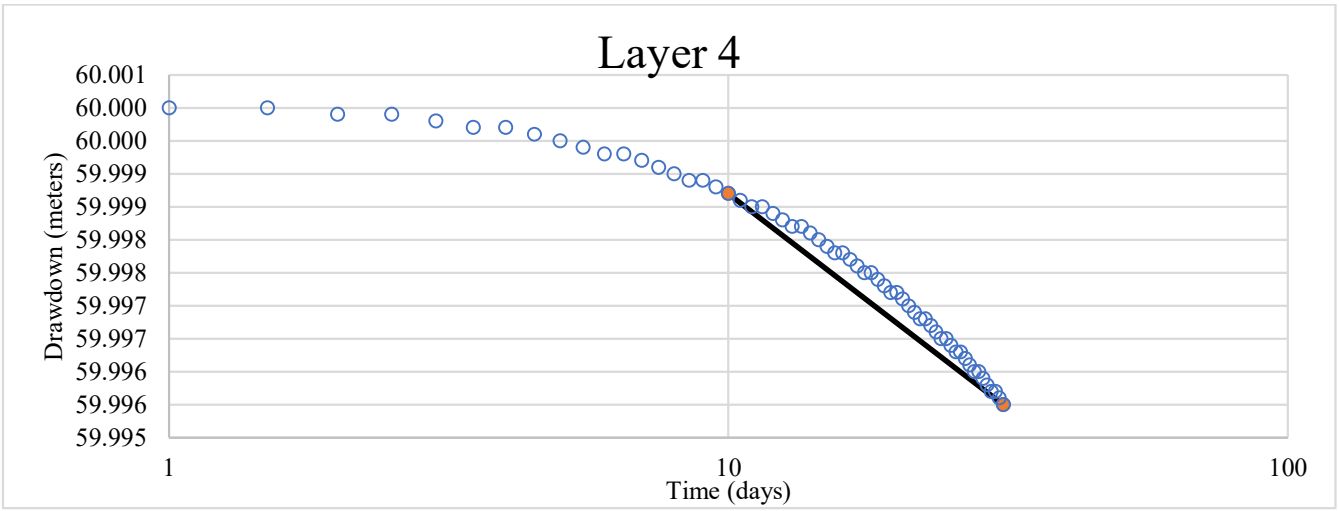
Layer 4
60.001
60.000
60.000
59.999
59.999
59.998
59.998
59.997
59.997
59.996
59.996
59.995
Drawdown (meters)
1
10
100
Time (days)

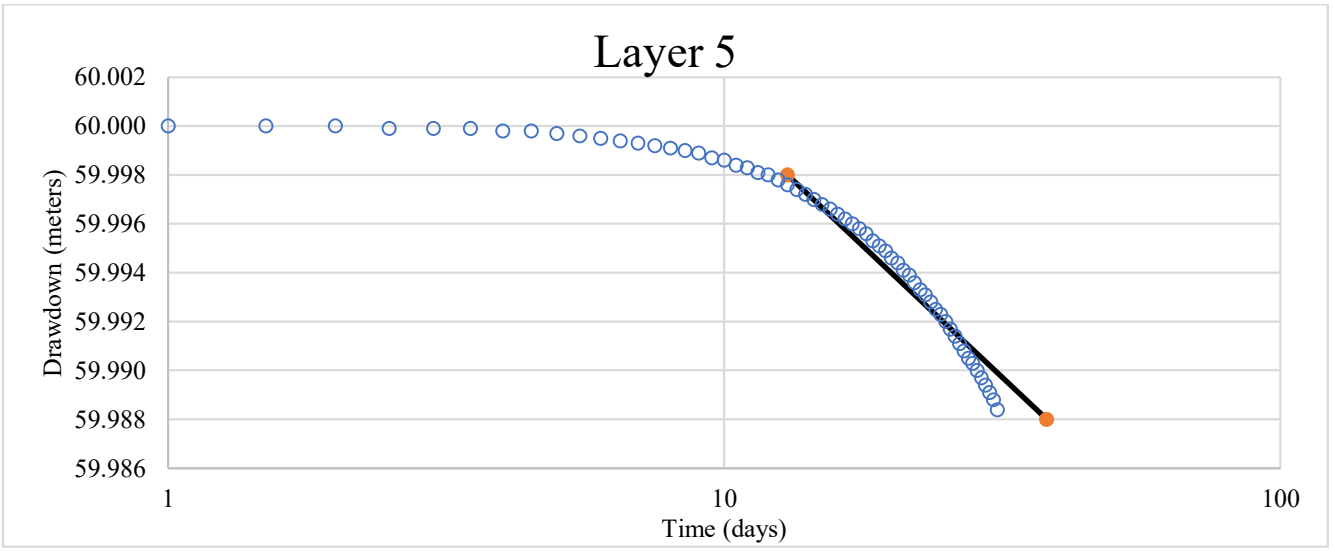
Layer 5
60.002
60.000
59.998
59.996
59.994
59.992
59.990
59.988
59.986
Drawdown (meters)
1
10
100
Time (days)

Test 17

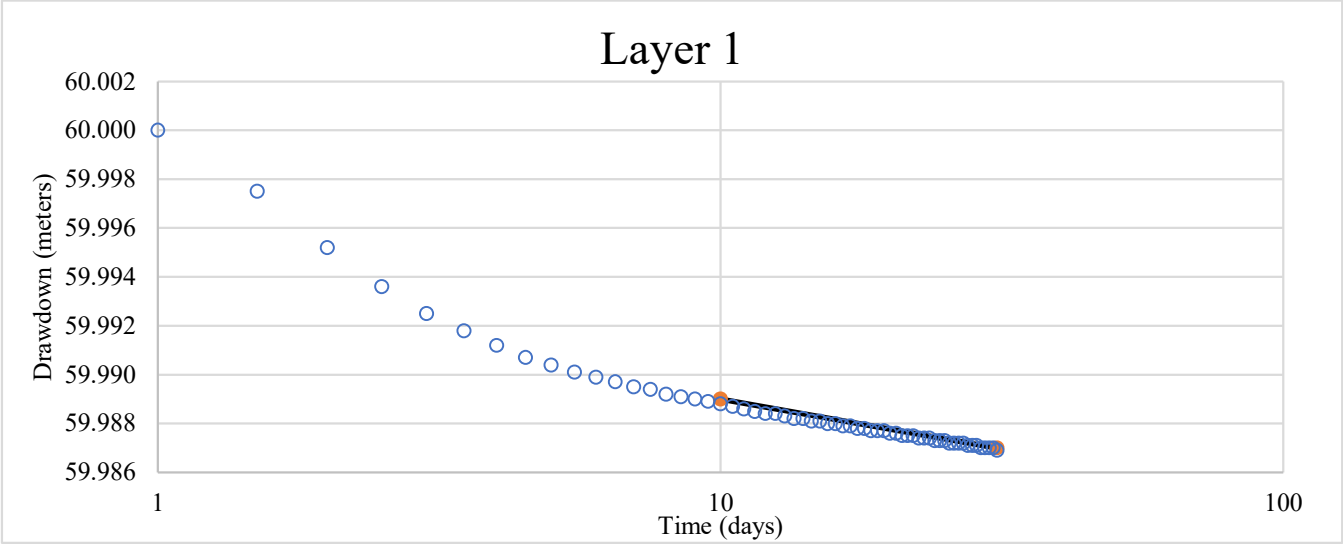
Layer 1
60.002
60.000
59.998
59.996
59.994
59.992
59.990
59.988
59.986
Drawdown (meters)
1
10
100
Time (days)

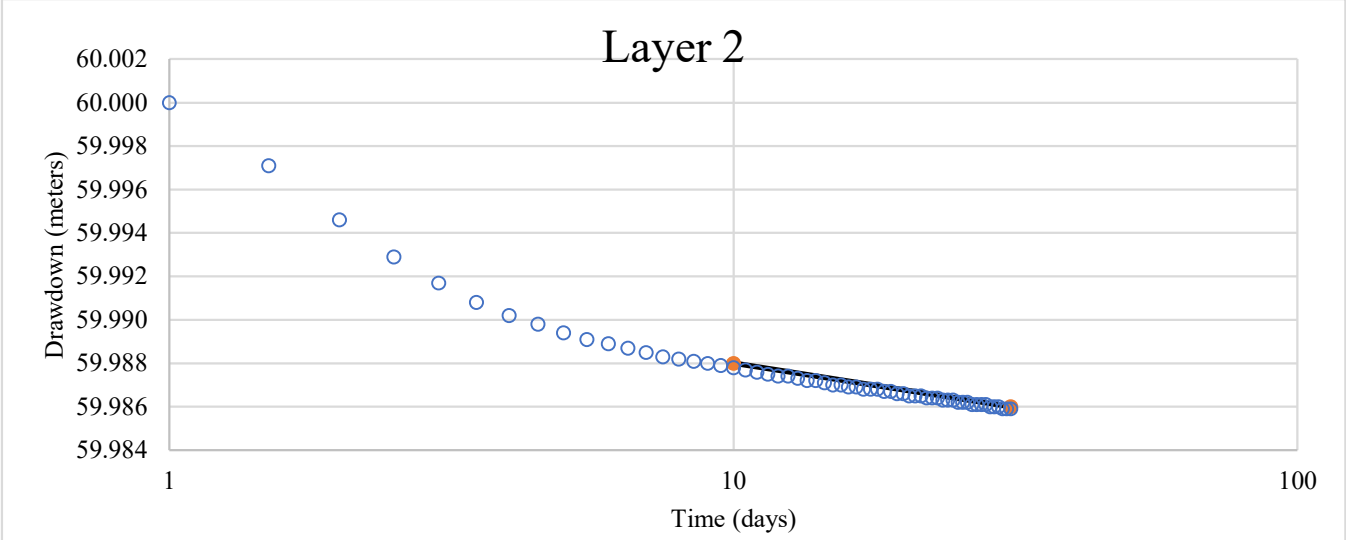
Layer 2
60.002
60.000
59.998
59.996
59.994
59.992
59.990
59.988
59.986
59.984
Drawdown (meters)
1
10
100
Time (days)

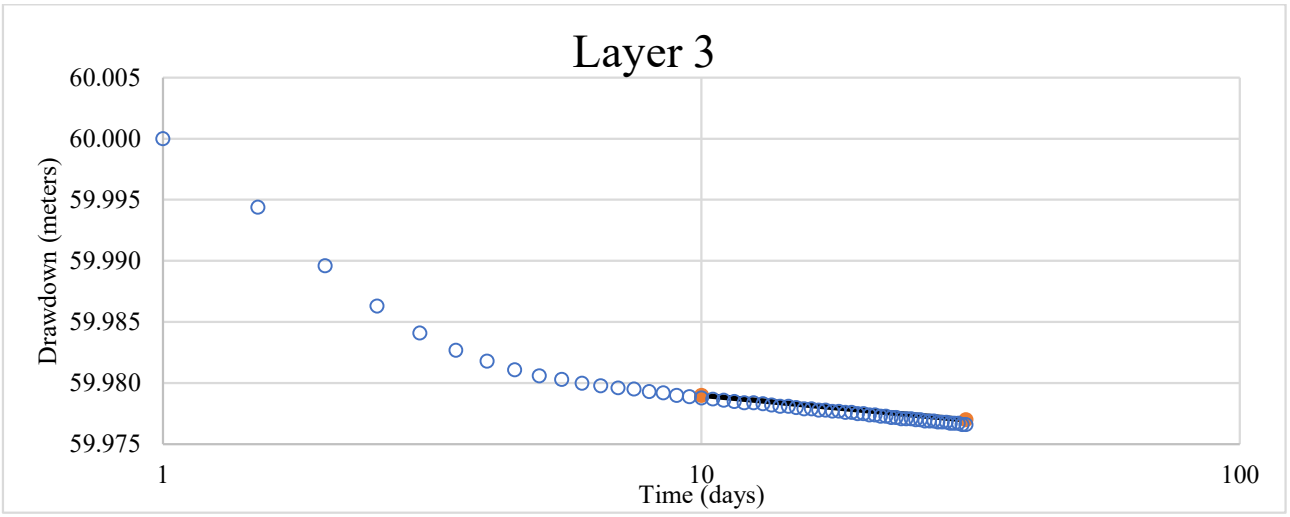
Layer 3
60.005
60.000
59.995
59.990
59.985
59.980
59.975
Drawdown (meters)
1
10
100
Time (days)

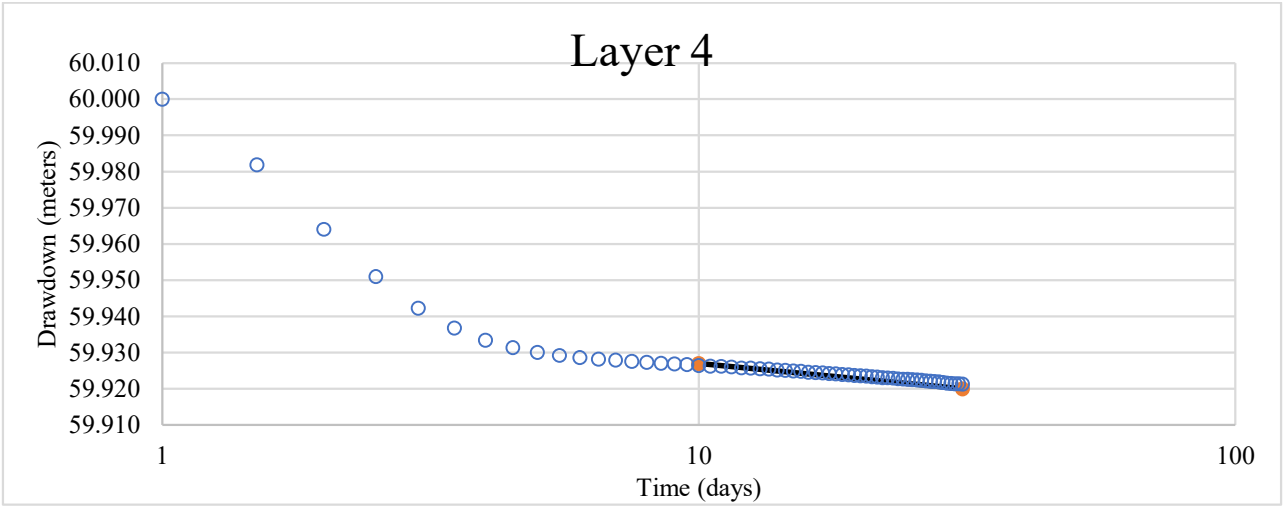
Layer 4
60.010
60.000
59.990
59.980
59.970
59.960
59.950
59.940
59.930
59.920
59.910
Drawdown (meters)
1
10
100
Time (days)

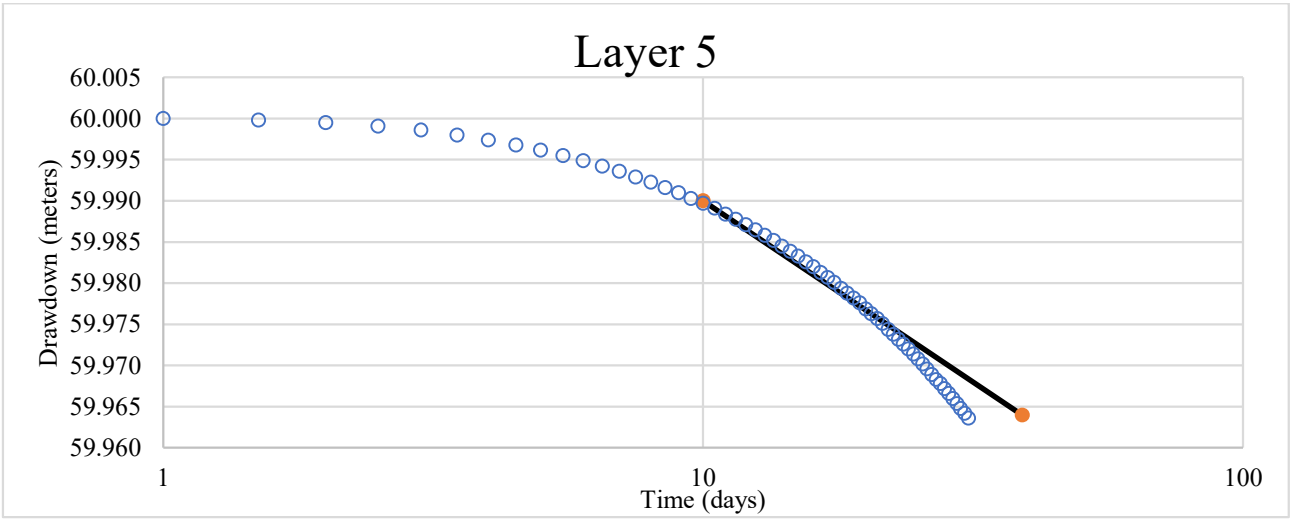
Layer 5
60.005
60.000
59.995
59.990
59.985
59.980
59.975
59.970
59.965
59.960
Drawdown (meters)
1
10
100
Time (days)

Test 18

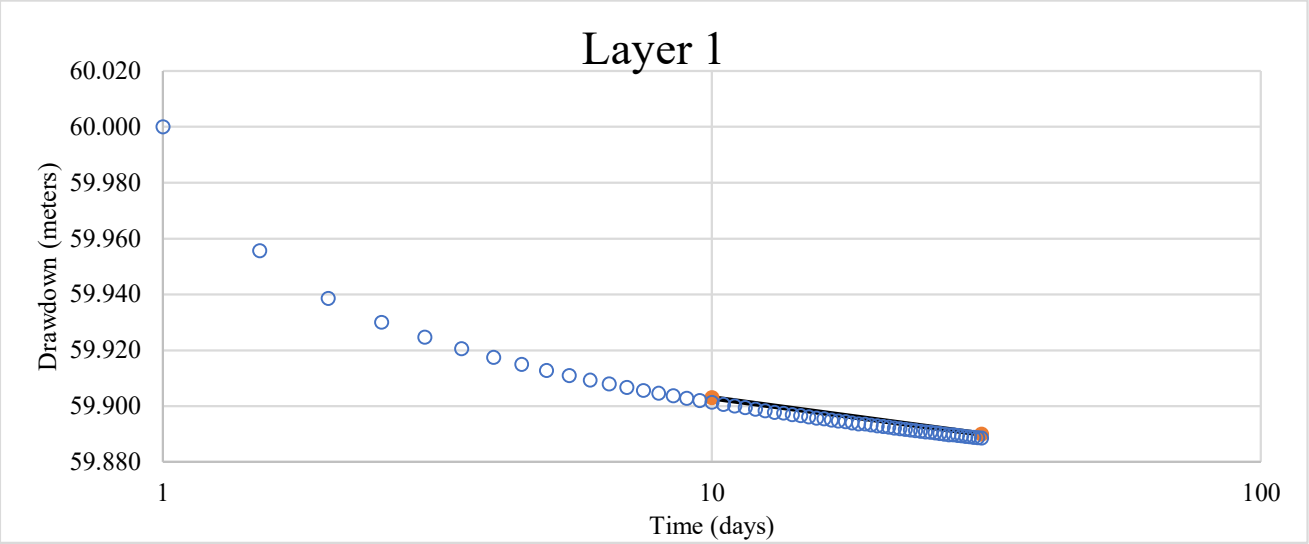
Layer 1
60.020
60.000
59.980
59.960
59.940
59.920
59.900
59.880
Drawdown (meters)
1
10
100
Time (days)

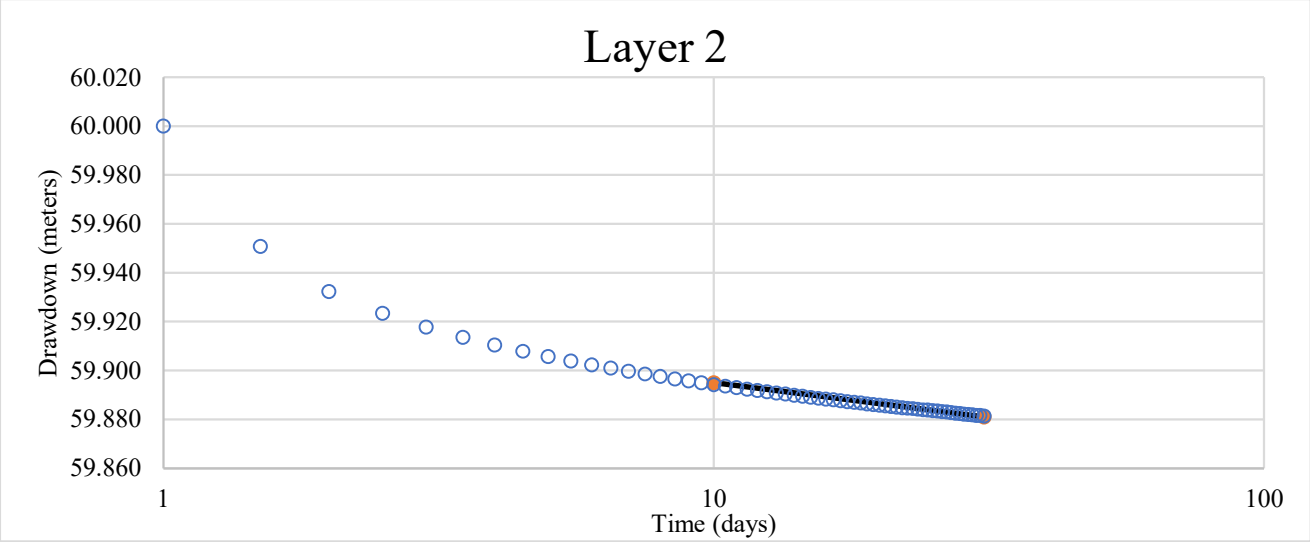
Layer 2
60.020
60.000
59.980
59.960
59.940
59.920
59.900
59.880
59.860
Drawdown (meters)
1
10
100
Time (days)

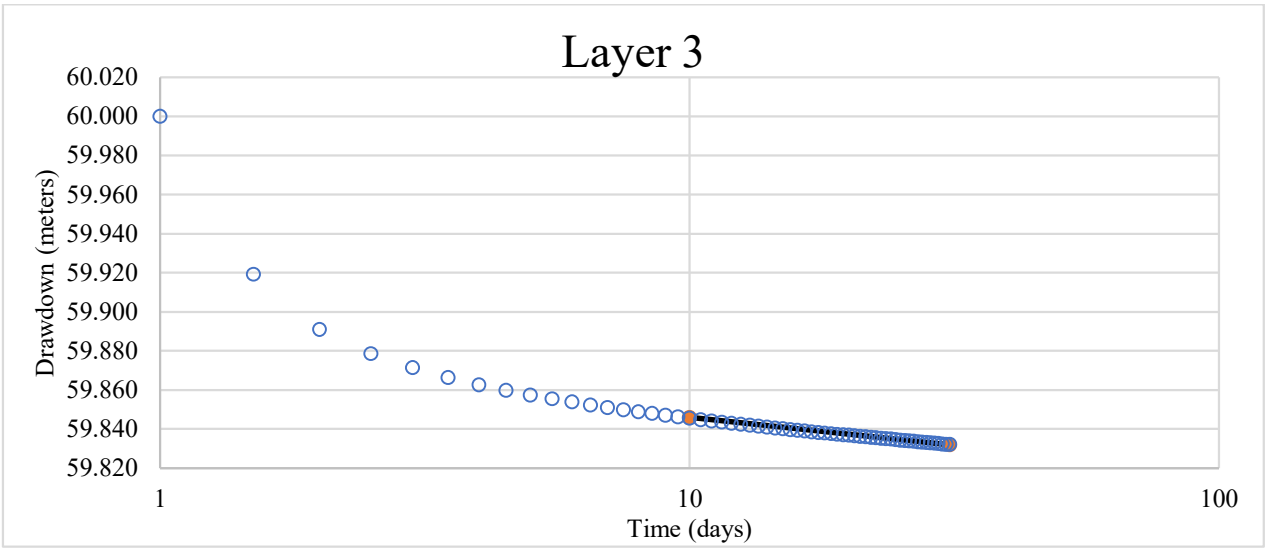
Layer 3
60.020
60.000
59.980
59.960
59.940
59.920
59.900
59.880
59.860
59.840
59.820
Drawdown (meters)
1
10
100
Time (days)

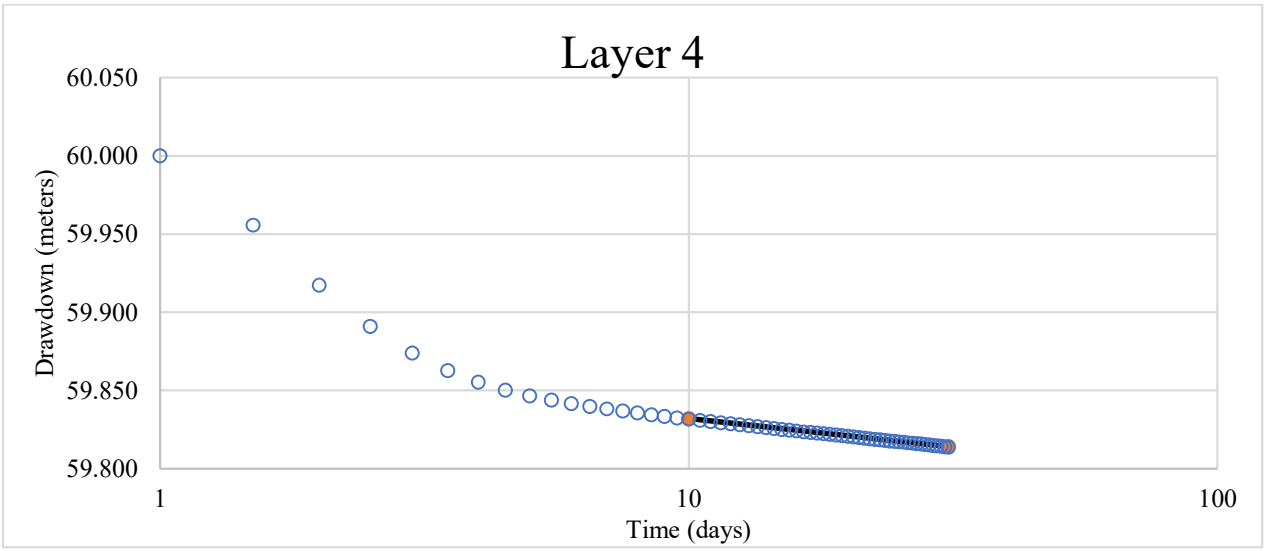
Layer 4
60.050
60.000
59.950
59.900
59.850
59.800
Drawdown (meters)
1
10
100
Time (days)

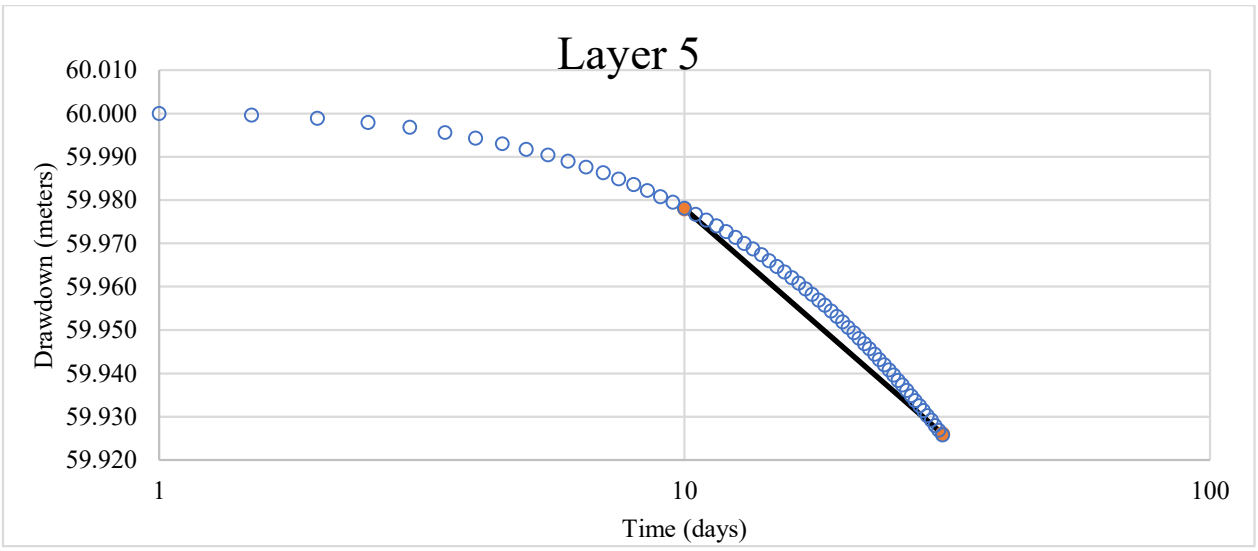
Layer 5
60.010
60.000
59.990
59.980
59.970
59.960
59.950
59.940
59.930
59.920
Drawdown (meters)
1
10
100
Time (days)

Test 19

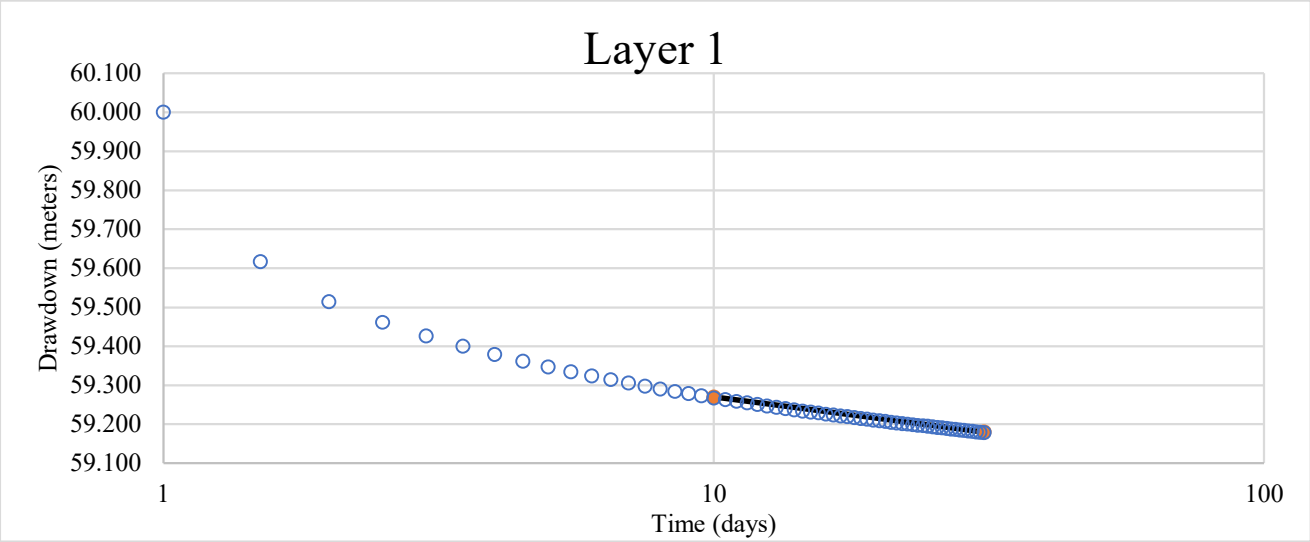
Layer 1
60.100
60.000
59.900
59.800
59.700
59.600
59.500
59.400
59.300
59.200
59.100
Drawdown (meters)
1
10
100
Time (days)

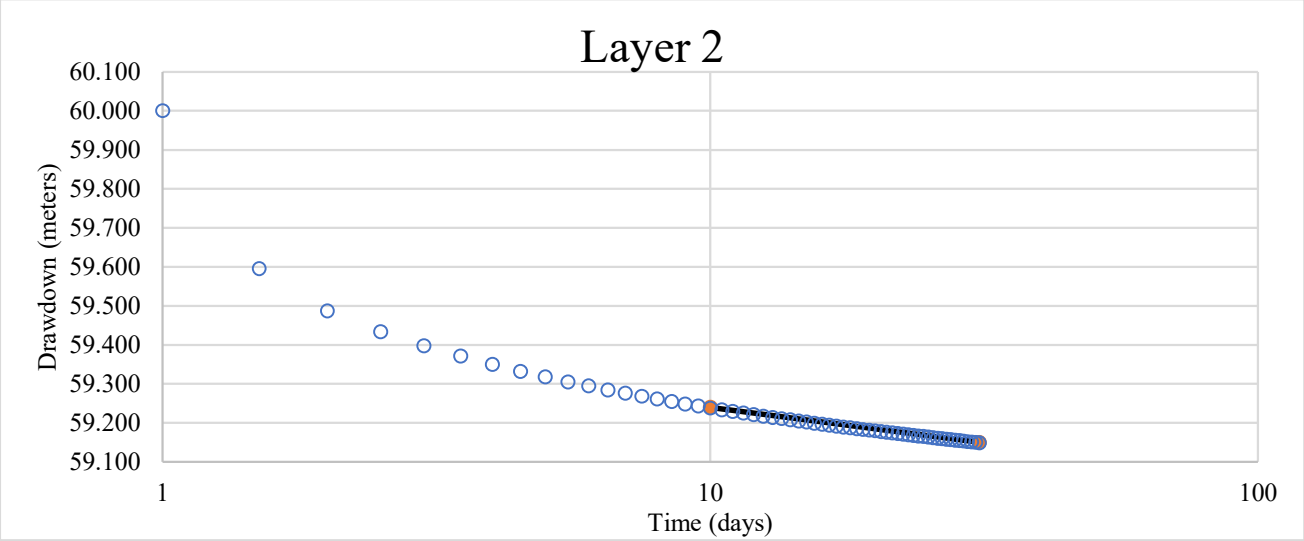
Layer 2
60.100
60.000
59.900
59.800
59.700
59.600
59.500
59.400
59.300
59.200
59.100
Drawdown (meters)
1
10
100
Time (days)

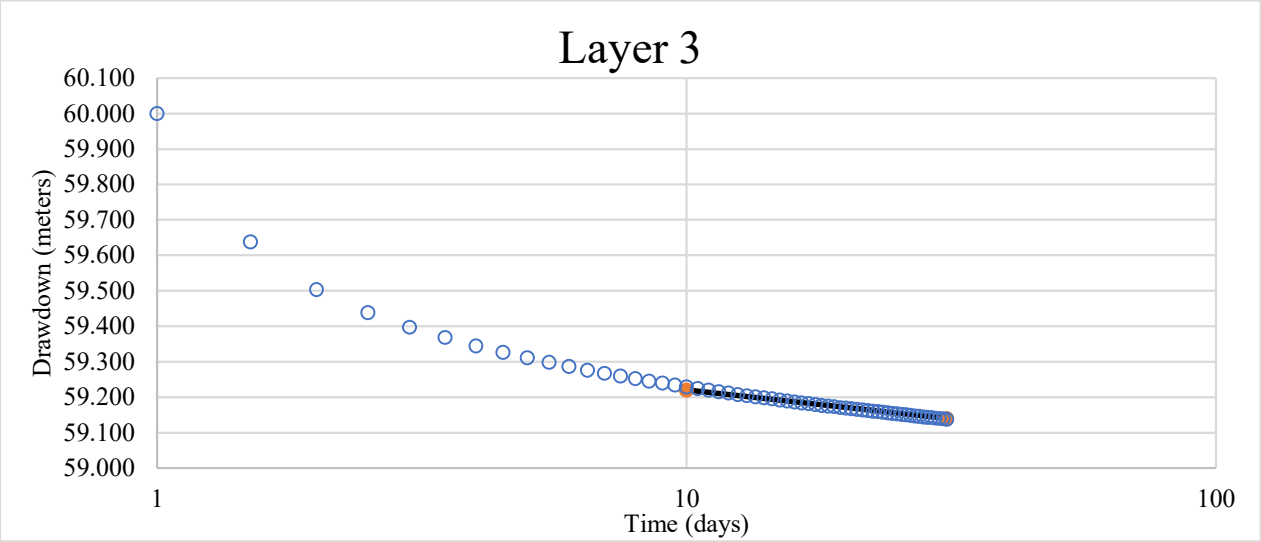
Layer 3
60.100
60.000
59.900
59.800
59.700
59.600
59.500
59.400
59.300
59.200
59.100
59.000
Drawdown (meters)
1
10
100
Time (days)

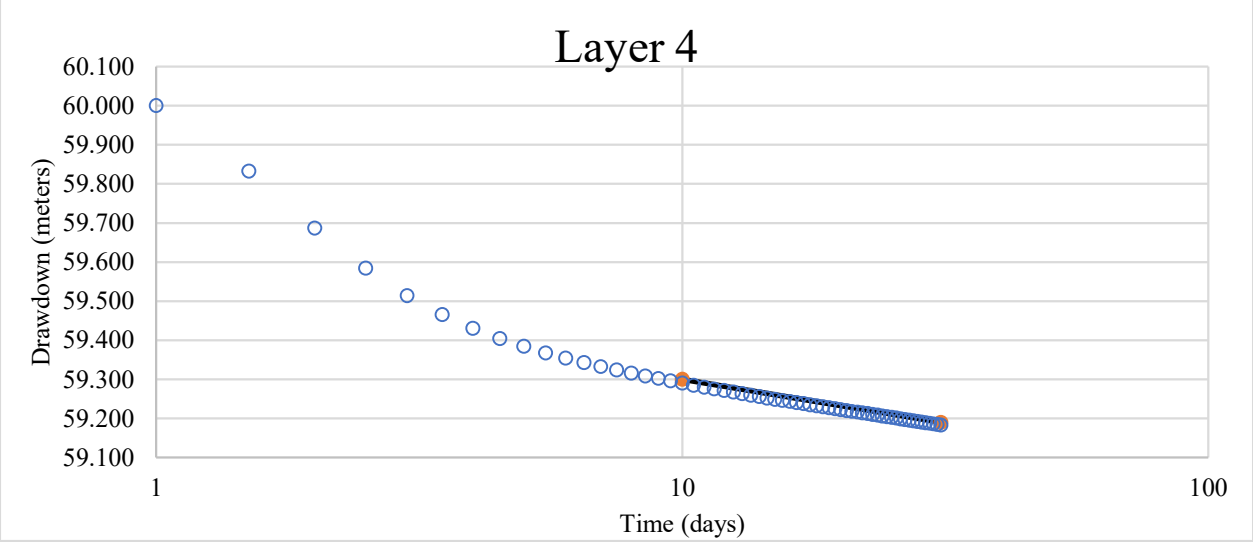
Layer 4
60.100
60.000
59.900
59.800
59.700
59.600
59.500
59.400
59.300
59.200
59.100
Drawdown (meters)
1
10
100
Time (days)

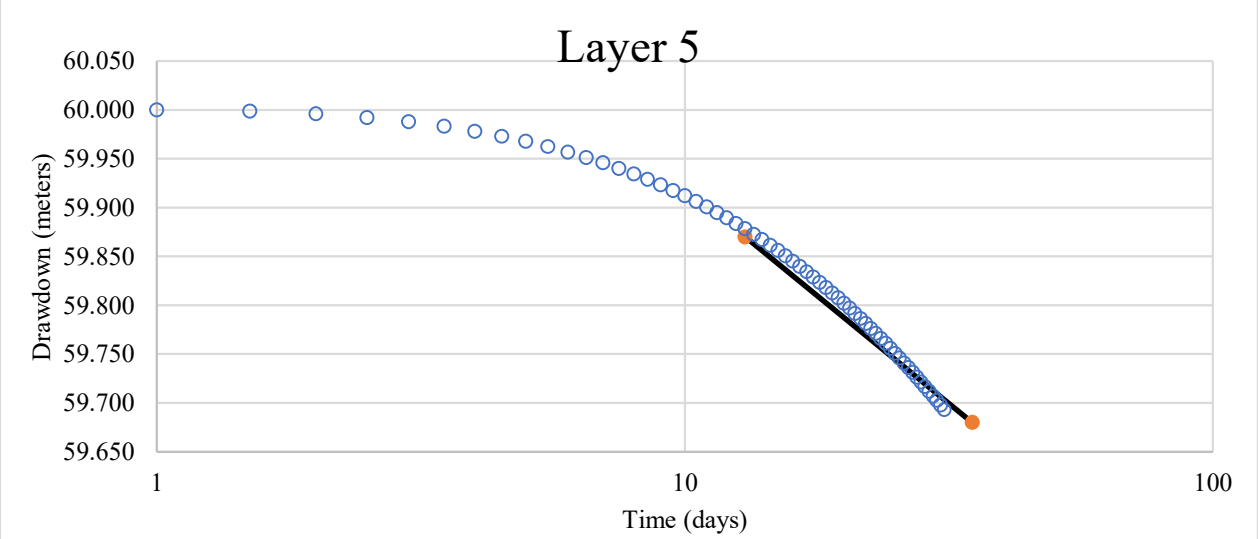
Layer 5
60.050
60.000
59.950
59.900
59.850
59.800
59.750
59.700
59.650
Drawdown (meters)
1
10
100
Time (days)

Test 20

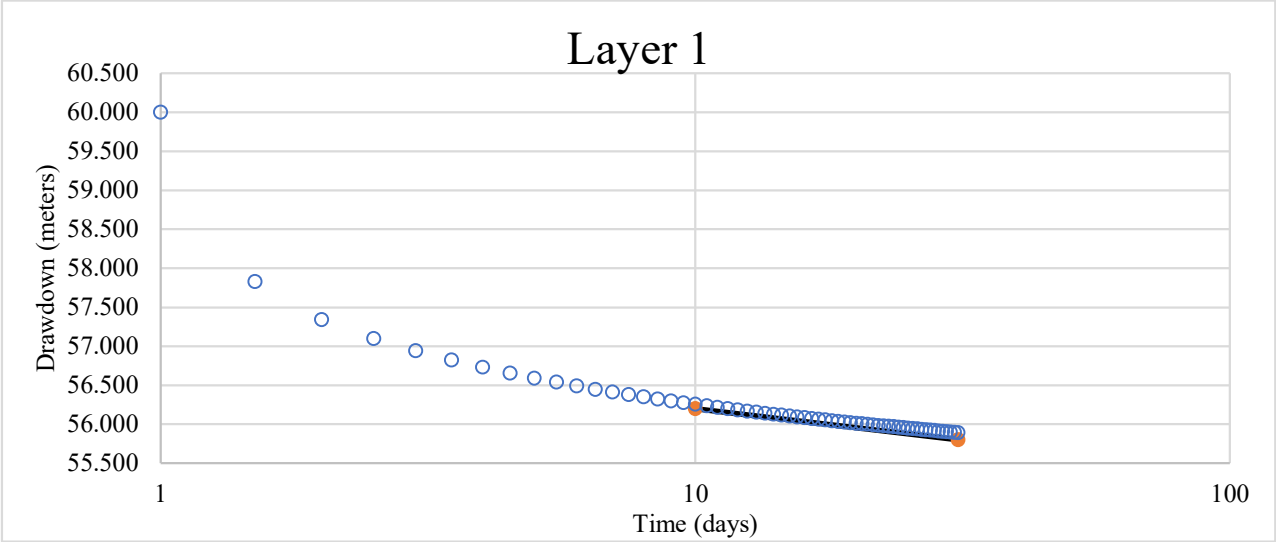
Layer 1
60.500
60.000
59.500
59.000
58.500
58.000
57.500
57.000
56.500
56.000
55.500
Drawdown (meters)
1
10
100
Time (days)

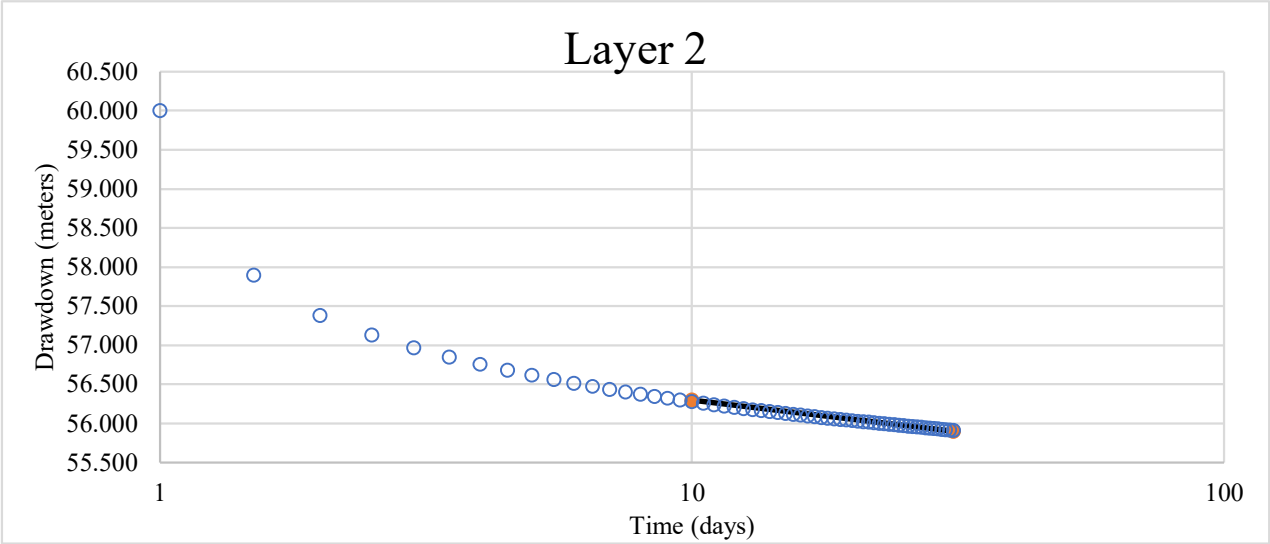
Layer 2
60.500
60.000
59.500
59.000
58.500
58.000
57.500
57.000
56.500
56.000
55.500
Drawdown (meters)
1
10
100
Time (days)

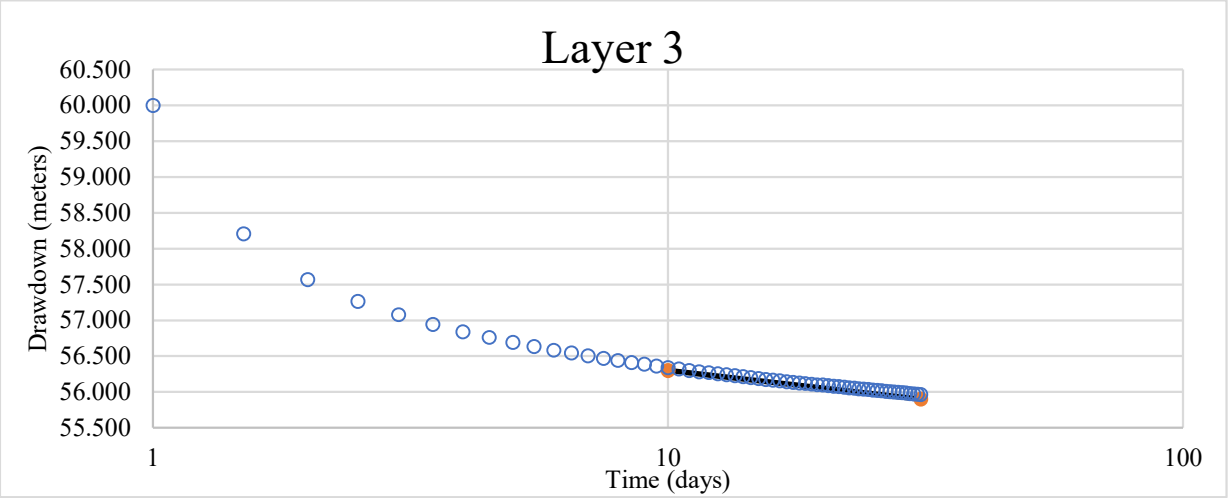
Layer 3
60.500
60.000
59.500
59.000
58.500
58.000
57.500
57.000
56.500
56.000
55.500
Drawdown (meters)
1
10
100
Time (days)

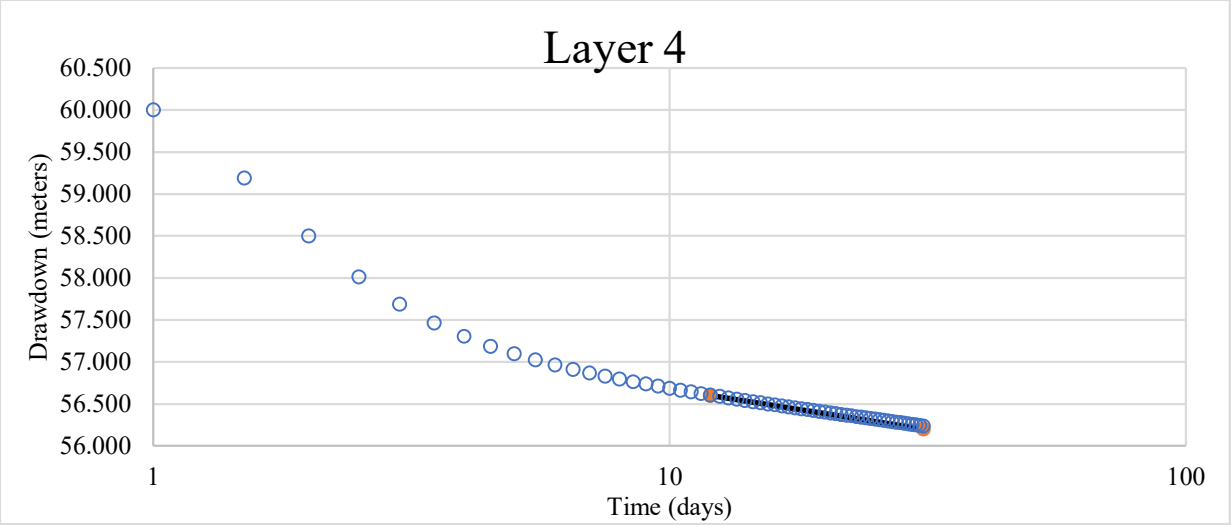
Layer 4
60.500
60.000
59.500
59.000
58.500
58.000
57.500
57.000
56.500
56.000
Drawdown (meters)
1
10
100
Time (days)

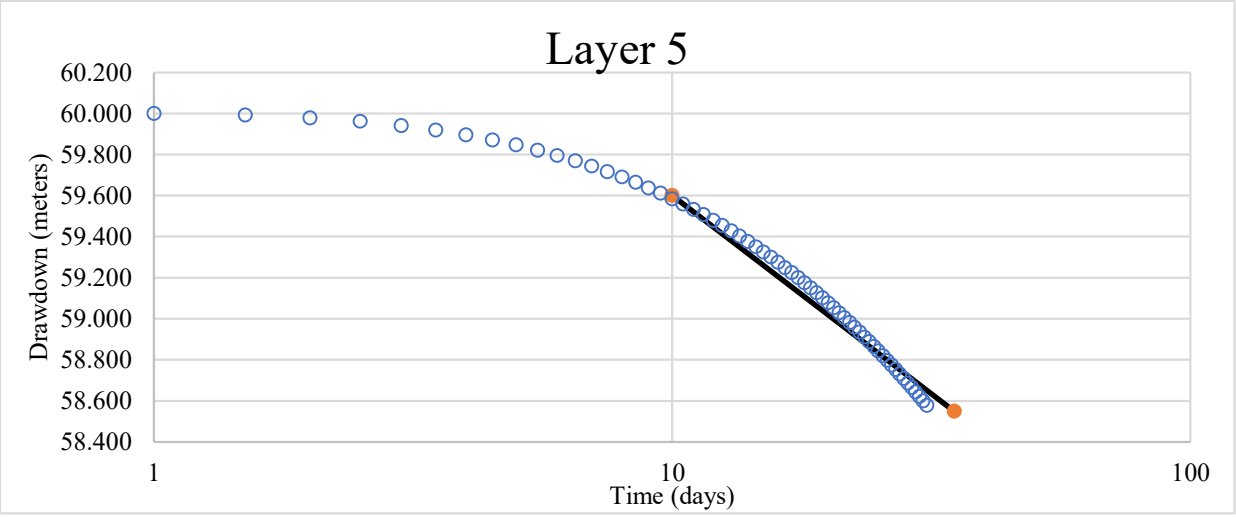
Layer 5
60.200
60.000
59.800
59.600
59.400
59.200
59.000
58.800
58.600
58.400
Drawdown (meters)
1
10
100
Time (days)

Test 21

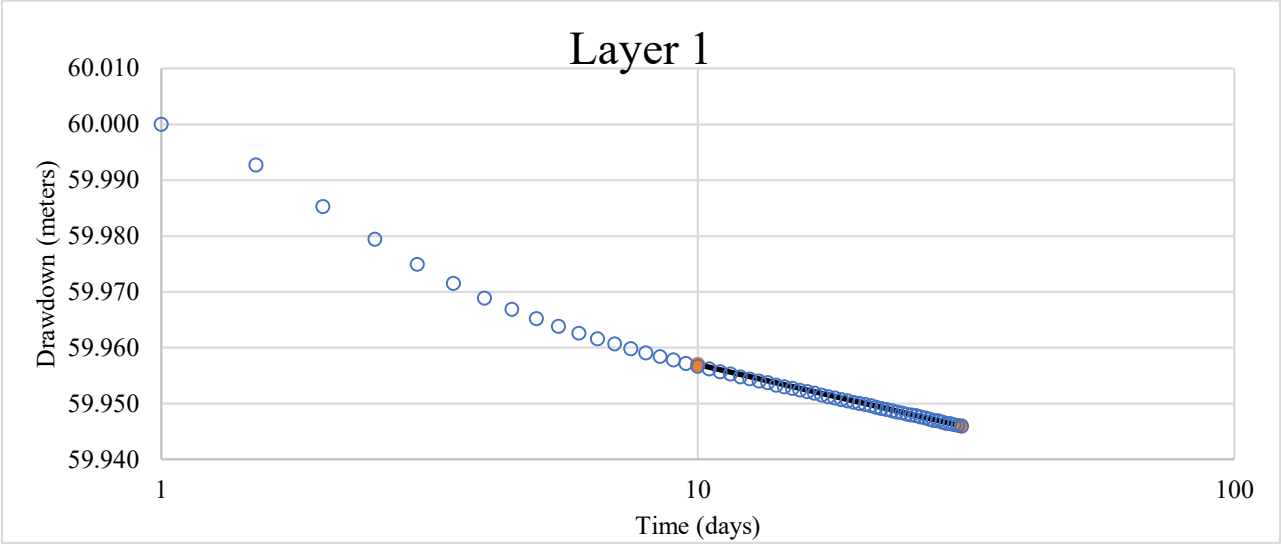
Layer 1
60.010
60.000
59.990
59.980
59.970
59.960
59.950
59.940
Drawdown (meters)
1
10
100
Time (days)

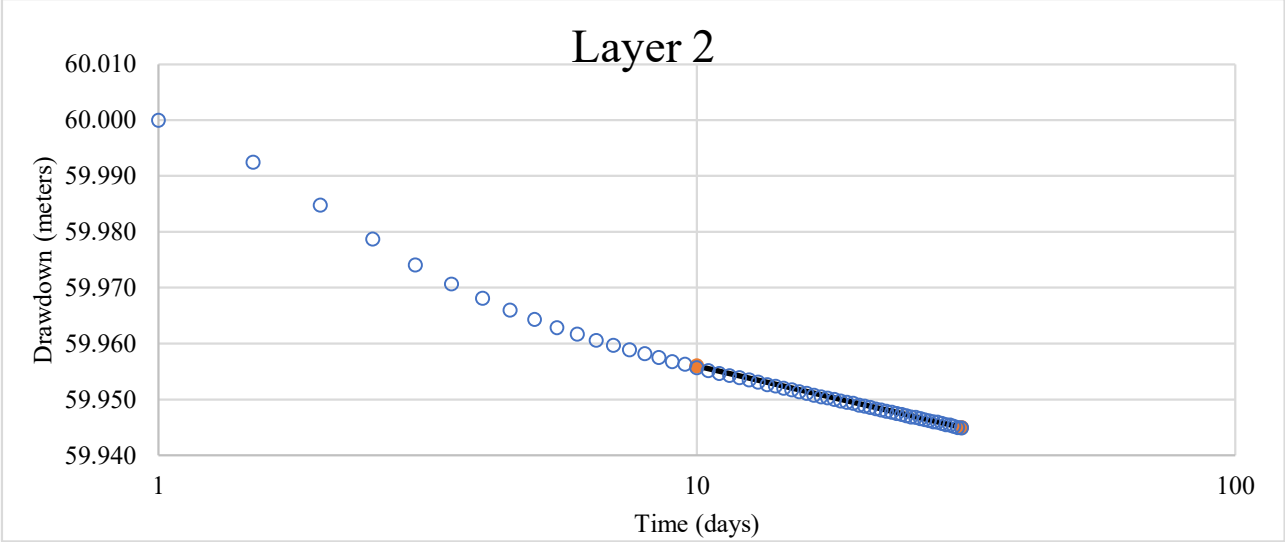
Layer 2
60.010
60.000
59.990
59.980
59.970
59.960
59.950
59.940
Drawdown (meters)
1
10
100
Time (days)

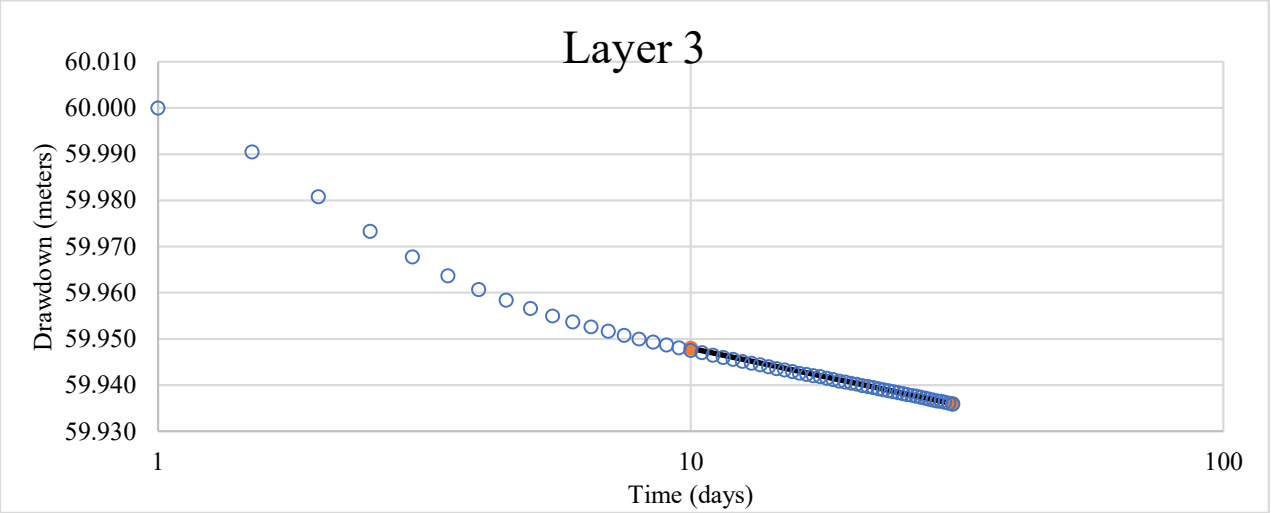
Layer 3
60.010
60.000
59.990
59.980
59.970
59.960
59.950
59.940
59.930
Drawdown (meters)
1
10
100
Time (days)

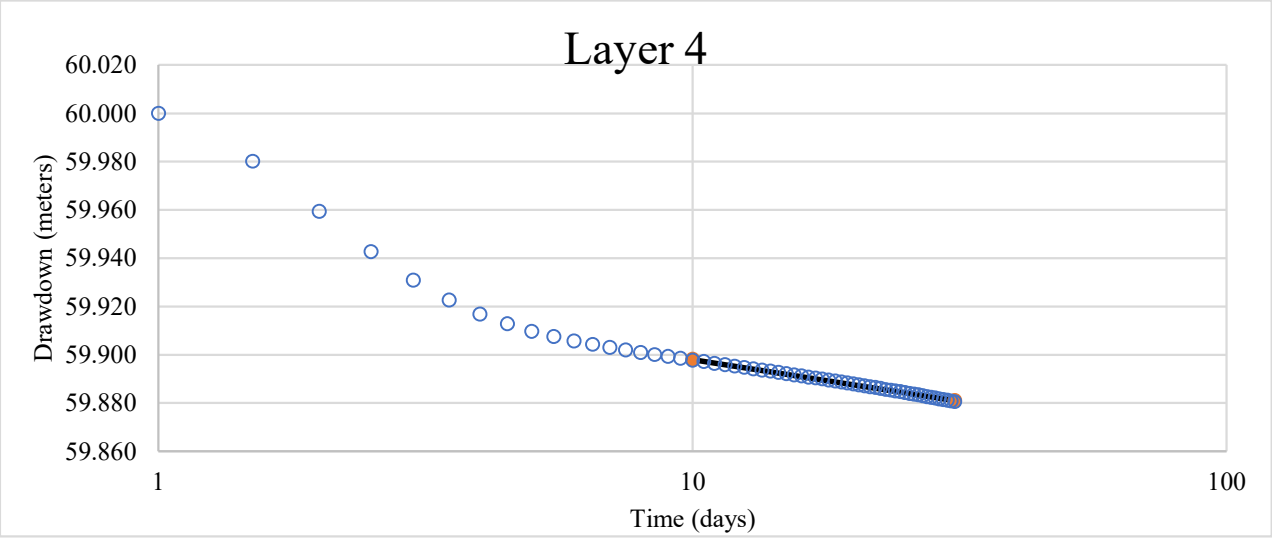
Layer 4
60.020
60.000
59.980
59.960
59.940
59.920
59.900
59.880
59.860
Drawdown (meters)
1
10
100
Time (days)

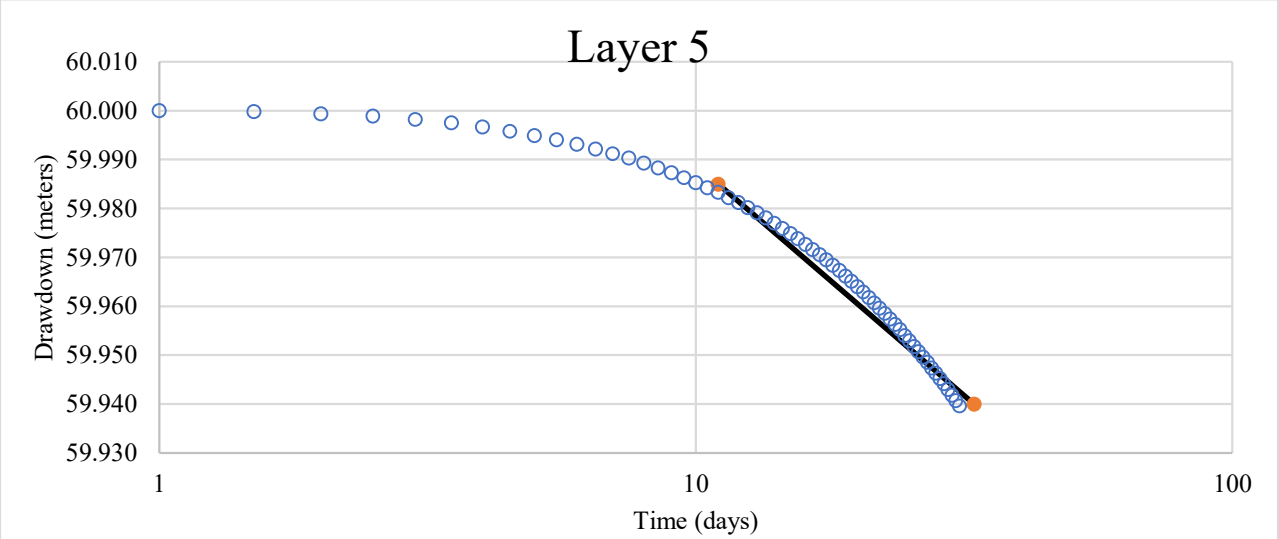
Layer 5
60.010
60.000
59.990
59.980
59.970
59.960
59.950
59.940
59.930
Drawdown (meters)
1
10
100
Time (days)

Test 22

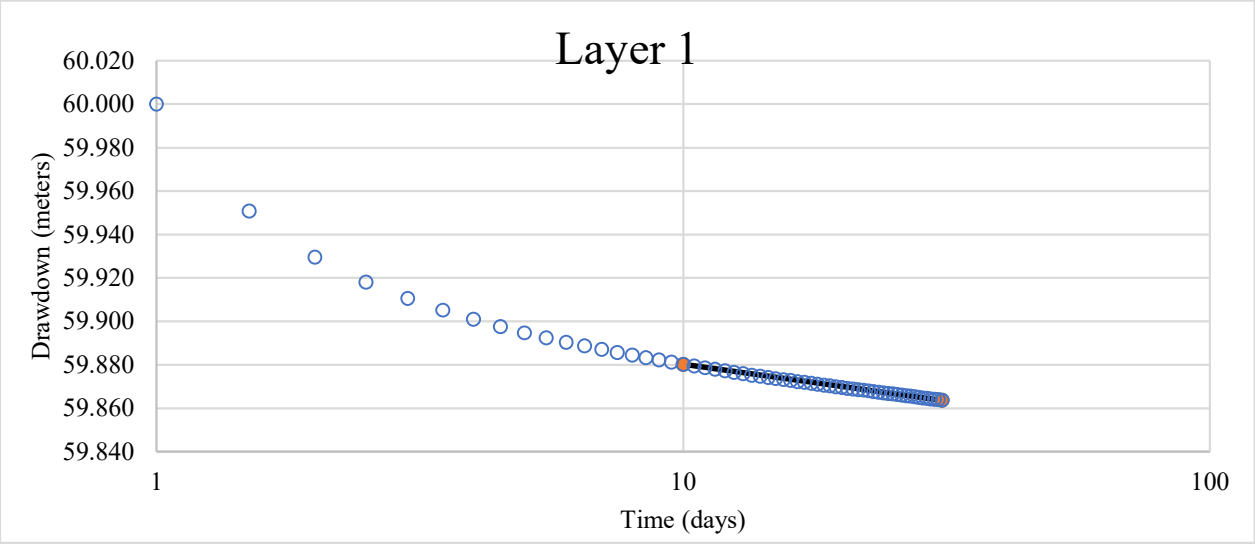
Layer 1
60.020
60.000
59.980
59.960
59.940
59.920
59.900
59.880
59.860
59.840
Drawdown (meters)
1
10
100
Time (days)

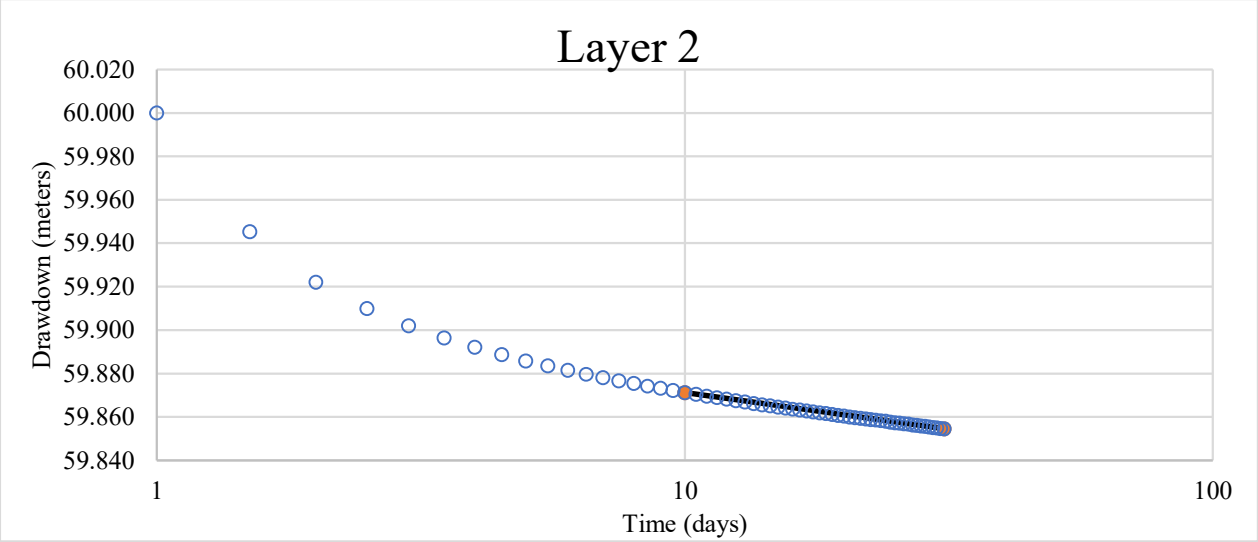
Layer 2
60.020
60.000
59.980
59.960
59.940
59.920
59.900
59.880
59.860
59.840
Drawdown (meters)
1
10
100
Time (days)

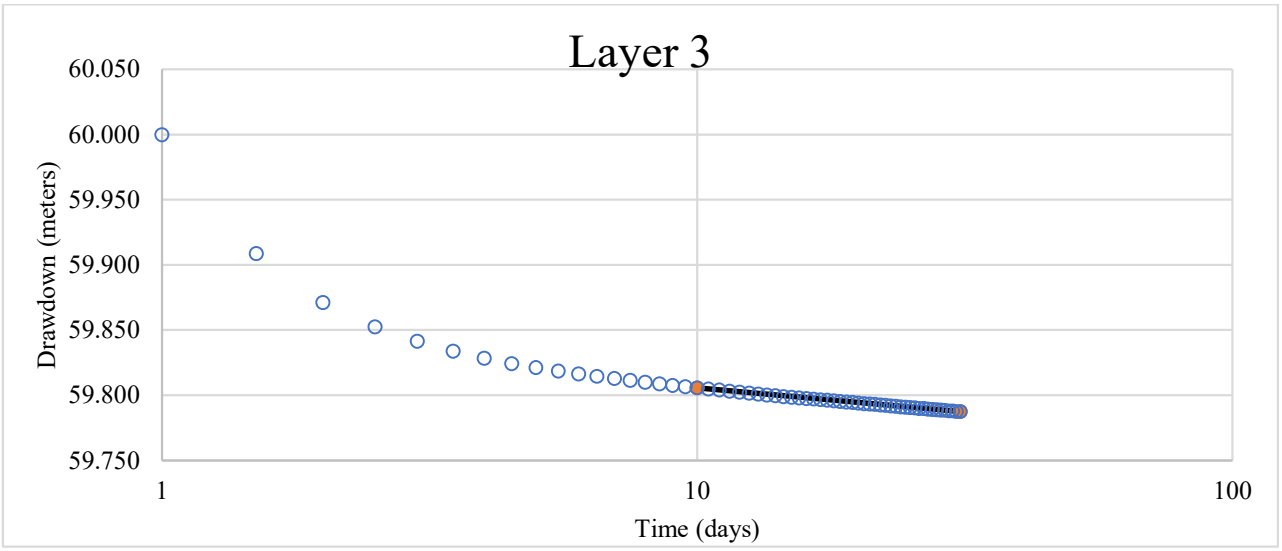
Layer 3
60.050
60.000
59.950
59.900
59.850
59.800
59.750
Drawdown (meters)
1
10
100
Time (days)

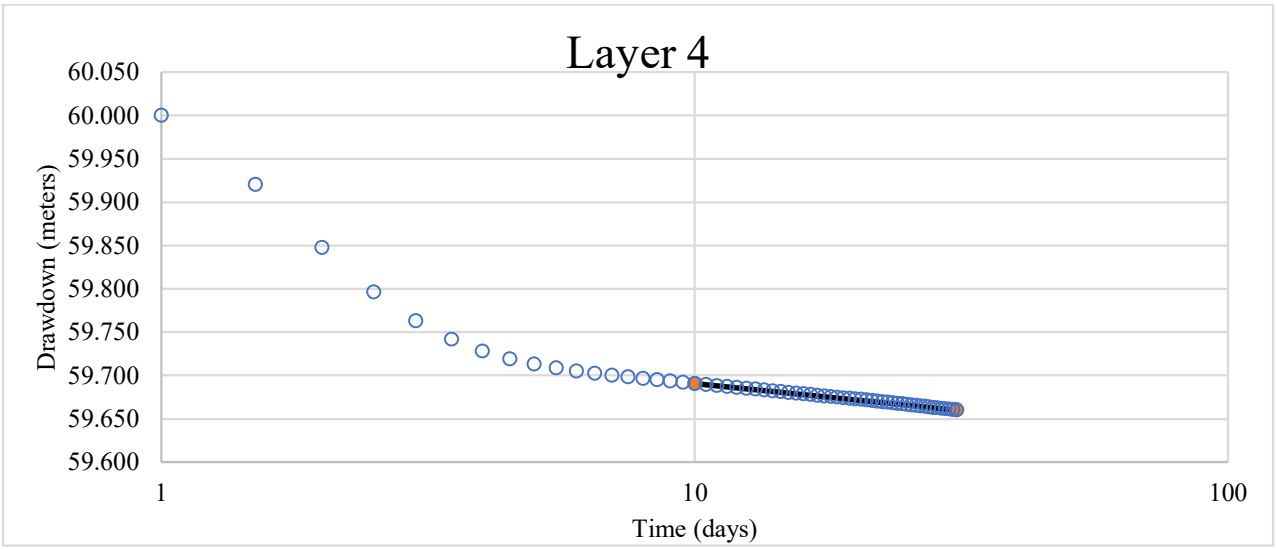
Layer 4
60.050
60.000
59.950
59.900
59.850
59.800
59.750
59.700
59.650
59.600
Drawdown (meters)
1
10
100
Time (days)

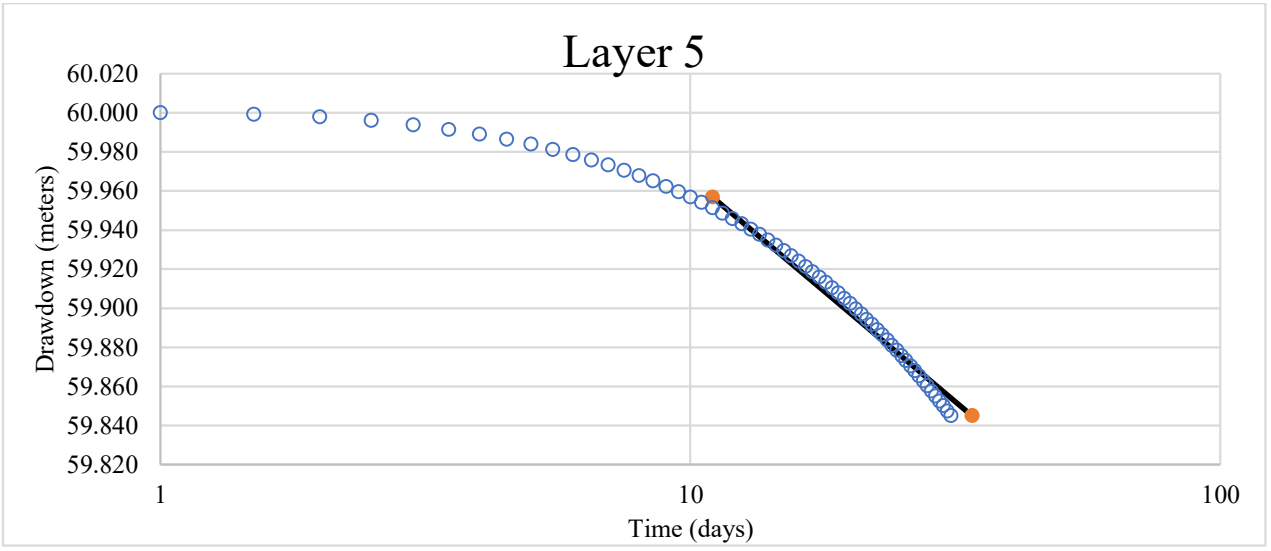
Layer 5
60.020
60.000
59.980
59.960
59.940
59.920
59.900
59.880
59.860
59.840
59.820
Drawdown (meters)
1
10
100
Time (days)

Test 23

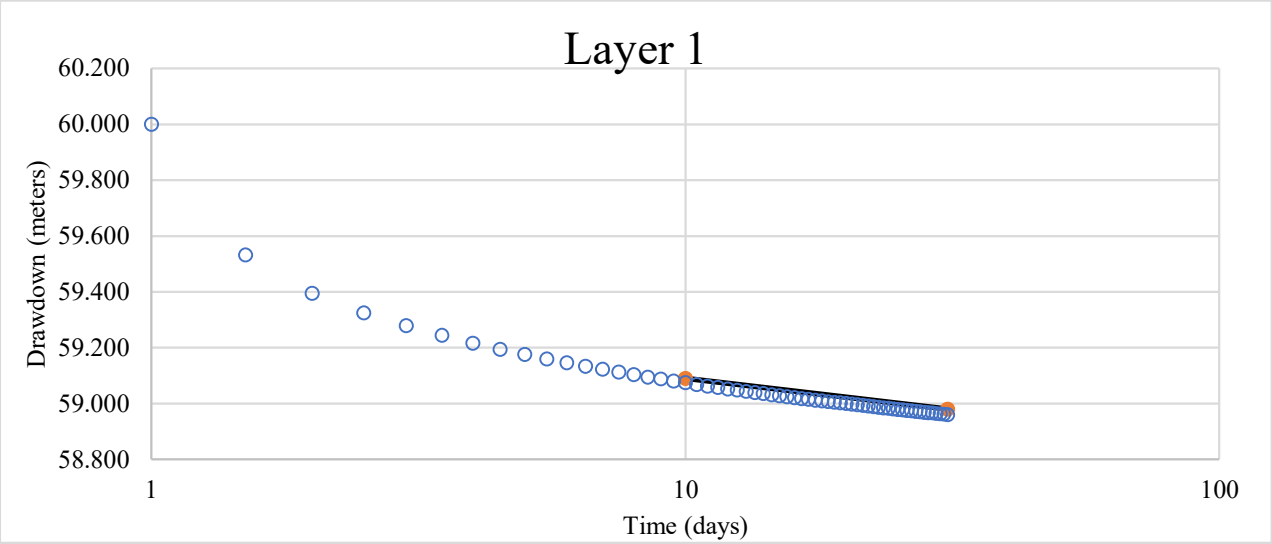
Layer 1
60.200
60.000
59.800
59.600
59.400
59.200
59.000
58.800
Drawdown (meters)
1
10
100
Time (days)

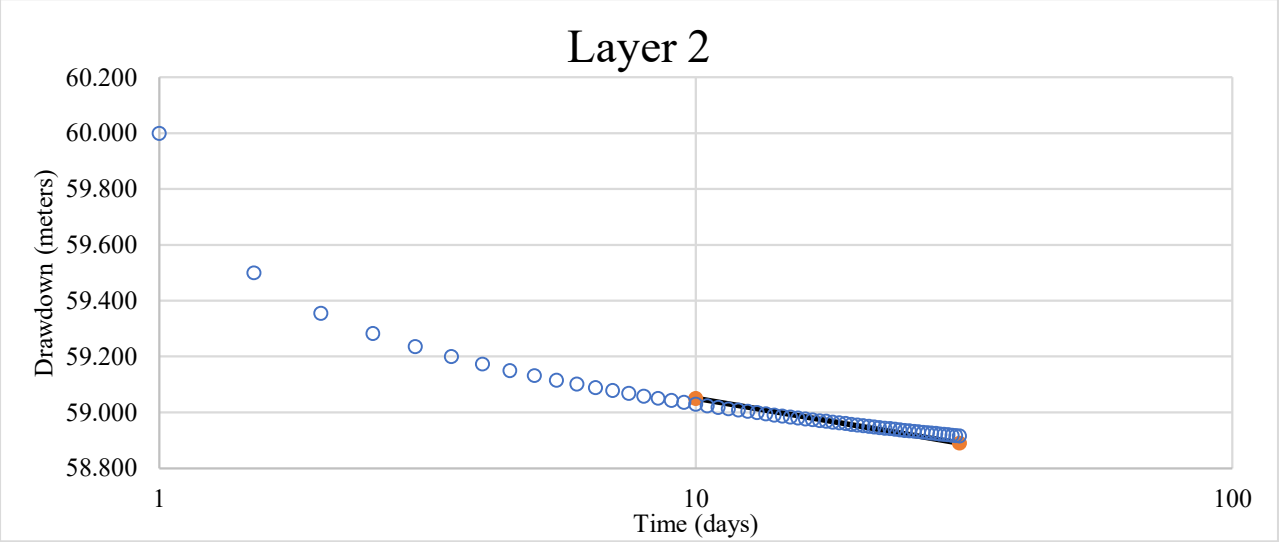
Layer 2
60.200
60.000
59.800
59.600
59.400
59.200
59.000
58.800
Drawdown (meters)
1
10
100
Time (days)

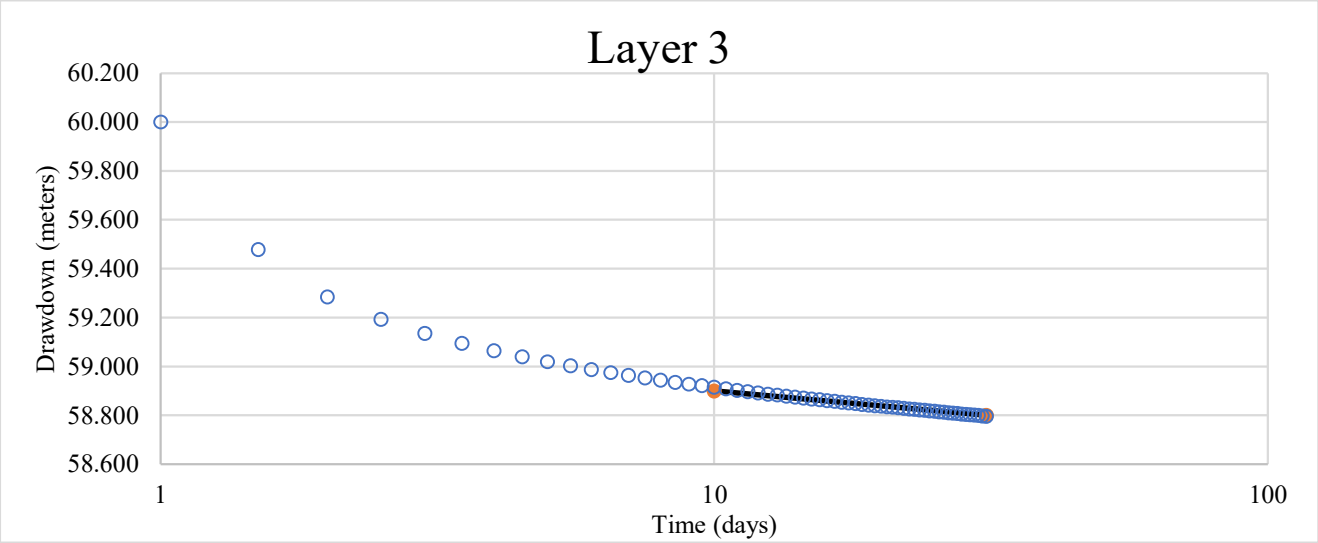
Layer 3
60.200
60.000
59.800
59.600
59.400
59.200
59.000
58.800
58.600
Drawdown (meters)
1
10
100
Time (days)

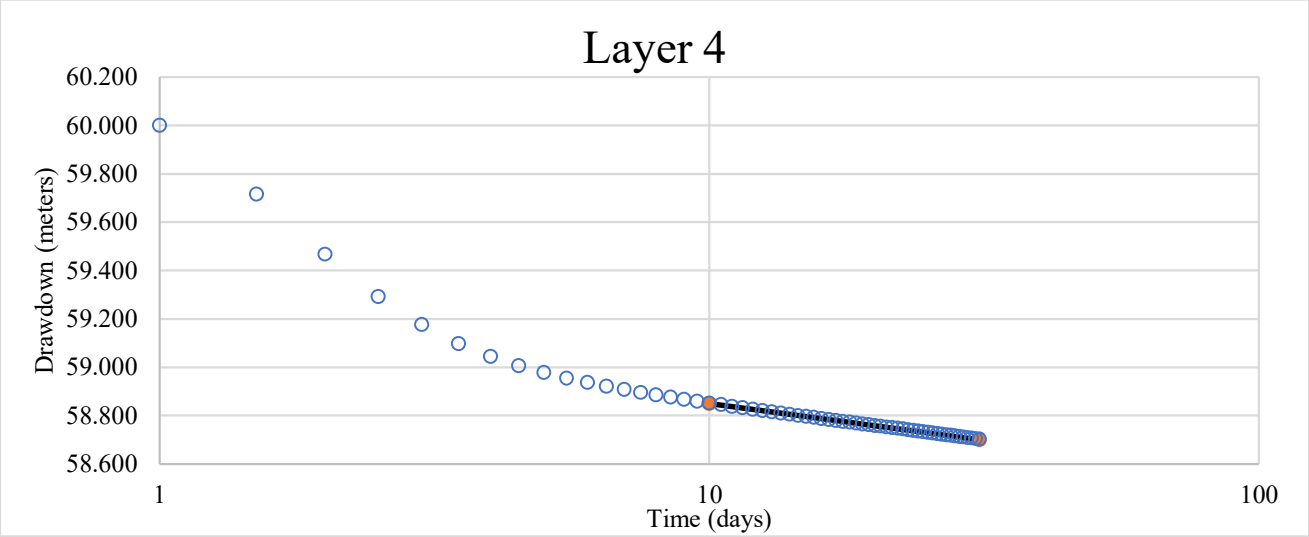
Layer 4
60.200
60.000
59.800
59.600
59.400
59.200
59.000
58.800
58.600
Drawdown (meters)
1
10
100
Time (days)

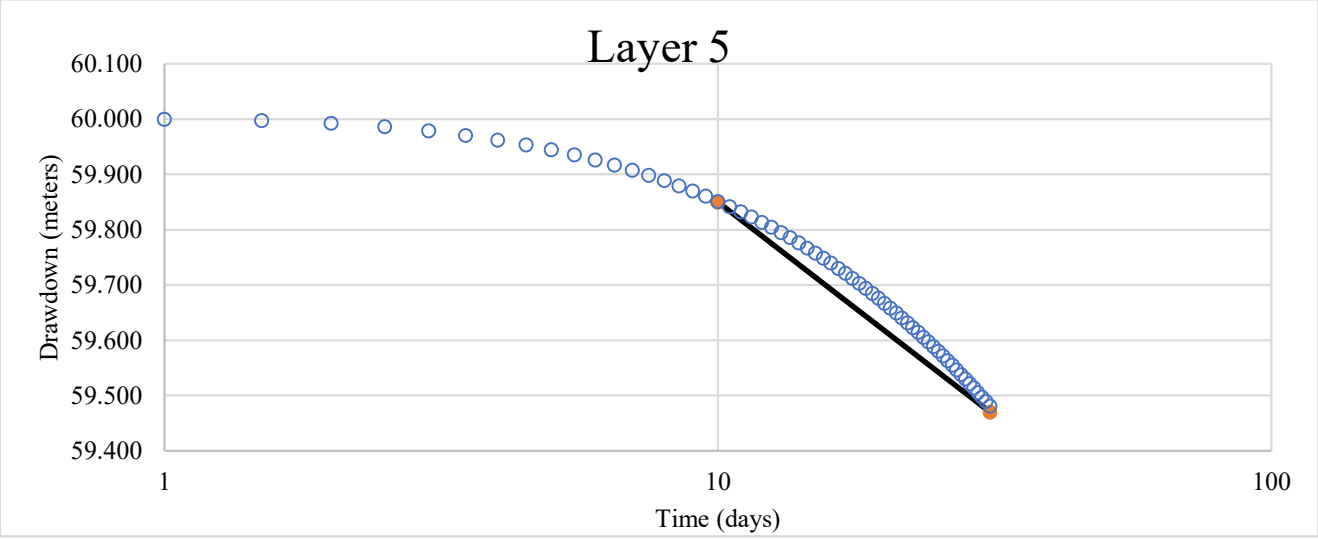
Layer 5
60.100
60.000
59.900
59.800
59.700
59.600
59.500
59.400
Drawdown (meters)
1
10
100
Time (days)

Test 24

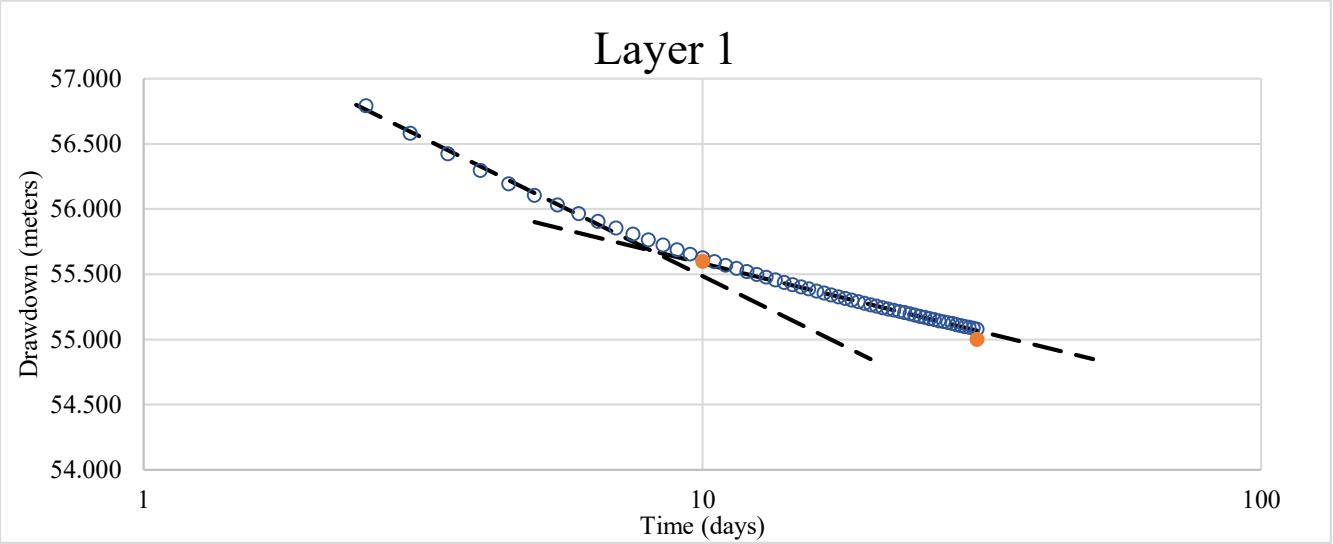
Layer 1
57.000
56.500
56.000
55.500
55.000
54.500
54.000
Drawdown (meters)
1
10
100
Time (days)

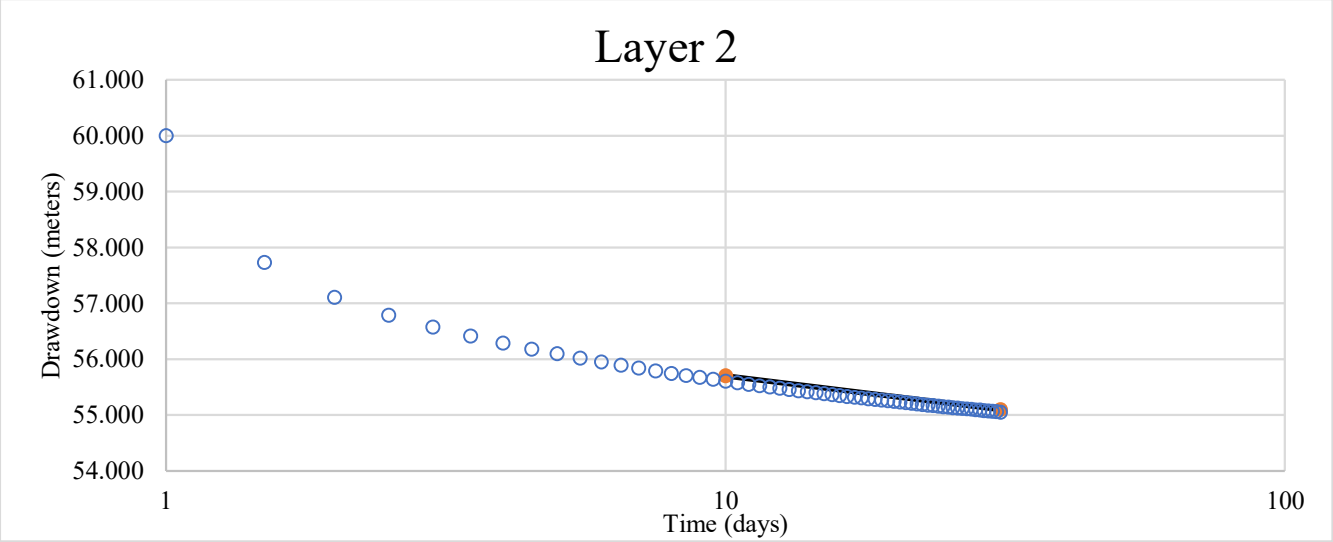
Layer 2
61.000
60.000
59.000
58.000
57.000
56.000
55.000
54.000
Drawdown (meters)
1
10
100
Time (days)

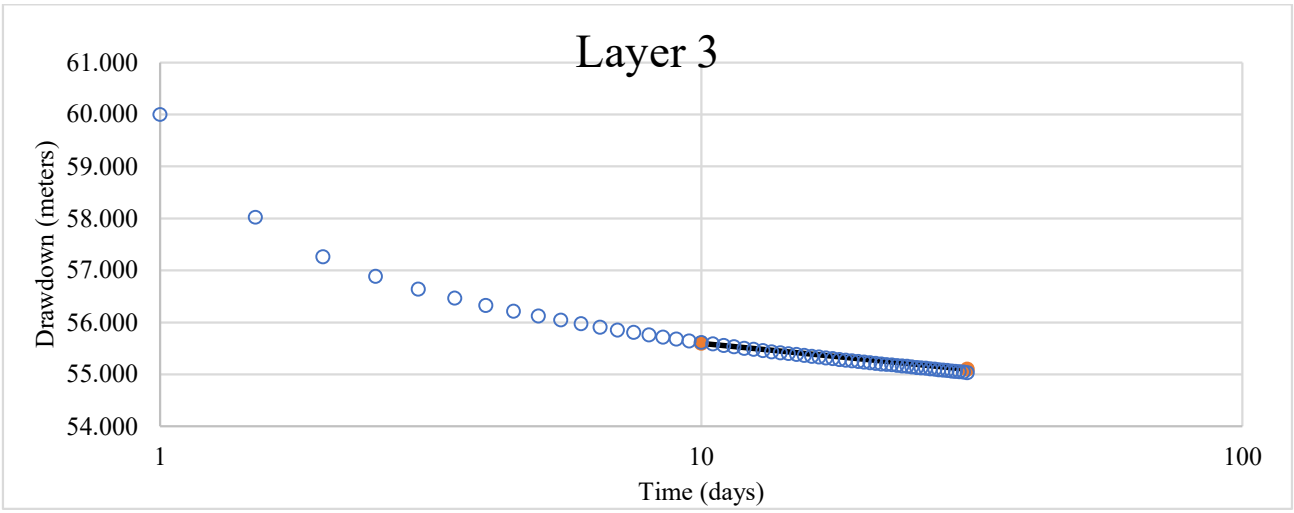
Layer 3
61.000
60.000
59.000
58.000
57.000
56.000
55.000
54.000
Drawdown (meters)
1
10
100
Time (days)

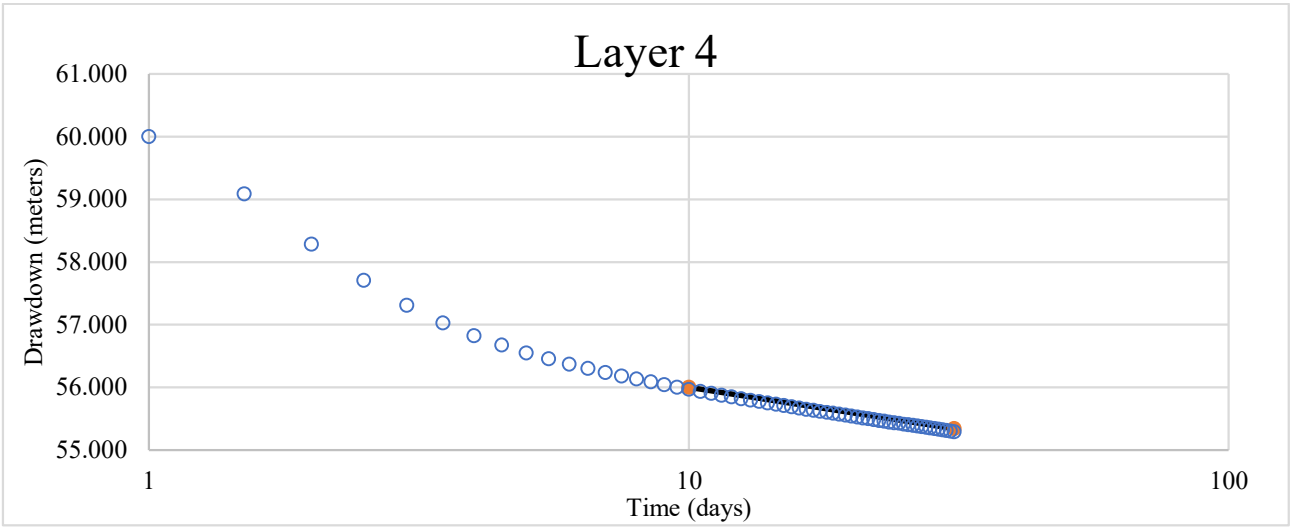
Layer 4
61.000
60.000
59.000
58.000
57.000
56.000
55.000
Drawdown (meters)
1
10
100
Time (days)

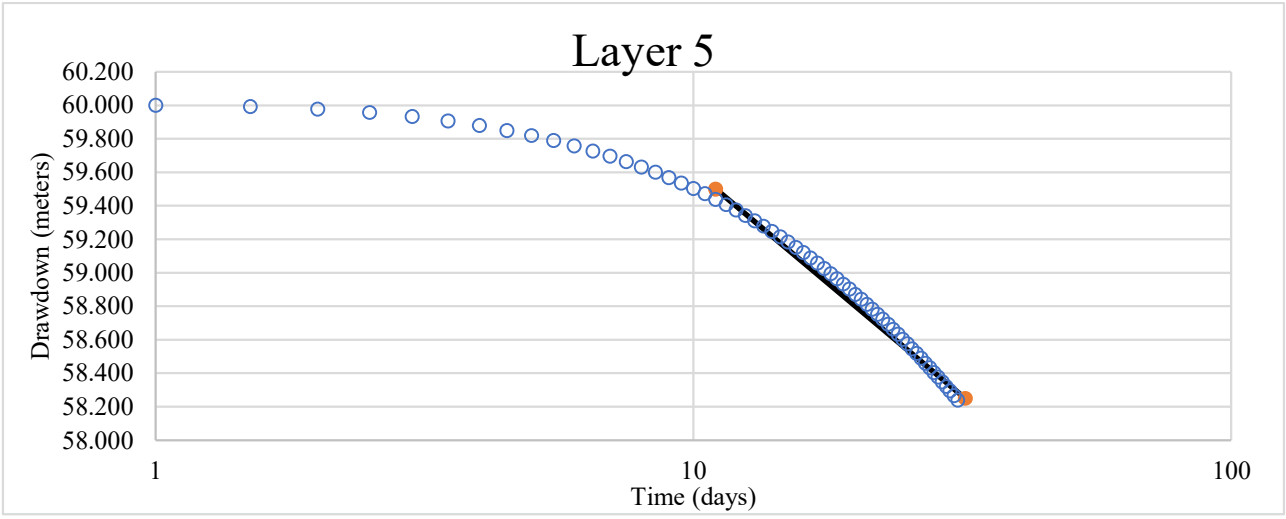
Layer 5
60.200
60.000
59.800
59.600
59.400
59.200
59.000
58.800
58.600
58.400
58.200
58.000
Drawdown (meters)
1
10
100
Time (days)

Test 25

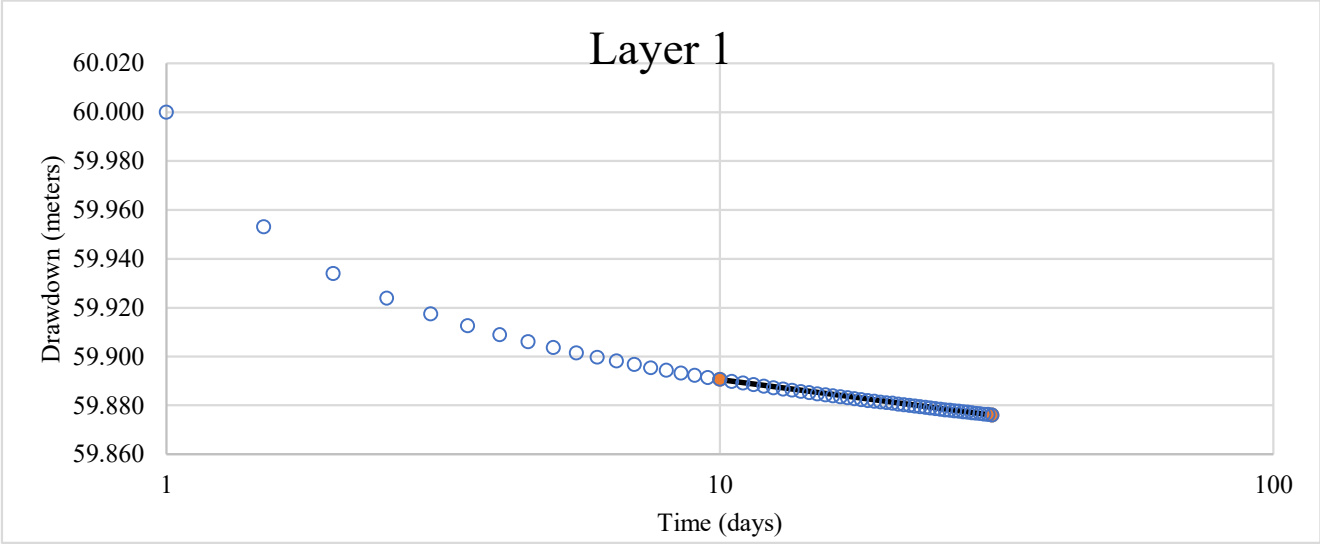
Layer 1
60.020
60.000
59.980
59.960
59.940
59.920
59.900
59.880
59.860
Drawdown (meters)
1
10
100
Time (days)

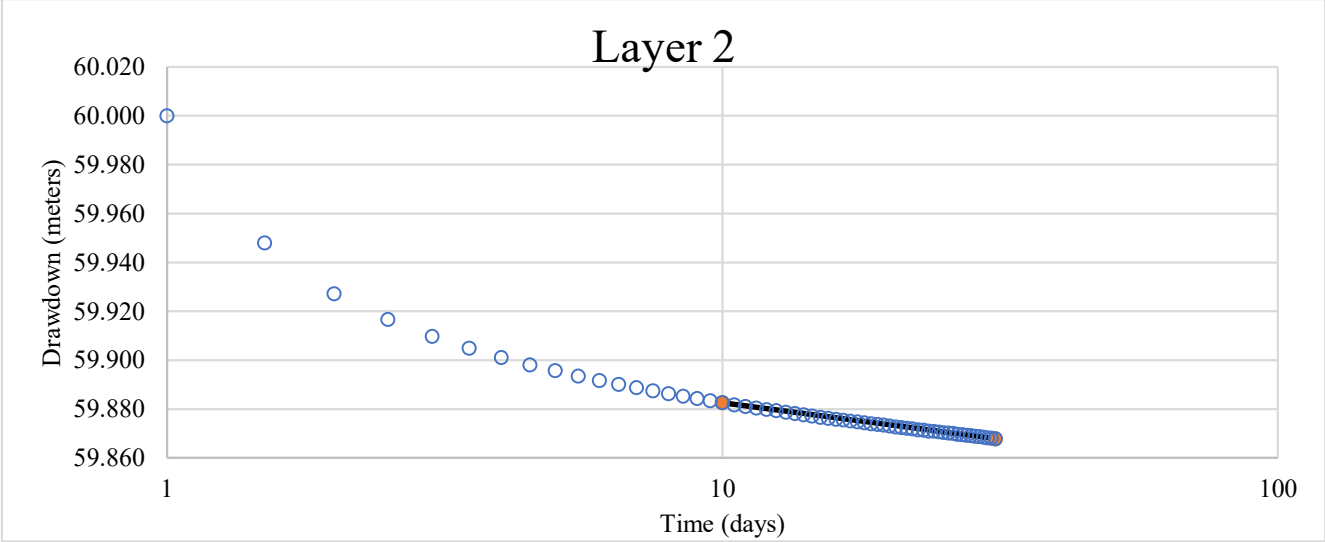
Layer 2
60.020
60.000
59.980
59.960
59.940
59.920
59.900
59.880
59.860
Drawdown (meters)
1
10
100
Time (days)

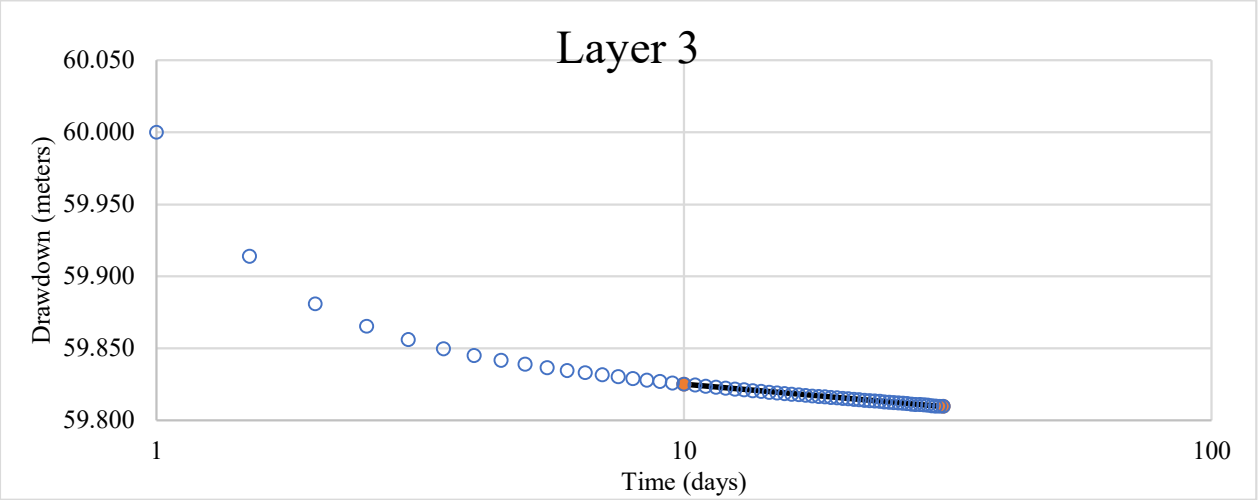
Layer 3
60.050
60.000
59.950
59.900
59.850
59.800
Drawdown (meters)
1
10
100
Time (days)

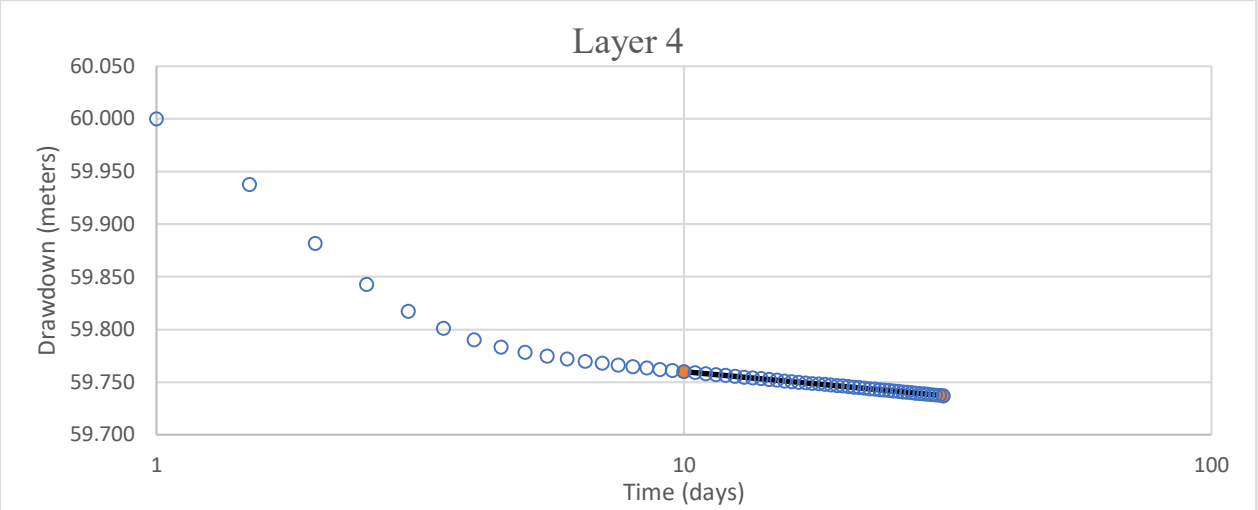
Layer 4
60.050
60.000
59.950
59.900
59.850
59.800
59.750
59.700
Drawdown (meters)
1
10
100
Time (days)

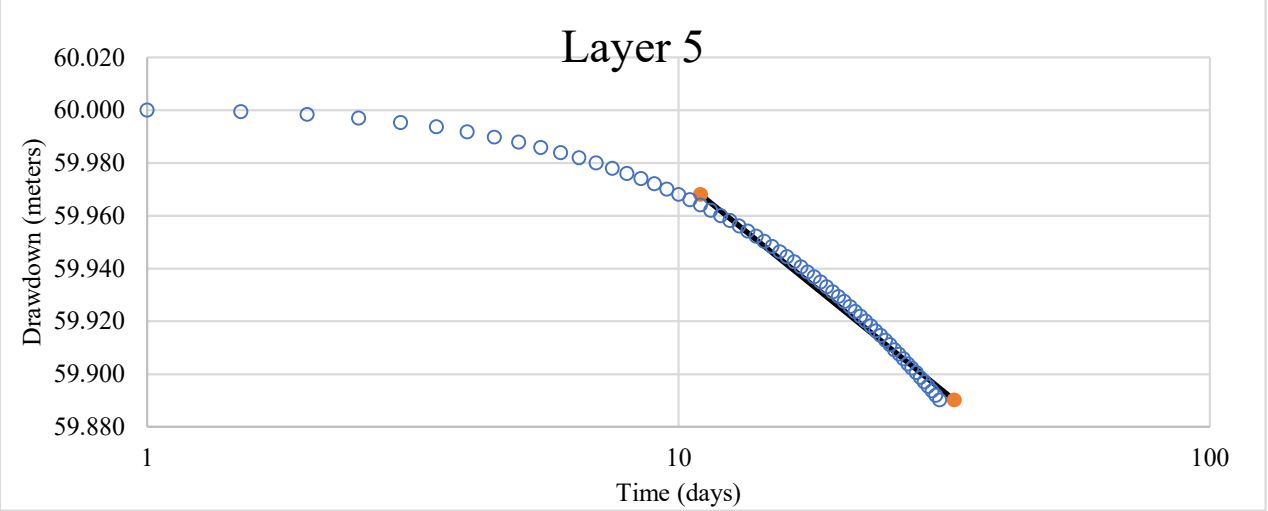
Layer 5
60.020
60.000
59.980
59.960
59.940
59.920
59.900
59.880
Drawdown (meters)
1
10
100
Time (days)

Test 26

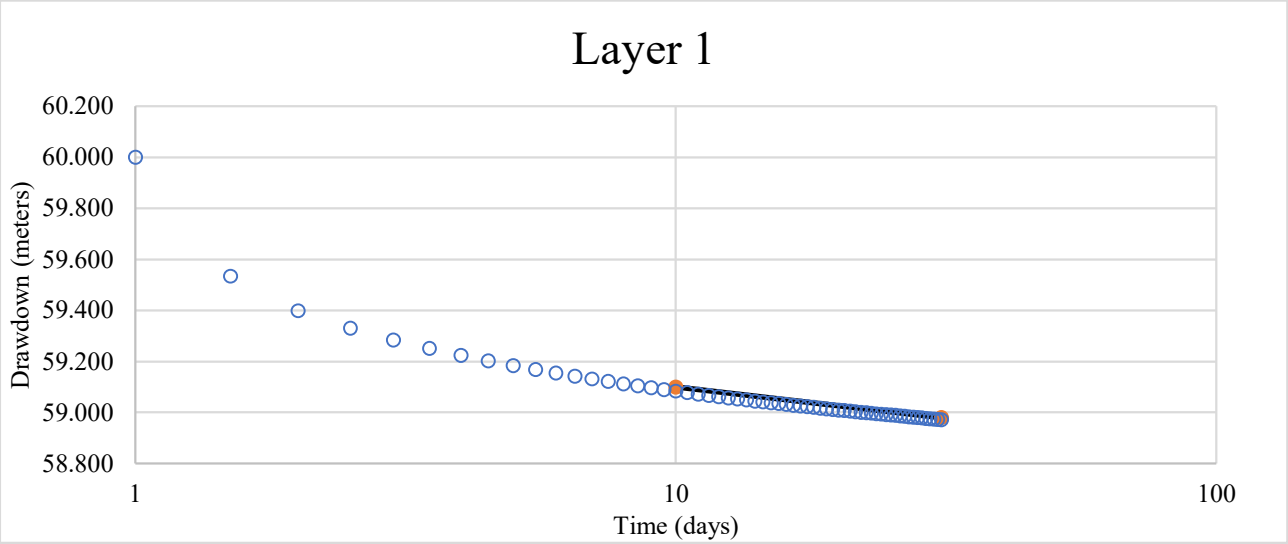
Layer 1
60.200
60.000
59.800
59.600
59.400
59.200
59.000
58.800
Drawdown (meters)
1
10
100
Time (days)

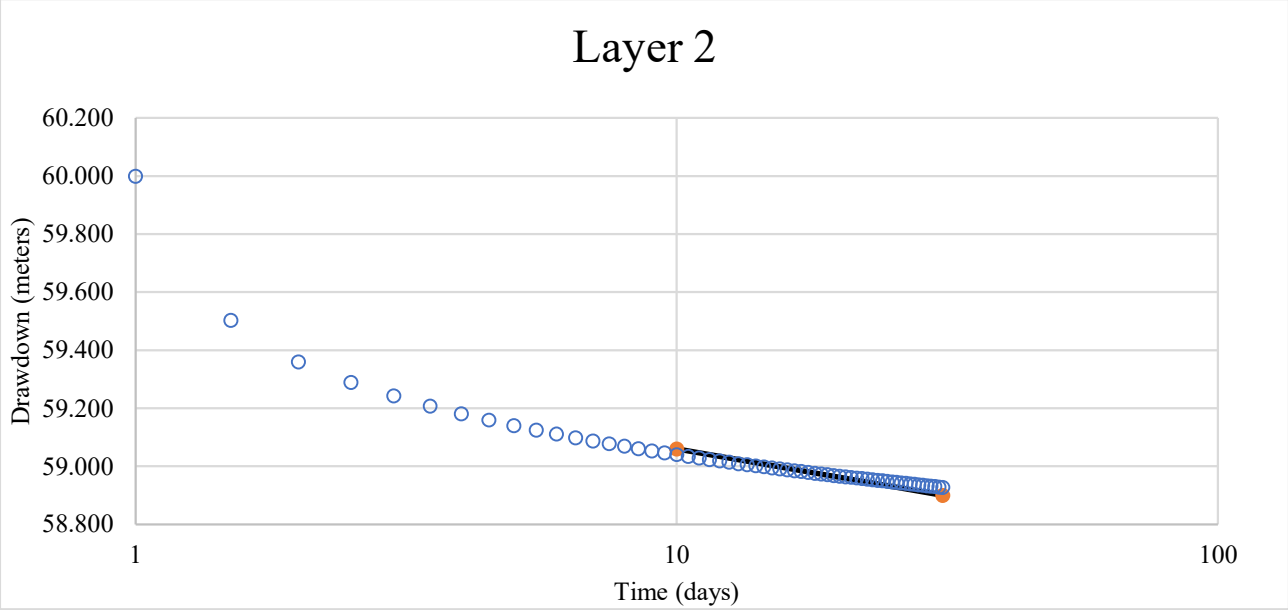
Layer 2
60.200
60.000
59.800
59.600
59.400
59.200
59.000
58.800
Drawdown (meters)
1
10
100
Time (days)

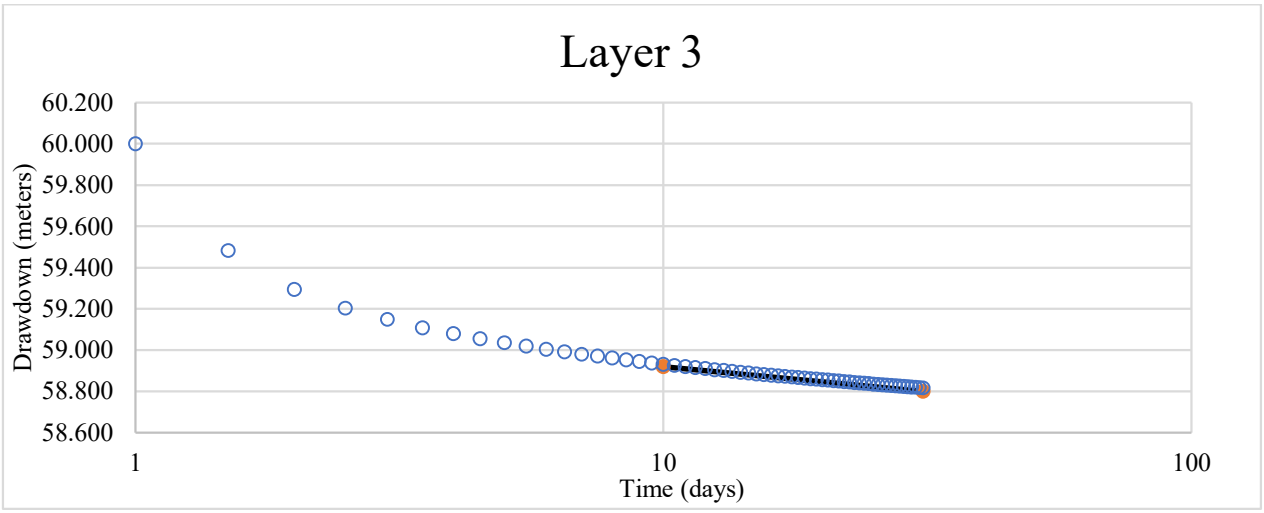
Layer 3
60.200
60.000
59.800
59.600
59.400
59.200
59.000
58.800
58.600
Drawdown (meters)
1
10
100
Time (days)

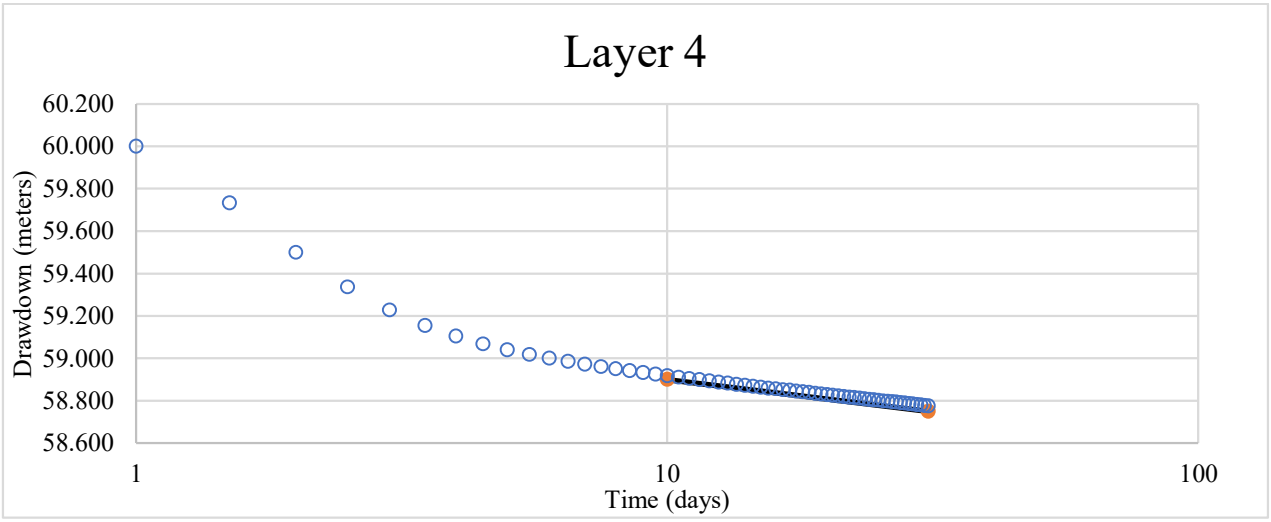
Layer 4
60.200
60.000
59.800
59.600
59.400
59.200
59.000
58.800
58.600
Drawdown (meters)
1
10
100
Time (days)

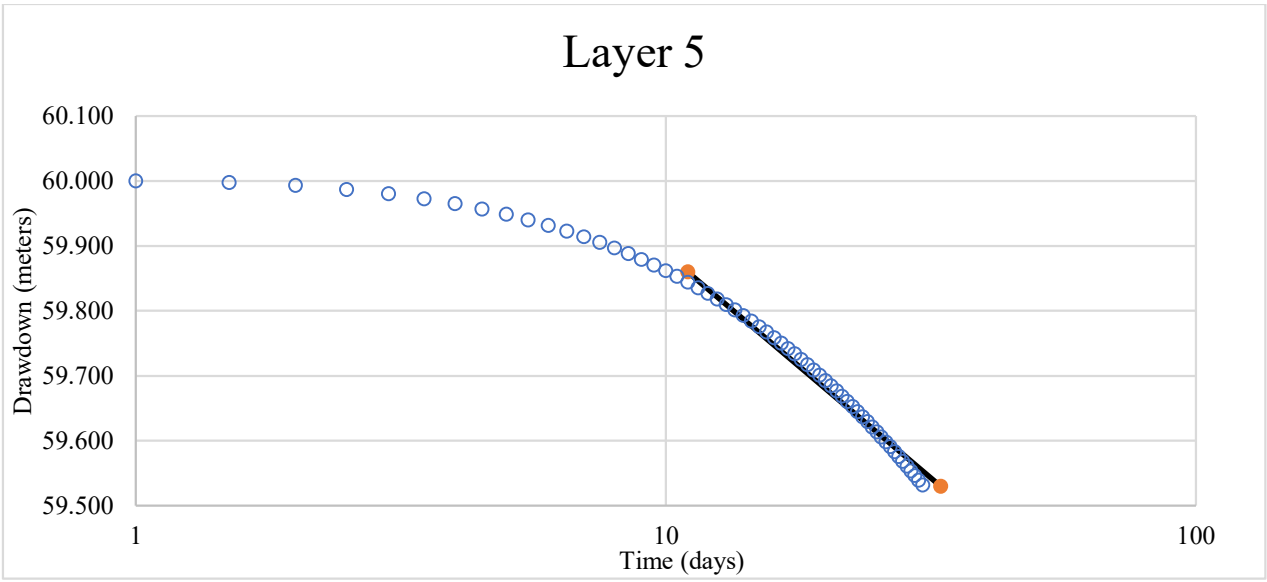
Layer 5
60.100
60.000
59.900
59.800
59.700
59.600
59.500
Drawdown (meters)
1
10
100
Time (days)

Test 27

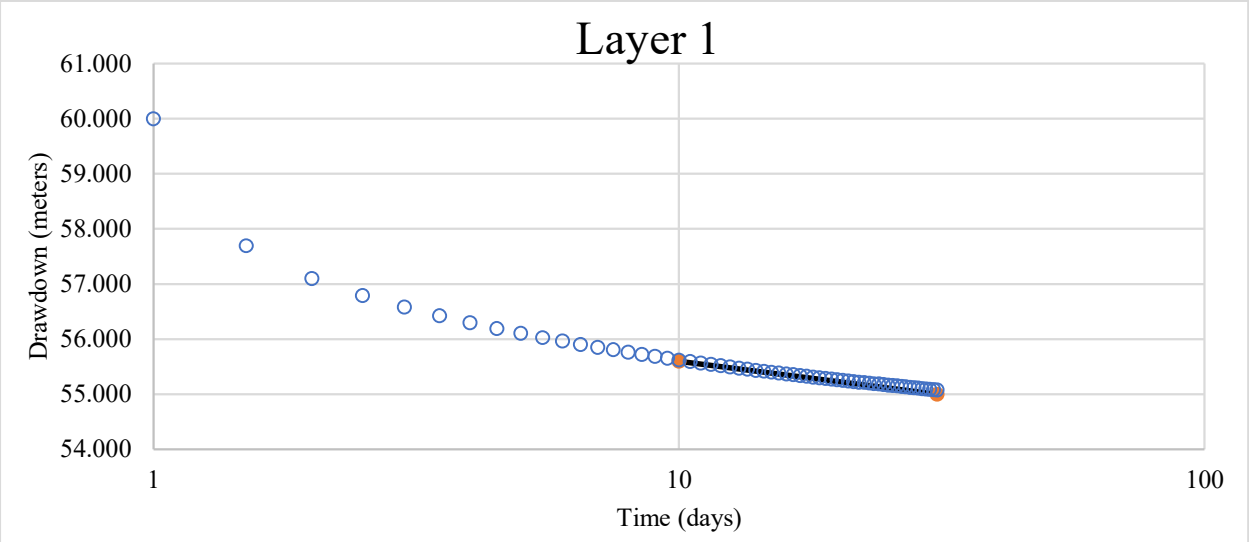
Layer 1
61.000
60.000
59.000
58.000
57.000
56.000
55.000
54.000
Drawdown (meters)
1
10
100
Time (days)

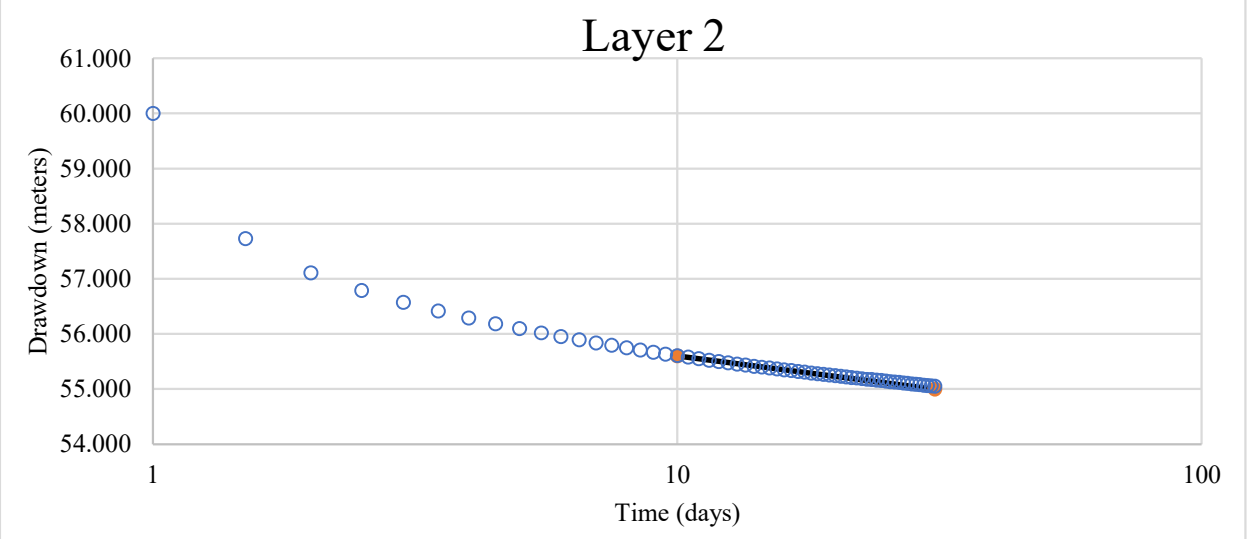
Layer 2
61.000
60.000
59.000
58.000
57.000
56.000
55.000
54.000
Drawdown (meters)
1
10
100
Time (days)

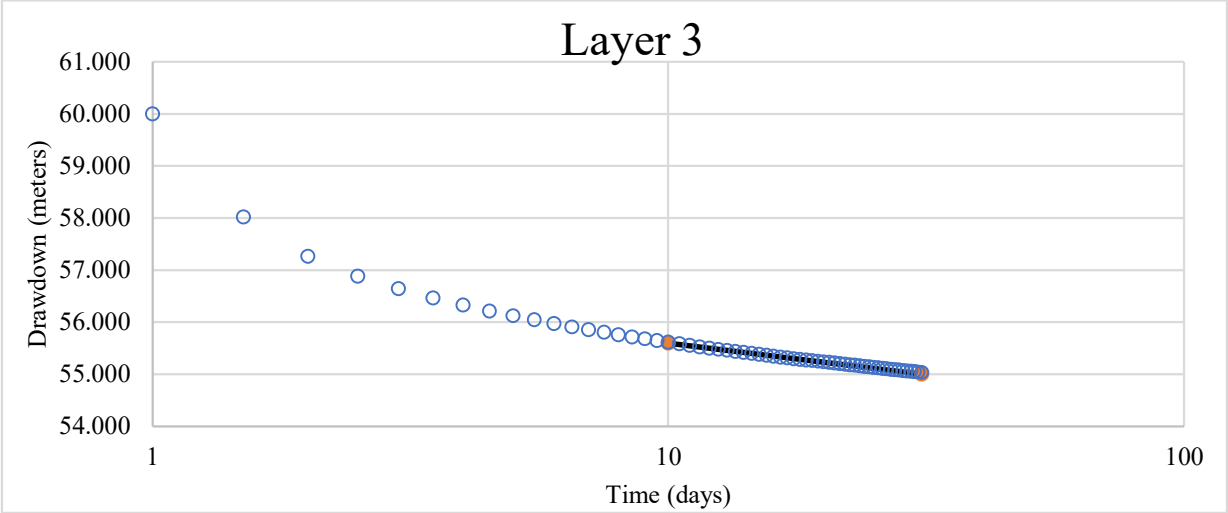
Layer 3
61.000
60.000
59.000
58.000
57.000
56.000
55.000
54.000
Drawdown (meters)
1
10
100
Time (days)

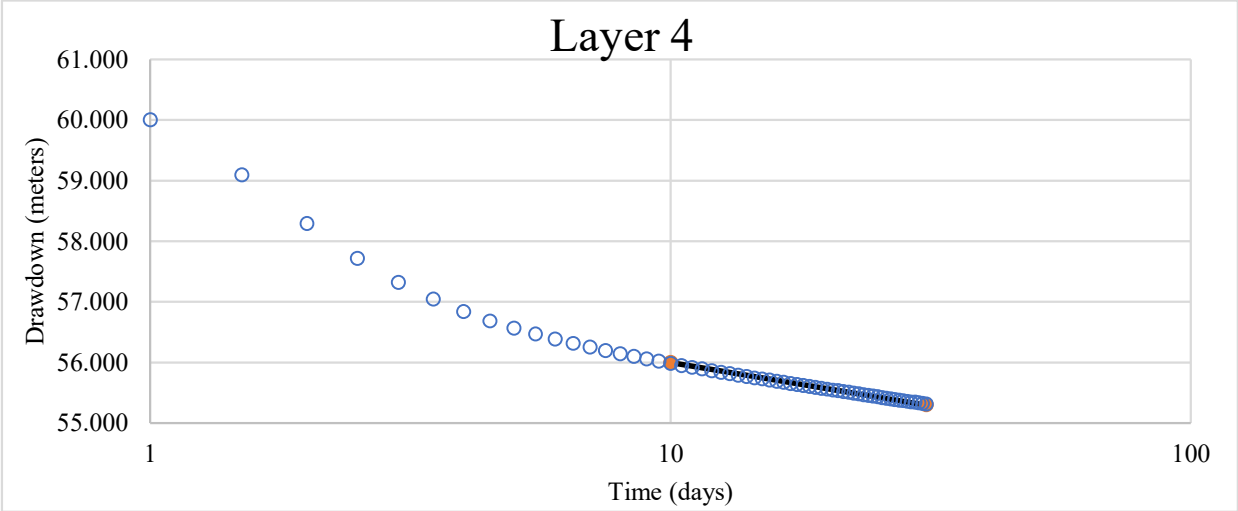
Layer 4
61.000
60.000
59.000
58.000
57.000
56.000
55.000
Drawdown (meters)
1
10
100
Time (days)

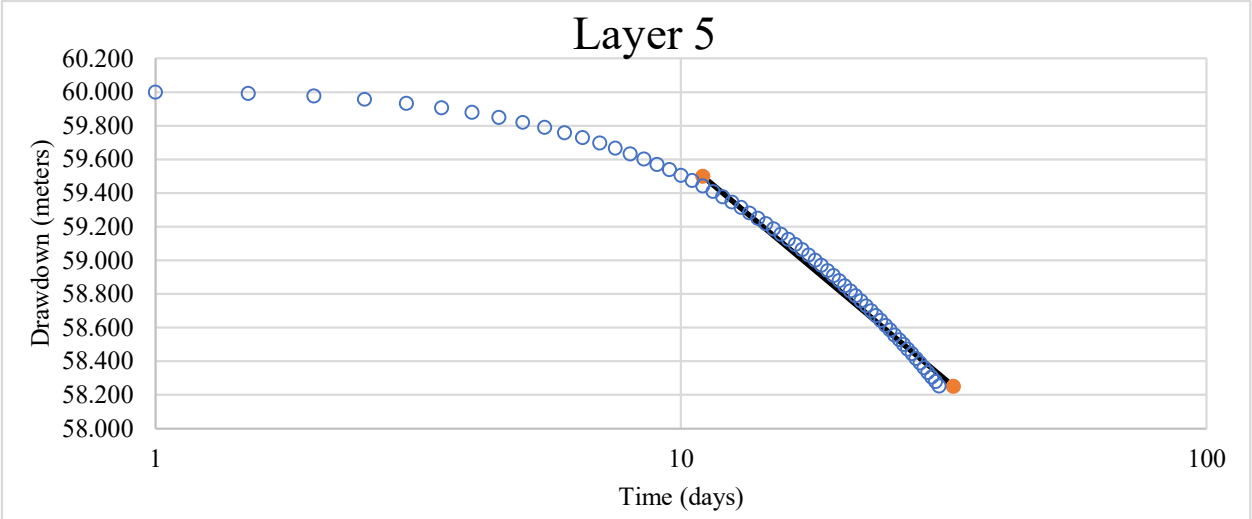
Layer 5
60.200
60.000
59.800
59.600
59.400
59.200
59.000
58.800
58.600
58.400
58.200
58.000
Drawdown (meters)
1
10
100
Time (days)

Test 28

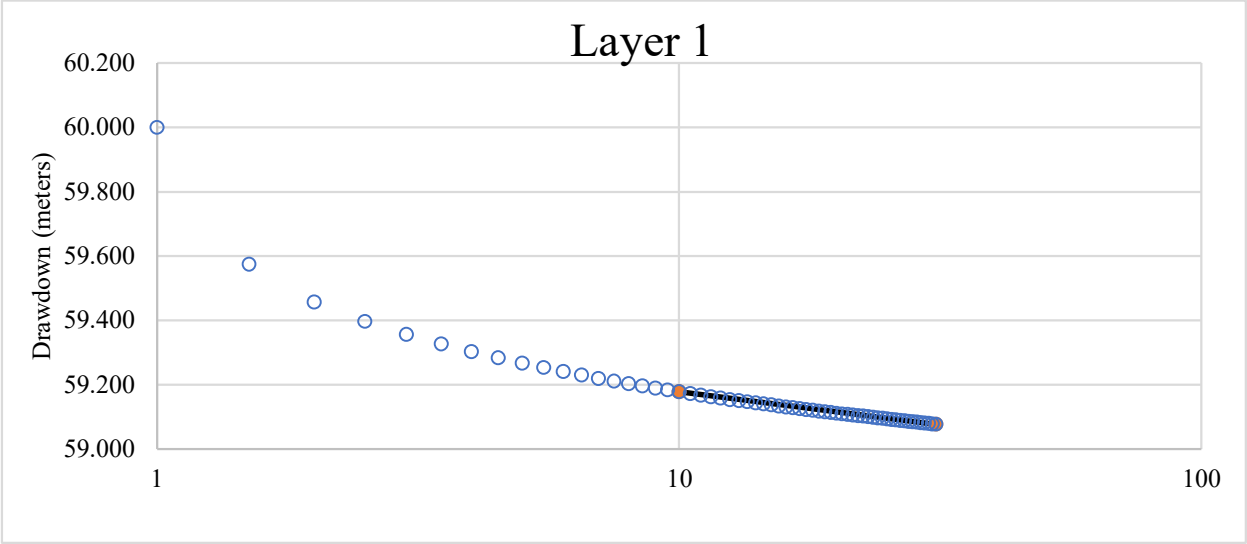
Layer 1
60.200
60.000
59.800
59.600
59.400
59.200
59.000
Drawdown (meters)
1
10
100

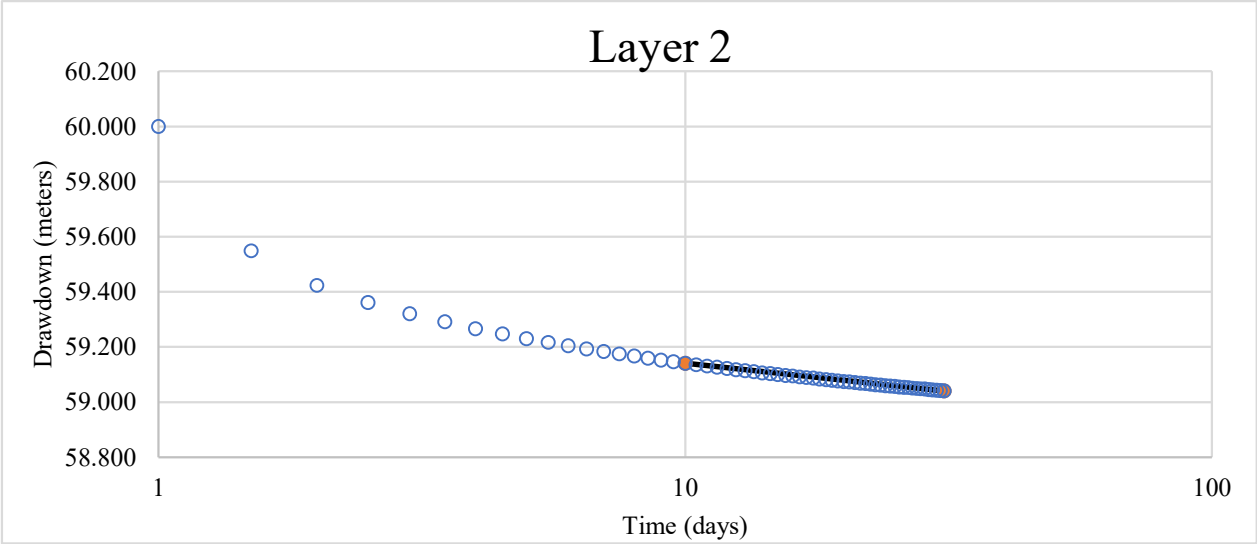
Layer 2
60.200
60.000
59.800
59.600
59.400
59.200
59.000
58.800
Drawdown (meters)
1
10
100
Time (days)

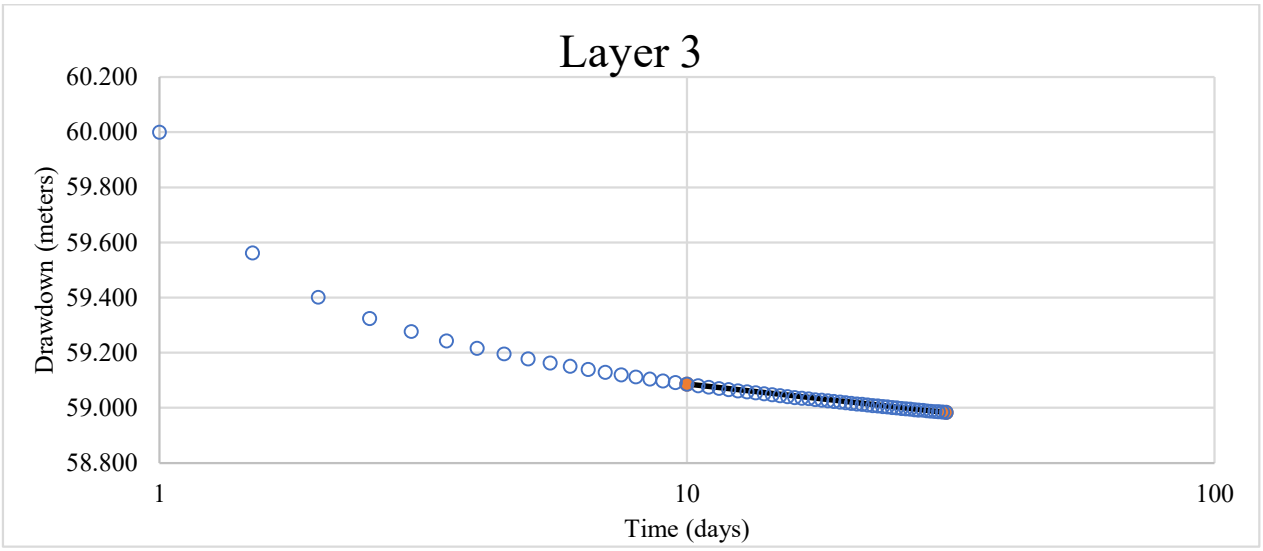
Layer 3
60.200
60.000
59.800
59.600
59.400
59.200
59.000
58.800
Drawdown (meters)
1
10
100
Time (days)

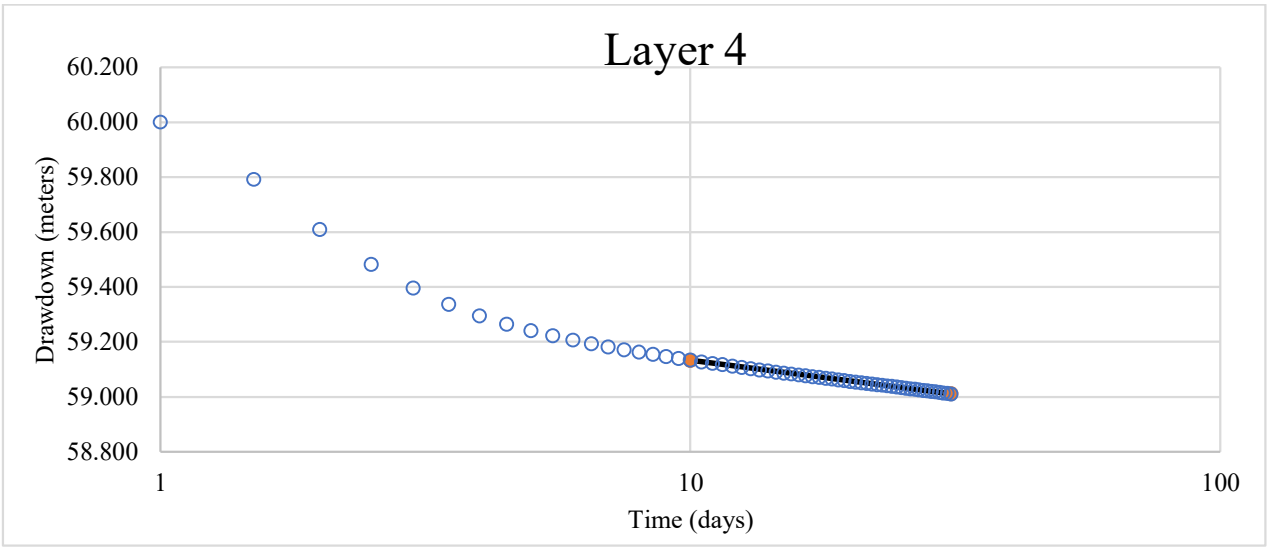
Layer 4
60.200
60.000
59.800
59.600
59.400
59.200
59.000
58.800
Drawdown (meters)
1
10
100
Time (days)

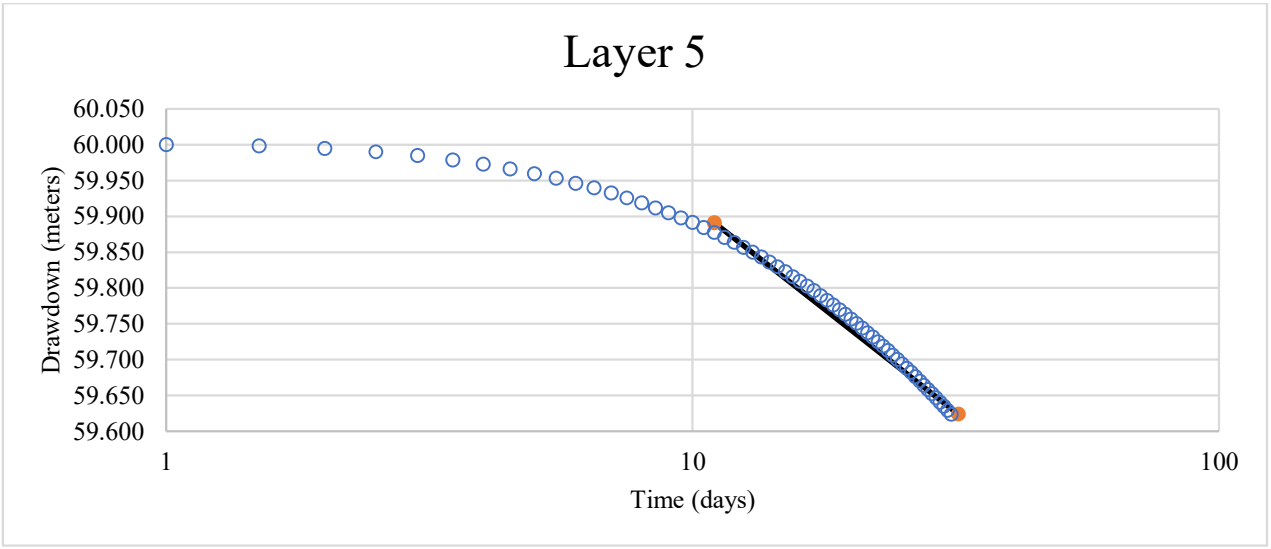
Layer 5
60.050
60.000
59.950
59.900
59.850
59.800
59.750
59.700
59.650
59.600
Drawdown (meters)
1
10
100
Time (days)

Test 29

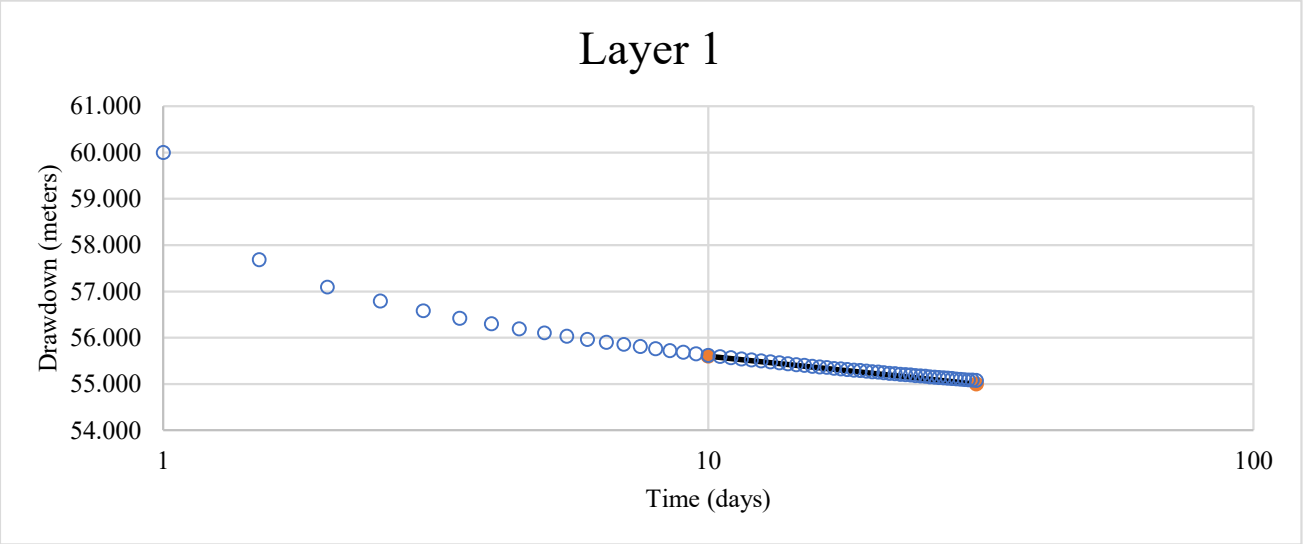
Layer 1
61.000
60.000
59.000
58.000
57.000
56.000
55.000
54.000
Drawdown (meters)
1
10
100
Time (days)

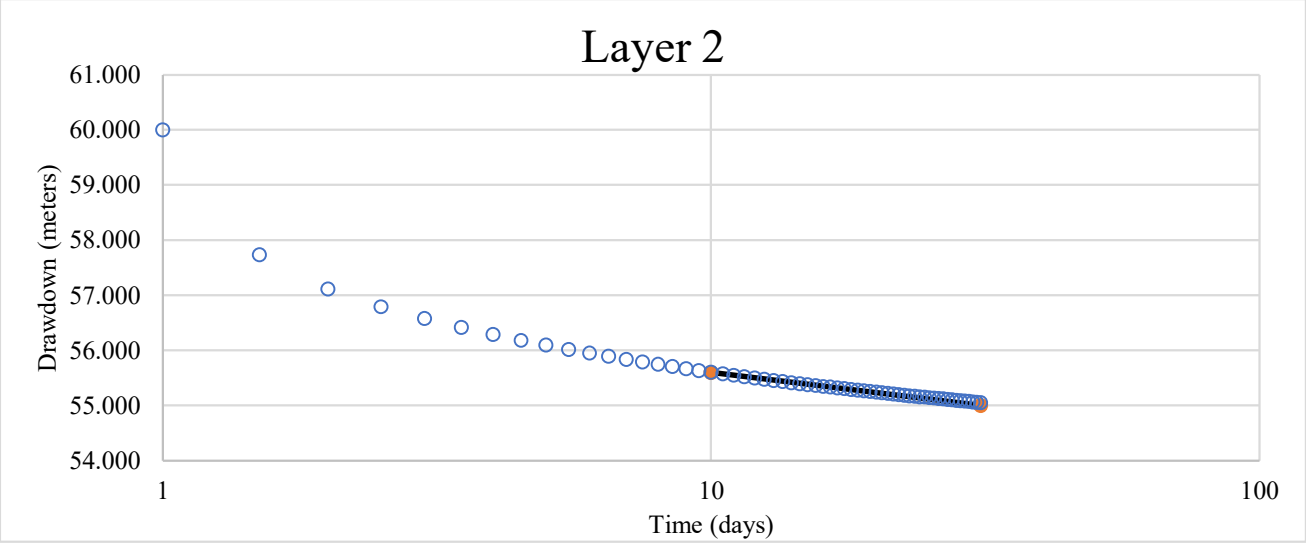
Layer 2
61.000
60.000
59.000
58.000
57.000
56.000
55.000
54.000
Drawdown (meters)
1
10
100
Time (days)

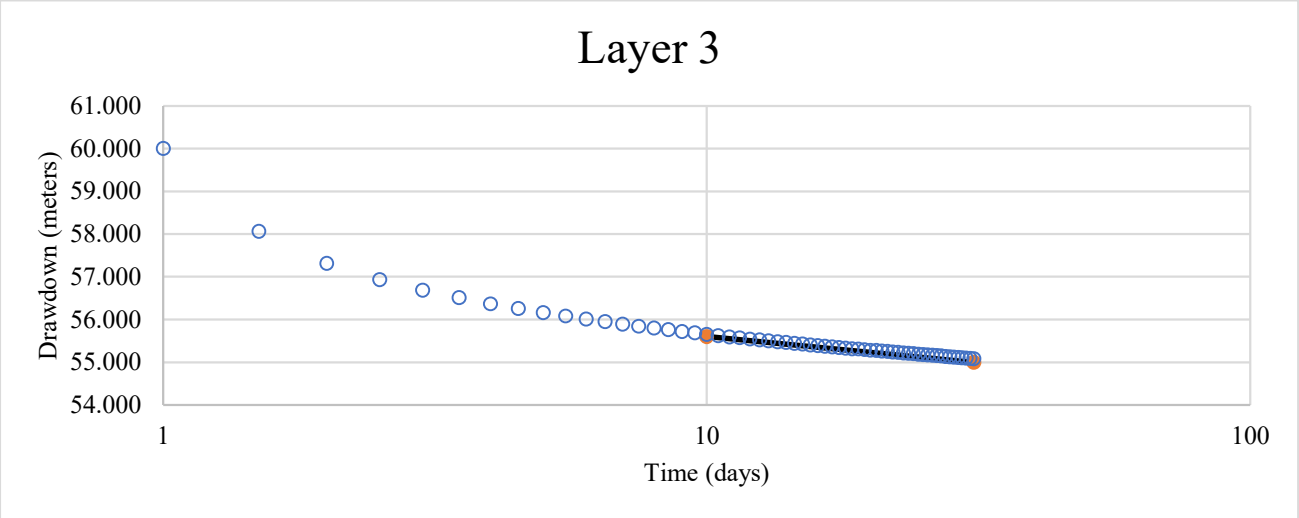
Layer 3
61.000
60.000
59.000
58.000
57.000
56.000
55.000
54.000
Drawdown (meters)
1
10
100
Time (days)

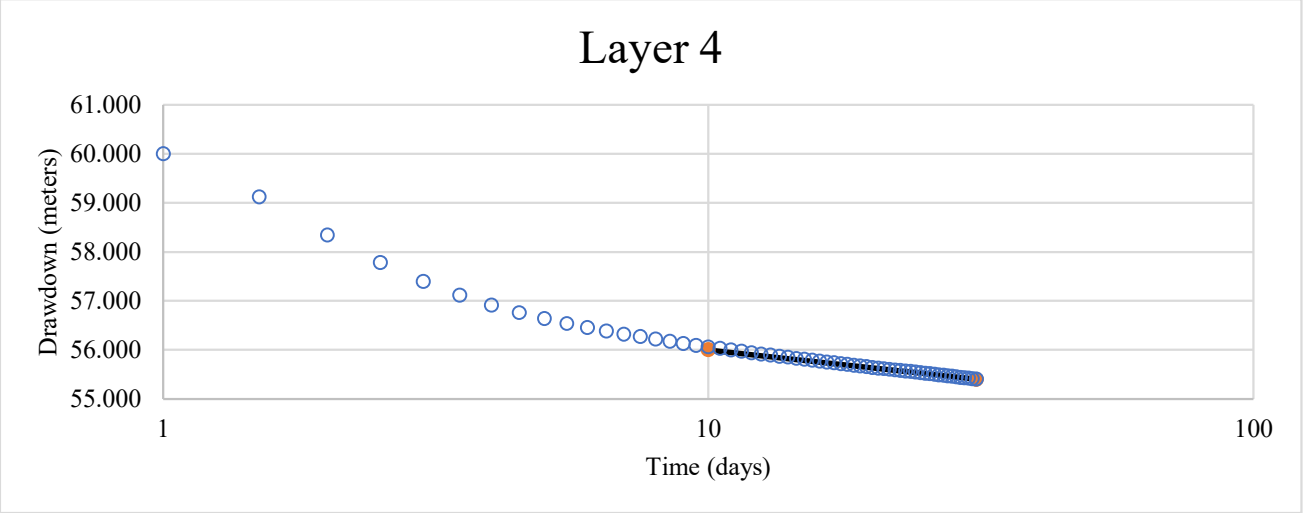
Layer 4
61.000
60.000
59.000
58.000
57.000
56.000
55.000
Drawdown (meters)
1
10
100
Time (days)

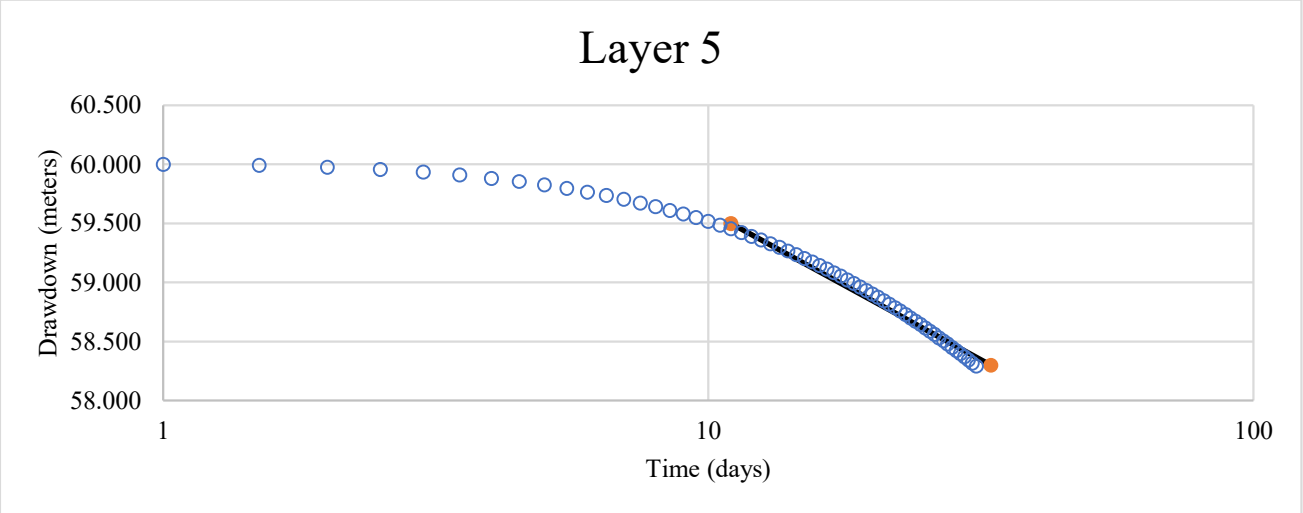
Layer 5
60.500
60.000
59.500
59.000
58.500
58.000
Drawdown (meters)
1
10
100
Time (days)

Test 30

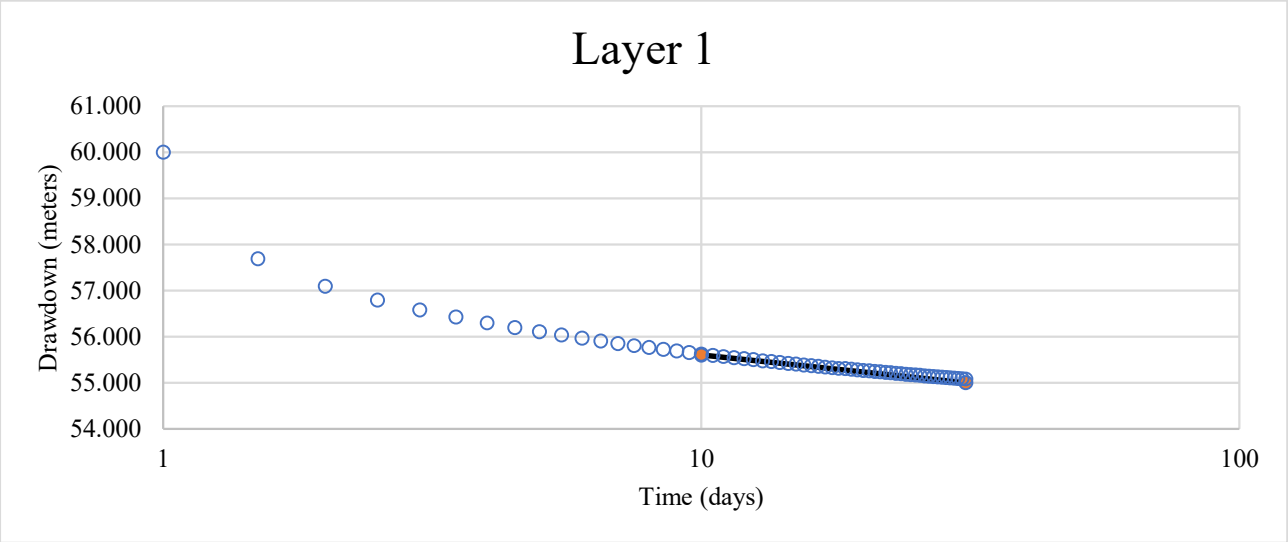
Layer 1
61.000
60.000
59.000
58.000
57.000
56.000
55.000
54.000
Drawdown (meters)
1
10
100
Time (days)

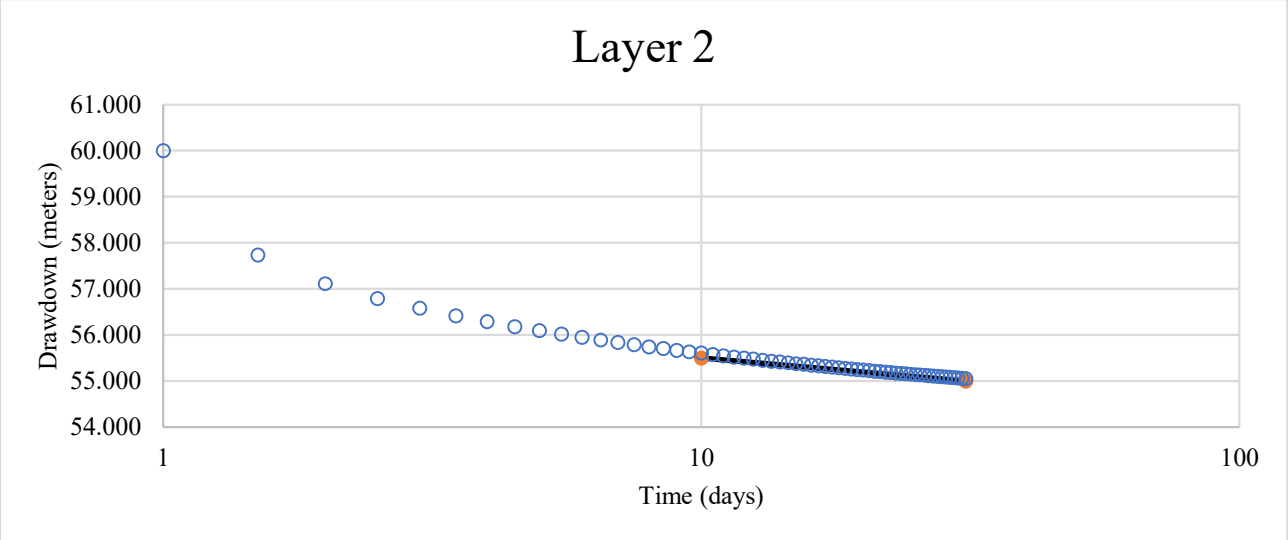
Layer 2
61.000
60.000
59.000
58.000
57.000
56.000
55.000
54.000
Drawdown (meters)
1
10
100
Time (days)

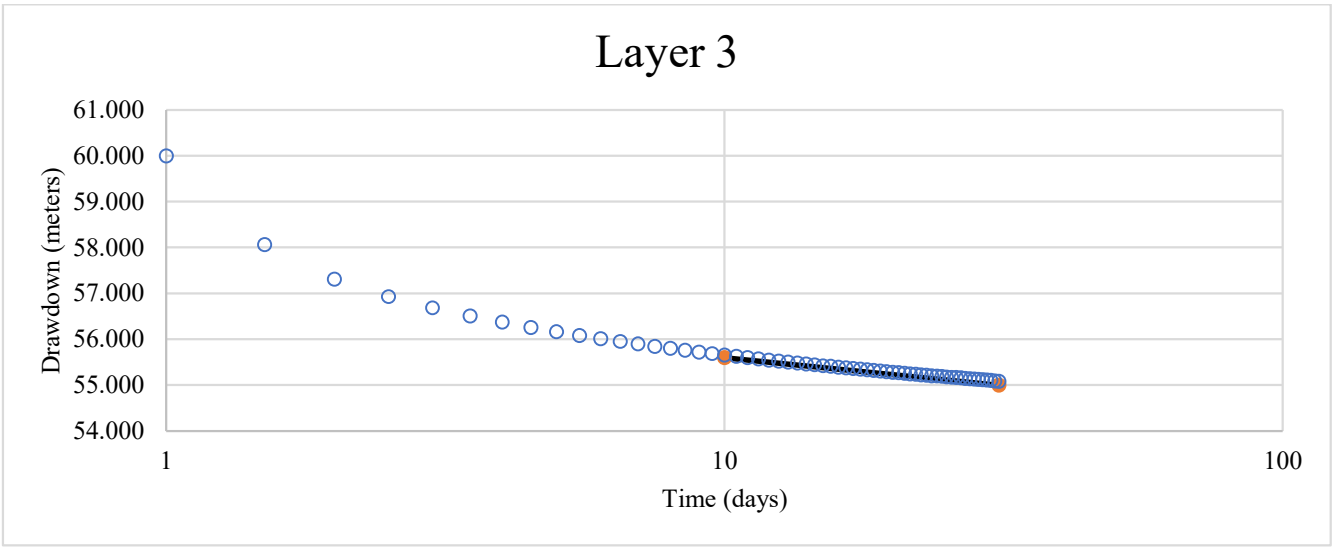
Layer 3
61.000
60.000
59.000
58.000
57.000
56.000
55.000
54.000
Drawdown (meters)
1
10
100
Time (days)

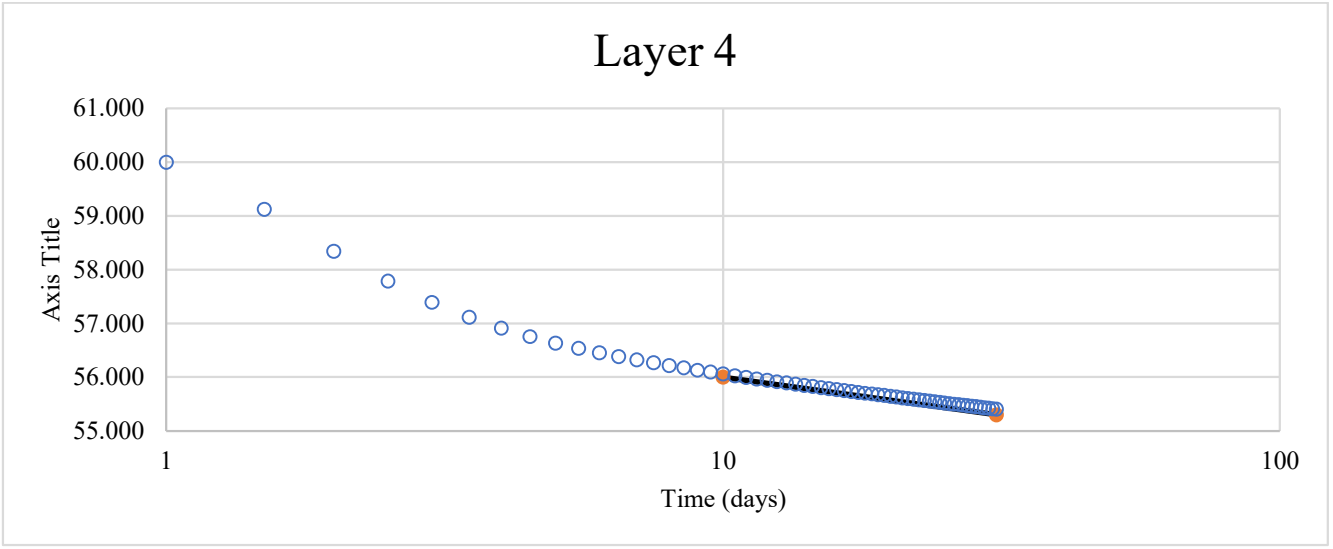
Layer 4
61.000
60.000
59.000
58.000
57.000
56.000
55.000
Axis Title
1
10
100
Time (days)

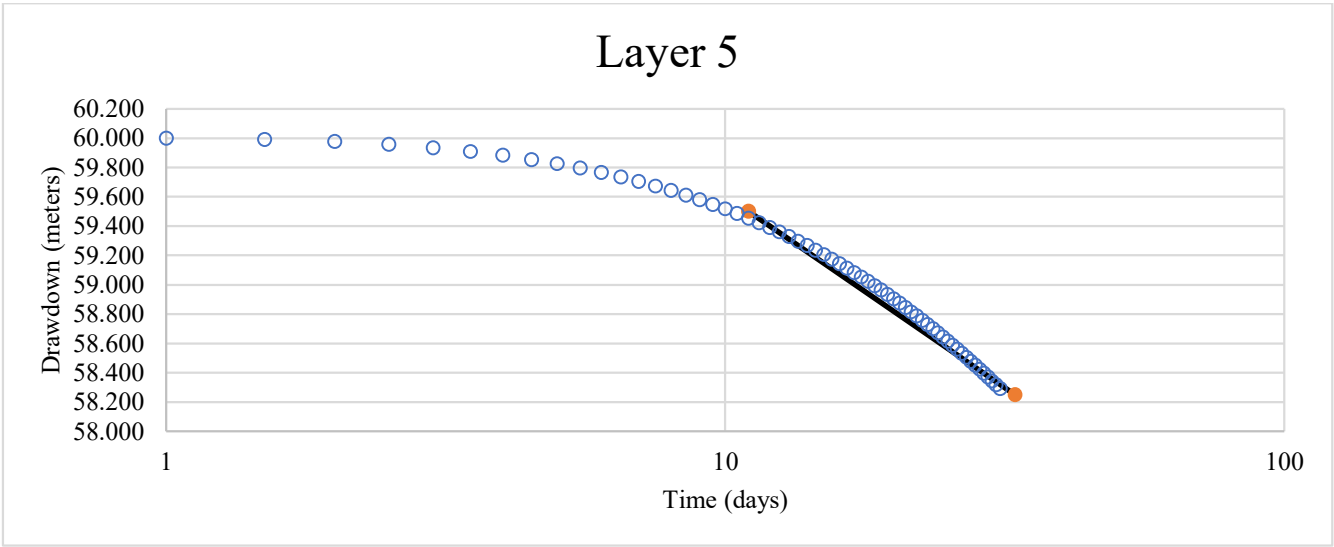
Layer 5
60.200
60.000
59.800
59.600
59.400
59.200
59.000
58.800
58.600
58.400
58.200
58.000
Drawdown (meters)
1
10
100
Time (days)

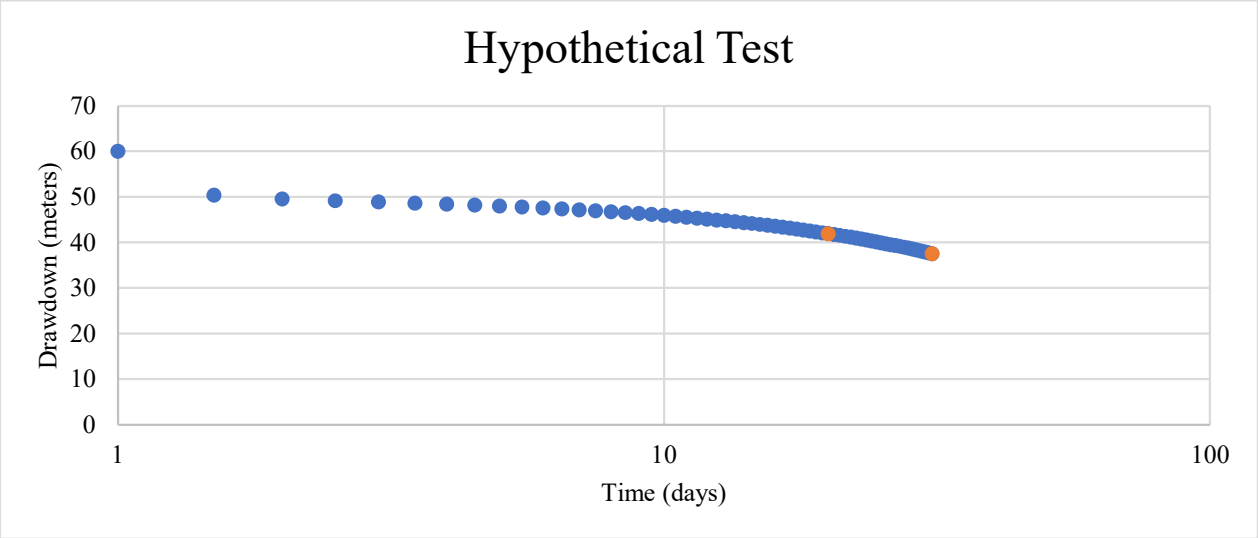

Theis Hypothetical Case

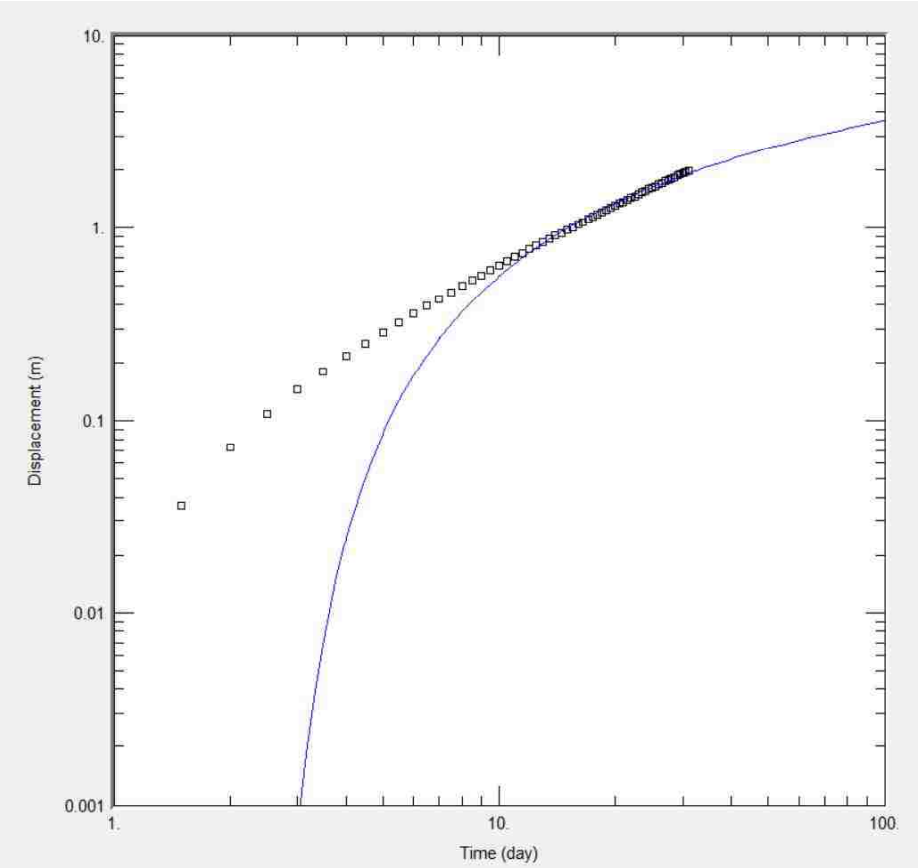

Works Cited

Anderson, M. P., and Woessener, W. W., 1992, Applied Groundwater Modeling: Simulation of Flow and Advective Transport. San Diego: Academic Press, Inc., 341 p.

Belcher, W.R., Elliott, P.E., and Geldon, A.L., 2001, Hydraulic-property estimates for use with a transient ground-water flow model for the Death Valley regional ground-water flow system, Nevada and California: U.S. Geological Survey Water-Resources Investigations Report 01-4210, 33 p., Accessed June 4, 2018, at *http://water.usgs.gov/pubs/wri/wri014210/*.

Belcher, W. R., Bedinger, M.S., Back, J. T., and Sweetkind, D.S., 2009, Interbasin flow in the Great Basin with special reference to the southern Funeral Mountains and the source of Furnace Creek springs, Death Valley, California. Journal of Hydrology v. 369, p. 30-43. Accessed June 4, 2018, at *https://doi.org/10.1016/j.jhydrol.2009.02.048*.

Belcher, W. R., Sweetkind, D. S., Faunt, C. C., Pavelko, M. T., and Hill, M. C., 2017, An update of the Death Valley regional groundwater flow system transient model, Nevada and California. U.S. Geological Survey Scientific Investigations Report 2016-5150, 74 p. Accessed June 4, 2018, at *https://doi.org/10.3133/sir20165150*.

Cooper, H. H. and Jacob, C. E., 1946, A Generalized graphical method of evaluating formation constants and summarizing well- field history. American Geophysical Union Transactions, v. 27, p. 526-534. Accessed June 4, 2018, at *https://doi.org/10.1029/TR027i004p00526*.

D'Agnese, F.A., Faunt, C. C., Turner, A. K., and Hill, M.C., 1997, Hydrogeologic evaluation and numerical simulation of the Death Valley regional ground-water flow system, Nevada and California. U.S. Geological Survey Water- Resources Investigations Report 96-4300, 124 p. Accessed June 4, 2018, at *https://pubs.usgs.gov/wri/1996/4300/report.pdf*.

Driscoll, F. G., 1987, Groundwater and Wells. St. Paul: Johnson Division, 1089 p.

Faunt, C. C., 1997, Effect of faulting on ground-water movement in the Death Valley region, Nevada and California. U.S. Geological Survey Water- Resources Investigations Report 95-4132, 42p. Accessed June 4, 2018, at *https://pubs.usgs.gov/wri/1995/4132/report.pdf*.

Faunt, C. C., Blainey, J.B., Hill, M. C., D`Agnese, F. A., and O'Brien, G.M., 2010, Chapter F. Transient flow model, in Belcher, W.R., and Sweetkind, D.S. eds., Death Valley regional groundwater flow system, Nevada and California--Hydrogeologic framework and transient groundwater flow model. U.S. Geological Survey Professional Paper 1711, p. 251-344. Accessed June 4, 2018, at *https://pubs.usgs.gov/pp/1711/*.

Fetter, C.W., 1994, Applied Hydrogeology (3rd ed). New Jersey: Prentice Hall., 691 p.

Freeze, A. R., and Cherry, J. A., 1979, Groundwater. Englewood Cliffs: Prentice Hall., 604 p.

Halford, K.J., 2016, T-COMP—A suite of programs for extracting transmissivity from MODFLOW models: U.S. Geological Survey Techniques and Methods, book 6, chap. A54, 17 p., Accessed June 4, 2018, at *http://dx.doi.org/10.3133/tm6A54*.

Halford, K.J., Weight, W.D., and Schreiber, R.P., 2006, Interpretation of Transmissivity Estimates from Single-Well Pumping Aquifer Tests. Groundwater v. 44, p. 467-471. Accessed, June 4, 2018, at *https://doi.org/10.1111/j.1745-6584.2005.00151.x*.

Harbaugh, A.W., 2005, MODFLOW-2005, The U.S. Geological Survey modular ground-water model-- The Ground-Water Flow Process. U.S. Geological Survey Techniques and Methods 6-A16., variously paginated. Accessed June 4, 2018, at *https://pubs.usgs.gov/tm/2005/tm6A16/*.

Harrill, J. R., and Bedinger, M.S., 2010, Appendix 2. Estimated boundary flows, in Belcher, W.R., and Sweetkind, D.S., eds., Death Valley regional groundwater flow system, Nevada and California-- hydrogeologic framework and transient groundwater flow model. U.S. Geological Survey Professional Paper 1711, p. 365-398. Accessed June 4, 2018, at *https://pubs.usgs.gov/pp/1711/*.

Hsieh, P.A., and Winston, R.B., 2002, User's Guide to Model Viewer: a program for three-Dimensional Visualization of Ground-Water Model Results. U.S. Geological Survey Open-File Report 20-106, 18 p. Accessed June 4, 2018, at *https://water.usgs.gov/nrp/gwsoftware/modelviewer/ModelViewer.html*.

Konikow, L. F., Hornberger, G. Z., and Halford, K. A.,2009, Revised multi-node well (MNW2) package for MODFLOW ground-water flow model. U.S. Geological Survey Techniques and Methods 6- A30, 67 p. Accessed June 4, 2018, at *https://pubs.usgs.gov/tm/tm6a30/*.

Lohman, S.W., 1979, Ground-Water Hydraulics. U.S. Geological Survey Professional Paper 708, 4 p. Accessed May 15, 2019, at *https://pubs.usgs.gov/pp/0708/report.pdf*.

Walton, W. C.,1987, Groundwater Pumping Tests: Design and Analysis. Chelsea: Lewis Publishers, Inc., 201 p.

Winston, R.B., 2000, Graphical User Interface for MODFLOW, Version 4: U.S. Geological Survey Open-File Report 00-315, 27 p. Accessed June 4, 2018, at https://water.usgs.gov/nrp/gwsoftware/GW_Chart/GW_Chart.html.

Winston, R.B.,2009, ModelMuse- A graphical user interface for MODFLOW-2005 and PHAST. U.S. Geological Survey Techniques and Methods 6-A29, 52 p. Accessed June 4, 2018, at *https://pubs.usgs.gov/tm/tm6A29/*.

Curriculum Vitae

Afan Tarar
Personal Email –afan.tarar@gmail.com

EDUCATION

M.S., Geology, University of Nevada, Las Vegas, May 2019

B.S., Molecular and Cellular Biology, University Nevada, Las Vegas, May 2012

GRANTS

USGS-NPS Grant, $50,000: June 2017